ORNL
ER COPY

ORNL-2148
Progress

HOMOGENEOUS REACTOR PROJECT

QUARTERLY PROGRESS REPORT

FOR PERIOD ENDING JULY 31, 1956

OAK RIDGE NATIONAL LABORATORY
OPERATED BY
UNION CARBIDE NUCLEAR COMPANY
A Division of Union Carbide and Carbon Corporation

UCC

POST OFFICE BOX P · OAK RIDGE, TENNESSEE

ORNL-2148

Cy. 34

Contract No. W-7405-eng-26

HOMOGENEOUS REACTOR PROJECT

QUARTERLY PROGRESS REPORT

For Period Ending July 31, 1956

Project Director — R. B. Briggs
Associate Director — C. E. Winters

Homogeneous Reactor Test — S. E. Beall
Reactor Design and Analysis — J. A. Lane
Engineering Development — J. A. Lane
Corrosion and Materials — E. G. Bohlmann
Chemical Engineering Development — F. R. Bruce
Supporting Chemical Research — E. H. Taylor

DATE ISSUED

SEP 20 1956

INTERNAL DISTRIBUTION

1. C. E. Center
2. Biology Library
3. Health Physics Library
4. Metallurgy Library
5-6. Reactor Experimental
     Engineering Library
7-9. Central Research Library
10-33. Laboratory Records Dept.
34. Laboratory Records, ORNL R.C.
35. G. M. Adamson
36. R. E. Aven
37. S. E. Beall
38. D. S. Billington
39. E. P. Blizard
40. E. G. Bohlmann
41. G. J. Borkowski
42. G. E. Boyd
43. F. R. Bruce
44. A. D. Callihan
45. D. W. Cardwell
46. W. L. Carter
47. G. H. Cartledge
48. R. A. Charpie
49. W. E. Clark
50. T. E. Cole
51. E. L. Compere
52. D. D. Cowen
53. S. Cromer
54. F. L. Culler
55. J. S. Culver
56. J. S. Drury
57. W. K. Eister
58. L. B. Emlet (K-25)
59. D. E. Ferguson
60. J. H. Frye, Jr.
61. J. L. Gabbard
62. W. R. Gall
63. H. E. Goeller
64. C. B. Graham
65. J. C. Griess
66. P. N. Haubenreich
67. J. W. Hill
68. C. J. Hochanadel
69. A. Hollaender
70. A. S. Householder
71. G. H. Jenks
72. W. H. Jordan
73. P. R. Kasten
74. C. P. Keim
75. M. T. Kelley
76. B. B. Korsmeyer
77. A. S. Kitzes
78. K. A. Kraus
79. J. A. Lane
80. R. E. Leuze
81. S. C. Lind
82. R. B. Lindauer
83. R. S. Livingston
84. M. I. Lundin
85. R. N. Lyon
86. J. L. Marsh (C&CCC, South Charleston)
87. W. R. Marshall
88. H. F. McDuffie
89. J. P. McBride
90. R. A. McNees
91. J. R. McWherter
92. O. Menis
93. E. C. Miller
94. K. Z. Morgan
95. E. J. Murphy
96. M. L. Nelson
97. E. O. Nurmi
98. J. P. Murray (Y-12)
99. L. F. Parsly
100. H. F. Poppendiek
101. L. R. Quarles
102. W. D. Reel
103. P. M. Reyling
104. A. M. Rom
105. W. L. Ross
106. H. C. Savage
107. C. H. Secoy
108. C. L. Segaser
109. E. D. Shipley
110. M. J. Skinner
111. R. W. Stoughton
112. A. H. Snell
113. I. Spiewak
114. C. D. Susano
115. J. A. Swartout
116. E. H. Taylor
117. D. G. Thomas
118. P. F. Thomason
119. M. Tobias

120. D. S. Toomb
121. W. E. Unger
122. R. Van Winkle
123. B. Weaver
124. A. M. Weinberg
125. T. A. Welton
126. E. P. Wigner (consultant)
127. G. C. Williams
128. J. C. Wilson

129. C. E. Winters
130. F. C. Zapp
131. J. E. Baker
132. H. P. Day
133. W. J. Leonard
134. M. L. Picklesimer
135. ORNL & Y-12 Technical Library,
  Document Reference Section
136. HRP Director's Office, Y-12

EXTERNAL DISTRIBUTION

137. Division of Research and Development, AEC, ORO
138-479. Given distribution as shown in M-3679 under Reactors-Research and Testing category

Reports previously issued in this series are as follows:

ORNL-527	Date Issued, December 28, 1949
ORNL-630	Period Ending February 28, 1950
ORNL-730	Feasibility Report — Date Issued, July 6, 1950
ORNL-826	Period Ending August 31, 1950
ORNL-925	Period Ending November 30, 1950
ORNL-990	Period Ending February 28, 1950
ORNL-1057	Period Ending May 15, 1951
ORNL-1121	Period Ending August 15, 1951
ORNL-1221	Period Ending November 15, 1951
ORNL-1280	Period Ending March 15, 1952
ORNL-1318	Period Ending July 1, 1952
ORNL-1424	Period Ending October 1, 1952
ORNL-1478	Period Ending January 1, 1953
ORNL-1554	Period Ending March 31, 1953
ORNL-1605	Period Ending July 31, 1953
ORNL-1658	Period Ending October 31, 1953
ORNL-1678	Period Ending January 31, 1954
ORNL-1753	Period Ending April 30, 1954
ORNL-1772	Period Ending July 31, 1954
ORNL-1813	Period Ending October 31, 1954
ORNL-1853	Period Ending January 31, 1955
ORNL-1895	Period Ending April 30, 1955
ORNL-1943	Period Ending July 31, 1955
ORNL-2004	Period Ending October 31, 1955
ORNL-2057	Period Ending January 31, 1956
ORNL-2096	Period Ending April 30, 1956

HRP QUARTERLY PROGRESS REPORT

SUMMARY

PART I. HOMOGENEOUS REACTOR TEST

1. HRT Operations

Engineering tests of 20 HRT components were completed during the quarter. These were followed by a three-week period of repairs and remote-maintenance practice. Preparations were completed for a series of dump tests and for experiments with unenriched uranyl sulfate at full design pressure and temperature.

2. HRT Design

The refrigeration system was modified to permit the installation of permanent freeze jackets on the feed and purge pumps. The remotely operated freeze jacket was redesigned to permit easier operation and to reduce fabrication costs. Provisions were made to meter the flow through the feed and purge pumps. Preliminary specifications and a drawing for a replacement pressure vessel for the HRT were prepared prior to placing a purchase order for this item. The remote-maintenance tooling program is considered to be approximately 40% complete.

3. HRT Component Development

The 400A-1 and 300A-1 circulating pumps have operated satisfactorily since their thermal barriers were seal-welded to their stator flanges. The spare reactor fuel pump, with its titanium thermal barrier sealed with a solid stainless steel gasket, completed a successful 1135-hr run on 0.04 m UO_2SO_4 solution. The spare reactor blanket pump circulated 1.3 m UO_2SO_4 successfully for 550 hr.

Proposals for a spare HRT heat exchanger were received and are being evaluated.

The new feed-pump check-valve design has apparently eliminated housing failures. A program aimed at increasing diaphragm life was initiated.

Pressure balance approaching that required on the HRT was attained in dump tests. The HRT sampler took satisfactory samples from the HRT mockup; some improvements were made in the sampler. Freezing stations were tested successfully on $\frac{1}{2}$- and $3\frac{1}{2}$-in. pipes. Test of an HRT pressurizer heater disclosed that heat transmission is adequate.

The HRT mockup ran for 1730 hr during the quarter; there were few operational difficulties. A special study was made of sampling and chemical analysis. Simulated reactor fission and corrosion products were introduced in connection with tests of a hydroclone removal unit.

4. HRT Controls and Instrumentation

4.1 Procurement. — The 20-channel remote-area radiation monitoring system is being modified by the vendor to decrease the sensitivity to noise signals that are introduced through the a-c power supply.

4.2 Equipment Installation. — The control valve and capillary pressure-drop metering stations proved to be satisfactory for oxygen injection into the high-pressure system in calibration tests. However, a "snubber" must be used to prevent the sudden addition of pressure to the metering system. A waterproof microphone assembly demonstrated sufficient sensitivity to be used as a noise detector on reactor equipment.

4.3 Liquid-Level Indicators. — A float-type level alarm indicator utilizing a packless flexible shaft to actuate a microswitch will be installed on the holdup tank in the low-pressure system.

4.4 Valves and Operators. — HRT-type valves have performed satisfactorily in tests to date. The plug design on the blanket dump valve and the sampler inlet valves was modified to eliminate sticky action caused by the tendency of the plugs to wedge in the seats.

5. HRT Fuel Processing Plant

Insoluble corrosion and fission products are to be removed centrifugally from the reactor fuel with a hydroclone. The question of whether or not the small particulates continue in suspension in the reactor fuel will be inferred from the concentration of these materials achieved by the hydroclone. The sampling of a slurry is rarely representative, however, and dependable sampling requires that the slurry concentrate first be completely dissolved.

Accordingly, a dissolver and two decay storage tanks will be installed in the HRT-CP to replace the former carrier-evaporators. The slurry will be

transferred to the dissolver, the heavy water recovered by evaporation, and the solids dissolved in a light-water solution of 10.8 M sulfuric acid. After dissolution and sampling, the dissolver solution will be stored for decay, and the dissolver will be dried in preparation for receiving the next batch of heavy-water slurry from the hydroclone underflow receiver.

The construction of the HRT-CP, exclusive of changes incidental to the installation of the dissolving equipment, has been essentially completed, and preparations are under way for the engineering tests required before the chemical plant is to be placed in operation. A shakedown loop, to supply simulated fuel solution at temperature and pressure to the chemical processing plant, will enable the testing operations to be performed while the chemical plant is isolated from the reactor system.

Octagonal ring gaskets have demonstrated much greater sealing reliability and resistance to deformation in laboratory tests than the oval ring gaskets used heretofore, and octagonal gaskets have been recommended for the chemical processing service. Special tools for the remote removal of the hydroclone and retainer plug were tested from a scaffolding to mock up the conditions under which the tools will be used in the chemical processing plant. The heat-transfer coefficients of the hydroclone underflow pot have been determined, as has the operability of the slurry outlet freeze plug. The latter held against 2000 psi pressure, even while the underflow pot itself was at 300°C.

The HRT will be operated initially with a D_2O blanket. Later, the D_2O reflector will be replaced with a concentrated uranyl sulfate solution of natural or depleted uranium to demonstrate the production of plutonium. Processing equipment is being designed to remove continuously the plutonium and corrosion products from the blanket solution. The process is similar to that of the core processing plant and is based upon the centrifugal concentration of these insoluble materials by a hydroclone.

PART II. REACTOR DESIGN AND ANALYSIS

6. Homogeneous Research Reactor

A study to determine the feasibility of constructing a circulating-fuel, aqueous homogeneous research reactor was completed. It was concluded from the study that a reactor of this nature, capable of providing neutron fluxes in the order of 10^{15} neutron/cm^2·sec, is practical from both economic and

technological aspects. A by-product of such a reactor would be the production of 125,000 kw of electrical energy.

7. Reactor Analysis

Preliminary calculations were made concerning fuel costs for single-region, UO_2SO_4-D_2O power reactors in which the fuel was considered to be processed on a batch basis. Slightly enriched uranium was assumed for the initial fuel loadings, and the fuel feed was considered to be fully enriched. In these studies the cost of the fuel feed was taken as $17.10 per gram of U^{235}. For a 6-ft-dia reactor, the total fuel cost was 2.5 mills/kwhr for initial U^{238} concentrations of 100 to 400 g/liter for no poison or plutonium removal and for operating periods greater than ten years. There was no apparent advantage in processing the fuel at the end of the operating period.

Calculations concerning the effects of xenon transients upon homogeneous reactor behavior were made for the case of complete retention of xenon within the reactor system. Average flux levels up to 10^{15} neutrons/cm^2·sec were considered. The maximum rate of reactivity addition associated with xenon burnout was less than 10^{-3} Δk_e/sec, which does not constitute a dangerous rate. However, at an operating flux of 10^{15} the increase in fuel concentration or the decrease in temperature required to maintain criticality following partial or total shutdown is so large that provisions should be made for elimination of xenon by external means. At 10^{14} average flux it appears that xenon poisoning may be overridden by decreasing the reactor temperature.

Previous Oracle codes were changed to comply with recent changes in Oracle operation. The Oracle code for calculating heat generation in materials due to gamma-ray absorption was used to calculate gamma-ray heating in lead, iron, and aluminum samples placed near the Bulk Shielding Reactor. The calculated results checked experimental measurements in the BSF to within ±23% for these target metals.

PART III. ENGINEERING DEVELOPMENT

8. Development of Fuel-System Components

Samples of titanium and zirconium exposed to the high-pressure recombiner loop reacted in such a way as to preclude their use as structural materials in the loop; rebuilding of the loop with type 309 stainless steel or Incoloy is being considered.

Syracuse University has determined detonation and explosion limits of H_2-O_2-steam in a long tube.

The 20-cfm canned-rotor blower failed to achieve the required head-flow characteristics, and a new impeller is being fabricated.

Three 5-gpm ORNL pumps continued to operate well on water, except for one stator failure. The 4000-gpm Byron Jackson pump suffered considerable loss of Stellite during a UO_2SO_4 run.

In the high-pressure flange test it was found that careful fitting of ring gasket to groove would produce a joint that leaked at low rates during thermal cycling.

9. Development of Blanket-System Components

Thorium oxide slurries have been circulated, since October 1953, for about 25,000 hr in 100- and 200-gpm loops, at temperatures from 250 to 300°C and concentrations from 200 to 1200 g of thorium per kilogram of H_2O. In 95 out of 130 runs (or 88% of the operating time) there were no difficulties in circulating the slurries. In the remaining runs, soft plugs in the pressurizers and plugged bypass lines predominated. One run ended in the formation of a thick, extremely hard cake throughout the system; the conditions which led to the formation of this cake are not understood.

Recalculation of laminar flow data for a variety of thorium oxide slurries in which correction is made for end effects has shown that the slurries are not thixotropic.

The pressure drop for the thorium oxide slurries studied in turbulent flow may be calculated by means of the usual friction-factor—Reynolds-number plot, provided that the density is taken as that of the slurry and the viscosity as that of water. From this fact, a generalized Hedstrom-type plot extending into the turbulent range was prepared wherein turbulent-friction-factor lines are drawn with the ratio of the slurry coefficient of rigidity to the viscosity of water as the parameter.

Atmospheric-pressure heat-transfer data are being obtained for slurries having an appreciable yield stress; some results are compared with measurements on water in the same system. It is possible to obtain high heat-transfer coefficients for slurries having a significant yield stress, but only at velocities high enough to make the ratio of yield stress to shear stress at the wall small.

For nearly 2000 hr the 200A loop circulated, at 300°C, a slurry containing 1000 g of thorium per kilogram of H_2O and from 1500 to 2800 ppm sulfate. The sulfate concentration was raised to the upper figure to eliminate erratic pump operation. No caking or unusual accumulations of solids were found when the equipment was dismantled, and the material was washed easily from the system. Considerable wear occurred on some pump components, such as the seal rings, portions of the casing liner (where high turbulence was encountered), and the front Graphitar radial bearing, which appears to have been eroded by oxidation rather than abrasion.

The development of types of dump tanks suitable for use with slurries has resulted in two feasible tank systems, one horizontal and the other vertical. Small-scale models of these were operated successfully for more than a thousand hours without caking or difficulties in moving the thorium oxide.

The slurry blanket test system has had three shakedowns on water and has undergone several alterations. Major changes include installation of a high-pressure condenser and flow-control system to supply purge water for the circulating pump and replacement of the pulsafeeder pump with an "acid egg" type of high-pressure feed system. Operation during the latest shakedown has been good, and the system is ready to operate on slurry.

10. Instrument and Valve Development

An experimental heated-thermocouple-type liquid-level indicator suitable for use at 2000 psi and 335°C was fabricated.

Six bellows suitable for sealing a $\frac{3}{4}$-in.-dia shaft had an average life of 43,000 cycles for a $\frac{1}{8}$-in. stroke in uranyl sulfate at 2000 psi and 300°C. Two titanium-alloy trim sets have suffered sudden drastic failures in dump-valve service on the valve test loop. Heliarc hard-facing of type 347 stainless steel with Stellite 6 appears to be superior to torch application for valve-trim service.

PART IV. CORROSION AND MATERIALS

11. Solution Corrosion

A mockup of the expansion joint and Zircaloy–stainless steel transition joint as used in the HRT reactor vessel was installed in a test loop for evaluation of corrosion and joint integrity.

Aluminum oxide bearings are being tested in the model 100A Westinghouse pumps. Preliminary results are encouraging.

Long-term tests with solutions containing 0.04 m UO_2SO_4, 0.005 m $CuSO_4$, and 0.015 m H_2SO_4 were completed at 200, 250, and 300°C. The results show low corrosion rates for stainless steel below about 40 fps except at 200°C, where corrosion

rates were high at flow rates as low as 34 fps. However, both uranium and copper were slowly lost from solution at 250 and 300°C.

A run made in the 4000-gpm loop at 250°C with a solution composed of 0.04 m UO_2SO_4, 0.005 m $CuSO_4$, and 0.02 m H_2SO_4 showed that the system was stable with even very low oxygen concentrations. The system was operated for 225 hr with 25 ppm oxygen and for 100 hr with approximately 3 ppm oxygen, with no evidence of accelerated corrosion or uranium precipitation.

Further corrosion testing with uranyl fluoride indicated that stainless steel is attacked to a lesser extent in uranyl fluoride than in uranyl sulfate solutions. The reverse is true with titanium, particularly in crevices, where the attack rate can be high in fluoride systems. Both titanium and stainless steel show adequate corrosion resistance in the gas phase above fluoride solutions, but zirconium is completely destroyed both in the gaseous and the liquid phase.

The addition of Cr(VI) ions to uranyl sulfate solutions was investigated further. It was shown that even very low concentrations of Cr(VI) increased the film-free corrosion rate of stainless steel in a very pronounced way. At low velocities the amount of metal that dissolved during the period of film formation decreased as the Cr(VI) concentration increased.

Quartz-tube investigations indicated that solutions containing equimolar concentrations of beryllium sulfate and uranyl sulfate are stable over quite wide temperature and concentration ranges. It was also shown that beryllium sulfate solutions will dissolve appreciable quantities of uranium trioxide and remain stable at high temperatures. No corrosion tests have been completed with beryllium-containing solutions.

A laboratory-scale corrosion study demonstrated the susceptibility of stainless steel to stress-corrosion cracking in boiling simulated HRT fuel solution (0.04 m UO_2SO_4, 0.005 m $CuSO_4$, and 0.02 m H_2SO_4) containing chloride ions. During a 500-hr test period stressed specimens showed cracking at chloride concentrations of 25 and 50 ppm; no cracks were apparent at the 5, 10, and 100 ppm levels. At the two lower chloride concentrations no accelerations of corrosion was noted. At all other concentrations generalized corrosion was appreciable, being the highest at the 100-ppm level. Preliminary tests with the simulated HRT

solution containing 100 ppm bromide or iodide revealed no cracking of the specimens.

One phase of a test program to examine the corrosion-fatigue behavior of type 347 stainless steel bellows in uranyl sulfate solutions at elevated temperatures was completed. The results indicate that the life of the bellows is not greatly shortened when a uranyl sulfate solution is used as the corrodent instead of distilled water.

12. Slurry Corrosion

12.1 Pump Loops. — Dynamic-corrosion data are presented for two slurry runs made in 100A pump loop CS. One test was terminated after 49 hr of 300°C operation at an average concentration of 534 g of thorium per kilogram of water, because of plugging in the loop pressurizer. The second test was terminated, as scheduled, after 300 hr of operation at an average circulating concentration of 426 g of thorium per kg of water. In this test, thoria was charged to the system in five batch additions while the loop was operating at 300°C and 1500 psi pressure.

Water runs and an attempted slurry run on the experimental in-pile slurry loop are described.

12.2 Toroids. — Studies of thorium oxide slurries circulated in toroids indicated some correlation between particle size and attack rate on stainless steel. The preparation and behavior of sized fractions of thorium oxide calcined at 1200, 1400, and 1600°C are described. Generally, less attack on type 347 stainless steel and titanium was observed with an original particle size below 1 μ; no effect of calcination temperature was evident. The effect of time of calcination at 1400°C, ranging from 2 to 96 hr, is discussed. Additions of sodium phosphate or pyrophosphate, at pH values from 7 to 11, caused severe attack of titanium by circulating thorium oxide slurries.

13. Radiation Corrosion

13.1 In-Pile Loops. — The fabrication and the operational testing of the all-titanium in-pile loop L-2-14 were completed, and the loop is now ready for installation in beam hole HB-2 of the LITR.

Two of the Byron Jackson in-pile circulating pumps have been received. Ten of these pumps are on order as replacement units for the ORNL pump now in use. The in-pile loop package design has been modified to allow use of the Byron Jackson pump pending satisfactory pump test results.

Metallographic examination of type 347 stainless steel components from loop EE indicates that there was some attack of the loop pressurizer above the liquid level and of the core cap. Zircaloy-2 and stainless steel coupons and stress specimens showed evidence of attack, but titanium appeared to be unaffected.

The sixth in-pile loop experiment, L-4-11, was completed. The loop operated in-pile for a total of 1109 hr, during which time the LITR energy output was 2175 Mwhr. The main-stream operating temperature was 250°C. During this run the loop was drained and then recharged with fresh solution. Based on oxygen data the generalized corrosion rate for the first 300 hr was about 4.1 mpy; the rate for the remainder of the run was about 2.0 mpy. The nickel data gave parallel results. The corrosion specimens consisted of a large variety of zirconium alloys, titanium alloys, and stainless steel. Specimens of synthetic sapphire, sintered alumina, platinum, and Incoloy were also included. Corrosion rates of most of the zirconium alloys, titanium alloys, and stainless steels were generally consistent with rates observed in the previous in-pile loops.

The zirconium alloys Zr-3 (3% Ag), Zr-3 (0.52% Sn, 5.71% Ti, 40 ppm N_2), Zr-3 (0.52% Sn, 0.28% Fe, 5.66% Ti, 60 ppm N_2), Zr-3 (1.4% Fe), and Zr-3 (0.7% Fe, 2.8% Cr) corroded at rates about two to three times those observed for Zircaloy-2 at the same power density. The zirconium alloy containing 3.84% Al and 2.5% Mn corroded at rates about 10 to 20 times those for Zircaloy-2.

The zirconium alloy containing 2% niobium corroded at the same rate as Zircaloy-2 in the core but at a much higher rate, 17 mpy, in the in-line position. However, a zirconium alloy containing 15% niobium corroded at less than one-third the Zircaloy-2 corrosion rates in the core and exhibited rates similar to Zircaloy-2 in the in-line position.

Corrosion rates for Incoloy were found to be about the same as those for stainless steel exposed to similar conditions.

All sintered aluminum oxide specimens in the main stream disintegrated; however, the aluminum oxide bearings in the low temperature region of the pump showed no measurable wear. Synthetic sapphire became cloudy and corroded at a rate of 12 mpy. Platinum was slightly affected in the core.

Exposure of in-pile loop experiment L-4-12 in the LITR has been completed. This loop had a tita-nium core and titanium coupon holders. There was not the initial period of high corrosion rate observed in previous experiments with stainless steel cores. The over-all corrosion rate as calculated from oxygen data was 1.1 mpy.

In-pile loop experiment L-2-10 is now inserted in the new loop facility in the HB-2 hole at the LITR. The main-stream operating temperature is 280°C, and the uranyl sulfate concentration is 0.04 m.

13.2 In-Pile Autoclave Tests. — Inspection of the data obtained in the various Zircaloy-2 corrosion experiments in the LITR has provided evidence that the rate of radiation-induced corrosion of Zircaloy-2 by uranyl sulfate solution is not directly proportional to the intensity of reactor radiations prevailing in the experiment. Data presently available from both loop and rocking-autoclave experiments can be expressed by equations of the form

$$CR = K(PD)^{2/3} ,$$

where CR is the corrosion rate (mpy) based on radiation time, PD is the fission power density (w/ml) which prevailed in solution during exposure, and K is a constant, the value of which depends upon exposure temperature and solution composition. A plot of the data is presented.

One titanium experiment was operated in HB-6 of the LITR, and three Zircaloy-2 experiments were operated in HB-5. The titanium experiment was performed in an attempt to evaluate the effects of power density and temperature on the radiation-induced corrosion. The results are inconclusive. The objectives of the Zircaloy-2 experiments were to determine, respectively, the effects on radiation corrosion of Cr(VI) in solution, addition of H_2MoO_4, and substitution of D_2O for H_2O. The results of these Zircaloy-2 experiments are incomplete, and only preliminary data are presented.

Data from earlier experiments which have become available since the last report are included in a table.

An all-stainless-steel system was operated in HB-3 of the MTR for 26 hr in the retracted position and for 14 hr in the inserted position. It was necessary to terminate the experiment before conclusive results could be obtained.

14. Metallurgy

Crystal-bar zirconium and Zircaloy-2 specimens were hydrided at 600 to 1000°C and quenched in mercury in the hydrogenation equipment. Specimens

examined so far indicate that at least 130 ppm H_2 can be dissolved in crystal-bar zirconium and retained on quenching from 600°C. Quenched specimens containing visible hydrides were submitted to x-ray diffraction examination and showed only the equilibrium hydride, $ZrH_{1.75}$.

Specimens of Zircaloy-2 core-tank material were held for one week at 840, 860, and 880°C and quenched. They showed no change in structure from the short-time specimens previously reported and confirmed the alpha/alpha-plus-beta temperature for Zircaloy-2 as 810°C. Zircaloy-2 specimens quenched from 1000°C, cold-rolled 20%, and annealed at 800°C showed a lessening (randomization) of the preferred-orientation texture over that of the starting material. A Zircaloy-2 weldment was examined extensively metallographically.

Examination of heat-treated specimens of several zirconium-base alloys containing Nb, Mo, Ta, Fe, and Pd as binary and ternary alloys showed that the beta structure can be fully retained on quenching a 5% Pd alloy from 800°C or higher. Two phases are present in the 10% Pd alloys held at 800°C and above, and neither phase is alpha zirconium. The addition of 2% Pd to a 15% Nb alloy does not eliminate the precipitation of alpha zirconium on quenching from 700°C and above. A 10% Mo alloy showed a second phase, not identified, on quenching from 800°C and above. The full decomposition of retained beta to a eutectoid structure occurred in less than 1 hr at 600 and 700°C in the palladium alloys.

Zirconium- and titanium-alloy specimens were corroded in a recombiner loop. Hydrogen analyses of the specimens revealed that Ti–6% Al–4% V, A-55 Ti, and Zircaloy-2 alloys picked up small amounts of hydrogen but that crystal-bar titanium and crystal-bar zirconium specimens, respectively, picked up 1200 and 1600 ppm H_2. The high-purity materials showed evidence of extensive recrystallization and grain growth in the process of hydrogen absorption at temperatures far below normal recrystallization temperatures.

Aging times up to 1500 hr at temperatures up to 450°C do not appear to have any appreciable effect on the impact strength of Zircaloy-2 as-received core-tank material.

Work was resumed in an effort to obtain a zirconium oxide corrosion film free of monoclinic phase in order to test the effect on corrosion resistance. Work in the present investigation has been con-centrated on making additions or changes to the zirconium-niobium system, which was shown in the previous study to be the most effective. Several oxide additions, as well as an increase in oxidation temperature, were shown to increase the amount of the orthorhombic phase. Alloys fabricated from sponge zirconium produced more orthorhombic phase than those fabricated from iodide zirconium.

A weld-joint design was developed for welding titanium pipe by which a flat preplaced insert may be used and a weld obtained with a quality and hardness equivalent to those of a weld made by the filler-wire method.

If welded 6% Al–4% V titanium alloy structures are to be used in reactor or other critical fabrication, a postweld heat treatment will be necessary to assure adequate bend properties.

PART V. CHEMICAL ENGINEERING DEVELOPMENT

15. Fuel Processing

Reactor solids may be dissolved in 10.8 M H_2SO_4 by treating 1 g of solids with 3 to 5 ml of acid at 165 to 170°C for 6 hr and then diluting to 1 to 2 M acidity. The solids must be well agitated during the process.

In 0.02 m UO_2SO_4–0.005 m H_2SO_4 solutions, gamma radiation displaces the free-iodine–ionic-iodine equilibrium. At 250°C the displacement favors the elemental form, but at 100°C it favors the ionic form. The vapor/liquid equilibrium mole ratio of free iodine in 0.02 m UO_2SO_4–0.005 m H_2SO_4 at 100°C was 0.37; in the presence of simulated mixed fission and corrosion products, it was 2.4; and for water at pH 4.5, it was 0.013. In the same solutions the ratio of free to combined iodine was 25/1, 1/1, and 10/1, respectively. Platinized alundum at 350 to 400°C absorbed iodine at low partial pressures from a gas stream of oxygen and water vapor.

Experiments in the Y-12 HRT mockup loop verified the chemical data obtained in loops and laboratory studies and confirmed the expectation that various portions of a large system such as the mockup would compete with the hydroclone in accumulating solids.

The results of loop tests indicated that placing the hydroclone upstream from the heater instead of downstream had no appreciable effect on the distribution of precipitated $Nd_2(SO_4)_3$ between the heater and hydroclone underflow pot. There was a marked

tendency for zirconium oxide which was precipitated in a loop by hydrolysis to plate out on all surfaces of the loop regardless of temperature or fluid velocity.

16. Plutonium-Producer Blanket Processing

When plutonium precipitation does not occur, plutonium adsorption on titanium and Zircaloy-2 surfaces at 250°C from 1.4 m UO_2SO_4 apparently reaches a maximum, or equilibrium, value. With solutions containing 4 mg of plutonium per kilogram of H_2O, the approximate maximum adsorption values are 0.3 $\mu g/cm^2$ on titanium and 3.5 $\mu g/cm^2$ on Zircaloy-2. In an actual reactor system this adsorption will probably be insignificant compared with the amount of precipitated PuO_2 adhering to the walls.

When 1.4 m UO_2SO_4 containing less than 25 mg of plutonium per kilogram of H_2O was heated at 250°C in pyrex under 200 psi H_2 and 100 psi O_2, PuO_2 did not always precipitate. In many cases precipitation occurred, but considerably more than 3 mg of plutonium per kilogram of H_2O remained in solution and in some cases precipitation was complete, leaving in solution from 0.5 to 3 mg of plutonium per kilogram of H_2O. With initial plutonium concentrations of 30 to 50 mg per kilogram of H_2O, some PuO_2 was always formed at 250°C, but often more than 3 mg of plutonium per kilogram of H_2O remained in solution. With initial plutonium concentrations greater than 100 mg per kilogram of H_2O, precipitation at 250°C was essentially complete, leaving in solution about 3 mg of plutonium per kilogram of H_2O. Iron added to these solutions hydrolyzed and precipitated but had no significant effect on the amount of plutonium remaining in solution.

Simulated HRT blanket solids containing 70% Fe_2O_3, 18% Cr_2O_3, 9.8% NiO, 1.2% ZrO_2, and 1.0% UO_3 were completely dissolved in anhydrous H_3PO_3 or H_3PO_4 at 230°C and were partially dissolved in 0.4 M $CrSO_4$–1.0 M H_2SO_4 at 80°C.

17. Thorium Oxide Slurry Development

The absence of a gross radiation-damage effect on thorium oxide slurry behavior was indicated by three irradiation experiments carried out at 300°C in the LITR with thorium oxide slurries containing enriched uranium. At a thorium concentration of 750 g per kilogram of H_2O and at radiation power densities approximately equal to the average power density of a TBR blanket, the slurries were stirred under irradiation for 168, 92, and 192 hr, with no apparent change in slurry viscosity.

Out-of-pile studies on the catalytic combination of hydrogen and oxygen in thorium oxide slurries containing MoO_3 catalyst (0.025 to 0.2 m) were continued. A slurry of thorium-uranium mixed oxides (1000 g of thorium per kilogram of H_2O, 0.5 mole % uranium) containing 0.025 m MoO_3, which had been activated by heating at 280°C with a hydrogen overpressure, gave a combination rate more than sufficient to maintain a slurry blanket at less than 2000 psi total pressure under expected TBR conditions. Maximum catalytic activity was observed for the MoO_3 catalyst at 0.05 m concentration, both in the slurry as prepared and after treatment with hydrogen.

The ratio of specific surface area, as measured by nitrogen adsorption, to the theoretically available surface area has been used to correlate the data on thorium oxide prepared by various methods and is indicative of the nature of crystallite packing in the thoria particles. The crystallites in the hydrothermally prepared oxides are apparently discrete particles in random orientation.

No crystallite growth was observed in a typical thorium oxide which was heated as an aqueous suspension at 300°C for 1766 hr. Lack of crystallite growth probably indicates an extremely low solubility of thorium oxide in water at 300°C.

Thorium oxide and mixed thorium-uranium oxide suitable for use in the preparation of aqueous suspensions were prepared by hydrothermal decomposition at 300°C of the nitrate solutions. These oxides are characterized by a small average crystallite size which does not grow on firing to 900°C.

The settling characteristics of pumped slurries were markedly changed by the presence of sulfate. The settling-rate–temperature-dependence curves for slurries containing sulfate were steeper and more irregular than those for slurries of the pure oxides or than would be predicted from the decrease in water viscosity with temperature. With 500 to 1000 ppm of sulfate and 5000 ppm of sulfate, changes occurred in the slurry flocculation characteristics at slurry temperatures of 100 to 300°C, as indicated by pronounced increases in the settling rates.

The preparation of thoria sols was continued. Nineteen sols containing nine different inorganic

stabilizers – NO_3, Cr_2O_3, CrO_3, Fe_2O_3, MoO_3, La_2O_3, Bi_2O_3, PdO, Y_2O_3 – were prepared; all were stable at 100°C but were decomposed by heating at 300°C. Nitrate ion, contained in all the sols, may have obscured the effect of the additive.

18. Equipment Decontamination

A short length of type 347 stainless steel pipe from an in-pile loop that had been used for circulating uranyl sulfate fuel at 250°C was decontaminated from 30 r/hr to 200 mr/hr by a 2-hr contact with 0.4 M $CrSO_4$–0.5 M H_2SO_4 at 85°C. The activity remaining was 99% ruthenium, which apparently replated from the chromous sulfate solution. Contacting the metal with alkaline-tartrate-peroxide solution at room temperature for 4 hr further reduced the activity to about 6 mr/hr. A solution containing 2% H_3PO_3 and 2% NaH_2PO_2 at 150°C completely removed the oxide film from similar specimens in 20 to 30 hr. However, the fission products replated. The phosphorous acid–hypophosphite solution did not dissolve ZrO_2 or PuO_2.

Thorium daughters that had been deposited on type 347 stainless steel from ThO_2 slurries at 250 to 300°C were reduced from 10^6 to 50 alpha counts/min/in.^{2} by contacting with 0.4 M $CrSO_4$–0.5 M H_2SO_4 at 80°C and then with alkaline-tartrate-peroxide solution at 23°C.

PART VI. SUPPORTING CHEMICAL RESEARCH

19. Aqueous Systems at Elevated Temperatures

Efforts were made to prepare a sol having an average crystallite size smaller than that of the sols studied previously; these efforts failed, however, apparently because of particle growth after the preparation of the hydrous ThO_2 precipitate. The use of the spectrophotometer to measure light transmission offers promise as a fast, easy method for estimating particle size.

Studies of the settling rates of ThO_2 slurried in a 53.5% $Ca(NO_3)_2$ solution and in water disclosed a large inhibition of settling by the dissolved salt, especially in the early unhindered part of the settling process. The effect is too great to be explained on the basis of a simple dependence on viscosity and density.

20. Radiation Studies of Thorium Nitrate Solutions

The in-pile irradiation of a solution consisting of 7 m $Th(NO_3)_4 \cdot Be(NO_3)_2$ and 0.05 m highly enriched $UO_2(NO_3)_2$ showed that the radiation decomposition of nitrate to yield N_2 is temperature-independent and that any back reaction involving N_2 is negligible up to 300°C. The G_{N_2} yield for the 49.3 wt % NO_3^- solution was found to be 0.16 molecule per 100 ev.

21. HRP Analytical Chemistry

A method was developed for the differential titration of acid in solutions of uranyl sulfate; interference studies and an evaluation of the precision were made with respect to an amperometric titration method for mercury; and an improvement was made in an internal electrolysis method for the determination of copper in solutions of uranyl sulfate.

In addition, improved methods were developed for the determination of fluoride, aluminum, and halides in thorium oxide. Reaction rates were determined for the conversion of pyrophosphate to orthophosphate in slurries of thorium oxide; the effect of graphite in the slurries of thorium oxide on the determination of sulfate was evaluated; and comparative studies were made of sedimentation methods for the determination of the particle-size distribution of ThO_2. Techniques for use with materials composed of extremely small particles (<2 μ diameter) are under study.

Satisfactory radiochemical procedures for Cs, Cu, Nb, P, and S in HRT samples have been developed.

A polarographic method for the determination of fission-product tellurium in HRT fuel solution is being studied, and two chelating agents are being studied for possible use in the spectrophotometric determination of uranium.

Installation of spectrographic equipment in the High-Radiation-Level Analytical Facility was completed, and testing is in progress. Separation and estimation procedures for the rare earths, zirconium, and niobium from thorium and uranium matrices such as the blanket or fuel of the HRT are being developed. An improved technique for operating an air-interrupted spark source was shown to give better day-to-day precision in quantitative spectrochemical analyses.

22. Isolation of Protactinium-231

Personnel at Mound Laboratory have concentrated approximately 1 g of Pa^{231} during the past two years from the residue that appeared in the aqueous raffinate from the diethyl ether extraction step of the uranium processing scheme used at the uranium refinery plant operated by the Mallinckrodt Chemical Works. A total of 19,360 lb of raffinate residue was processed to yield 130 gal of carrier.

The Pa^{231} in the carrier precipitate was concentrated by four solvent-extraction cycles. The protactinium from the fourth solvent-extraction cycle was stored in 500 ml of a solution of approximately 2.5 M H_2SO_4 and 7 M HCl; it is estimated that the 500 ml contains about 700 mg of protactinium. The protactinium concentrations and losses are summarized.

CONTENTS

PART II. REACTOR DESIGN AND ANALYSIS

PART III. ENGINEERING DEVELOPMENT

PART IV. CORROSION AND MATERIALS

PART V. CHEMICAL ENGINEERING DEVELOPMENT

Part I

HOMOGENEOUS REACTOR TEST

S. E. Beall

1. HRT OPERATIONS

S. E. Beall

R. E. Brooksbank
W. D. Burch
C. C. Cardwell[1]
J. S. Culver
N. W. Curtis[2]
J. R. Engel
K. E. Estes
J. D. Flynn

D. F. Frech
T. H. Gladney
J. L. Gory
B. H. Hamling[3]
P. N. Haubenreich
J. W. Hill, Jr.
D. M. Johnson[4]

R. W. Jurgensen[5]
S. I. Kaplan
J. O. Kolb
J. D. Perret, Jr.
G. W. Rivenbark
H. K. Search[2]
R. Van Winkle
H. E. Williamson

1.1 REACTOR OPERATIONS

The past quarter was devoted to the program of engineering tests, which began with the flushing of process lines early in May.

1.1.1 Component Testing

The experiments enumerated below were conducted on a three-shift basis and were made in preparation for operation with unenriched uranyl sulfate solution.

1. The load cells which indicate the quantities of liquids in the dump tanks and condensate tanks were calibrated.

2. Pressure drop as a function of oxygen flow through the charcoal adsorber beds was measured. This pressure drop determines the operating pressure of the reactor low-pressure system for various oxygen inputs.

3. Steam-system components were tested for adequacy of performance:

(a) The pressure relief valve on the feedwater pumps was too small; so it was replaced.

(b) The turbine hot-well condensate pump and condensate level controller operated satisfactorily. It was determined that 130 kw of electricity can be generated with building steam; the output is limited by the building steam supply. The building electrical load was picked up and carried by the turbine-generator from a cold start with no outside power other than the steam supplied to the 7500 area from the X-10 steam plant.

(c) The package boiler for reactor warmup was tested and, after some initial difficulties, was found to produce 1750 lb of steam per hour at 1500 psig as guaranteed.[6]

(d) The air-cooled condenser was operated at about 50% of the heat load it is expected to carry when the reactor operates at 5 Mw; although its performance seems to be satisfactory, the full 10-Mw heat load cannot be applied until the reactor is in operation.

(e) The performance of the deaerator has not been proved. Although attempts were made to test it by using the limited condensate load that could be applied from the turbine condenser and the air-cooled condenser, an adequate check must await reactor operation.

4. The cooling-water system was tested, including the cooling tower[7] and the branch circuits which distribute water to various reactor components.[8]

5. The refrigeration system which supplies coolant to cold traps and freeze plugs was partly tested. Although much time was spent, several errors and minor mechanical difficulties with solenoids, check valves, rupture disks, and electrical program timers prevented a satisfactory test of the complete system.

6. The leak-detector system failed to operate in a satisfactory manner because of several shortcomings in the high-pressure needle valves: surface finish on stems and tolerances on retaining washers were poor, resulting in the extrusion of plastic from the stem packing gland onto the seating area, and general quality control on tolerances

[1]On loan from Babcock & Wilcox Co.

[2]On loan from Pennsylvania Power and Light Co.

[3]On loan from Union Carbide Nuclear Co., New York Office.

[4]On loan from The Glenn L. Martin Co.

[5]On loan from American Gas and Electric Co.

[6]J. L. Gory, *Results of Package Boiler Test, HRT Test No. V 4a*, ORNL CF-56-6-165 (June 28, 1956).

[7]R. E. Brooksbank, *HRT Cooling Tower Performance Test Evaluation*, ORNL CF-56-6-171 (June 28, 1956).

[8]R. E. Brooksbank, *HRT Cooling Water System Evaluation, Results of HRT Engineering Tests VI A-2, 3, 4, 5; B-1 a,b, and B-3*, ORNL CF-56-4-194 (April 30, 1956).

and materials appeared to be poor. New bellows-sealed, soft-seated valves manufactured by Hoke, Inc., were ordered to replace all the original valves.

7. The entire reactor system was subjected to a hydrostatic test.[9] The low-pressure system was pressurized to 750 psig and the high-pressure system to 3000 psig. The only leak found during the test was traced to a valve-bellows seal weld in the valve bonnet.

8. The entire reactor system was cleaned with 3% trisodium phosphate solution[10] at 100°C for 3 hr and then rinsed with water.

9. Following the TSP treatment the process-piping system was treated with nitric acid to complete the cleaning and to determine whether any off-specification materials had been used accidentally in construction. The system was exposed to a 5% solution of nitric acid at 85°C for 49 hr. Solution samples were withdrawn periodically from various points and analyzed both chemically and spectrographically. No significant buildup of metallic ions from foreign materials was observed in treating the reactor system.

10. Preliminary tests on the fuel recombiner had indicated[11] incomplete recombination of hydrogen and oxygen at catalyst bed temperatures below 200°C. Such low catalyst temperatures result at hydrogen flows of less than 2 scfm with normal steam-dilution flow rates of about 8 lb/min. Tests were run with the blanket recombiner at hydrogen flow rates of between 0.2 and 2.0 scfm to evaluate recombination at steam dilution rates of only 2 lb/min. Gas samples obtained during these tests indicated complete recombination; the catalyst bed temperature was about 165°C at 0.2 scfm and increased linearly up to about 290°C at 2 scfm.

11. The performance of the blanket entrainment separator was measured by analyzing samples of condensate from the condenser while potassium sulfate solution was being boiled in the dump tank. The decontamination factor, defined as the ratio of the concentration of potassium in the dump tank to that in the condensate, was observed to be 1000 to 2000 in one set of tests which agreed with earlier results[12,13] when sodium was used as a tracer. The earlier data had been questioned because of the possibility that sodium from other sources had contaminated the condensate samples. A second set of tests on the blanket entrainment separator was performed with a higher concentration of potassium, greater sampling frequency, and greater care to prevent sample contamination. In the later test all samples indicated decontamination factors greater than 150,000. Decontamination factors of about 80,000 will be required to produce condensate containing less than 5 ppm uranium when D_2O is being boiled from a 350-g/liter blanket solution of uranyl sulfate. Further entrainment tests will be conducted when the fuel system is operated with uranyl sulfate solutions.

12. Flows were determined in the fuel and blanket high-pressure circulating systems by measuring pressure drops across the heat exchangers and referring to the calibration curves of pressure vs flow.[14] At 25°C the blanket flow rate was 208 gpm and the fuel flow rate was 385 gpm. These flow rates are lower than the design rates because of additional pressure drop resulting from special strainers which were installed to remove particulate matter during the system cleanup. When the strainers were removed, it was found that the blanket strainer had collected about a teaspoonful of brown fibrous material (like tobacco) and that the fuel strainer contained a few small particles (mass estimated to be a few milligrams) and one small metal chip.

13. Flow rates and heels remaining were measured for the following transfers (steam pressure was used to accomplish the transfers):

(a) fuel dump tank to fuel storage tank, where the flow rate was 28 lb/min at about 20 psig driving pressure and the heels remaining weighed 16 and 26 lb;

(b) fuel storage tank to fuel dump tank, where the flow rates were 25 and 37 lb/min, respectively,

[9]H. E. Williamson, *Procedure for Initial Hydrostatic Test on HRT Fuel and Blanket Systems*, ORNL CF-56-4-167 (April 20, 1956).

[10]J. R. Engel, *Treatment of the Reactor System with 3% Trisodium Phosphate Solution*, ORNL CF-56-7-67 (July 17, 1956).

[11]Unreported data taken in October 1955.

[12]P. H. Harley, *Performance Tests of HRT Fuel Solution Evaporator and Entrainment Separator*, ORNL CF-54-10-51 (Oct. 13, 1954).

[13]P. N. Haubenreich and R. Van Winkle, *Efficiency of Fuel System Entrainment Separator During Normal Operation*, HRT Report II A(7c)b, ORNL CF-56-5-167 (May 25, 1956).

[14]J. R. Engel, *Pressure Drop Calibration of Fuel Heat Exchanger*, HRT Report No. 1 A(4)a, ORNL CF-56-3-14 (March 6, 1956).

at 5 and 37 psig driving pressures and the heels remaining weighed 22.5 and 39 lb;

(c) blanket dump tank to blanket storage tank, where the flow rate was 33 lb/min at 39 psig driving pressure and the heel remaining weighed 24 lb;

(d) blanket storage tank to blanket dump tank, where the flow rates were 19 and 40 lb/min, respectively, at 15 and 37 psig driving pressures and the heels remaining weighed 1.5 and 35 lb;

(e) blanket dump tank to fuel dump tank, where the transfer was performed by using 30 psig N_2 pressure, and the flow rate was 54 lb/min. (It is believed that flashing of the saturated liquid flowing in the transfer lines, when steam is used for pressurization, results in the lower flow rates.)

14. The fuel and blanket reflux condensers were tested for performance, and the results were reported.[15,16] The fuel reflux condenser removed 176 kw of heat when 20 gpm of 77°F cooling water was used; this almost duplicates the design value of 170 kw with 21.5 gpm of 100°F cooling water.[17] This is the estimated heat release from the fuel solution 15 min after shutdown following 10-Mw operation for a long time.

The blanket reflux condenser, although of identical design, removed only 148 kw of heat at atmospheric pressure when 21 gpm of 83°F cooling water was used. It is likely that the presence of non-condensables caused the poorer performance of the blanket reflux condenser.

15. Fuel and blanket feed coolers and the fuel purge-water coolers were tested and were found to meet design specifications.

In addition to the reports referred to above, other HRT engineering tests have been reported in the following memoranda:

HRT Test No.	Title	ORNL CF No.
I-A, 4e	Fuel Heat Exchanger Heat Loss and Insulation Performance	56-3-13

[15]P. N. Haubenreich, *Rate of Heat Removal from Fuel Reflux Condenser*, HRT Report II A 15b, ORNL CF-56-6-80 (June 13, 1956).

[16]P. N. Haubenreich and H. E. Williamson, *Rate of Heat Removal from Blanket Reflux Condenser*, HRT Report IV A, 39b, ORNL CF-56-6-137 (June 21, 1956).

[17]C. L. Segaser, *Bayonet Tube Reflux Condenser for the HRT Outer Dump Tanks*, ORNL CF-55-1-49 (Jan. 4, 1955).

HRT Test No.	Title	ORNL CF No.
I-B, 5a	Fuel High-Pressure System Volume Calibration	56-7-116
II-A, (7a,b)a	Fuel Dump Tank Evaporation Rate	55-12-25
II-A, (7a,b)e	Fuel Dump Tank Volume Calibration	55-12-23
II-A, (14)c	Fuel Condensate Tank Volume Calibration	55-12-24
II-B, 1b	Head Losses in Lines Between Condenser and Condensate Tank	55-12-38
II-B, 8a	Fuel Dump Tank Heat Loss and Insulation Performance	55-12-115
III-B, 5a	Blanket High-Pressure System Volume Calibration	56-7-117
IV-A, (34a,b)a	Blanket Dump Tank Evaporation Rate	55-12-37
IV-B, 8a	Blanket Dump Tank Heat Loss and Insulation Performance	55-12-114
V-A, 2a,b,c	Turbine Condenser Performance	56-7-27

1.1.2 Remote Maintenance Practice

On July 16 experimental work was discontinued for a two-week period for maintenance and revisions. This period was also used for practice in the use of tools constructed for the remote replacement of various reactor parts, should they fail after the reactor is operated at power.

Twelve different remote-maintenance jobs were practiced, with varying degrees of success. All the jobs (described below) were accomplished by personnel standing on top of the cell and working with long-handled tools. This phase of the program was done with the cell dry. The times reported here do not include opening or flooding the shield.

Both fuel feed-pump heads were removed and reinstalled easily by means of remote handling tools in less than 8 hr.

The blanket circulating pump was removed and reinstalled by means of extended-handle tools to break and remake the flanged joints in the $3\frac{1}{2}$-in.

5

high-pressure lines. There was some interference with the high-torque hydraulic wrench, but simple modifications eliminated the obstructions. Television was employed with considerable success; waterproof equipment will be required when the system is flooded. All the tools required for the main flanged joints performed satisfactorily. However, the making and breaking of the joints in the cooling-water lines to the pump were not done remotely, because those lines had not been anchored properly. Although 14 to 16 hr was required to remove and replace the pump, it is believed that less time will be required on future replacements.

Two high-pressure valves were removed and reinstalled remotely with no difficulty. Five low-pressure valves which had been previously removed by hand were reinstalled by use of remote handling tools. Valve removal and reinstallation appear to be an easy operation, requiring approximately 2 hr per valve.

The fuel-pressurizer purge pump was removed remotely, but it has not yet been reinstalled because certain handling tools do not perform satisfactorily.

The removal procedure for the blanket recombiner was only fairly successful because of several interferences and lack of proper tools. Portions of this procedure must be repeated at a later time.

A core-tank thickness measurement was made to gain experience with the ultrasonic measuring equipment which will be used after the reactor has operated for a period of time. J. K. White of the Metallurgy Division obtained a reading of 0.3163 ± 0.0002 in., which agrees with an earlier measurement to within 0.0005 in. It will be possible to determine whether significant corrosion has occurred by comparison of future measurements with this reference thickness.

The removable floodgate, which separates the reactor tank into two cells of approximately equal volume, was difficult to install. The guide rails must be repositioned to permit the gate to slide easily into place.

All except one of the eight pressurizer electric heaters were removed in a total of approximately 8 hr. The removal of the other heater cannot be accomplished until an interfering pipe is moved.

No additional remote handling work is scheduled until the natural-uranium run is finished.

1.2 OPERATIONS ANALYSES

P. N. Haubenreich

1.2.1 Reactor Operation at Reduced Pressure and Temperature

A study was made of the gas-recombination problems involved in operating the HRT initially at reduced temperature and pressure. The maximum rate at which the low-pressure system is capable of recombining gas is equivalent to the gas production at about 2 Mw without internal recombination. Thus, for operation at powers above 2 Mw, it has been intended that part of the gas be recombined internally. Because the effectiveness of the internal copper catalyst is strongly temperature-dependent, the copper concentration required for full-power operation at an average core temperature of 250°C and any pressure below 2000 psia is several times that required at an average core temperature of 280°C and a pressure of 2000 psia.

If the reactor is operated initially at 250°C and later at 280°C, any one of the following plans could be used:

(a) Put in only the copper required for high-temperature operation and limit the power during 250°C operation to 2.5 to 3.0 Mw.

(b) Put in sufficient copper for full power at 250°C. Leave the copper in the reactor and have complete internal recombination in subsequent high-temperature operation.

(c) Put in sufficient copper for full power at 250°C. Before operating the reactor at 280°C, remove part of the copper from the reactor so that there will be some gas letdown at the higher temperatures.

Course c is the most desirable, in that it achieves the goal of full power during the early operation of the reactor and also permits efficient stripping of gaseous fission products during later high-temperature operation. It requires, however, either some means of removing copper from the fuel solution or replacement of part of the fuel charge with fresh fuel containing no copper. About 10 months would be required to reduce the copper concentration by a factor of 2 by normal chemical processing.

1.2.2 Dump Tests

Before the system is operated any length of time at elevated temperatures and pressures, a series of tests will be carried out to check the functioning of the dump control system. The first tests will

be at pressures low enough for the reactor not to be damaged as a result of the dump controls failing to operate properly. Afterwards, the reactor will be dumped from conditions of 250°C–1400 psia and 280°C–2000 psia.

The tests will specifically check the action of the dump valves, pressurizer bleed valves, condenser emergency cooling water, and all other parts of the reactor system interlocked with the dump signal. During each dump, chart records will be obtained of pressures in the core, blanket, fuel dump tanks, and blanket dump tanks, of the core-blanket differential pressure, and of the position of the dump valves and the pressurizer bleed throttling valves. Dump-tank weights will be read at intervals throughout each dump. Temperatures at strategic points in the reactor will be recorded continuously.

1.2.3 Neutron Source

A neutron source was designed and constructed and is being irradiated in the LITR lattice. The source consists of a $\frac{1}{2}$-in.-OD × $3\frac{3}{4}$-in.-long cylindrical slug of antimony surrounded by a beryllium shell, and is enclosed in a stainless steel can (ORNL-LR-Dwg. C-25527). The source strength after saturation irradiation is designed to be 5×10^8 neutrons/sec. Because the fission chambers are located outside the thick steel pressure vessel and blast shield, a very strong source is required to produce a detectable flux when the

reactor is subcritical. During the initial critical experiment the source will be suspended in a tube in the center of the core. During all subsequent operation it will be located in the blanket thimble, where it will be continuously regenerated by irradiation of the antimony. Thus a strong source will always be present during startup.

1.2.4 Test Procedures

During the quarter the following memoranda were issued describing procedures and methods of testing:

HRT Test No.	Title	ORNL CF No.
	Procedure for Cleaning the Low- and High-Pressure Fuel and Blanket Systems with Trisodium Phosphate	56-4-186
	Detailed Procedure for Cleaning the Low- and High-Pressure Fuel and Blanket Systems with Trisodium Phosphate	56-5-123
II-A, 19a,b IV-A, 42a,b	Procedure for Testing of Transfer Tanks	56-5-129
II-A, 22a,b	Procedure for Testing Holdup Tank	56-5-168

2. HRT DESIGN

W. R. Gall

R. E. Aven
C. A. Burchsted
C. J. Claffey
H. N. Culver[1]
R. F. Hughes[2]
J. E. Kuster[3]

M. C. Lawrence[4]
M. I. Lundin
H. A. McLain
C. Michelson[1]
R. C. Moren[5]
R. C. Robertson

J. N. Robinson
C. L. Segaser
W. F. Taylor[6]
W. Terry
T. H. Thomas
F. C. Zapp

2.1 GENERAL STATUS OF DESIGN

Design of the HRT is complete except for revisions being made in order to benefit by new developments and to overcome problems that materialized during construction and testing. Among these changes are piping revisions incidental to installation of the rupture-disk assembly[7] and alteration of the cooling-water system to overcome possible stress-corrosion problems. Work on the following items concerned with the HRT, in addition to numerous minor design changes, is still in progress and will be summarized in future reports:

1. corrosion-specimen holders for installation within the core and blanket areas of the HRT pressure vessel;
2. design of pipeline monitor boxes and/or shielding;
3. redesign of the diaphragm pump heads, incorporating a bolted-type closure;
4. off-gas vent for the fuel storage tanks (the possible discharge of Kr^{83}, Xe^{133}, and Xe^{135} must be considered);
5. evaluation of flanged joints;
6. installation of a flowmeter in the water lines to the main heat exchanger of the fuel system as a means of obtaining more dependable heat-balance data;
7. provision for the placement of portable shielding within the reactor cell during shutdown;

8. determination of activity levels at various points of interest within the reactor cell, after shutdown, as a factor in maintenance operations.

The present program for design of tooling for remote maintenance is approximately 40% complete. Several tools for use in opening and bolting of flanged joints and a tool for movement of diaphragm pump heads into position preparatory to removal from the cell were designed by the Vitro Corp. Designs for the following items under this program were completed by ORNL:

1. bolt wrenches for use in conjunction with the Vitro-designed tools,
2. extension-handle mirrors for examining equipment remotely,
3. tools for removing ring-joint gaskets from flanged joints,
4. torque-multiplier adaptor,
5. disconnects for air and leak-detector lines,
6. tools for replacing the rupture-disk assembly,[7]
7. hydraulic movers for removing struts from the reactor cell,
8. fly crane for handling and spotting equipment and tools over the reactor cell.

Reports issued by the Mechanical Design Section during the quarter include:

ORNL CF NO.	Author	Title
56-4-105	J. E. Kuster	HRT Leak Detection System
56-4-202	R. F. Hughes	Stresses in Spherical Shells Resulting from Linear Heating of Inside Wall
(Memo)	J. N. Robinson	Purchase Specification HRT Ring Joint Flanges and Gaskets
56-4-188	H. A. McLain	HRT Core and Blanket Vent Piping

---

[1]On loan from TVA.

[2]On loan from Kaighin & Hughes, Inc.

[3]On loan from Maxon Construction Co.

[4]On loan from General Dynamics Corp.

[5]On loan from Westinghouse Electric Corp.

[6]On loan from Pioneer Service & Engineering Co.

[7]W. R. Gall *et al.*, *HRP Quar. Prog. Rep. April 30, 1956*, ORNL-2096, p 19—20.

2.2 REFRIGERATION SYSTEM

New lines were added to the refrigeration system to permit the installation of type B (permanent) freeze jackets[8] on the fuel and blanket feed and purge pumps and to provide spares for unforeseeable future needs. Eight new line pairs, involving four penetrations of the north wall, were specified. Two line pairs in the fuel system and three in the blanket system are spares.

The design for a remotely operated temporary freeze jacket reported previously[8] was replaced with the simplified design shown in Fig. 2.1. This jacket, based on a stock C-clamp, is more easily operated remotely than the previous model, in addition to being somewhat less expensive. Following successful operation of a prototype on a $\frac{1}{2}$-in. line, design of the jacket was modified for use on larger pipe sizes also.

2.3 FEED- AND PURGE-PUMP FLOW MEASUREMENT

Differential-temperature flow metering devices were designed for the HRT feed and purge pumps to assure that adequate flow will be maintained

---

[8]*Ibid.*, p 17–19.

Fig. 2.1. Modified Clamp-on Type of Freeze Jacket.

through these units. A metering installation consists of a jacketed sector of pipe leading to or from a pump, with a thermocouple assembly at each end; Fig. 2.2 shows a typical thermocouple assembly. Differential temperatures across the length of the cooled jacket and the corresponding process line are transmitted to a multipoint recorder in the control room, where flow in the process line is calculated as a function of the ratio of temperature differentials and the known flow of water through the jacket.

The existing feed-pump coolers will be utilized as the jacketed sectors for the feed pumps. Two pumps are served by each purge-pump cooler. Additional heat-exchange jackets will be provided on the discharge lines from the 3.5-gph pumps to determine the purge flow to the main circulating pumps; the flow through the pressurizer purge pumps will be found as the difference between the flow through the purge-pump cooler lines entering the pumps and the flow from the 3.5-gph pumps.
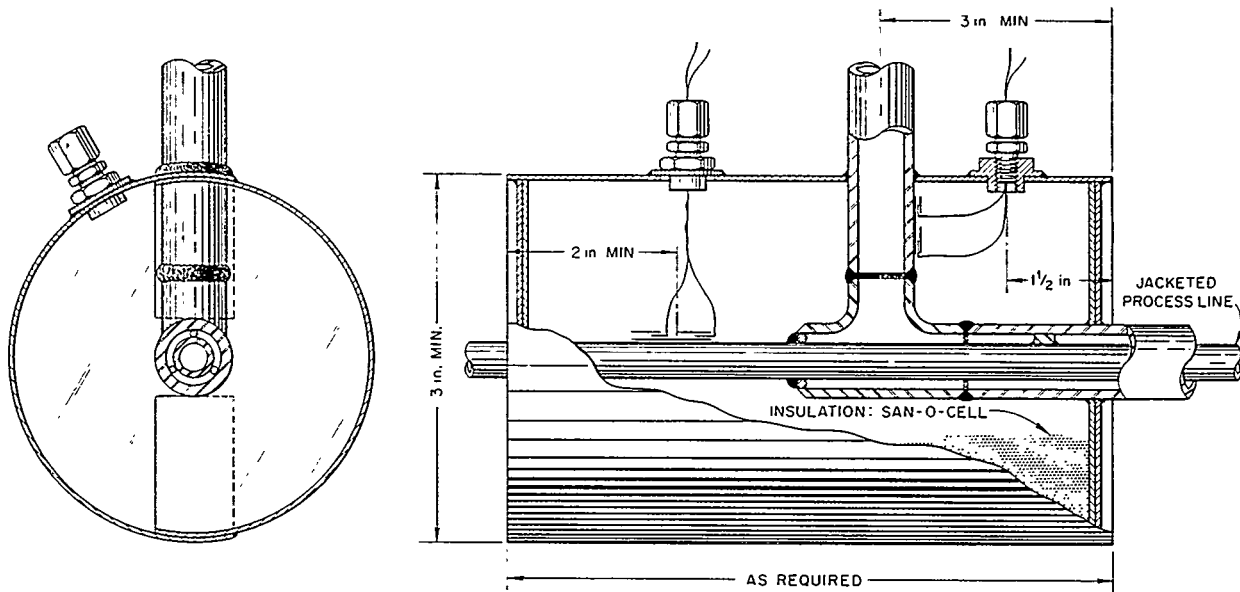
Fig. 2.2. Typical Thermocouple Assembly, Differential-Temperature Flowmeter.

2.4 REPLACEMENT PRESSURE VESSEL

Preliminary specifications and drawings have been completed for a replacement pressure vessel, core tank, and blast shield in the event of failure of the present HRT core tank. The replacement vessel shown in Fig. 2.3 incorporates two basic departures from the original vessel: first, future access to the core tank is provided through a 34-in. opening; second, the complicated transition section and second penetration of the present core tank are eliminated through the use of a re-entrant nozzle at the top of the tank. The blast-shield design is based on containment of any impact forces which might be developed in the event of pressure-vessel failure.
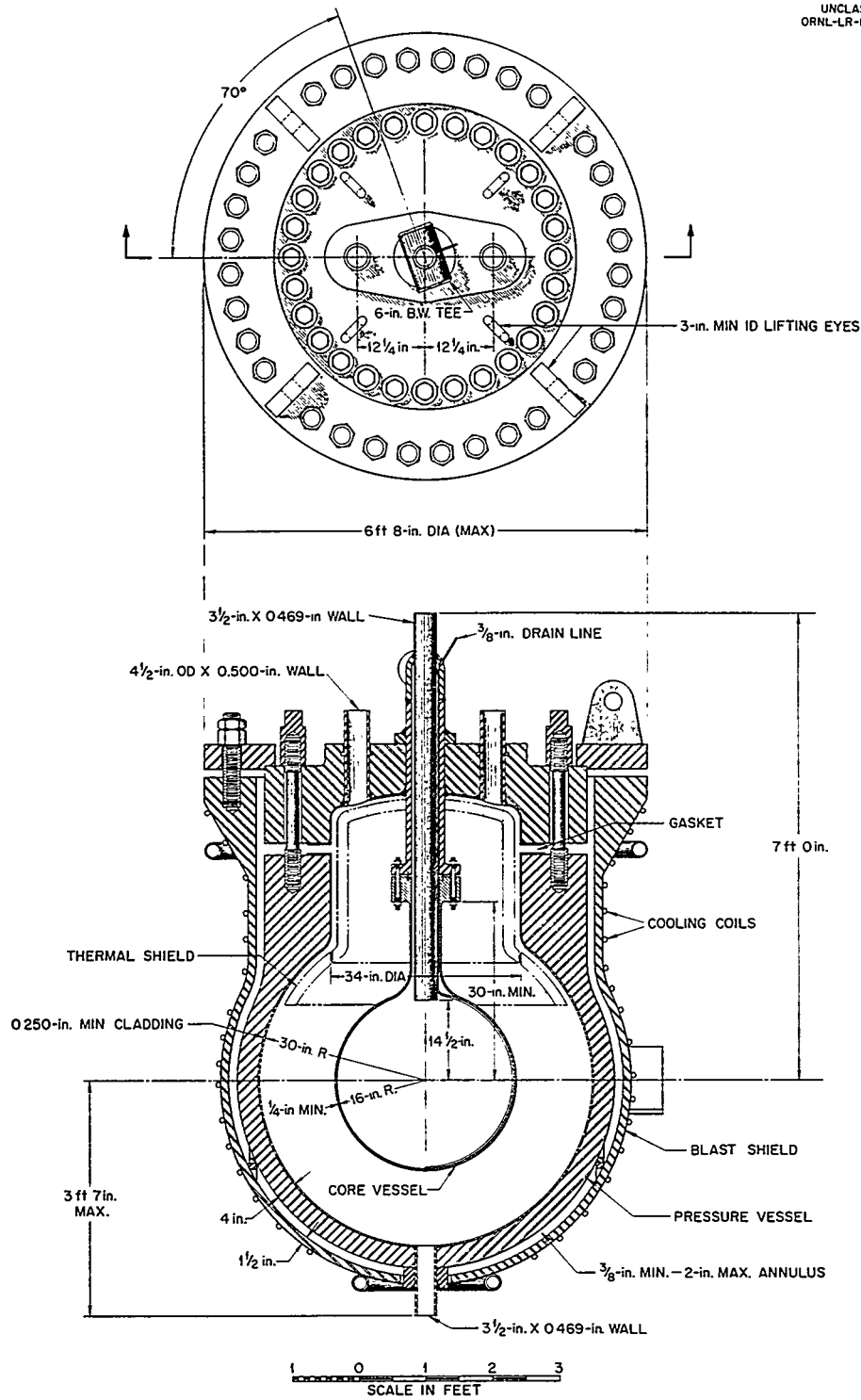
Fig. 2.3. Replacement Pressure Vessel and Blast Shield, HRT.

3. HRT COMPONENT DEVELOPMENT

C. B. Graham

R. Blumberg	E. C. Hise	W. L. Ross
B. D. Draper[1]	J. C. Moyers	I. Spiewak
C. H. Gabbard	P. F. Pasqua[2]	L. C. Wilbur[3]
B. A. Hannaford	D. M. Richardson	D. E. Willis
P. H. Harley		H. D. Wills

3.1 PUMP DEVELOPMENT

HRT-size pumps are being tested in the HRT mockup and in test loops to establish the reliability of thermal-barrier seals and titanium parts.

3.1.1 400A-1 Pump and Loop

The 400A-1 Westinghouse pump, which contains a titanium impeller and a titanium thermal barrier, has operated for 2285 hr since the thermal barrier was welded to the stator flange. For most of this time, 2163 hr, a solution of 0.04 m UO_2SO_4, 0.005 m $CuSO_4$, and 50 mole % excess H_2SO_4 was circulated at 255°C. Heat-balance checks on the pump cooling water indicated no leakage around the thermal barrier. Chemical analyses indicated low corrosion rates during the run.

3.1.2 300A-1 Pump

Since the thermal barrier and the main flange were seal-welded, the 300A-1 pump has operated without incident in the HRT mockup for 3357 hr, including 2964 hr on uranyl sulfate solution at 300°C.

3.2 REACTOR FUEL AND BLANKET PUMPS

3.2.1 Spare Reactor Fuel Pump and 400A-2 Test Loop

During the past quarter, the spare reactor fuel pump with titanium parts operated for 1135 hr on a solution containing 0.04 m UO_2SO_4, 0.005 m $CuSO_4$, and 50 mole % excess H_2SO_4 at 250°C. A solid gold-plated stainless steel gasket is being used to seal between the stator and the titanium thermal barrier. A high seating force on the gasket is obtained with cap screws of high strength titanium alloy. Pump cooling-water heat-balance checks indicate no leakage around the thermal

---

[1]On loan from TVA.

[2]Consultant.

[3]Research participant.

barrier. A pump inspection after operation for 1057 hr on the 0.04 m UO_2SO_4 solution revealed no abnormal corrosion or wear.

3.2.2 Spare Reactor Blanket Pump and 230A Test Loop

The spare blanket pump, with a stainless steel barrier welded to the stator, was installed in the 230A loop. The barrier has a titanium insert at the wearing-ring and labyrinth shaft seal.

During the quarter the pump circulated 1.3 m UO_2SO_4 solution at 250°C for 550 hr. Nickel analyses during the run, confirmed by manganese analyses, indicated a generalized corrosion rate of approximately 2 mpy. Figure 3.1 shows the chemical analyses obtained during the run; chromium went into solution at a rate higher than that usually obtained from type 347 stainless steel in contact with UO_2SO_4 solution.

After disassembly, inspection of the pump and loop showed that the only pitting or severe corrosive attack had occurred on one HRT-type corrosion specimen (Fig. 3.2) and in the pump itself. The loop was covered with a fairly heavy black film; machining and weld patterns were visible through the scale.

The pump suffered corrosive attack on three stainless steel surfaces:

1. There was one pit, about $\frac{1}{16}$ in. deep, on the hot face of the stainless steel thermal barrier.

2. The newly machined surface of the barrier where the barrier-stator seal weld was cleaned up was corroded around the circumference, as shown in Fig. 3.3. The maximum penetration was about 0.025 in. The barrier provides one wall of a 2-in.-deep cylindrical crevice of about 0.015-in. width.

3. The pump casing between the titanium liner and the gasket seat was corroded on the other boundary of the above crevice as shown in Fig. 3.4. The attack was more random than on the barrier, with penetration about the same. The corrosion occurred at the cool end of the crevice.
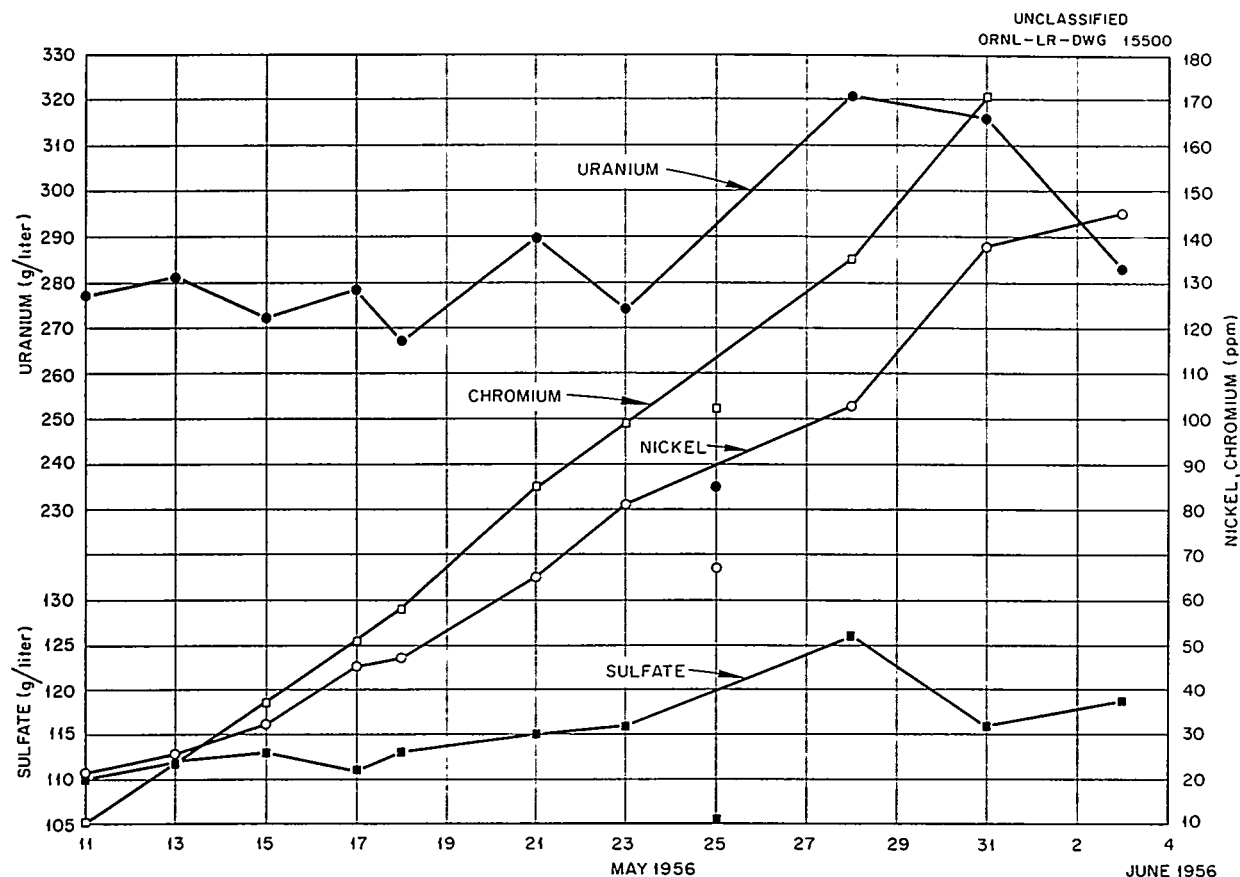
Fig. 3.1. Chemical Analyses of 1.3 m UO$_2$SO$_4$ Solution Circulated by the Spare Reactor Blanket Pumps.

Figure 3.5 shows the titanium impeller, which was not attacked.

3.3 HRT SPARE HEAT EXCHANGER

Proposals for the fabrication of a 5-Mw spare heat exchanger were received from three vendors: Alco Products, Inc., Babcock & Wilcox Co., and Foster Wheeler Corp. Selection of a vendor will be made after further discussion of engineering details with the three companies.

The Alco design uses 252 ⅜-in. tubes arranged in single U-bends. It features a strength-welded head closure and a welded water-box pass partition. Fuel solution holdup is 17 gal. This design eliminates the leakage problems at the pass partition and the head but makes tube-joint repair costly.

Babcock & Wilcox presented a unique design which brings all the tubes out through the shell individually and collects them in an external header. There are 84 ⅝-in. tubes arranged in triple U-bends. A thermal sleeve at each tube-shell joint minimizes stress concentration. Fuel holdup, 28 gal, is relatively high. This design might eliminate the problem of corrosion cracking of tubes in the tube sheet but would do so at the cost of many difficult tube welds.

Foster Wheeler bid on a unit essentially identical to the two 5-Mw heat exchangers delivered to ORNL earlier.[4,5] The design uses 251 single U-bend ⅜-in.-dia tubes.

[4]C. B. Graham *et al.*, *HRP Quar. Prog. Rep. Jan. 31, 1956*, ORNL-2057, p 22.

[5]C. B. Graham *et al.*, *HRP Quar. Prog. Rep. April 30, 1956*, ORNL-2096, p 23.

13
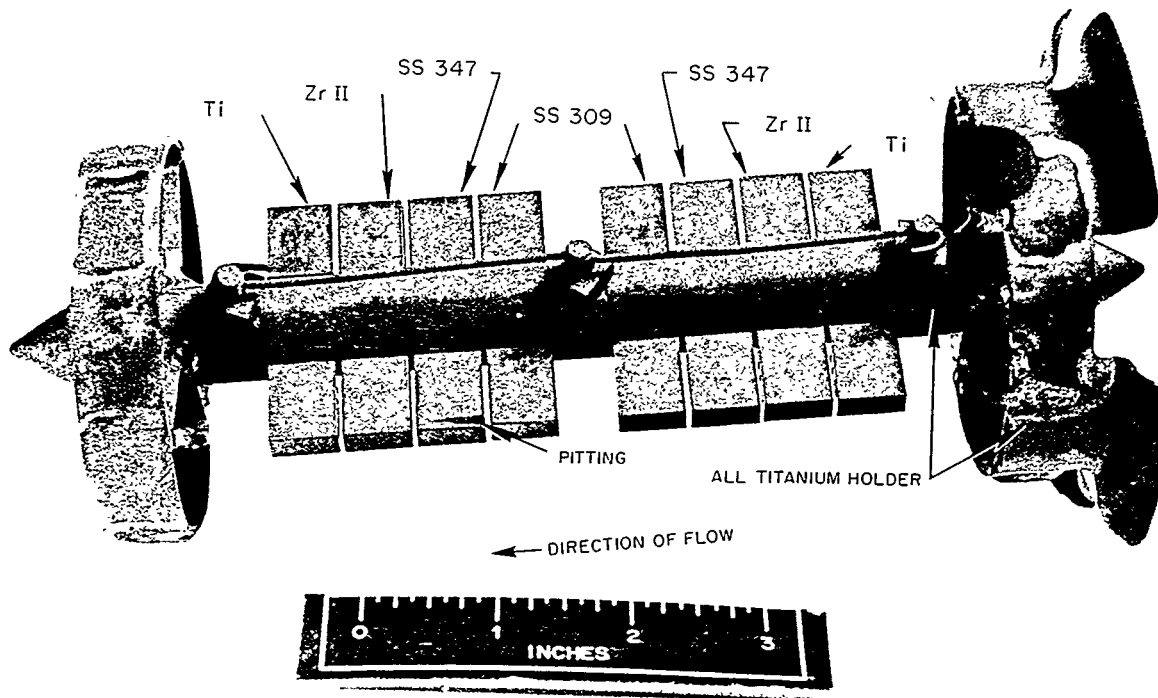
Fig. 3.2. Corrosion Specimens Exposed to 1.3 m UO$_2$SO$_4$ in the Spare Blanket Pump for 550 hr.

An order has been placed by ORNL for the tubing stock to be used in the spare exchanger.

3.4 DIAPHRAGM PUMPS

3.4.1 HRT Feed Pumps

The new girth-welded check-valve design[6] has apparently eliminated the problem of housing failures in the suction check valves. No check-valve failures have occurred in 8000 hr of operation, accumulated on three pumps. Therefore the improvement of diaphragm life is currently the main problem of the feed-pump development program.

Tests conducted on feed-pump test loop No. 1 showed that diaphragm motion is not uniform and that diaphragm failures may be partly caused by high stresses induced by wave motions and vibrations. The tests also showed that a 0.031-in.-

thick diaphragm had a smoother deflection than the standard 0.019-in. diaphragm. Although the maximum theoretical stress is higher for the thicker diaphragm, life may be longer owing to the more uniform deflection.

Stress calculations were completed for different diaphragm thicknesses, materials, and deflection contours; the results are tabulated below:

Deflection Contour		Material and Thickness (in.)	Maximum Stress (psi)
Type	Depth		
Existing	0.100-in.	0.019-in. SS	16,000
		0.031-in. SS	21,000
		0.020-in. titanium	9,000
		0.028-in. titanium	11,500
Purge pump		0.019-in. SS	29,000
Free deflection	0.100-in.	0.019 in. SS	15,000
		0.030-in. SS	18,000

[6]W. R. Gall *et al., HRP Quar. Prog. Rep. April 30, 1956,* ORNL-2096, p 16.
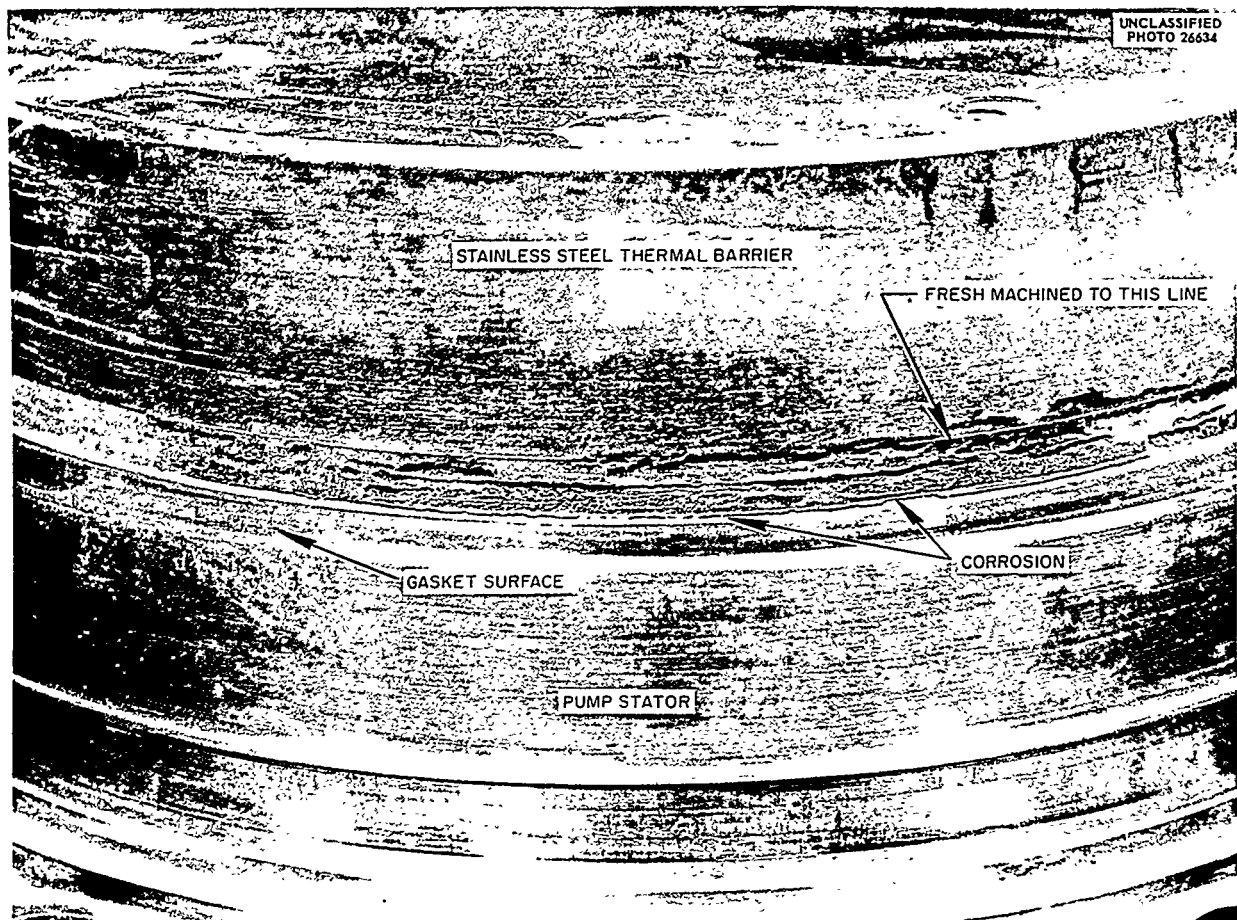
Fig. 3.3. Spare Blanket Pump and Thermal Barrier After 550 hr of Operation with 1.3 m UO$_2$SO$_4$.

The experimental evidence that the purge pump has a longer life than the feed pump, while operating with almost twice the theoretical stress, indicates that a more rigid diaphragm might extend the life of the feed pump or that corrosion fatigue is limiting its life. A program is being initiated to determine the effect of uranyl sulfate solution on the endurance limit of annealed and work-hardened type 347 stainless steel sheet and possibly other materials.

A second feed-pump test loop is being constructed so that a new pump-head design can be evaluated and so that diaphragm materials can be tested for endurance. The new head design contains a bolted closure, with finer mesh screening and a more evenly distributed flow into the diaphragm cavity. The new design should eliminate the problem of dirt particles embedding into the diaphragm and should provide better diaphragm motion. The test loop is approximately 90% complete.

3.4.2 HRT Purge Pump

The purge pump on the HRT mockup was found to have a ruptured diaphragm and a leaking discharge check valve after 2550 hr of pumping pure condensate. The diaphragm failure was caused by a relatively large metallic chip in the diaphragm cavity. With the exception of the area around the chip, the diaphragm was in excellent condition. The seats of the discharge check valve had eroded severely, as shown in Fig. 3.6. A metallographic examination is being made to determine the cause of the erosion.

3.5 HRT DUMP TEST

The HRT dump-test unit, which consists of concentric core and blanket vessels with a $\frac{1}{18}$

15
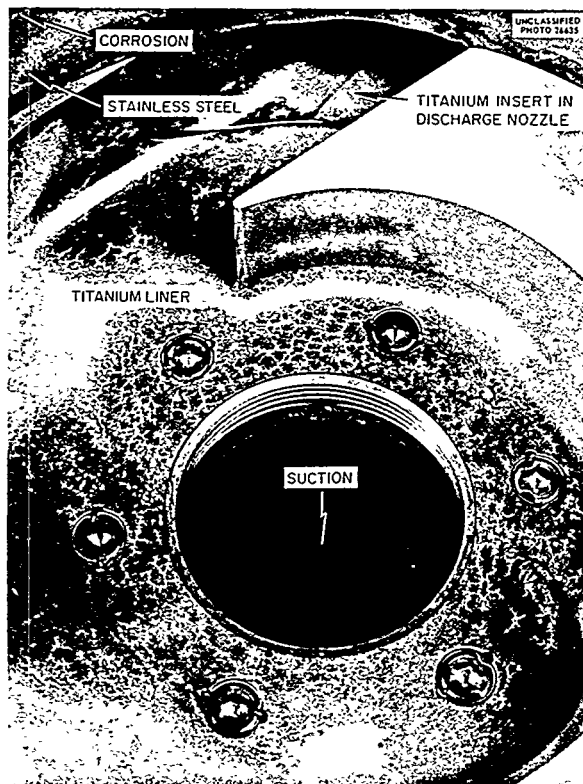
Fig. 3.4. Volute Casing of Spare Blanket Pump After 550 hr with 1.3 m UO_2SO_4.

Fig. 3.5. Titanium Impeller of Spare Pump After 550 hr with 1.3 m UO_2SO_4.

volume ratio to the reactor core and blanket systems, is being used to determine the effectiveness of the reactor dump control system. Starting conditions in both vessels were 300°C and 2000 psi.

During the initial part of the dump process the steam superpressures were relieved by means of throttling vent valves. The differential pressure between the core and the blanket exceeded ±75 psi when the vent controller had proportional and derivative functions. With proportional control only, the pressure differences remained within ±35 psi.

After the superpressure was relieved, the dump valves were opened. During this period, the pressure balance was within the control range of ±40 psi on all the runs.

3.6 HRT SAMPLER

Representative solution samples were taken from the HRT mockup with the prototype HRT sampler.

Deposition of drops of sample on the flask diaphragm was eliminated by providing vent holes in the flask holder and permitting longer drainage time.

This operation suggested that limit switches to indicate flask-holder position and isolation-chamber stem position should make the remote sampling procedure more reliable. These changes have been incorporated into the sampler and are being tested.

3.7 FREEZE JACKETS

HRT-type freezer stations[7] were tested on $3\frac{1}{2}$-in. and $\frac{1}{2}$-in. pipes. Leaktight ice plugs inside the pipes were produced by using refrigerant tubing coils welded or soldered to the test sections. Loosely wrapped coils produced satisfactory freeze plugs only under water; in air there was insufficient thermal conduction from the pipe to the coil.

---

[7]*Ibid.*, p 17–18.
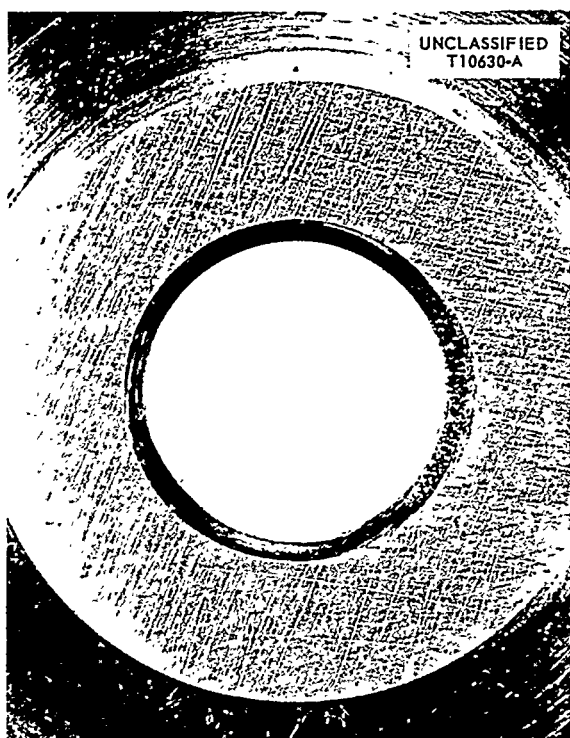
Fig. 3.6. Purge-Pump Discharge-Check-Valve Seat After 2550 hr of Operation.

The $3\frac{1}{2}$-in. plug was frozen in 75 min with −40°C refrigerant. The ends of the test pipe were open and the pipe was mounted vertically in a tank of stagnant hydrant water. This presented a most difficult arrangement for freezing because no attempt was made to hinder thermal convection of the water through the pipe.

The $\frac{1}{2}$-in. station is being tested under flow conditions, with varying internal temperature, pressure, and leak rate. The results of these tests should define the utility of freezer stations in plugging leaks while the HRT is operating.

3.8 HRT PRESSURIZER-HEATER TESTS

Preliminary tests were made on one clampon-type HRT pressurizer-heater unit. The heater clamps had to be tightened at the operating temperature to provide the proper heat transfer. Heat-transfer coefficients from heater to pipe varied between 85 and 99 Btu/hr·ft^2·°F, which is satisfactory.

Heat losses from the heater to the air were measured at various temperatures. At the normal heater temperature of 390°C the loss was 0.5 kw.

3.9 HRT MOCKUP

The HRT mockup contains a number of prototype HRT components operating under reactor conditions in an integrated system.[8,9]

3.9.1 Operation

The mockup operated for 1730 hr during the past quarter, circulating a solution containing 0.042 m UO_2SO_4, 0.021 m H_2SO_4, 0.005 m $CuSO_4$, and 500 ppm O_2. High-pressure oxygen injection was employed. There were no major shutdowns, but the system was down several times for short periods as required by special experiments. Maintenance was performed on those occasions.

The corrosion rate averaged 1.5 mpy based on nickel analysis. Analysis and sampling methods were improved and show a more uniform rise of nickel concentration from day to day than had been obtained previously.

3.9.2 Behavior of Loop Components

The main loop components performed satisfactorily during the report period. The incidence of feed-pump trouble was reduced considerably below that of the previous quarter; this was achieved partly as a result of slowing the pump down to 40 strokes per minute.

Failures which occurred in loop components were:

1. The titanium diaphragm of the bolted, south injection pump head failed after 425 hr of operation. This is not considered to be a valid test of titanium as a diaphragm material, because of irregularities in the head contour introduced while an originally welded head was being converted into a bolted head.

2. The purge-pump flow rate was noted to be falling off after 2200 hr of operation. When the diaphragm head and the check-valve assembly were replaced 300 hr later, failures were noted in the diaphragm and in the discharge check valve (see Sec. 3.4.2).

3. A Hammel-Dahl air-operated drain valve developed a bad leak as a result of exposure to hot fuel solution. The valve was replaced with a hand valve.

[8]C. B. Graham *et al.*, *HRP Quar. Prog. Rep. Jan. 31, 1956*, ORNL-2057, p 25–26.

[9]C. B. Graham *et al.*, *HRP Quar. Prog. Rep. April 30, 1956*, ORNL-2096, p 26.

A heat-balance-type purge flowmeter was built and calibrated. This device, which uses a small steam heater on the purge-pump discharge,[10] will be used in the reactor to monitor the flow of purge water to the circulating pumps and pressurizers.

The HRT-prototype letdown valve was inspected after 3100 hr of service and was found to be in excellent condition.

3.9.3 Special Test – Sampling Procedure and Analysis

In conjunction with testing of the HRT sampler, numerous solution and condensate samples were withdrawn from eight sample points over a 16-day period. Duplicates of each sample were submitted to the 9204-1 analytical laboratory, as well as stock control samples. The 5-ml samples from the HRT sampler were analyzed by the X-10 group that will analyze HRT samples.

The following conclusions were made after the analyses were interpreted:

1. Adequate flushing of sample lines is required to give representative samples.

2. The analyses of all concurrent high- and low-pressure samples gave the same results except for

some dilution in the high-pressure system as a result of purge flow.

3. The standard deviations of stock control analyses (Table 3.1) are of the same order of magnitude as the analytical changes of interest in inventory control. Therefore small amounts of precipitation of uranium and copper cannot be detected by solution analyses. On the mockup, for example, the uranium inventory averages 1360 g, and about 100 g would have to precipitate before that fact could be established from solution analysis.

4. Copper analyses at both laboratories and nickel and excess-acid analyses at the X-10 laboratory were subject to errors of more than 10%. The X-10 analyses were less precise, probably because of the smaller samples involved.

5. Submittal of duplicate samples revealed occasional erroneous analytical reports, which could be discarded in evaluating the chemical data.

3.9.4 Special Test – Solids Separation

Two seven-day runs were made for the Chemical Technology Division to test removal of rare-earth and corrosion-product solids with a hydroclone. Results of the tests are reported in Sec. 6.4.3.

---

[10]P. H. Harley, *Feed Pump and Purge Water Flow Measurements*, ORNL CF-56-5-169 (May 24, 1956).

TABLE 3.1. STANDARD DEVIATIONS OF CONTROL SAMPLES

Element or Ion	9204-1 Analytical Laboratory			X-10 Hot Lab		
	Concentration (g/liter)	Number of Times Submitted	Standard Deviation (%)	Concentration (g/liter)	Number of Times Submitted	Standard Deviation (%)
U	9.74	46	3.84	9.92	20	2.41
SO_4^{--}	6.67	40	2.20	6.73	20	8.09
Excess acid (as SO_4^{--})	2.33	43	1.36	2.09	20	12.1
Cu	0.315	47	17.8	0.293	20	10.9
Ni	0.038	40	7.59	0.041	20	19.4
pH	1.631	47	0.236 pH units	1.573	19	0.111 pH units

4. HRT CONTROLS AND INSTRUMENTATION

D. S. Toomb

A. M. Billings	R. L. Moore
J. D. Grimes[1]	L. R. Quarles[2]
J. C. Gundlach	W. P. Walker[2]

K. W. West

4.1 PROCUREMENT

The only major control or instrumentation equipment not yet received is a 20-channel remote-area radiation monitoring system being fabricated by the Victoreen Instrument Co. The system was approved by ORNL engineers subject to modifications by the vendor to decrease the sensitivity to noise signals that are present when the unit is being supplied by standard 60-cycle mains. It is thought that the recabling of internal wiring to separate power and signal leads will eliminate the "pickup."

4.2 EQUIPMENT INSTALLATION

4.2.1 Oxygen Metering Systems

The calibration of the metering stations (consisting of a control valve and a pressure-drop capillary) for high-pressure-oxygen injection in the HRT fuel and blanket systems was completed.[3] It was necessary to install a "snubber" in the oxygen supply line to avoid shifting the calibration of the differential-pressure cell by the sudden application of high pressure. The slow application of pressure that results from use of the snubber allows the pressure drop across the metering capillary to equalize within the range of the differential-pressure cell.

4.2.2 Sound Transmitters

Drawings were prepared for the waterproof microphone assemblies that are to be installed on equipment located in the reactor cell. The microphones will be used to sense motor-bearing and check-valve noises. Figure 4.1 shows the construction of the waterproof assembly, which demonstrated satisfactory sensitivity on HRT loop equipment.

4.3 LIQUID-LEVEL INDICATORS

4.3.1 Pressurizer and Storage-Tank Level Indicators[4]

The original Iso-Elastic alloy helical springs utilized in the pressurizer and storage-tank level indicators were replaced with gold-plated springs of the same alloy to achieve corrosion resistance. Elgiloy suspension springs have shown a susceptibility to stress-corrosion cracking[5] in the heat-treated states tested to date.

4.3.2 Level Alarm Transmitter

A float-type level indicator, utilizing a unique packless flexible shaft, is shown in Fig. 4.2. The transmitter, which was supplied by the Moore Products Co., will be installed on the holdup tank in the reactor low-pressure system to annunciate high liquid level in the tank. The tubular float shaft has a flattened center section which permits vertical float motion only. A tongue within the shaft transmits the float motion to a microswitch, which provides an electric off-on contact. The float motion of approximately $\frac{1}{32}$ in. is produced by the buoyant force of the displaced liquid. A limit stop yoke is provided to keep stresses in the shaft well within the elastic limit.

4.4 VALVES AND OPERATORS

4.4.1 Dump Valves

The dump valves of the fuel and blanket systems were both tested for 400 cycles in the valve test loop, and the leak rates did not change appreciably.

---

[1]On loan from TVA.

[2]Consultant from University of Virginia.

[3]A. M. Billings, *HRT Oxygen Metering Stations*, ORNL CF-56-7-72 (to be issued).

[4]D. S. Toomb *et al.*, *HRP Quar. Prog. Rep. April 30, 1956*, ORNL-2096, p 32.

[5]J. L. English and J. C. Griess, *HRP Quar. Prog. Rep. April 30, 1956*, ORNL-2096, p 85.
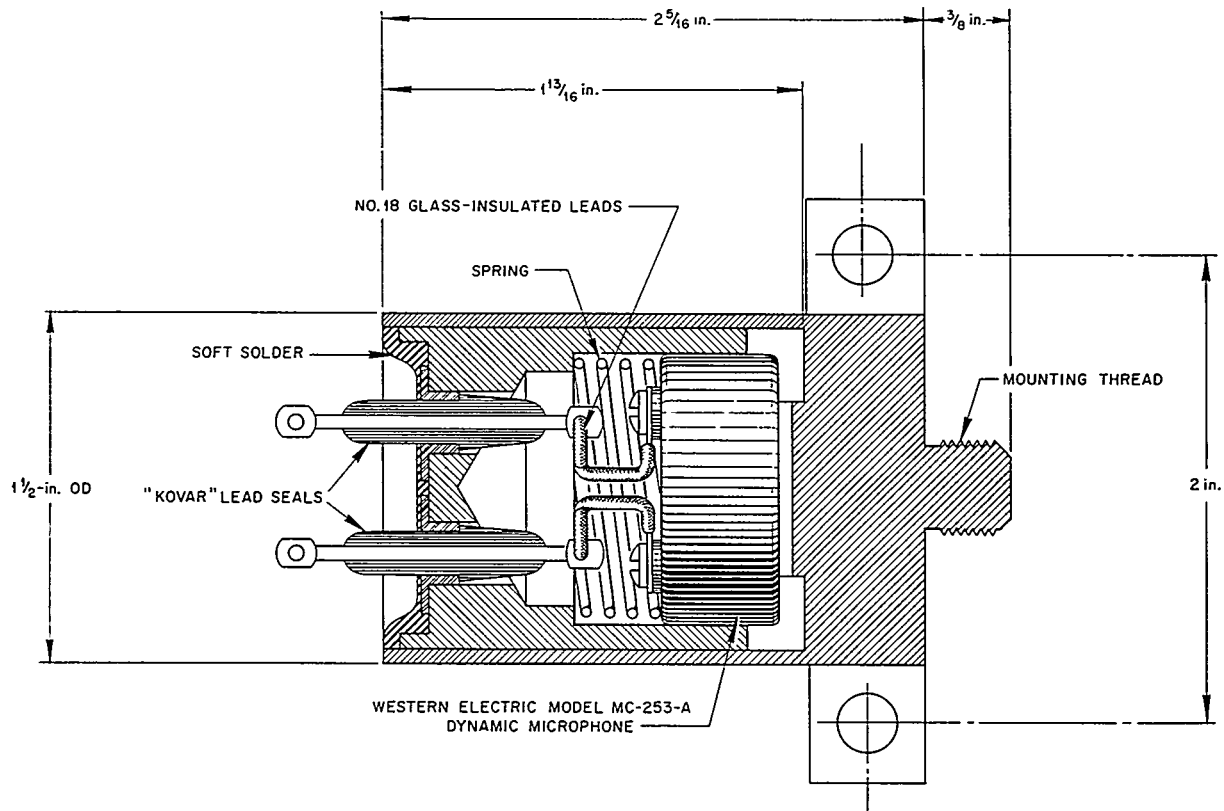
Fig. 4.1. Microphone Assembly for Underwater Service.

The leak rates, after testing, were less than the rate specified by HRP-303, which is 500 standard cc/day for nitrogen applied to the valve inlet at 2000 psi. The fuel dump-valve plug, which is of nominal $\frac{1}{2}$-in.-dia type 347 stainless steel construction, is shown after the test in Fig. 4.3. Figure 4.4 illustrates the nominal 1-in.-dia Stellite 6 plug of the blanket dump valve after it was tested.

The blanket dump-valve and actuator assembly is shown in Fig. 4.5; the valve is identical to the fuel-system dump valve, except for the plug material and the geometry (Fig. 4.3).

4.4.2 Letdown Valve

An HRT-type letdown valve[4] installed on the HRT mockup showed virtually no wear upon inspection after 3000 hr of service. The valve was reinstalled for further testing.

4.4.3 Sampler Inlet Valves

The high-pressure sampler inlet valves for the fuel and blanket systems were found to be sticky in operation; the plug tended to wedge in the valve seat. These valves were returned to the Fulton-Sylphon Division, where modifications in the plug shape were made. The operation of a modified valve (HCV-236) has been satisfactory to date in preliminary reactor tests.

Fig. 4.2. Level Alarm Transmitter.

UNCLASSIFIED
PHOTO 26577
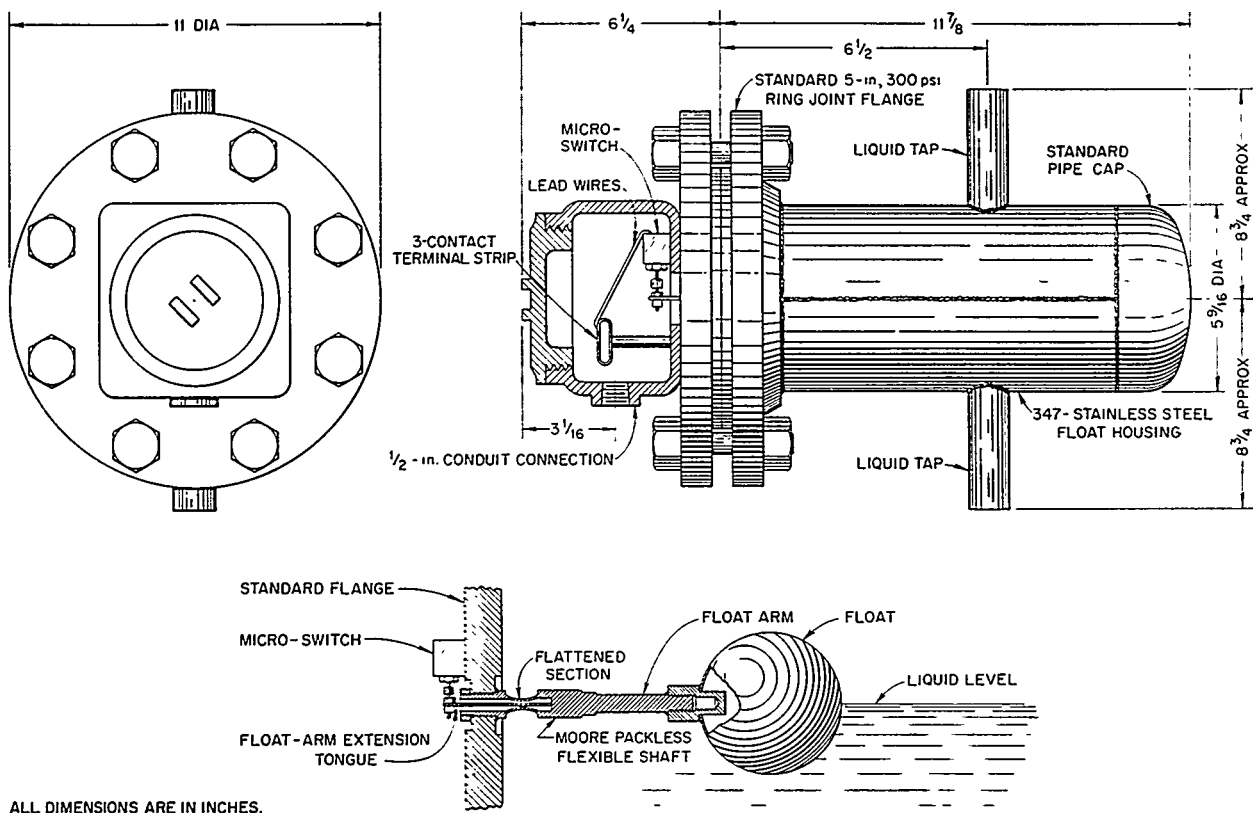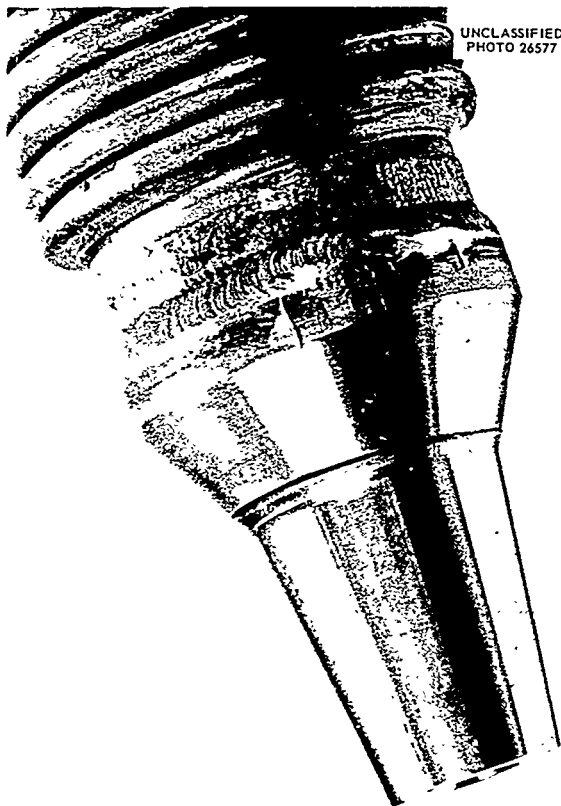
Fig. 4.3. Fuel Dump-Valve Plug After Test.

UNCLASSIFIED
PHOTO 26363

1   2
INCHES
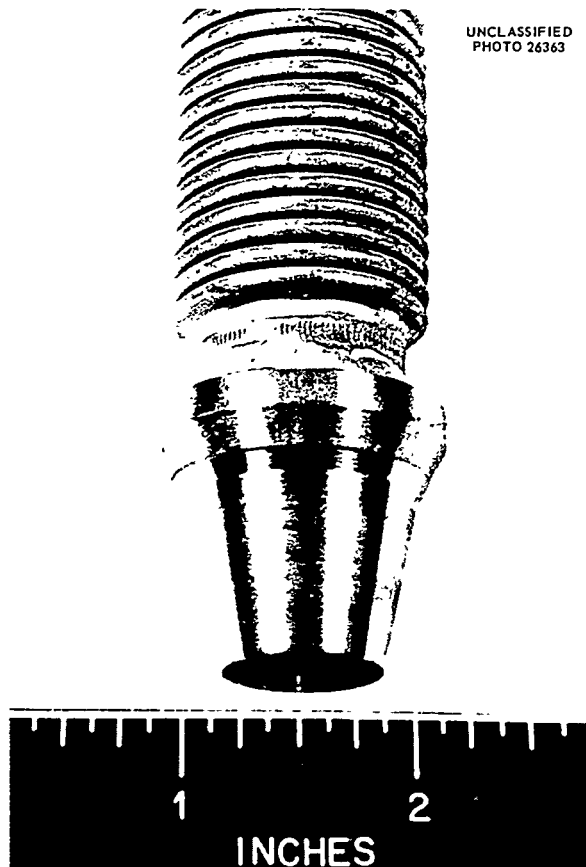
Fig. 4.4. Blanket Dump-Valve Plug After Test.

UNCLASSIFIED
ORNL-LR-DWG 15503

ACTUATING BELLOWS
2-PLY, TYPE 321
STAINLESS STEEL

AIR LOADING PORT

BRASS STEM
SEALING BELLOWS

ACTUATING AIR PORT

STAINLESS STEEL SPRING

BACKSEATING STEM
(STROKE - $\frac{5}{8}$ in.)

SECONDARY PACKING SEAL
(GRAPHITED ASBESTOS)

BELLOWS LEAK-DETECTING TAP

BELLOWS SEAL WELD

OPERATOR EFFECTIVE AREA — 68 in.^{2}

MAX AIR-OPERATING PRESSURE — 80 psi

ACTION — AIR LOADED CLOSED, AIR
PRESSURE TO OPEN, SPRING
ACTION AIDS OPENING.

PRIMARY BELLOWS SEAL
(3 PLIES OF 0.0085-in. TYPE
347 STAINLESS STEEL)

BODY WITH INTEGRAL SEAT
(347 STAINLESS STEEL)

DISCHARGE
(MAXIMUM PRESSURE 500 psi)

STELLITE NO 6 PLUG
$C_v = 10$

2000-psi INLET PRESSURE

Fig. 4.5. Blanket Dump-Valve and Actuator Assembly.

23

5. HRT FUEL PROCESSING PLANT

W. E. Unger

T. A. Arehart	G. W. Gray	E. O. Nurmi
N. A. Brown	P. A. Haas	A. M. Rom
W. D. Burch	C. C. Haws	W. F. Schaffer
W. L. Carter	R. H. Horton	H. O. Weeren
S. D. Clinton	F. C. McCullough	R. H. Winget

5.1 FLOWSHEET – CORE FUEL PROCESSING

The corrosion and fission products that hydrolyze and precipitate as oxides from the core fuel and the fission products that have retrograde solubilities and are essentially insoluble in the core fuel at the reactor operating temperature of 300°C are to be concentrated centrifugally with a hydroclone. The concentrate, after having been sampled, is to be discharged periodically.

There is no question as to the effectiveness of the hydroclone in concentrating particulates with a mean diameter of 1 μ or greater. But the propensity of small particulates for depositing on container walls at 300°C has been observed in loop experiments, and whether or not the small particulates continue in suspension in the reactor fuel will be inferred from the concentration of these materials achieved by the hydroclone. The concentration will be determined by comparison of analyses of samples of the clarified overflow stream with samples of the concentrate in the underflow receiver. Slurry samples are rarely representative, however, and dependable sampling requires that the underflow-receiver contents be completely dissolved and that the resultant solution be sampled for analysis.

As mentioned in the last progress report,[1] the solids dissolution was formerly to have been accomplished in a remote facility, mainly to avoid the risk of contaminating the reactor fuel with the light-water dissolving solution. The risk is justified by the convenience and the promptness of results, however, and the dissolution now is to be carried out in the processing cells. Figure 5.1 is a schematic drawing of the modified flowsheet for the core processing plant. The high-pressure system is unchanged. A dissolver and two decay storage tanks will replace the former carrier-evaporators. Both recombiner-condensers will lead

into the dissolver — one for the recovery of heavy water and the other for the light water driven off during the dissolving operation.

The dissolving process now consists in

1. boiling in 10.8 M H_2SO_4 (170°C) for 6 hr,
2. digestion at 100°F for 48 hr to convert the solids to sulfates,
3. dilution to 4 m H_2SO_4 to dissolve the sulfates.

The solids collected in the underflow receiver will be discharged once a week to the dissolver, where the D_2O will be recovered by evaporation. When the solids approach dryness, as indicated by an abrupt rise in the dissolver temperature, the dissolver will be isolated from the D_2O system by a combination of valves and freeze plugs. Then 10.8 M H_2SO_4 will be added to dissolve the solids; agitation will be supplied by steam admitted through the drawoff line. After the dissolution and sampling operations are completed, the solution will be transferred to one of the two decay tanks and stored until its activity has decreased enough to permit convenient transport and processing by solvent extraction.

The emptied dissolver will be given a water wash and will then be dried by heating. The connections with the equipment containing H_2O will be closed by a combination of valves and freeze plugs, and the dissolver will be vented back to the D_2O system to receive the next batch from the underflow receiver.

The new equipment in the cell will be a 6-gal tantalum-lined dissolver; an additional sampler; and two decay storage tanks, each of 120-gal capacity.

5.2 CONSTRUCTION STATUS

Construction of the HRT Chemical Plant (exclusive of changes incidental to the installation of dissolving equipment) was essentially completed, approximately one month after the scheduled completion date of July 1. Construction was delayed

---

[1]W. E. Unger *et al.*, *HRP Quar. Prog. Rep. April 30, 1956*, ORNL-2096, p 37.
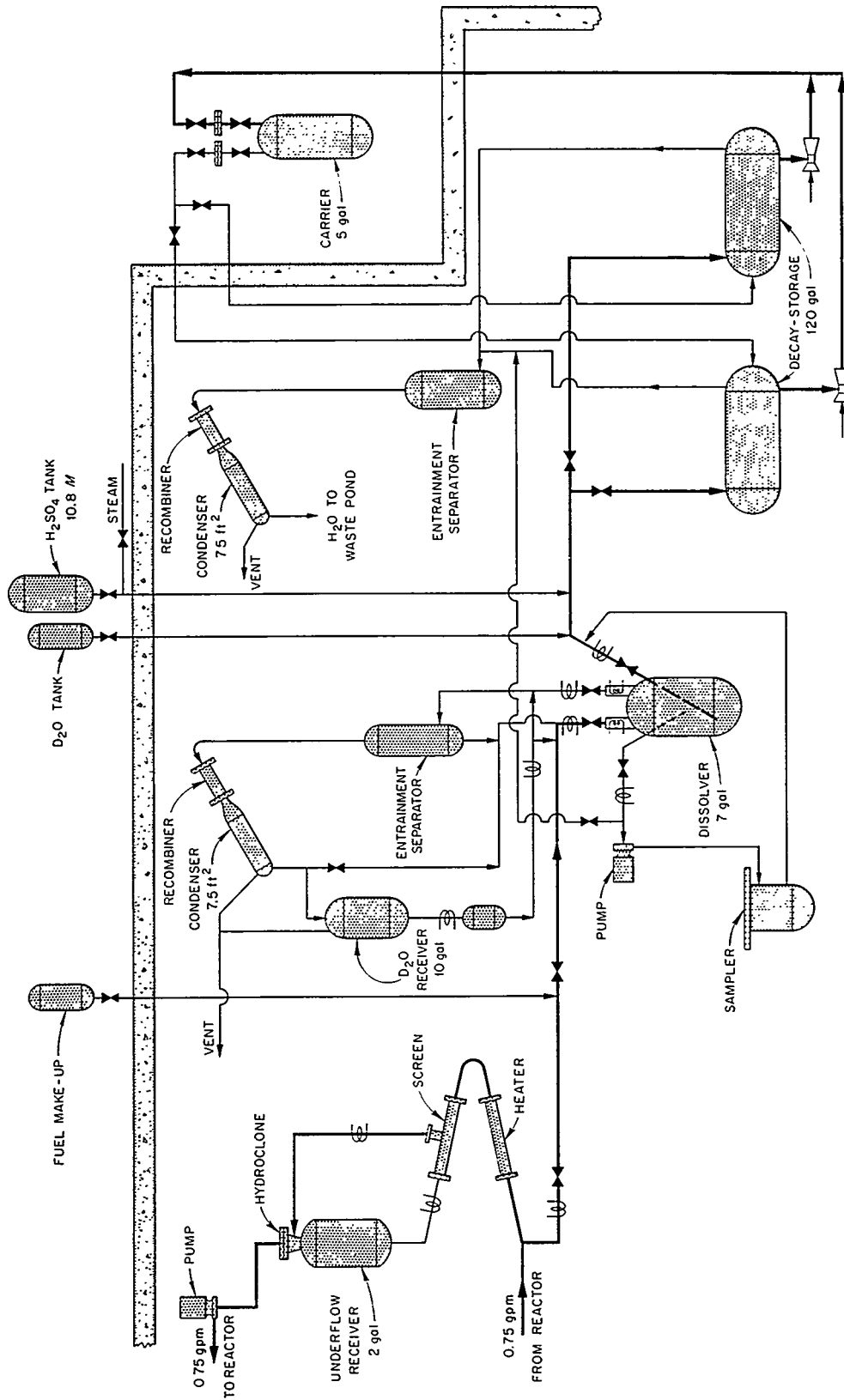
Fig. 5.1. Core Processing Plant.

mainly by the late delivery of the $\frac{1}{4}$-in. IPS sched-80 pipe from which the high-pressure system was fabricated.

The graphic control panel in the main control room at the ground level immediately east of the processing cell and the transducer rack in cell D immediately below the control room were prefabricated and installed as units (see Fig. 5.2).

Figure 5.3 shows the graphic panel, and the transducer rack is visible in Fig. 5.4. The panels to the right of the transducer rack (foreground of Fig. 5.4) will be used for blanket processing equipment to be installed in the future. Also visible in this photograph are the blowers which supply hot air to the underflow-receiver jacket for temperature control, valve air lines with safety shutoff valves, and the electrical conduit which pierces the wall between cell D and the processing cell C.

The high-pressure equipment is shown partially installed in Fig. 5.5. Visible in the photograph are three high-pressure valves, the Westinghouse circulating pump, the overflow sample cooler (H-5), and heater H-3, immediately below valves T-1-4 and P-1-4. The refrigeration lines (in bundles) are attached to the freeze coils, one of which is shown complete (just in front of the pump). Connecting lines to the reactor core system penetrate the wall on the right (shown to the right of and slightly above valve P-1-2 in Fig. 5.5). The integrally flanged hydroclone and underflow receiver have been installed directly above the refrigeration bundles.

5.3 ENGINEERING TESTS AND PLANT SHAKEDOWN

Preparations are under way for the engineering tests required to place the chemical plant in operation. In these tests individual items of equipment will first be operated at room temperature, and then all equipment will be operated as a unit at design temperature and pressure. In order to isolate the chemical-plant testing operation from reactor operations, a shakedown loop,[2] built around the spare 400A pump and a gas pressurizer, was fabricated and is to be installed temporarily in cell B for the period of the test (see Fig. 5.6). This loop will provide simulated fuel solution at 300°C to the chemical plant during testing opera-

tions. Simulated fission and corrosion products for testing will be injected into the loop.

5.4 REMOTE TOOLS

A mockup removal of the hydroclone and the retainer plug from the hydroclone flange was carried out in Building 4505 from a wooden scaffold above the hydroclone flange to simulate the distance between the underflow pot and the roof plug in the HRT Chemical Processing Plant. Although several minor difficulties developed during the test, the tools were found to be adequate in removing the hydroclone flange, the retainer plug, and the hydroclone itself.

Several changes were made as a result of the tests. The collet on the hydroclone tool will be fabricated from Carpenter RDS steel, which retains its elasticity better than the Carpenter "solar" steel formerly used. The collet will be spring-loaded to keep it open while engaging the clone. The retainer ring which holds the two pawls on the retainer-plug removal tool was chromium-plated for protection against corrosion. The hydroclone flange was fitted with $\frac{1}{2}$- and $\frac{3}{4}$-in. guide pins to ensure perfect alignment when the top flange is being replaced. The hydroclone standpipe flange was fitted with sockets to mate with two corresponding guide pins installed on the hydroclone flange. A limiting stop was welded into the socket wrench to prevent the bolt heads from bottoming and wedging in the socket. Also, a handle and an eye bolt were added to the socket wrench to permit its suspension from the crane hook, relieving the operator of its weight while torquing the bolts.

Designed but not tested are vertical valve wrench tools (Fig. 5.7), a right-angle drive tool for removing horizontally mounted bolts, and an adapter for holding a magnet of 20-lb force (Fig. 5.8).

5.4.1 Flange Leakage Tests

The octagonal ring gasket has been recommended for the HRT Chemical Processing Plant. Repeated cycling between 70 and 300°C failed to produce any leaks in two pairs of flanges assembled with octagonal rings, whereas similar temperature cycling resulted in leaks in all flanges assembled with oval rings.

The octagonal gaskets were subjected to nine cycles, the heating and cooling extending over several hours. One severe cycle, 30 min of heating and 45 min of cooling (by removing the flange

---

[2]B. H. Hamling, *Design of Solids Feed Loop for Shakedown of the HRT Chemical Plant,* ORNL CF-56-3-34 (March 5, 1956).
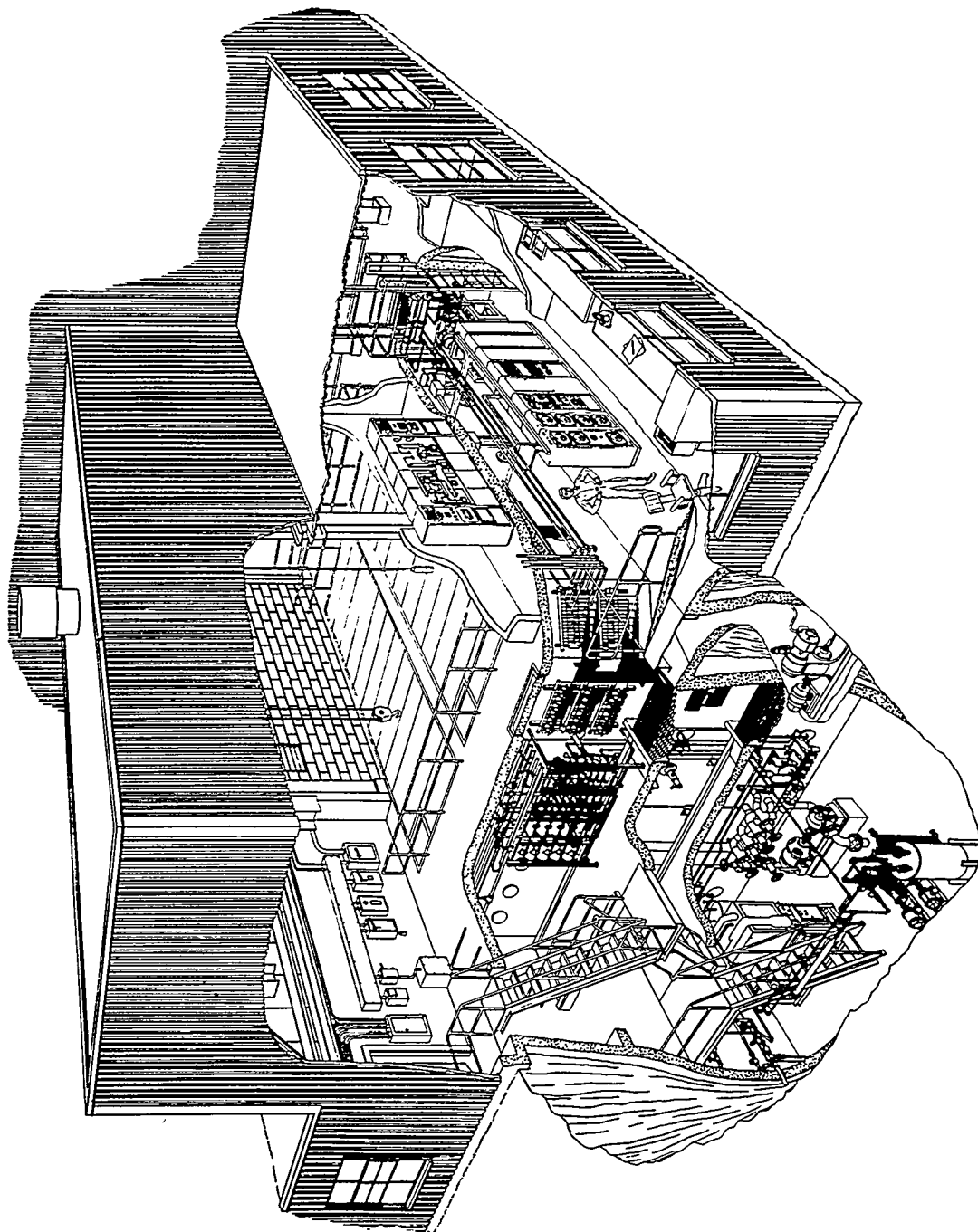
Fig. 5.2. Chemical Processing Plant Operating Area.
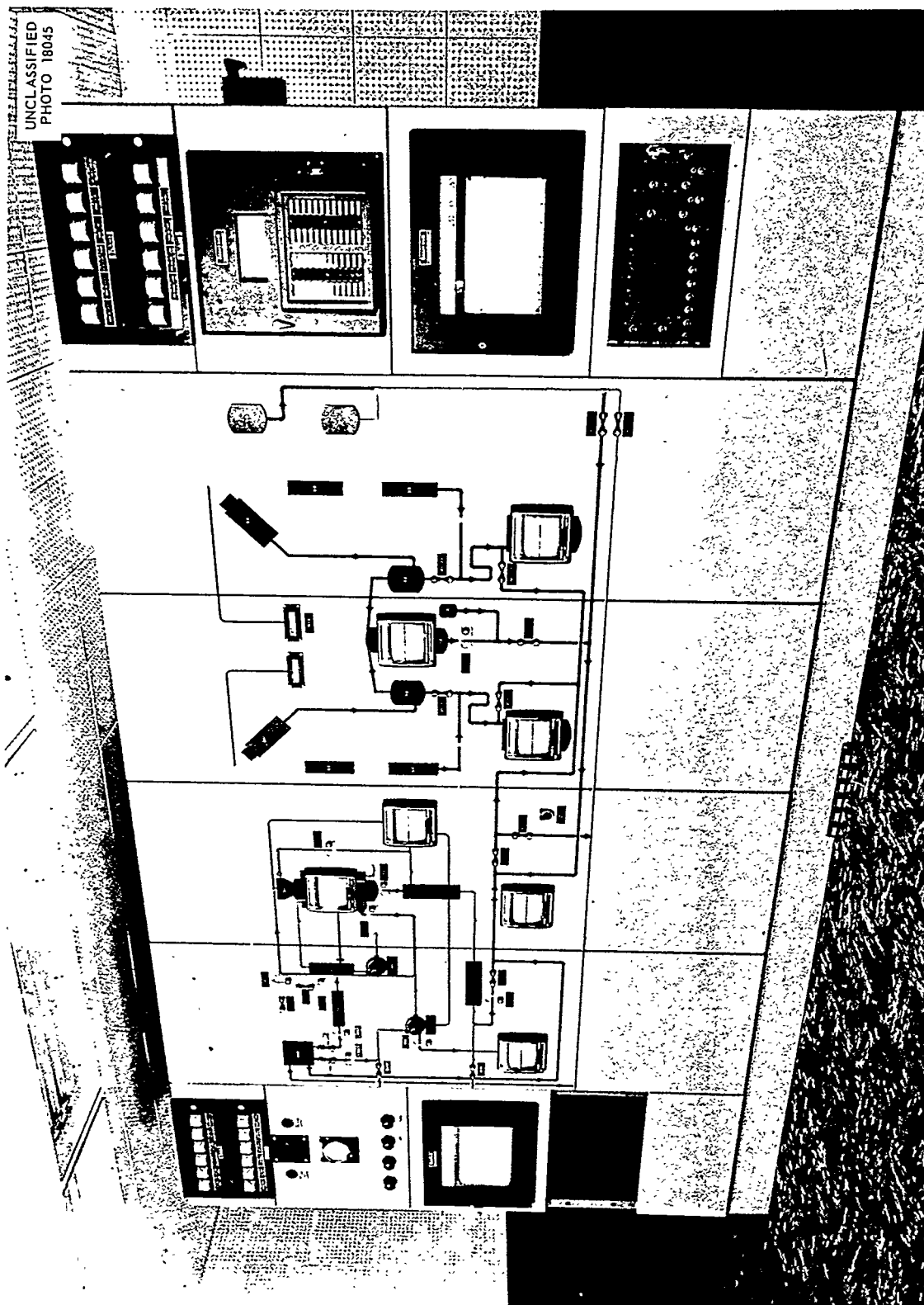
Fig. 5.3. HRT-CP Graphic Control Board.
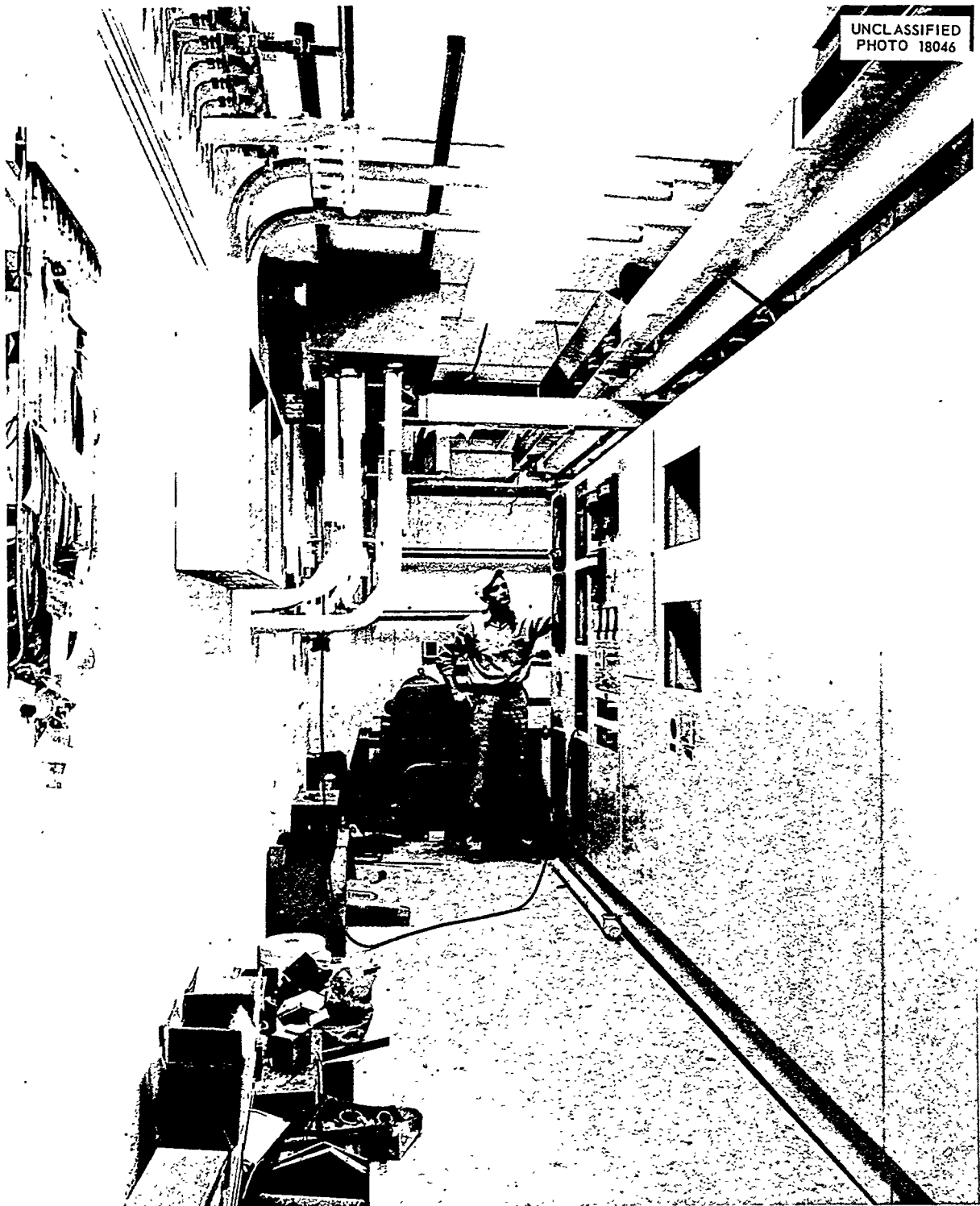
Fig. 5.4. Transducer Rack in Cell D.
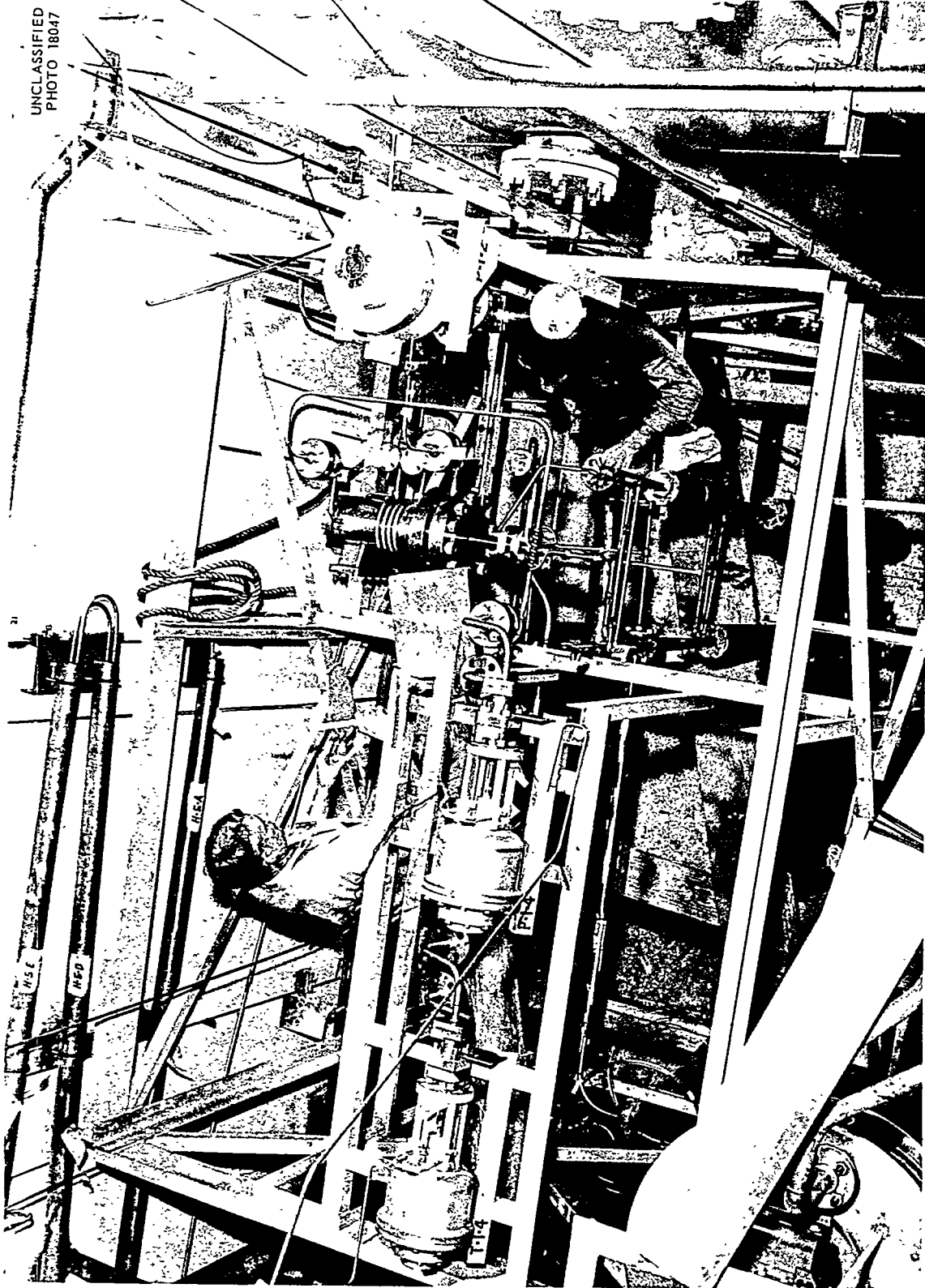
Fig. 5.5. North End of Process Cell Showing High-Pressure Equipment Installation.

VENT

VACUUM

O₂ ADDITION

RUPTURE DISK

P PRESSURE GAUGE

T THERMOCOUPLE

REDUCER

FLOW RESTRICTOR

FIGURES ON LINES INDICATE
NOMINAL PIPE SIZE.

PRESSURIZER (6–SCH 160, 52 in. LONG)

LIQUID LEVEL AT 300°C

VENT

T

400A
PUMP

0–10 gpm
COOLING
WATER

T

T

⅛–SCH 80; FLOW 2 2 gpm, 19 fps

LIQUID LEVEL AT
ROOM TEMPERATURE

SOLIDS FEED
~900 cm³/hr

¼–SCH 80
0.75 gpm

TO CHEMICAL PLANT

3½

FLOW

3

4

T

¼–SCH 80

RETURN

3–SCH 80

400 gpm
19.3 fps

DRAIN
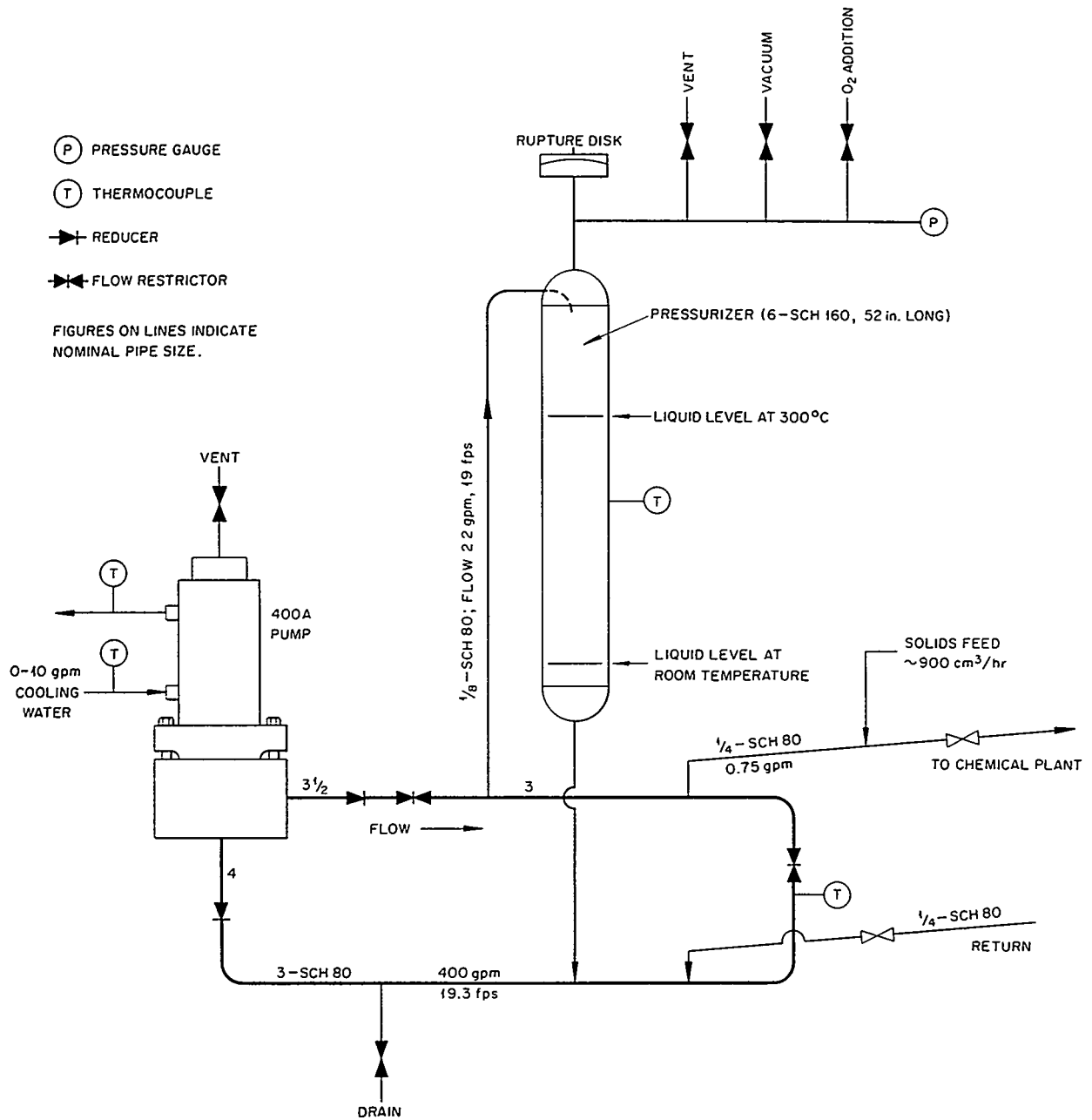
Fig. 5.6. Schematic Diagram of Shakedown Loop.

TORQUE INDICATOR LEVER ARM

SCALE IN INCHES

CLAMP JAW FOR SECURING LOOSENED
BOLT IN SOCKET

EXTENSION CONNECTOR
(FOR VARYING OVERALL LENGTH)

REMOVABLE SOCKET
(ASSORTED SIZES)
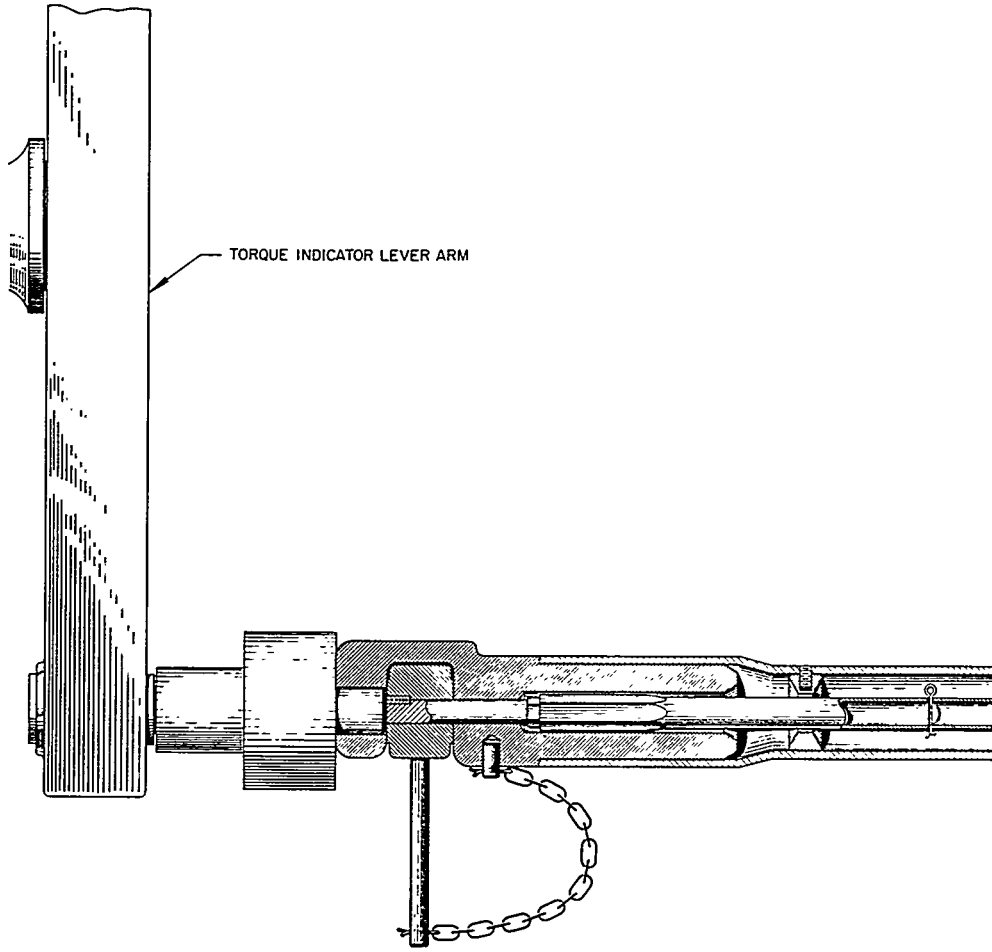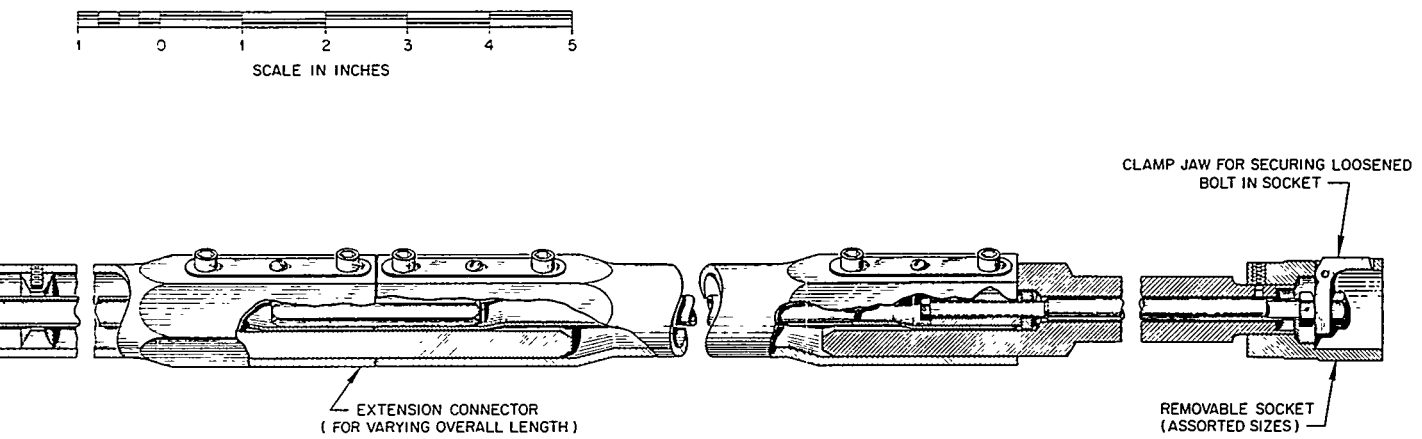
Fig. 5.7. Vertical Valve Wrench Tool.
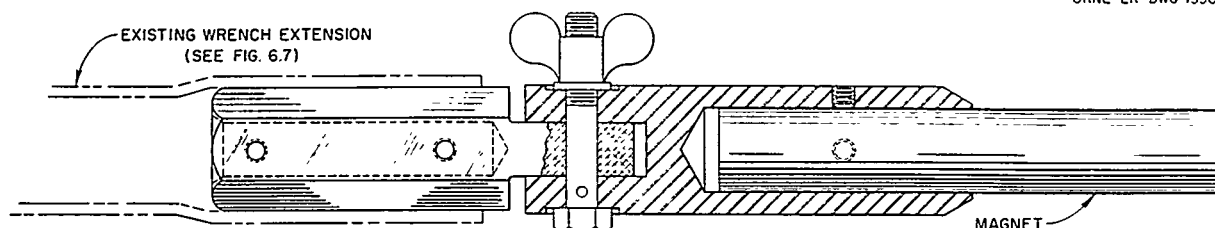
Fig. 5.8. Magnet Adapter.

insulation), failed to produce any indication of leakage. The flanges were equipped with the same leak-detector system planned for the HRT-CP process equipment. The octagonal gasket offers considerably greater mechanical strength, suffering only negligible sealing-face deformation under high compression. The only disadvantage of the octagonal gasket — increased bolt loading during temperature cycling — derives from the resistance of the octagonal gasket to deformation. Compression sleeves, or disk springs, may be required to increase the effective extensibility of the bolts to reduce bolt loading during temperature cycling.

5.4.2 Underflow-Pot Test

The heat-transfer coefficient of the HRT-CP underflow pot was measured for both heating and cooling conditions with water in the pot and air circulated through the jacket. The coefficient was determined as 25 Btu/hr·ft²·°F for an air flow of 45 scfm and 35 Btu/hr·ft²·°F for an air flow of 86 scfm. (The underflow pot was designed on an assumed coefficient of 15 Btu/hr·ft²·°F.)

Heating of the underflow pot from room temperature to 300°C, when the design air-heater capacity of 13.6 kw was used, required 6 hr. Since the desired heatup time is 4 hr, two additional heaters of 3.4 kw each have been added, to give a total of 20.4-kw capacity.

It was determined from tests that the freeze plug located on the lower outlet immediately adjacent to the base of the underflow pot could be frozen satisfactorily, even while the pot was at 300°C. The ice plug held against 2000 psi while the contents of the pot were at 300°C.

5.5 HRT BLANKET PROCESSING

The HRT will be operated initially with a D_2O blanket. Later, the D_2O blanket will be replaced with a uranyl sulfate solution containing ~355 g of natural or depleted uranium per kilogram of D_2O to demonstrate the production of plutonium. The expected corrosion of the reactor components by the concentrated uranyl sulfate solution will limit the period of the demonstration from 30 to 60 days of operation at a blanket temperature of 260°C.

The procedure for processing the blanket (Fig. 5.9) will be similar to that for the core solution. A stream of blanket solution of about 1 gpm rate will be removed on the high-temperature side of the blanket-system heat exchanger and routed through a hydroclone for solid-liquid separation. Plutonium, as PuO_2, and insoluble corrosion-product oxides, will be concentrated by the hydroclone in the underflow receiver.

The hydroclone and underflow receiver will be an integral unit of about 10-gal capacity. It has been calculated that in ten days sufficient PuO_2 should collect in the underflow receiver for a readily measurable concentration to be obtained, at which time the unit will be isolated from the blanket, lowered in temperature and pressure, and drained to the subsequent processing step. In the meantime the hydroclone will be put on-stream for another 10-day cycle.

The discharged underflow-receiver contents will be evaporated for D_2O recovery, and the solids will be dissolved for sampling. The dissolver solution will be stored for decay. Although a dissolving process has not been developed, it is expected to be similar to the 10.8 M H_2SO_4 process to be employed for dissolving solids collected from the core fuel. The solids from the two processes will be the same except that PuO_2 will be in the blanket solids. The evaporation for D_2O recovery and the light-water dissolving will be carried out in the same vessel, with the attendant risk of contamination of the D_2O reactor system with H_2O from the dissolving operation.

35
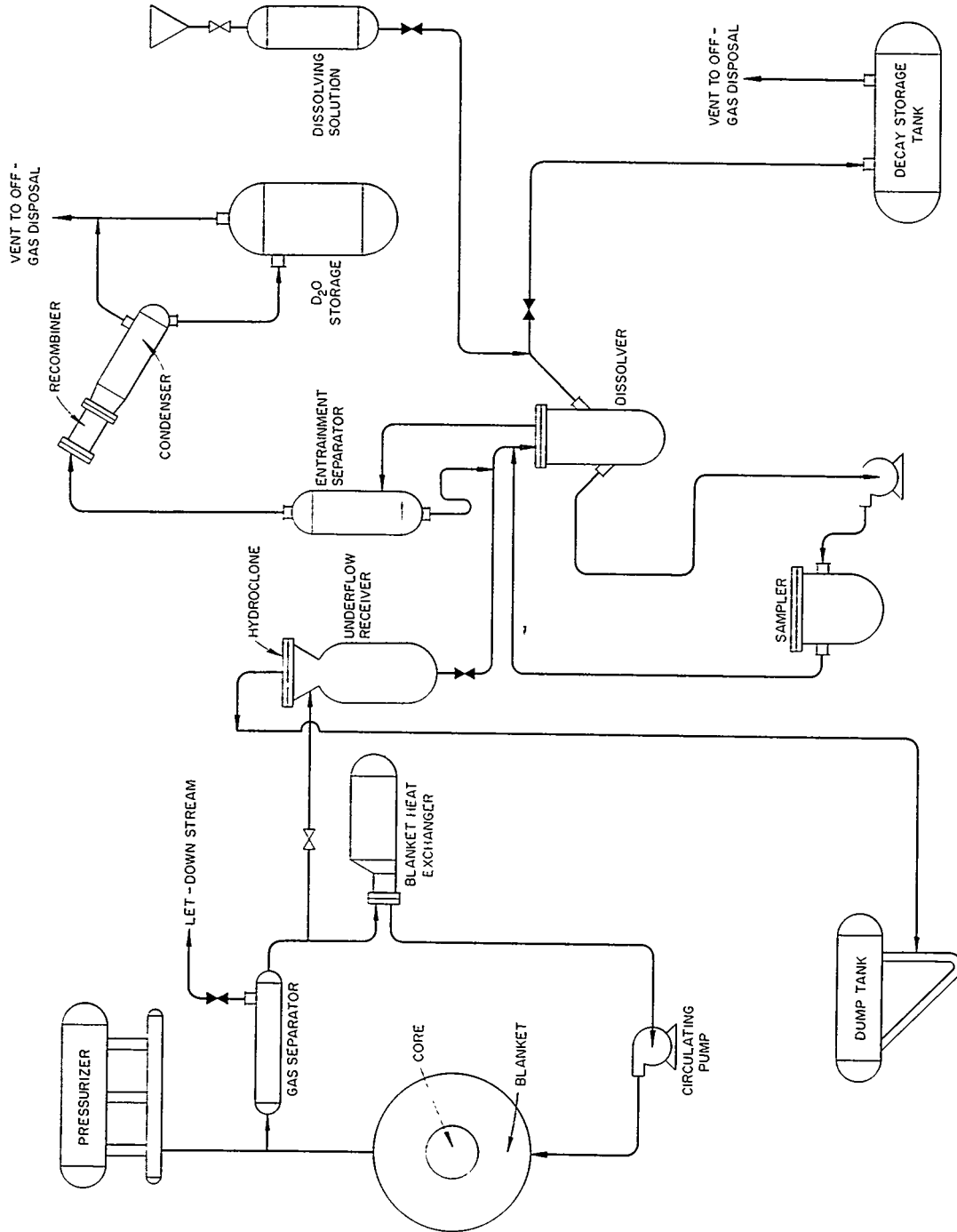
Fig. 5.9. Schematic Flow Diagram of Blanket Processing Plant.

36

Part II

REACTOR DESIGN AND ANALYSIS

J. A. Lane

6. HOMOGENEOUS RESEARCH REACTOR

W. R. Gall

R. E. Aven	P. R. Kasten	R. A. McNees
M. L. Carter	M. I. Lundin	C. Michelson[1]
D. R. Gilfillan[1]	M. C. Lawrence[3]	C. W. Nestor, Jr.
R. F. Hughes[2]	H. A. McLain	C. L. Segaser

A study to determine the feasibility of a circulating-fuel, aqueous homogeneous reactor to provide high-neutron-flux (10^{15} to 10^{16} neutrons/$cm^2 \cdot$ sec) facilities for research purposes was completed. As the purpose of the study was to delineate the nature, scope, and relative importance of the problems related to the construction of such a reactor rather than to obtain the optimum solutions of such problems, the study was limited to consideration of the design and layout of only the major components.

A single-region reactor, with enriched uranium as fuel and with heavy water as moderator and coolant, was selected for the study. The core vessel, constructed of stainless-steel-clad carbon steel and designed for an internal operating pressure of 1400 psi, has an inside diameter of 10 ft and a gross volume of 14,800 liters. One vertical and six horizontal zirconium thimbles are provided in the core for the insertion of experimental facilities. Two 17,650-gpm canned-rotor pumps circulate the fuel solution to the six main heat exchangers. The latter are two-drum units consisting of steam drums and vaporization sections interconnected with risers and downcomers to enhance circulation.

Although the development of economical power was not considered as a major design criterion, 500 Mw of heat energy, at temperatures ranging from 225 to 275°C, would be produced; therefore the generation of usable electric power as a means of heat dissipation was investigated.

The principal conclusion drawn from the study is that the construction of a homogeneous reactor with the parameters indicated by Table 6.1 is within the realm of economic and technological feasibility.

The present state of homogeneous reactor technology is deemed adequate for the design, development, and construction of a reactor of this scale. An intensive engineering effort to resolve such problems as assuring the integrity of the large-scale components involved under the conditions imposed by the use of uranyl sulfate, maintaining the plant under long-term continuous operating conditions (particularly in light of the primitive state of the maintenance art), and developing adequate fast flux and experimental facilities would be associated with the construction of the proposed reactor.

---

[1]On loan from TVA.

[2]On loan from Kaighin & Hughes, Inc.

[3]On loan from General Dynamics Corp.

TABLE 6.1. DESIGN CRITERIA FOR THE HOMOGENEOUS RESEARCH REACTOR

Reactor type	Single region, circulating fuel, homogeneous
Fuel solution	$UO_2SO_4 + D_2O + CuSO_4 + D_2SO_4$
Moderator	D_2O
Coolant	D_2O
Total uranium concentration, g/liter at 250°C	10
U^{235} concentration, g/liter at 250°C	0.8
$CuSO_4$ to recombine 100% of gas, M	0.02
D_2SO_4 to stabilize uranium and copper, M	0.02
Maximum nickel concentration, M	0.01

TABLE 6.1 (continued)

Fuel-solution temperature, °C	
Inlet to reactor vessel	225
Outlet of reactor vessel	275
Average	250
Fuel-system pressure, psia	1400
Neutron flux, neutrons/cm^2·sec	
Thermal (maximum)	6.5×10^{15}
Fast (maximum)	1×10^{15}
Power density, kw/liter	
Maximum (at reactor center)	110
Average	34
Minimum (at reactor wall)	1.9
Gross heat, Mw	500
Reactor vessel	
Inside diameter, ft	10
Total volume, liters	14,800
Net fluid volume (approx), liters	12,000
Shell material	Carbon steel clad with type 347 stainless steel
Experimental facilities	
Horizontal	Six Zircaloy-2 thimbles
Vertical	One Zircaloy-2 thimble
Inside diameter, in.	6
Wall thickness, in.	3/4
External system	
Construction material	Type 347 stainless steel, HRP-grade
Allowable velocities, fps	
225°C	10–15
250°C	25–35
275°C	30–40
300°C	40–50
Total external system holdup (approx), liters	46,000
Reactor control	Negative temperature co-efficient of reactivity
	Fuel concentration
Heat dissipation	Equivalent to 125 Mw of electrical power

7. REACTOR ANALYSIS

P. R. Kasten

H. C. Claiborne   M. P. Lietzke

T. B. Fowler   C. W. Nestor, Jr.

M. Tobias

7.1 FUEL COSTS FOR BATCH-OPERATED REACTORS

H. C. Claiborne   T. B. Fowler

The fuel costs of homogeneous reactors whose fuel is processed on a batch basis rather than on a continuous basis are still being investigated. Previous studies[1] have dealt with U^{235} burner-type reactors.

The studies reported here were confined to those of spherical, one-region power reactors utilizing an initial loading of slightly enriched uranium in the form of a UO_2SO_4-D_2O solution, both with and without Li_2SO_4 additive. In all cases the subsequent feed enrichment was 93.5% U^{235}. The total reactor power was assumed to be 480 Mw (thermal), and the corresponding net electrical capability was taken as 125 Mw, with an 0.8 load factor. All inventory charges were based on 4% per year, the cost of D_2O was taken as $28 per pound, and the cost (and value) of uranium as a function of enrichment was taken from the current AEC-listed values.

A summary of the fuel costs obtained is given in Table 7.1. More details for costs and isotope concentrations for five reactors are reported in Table 7.2. Examination of Table 7.1 indicates that the following general conclusions reached for burner reactors[1] are also applicable for these cases:

1. Economical operation is possible with no fuel processing for periods of time exceeding the probable reactor lifetime.

2. From an economic viewpoint the desirability of chemical processing of the spent fuel at reactor shutdown is at best marginal on the basis of the current AEC-listed value for fully enriched uranium ($17.10 per gram of U^{235}).

A comparison of previous results with the data given in Table 7.1 indicates that it may be possible to lower the fuel costs from 4 mills/kwhr to nearly 2 mills/kwhr if the initial fuel enrichment

is lowered from 93.5 to about 8%. For uranium concentrations of several hundred grams per liter, however, the formation of two phases is almost certain to occur at the 300°C maximum reactor temperature. It has also been demonstrated that the addition of Li_2SO_4 in molar concentration equal to the uranium will increase the temperature at which phase separation occurs. The addition of Li_2SO_4 (99 to 98% Li^7) (cases 5, 6, and 7) to the fuel solution raised the fuel cost slightly, the maximum increase being about 0.1 mill/kwhr.

The use of hydroclones (cases 9 and 10) for partial poison removal (assuming no plutonium removal) for these reactors showed an economic advantage, particularly in the "throwaway" fuel costs (no uranium or plutonium recovery). In these latter costs the removal of fission-product poisons reduced the fuel costs by 0.3 to 0.4 mill/kwhr for 20-year operation. The results indicate that operation in this manner makes chemical processing of the fuel uneconomical if the fuel costs used here apply. In view of its low solubility, however, plutonium would be extracted along with the fission-product poisons. The economic feasibility of hydroclones under these circumstances, in a power-only economy, would thus be dependent upon the savings effected by poison removal relative to the costs associated with recovery of the plutonium for fuel use.

The use of Li_2SO_4, high uranium concentrations, and excess acid increases the solubility of plutonium, but at present the complete picture is unavailable. If plutonium is considered to be removed continuously by the hydroclones (case 8), a slightly negative fuel cost results when a premium credit of $40 per gram is taken for the high-quality plutonium produced. This value, however, would not be realistic in a power-only economy.

7.2 EFFECT OF Xe^{135} RETENTION UPON REACTOR BEHAVIOR

M. Tobias   M. P. Lietzke

If aqueous homogeneous reactors are operated with complete recombination of the decomposition

---

[1]H. C. Claiborne and T. B. Fowler, *HRP Quar. Prog. Rep. April 30, 1956*, ORNL-2096, p 57.

TABLE 7.1. FUEL COSTS FOR BATCH-OPERATED HOMOGENEOUS REACTORS[a]

Case No.	Hydroclone Cycle (days)	Additive[b]	Initial Uranium Concentration (g/liter)		Fuel Costs[c] (mills/kwhr)			
					10-Year Operation		20-Year Operation	
			U^{238}	U^{235}	Uranium and Plutonium Recovered	No Uranium and Plutonium Recovered	Uranium and Plutonium Recovered	No Uranium and Plutonium Recovered
1	∞		100	2.72	2.94	2.99		
2	∞		200	4.18	2.67	2.66	2.61	2.67
3	∞		300	5.99	2.59	2.55	2.42[d]	2.48
4	∞		400	8.32	2.64	2.61	2.34[d]	2.44
5	∞	Li_2SO_4	100	2.99	2.96	3.02	2.96	3.03
6	∞	Li_2SO_4	200	4.82	2.70	2.71	2.62	2.69
7	∞	Li_2SO_4	300	7.21	2.64	2.65	2.44[d]	2.53
8	1		300	5.99	-0.14			
9	1[e]		300	5.99	2.43	2.23	2.24[d]	2.16
10	1[e]		400	8.32	2.49	2.26	2.16[d]	2.07

[a]Average temperature, 280°C; power, 480 thermal Mw, 125 electrical Mw; diameter, 6 ft; system volume, 27,240 liters; fuel solution, UO_2SO_4-D_2O.

[b]Molar concentration of additive was assumed to be equal to the total molar concentration of uranium.

[c]Based on the assumption that the fuel processing plants are servicing fuel solutions of reactors large enough to make the fixed charges for chemical processing negligible.

[d]Details in these cases are shown in Table 7.2.

[e]Plutonium was assumed to be completely soluble and not removed by hydroclones.

TABLE 7.2. ISOTOPE CONCENTRATIONS AND COST BREAKDOWN FOR BATCH-OPERATED
HOMOGENEOUS REACTORS*

(20-Year Operation)

Initial U^{238} concentration, g/liter	300	400	300	300	400
Initial U^{235} concentration, g/liter	5.99	8.32	7.21	5.99	8.32
Hydroclone cycle, days	∞	∞	∞	1	1
Additive	0	0	Li_2SO_4	0	0
Average U^{235} feed rate, kg/year	136	128	136	114	104
Initial U^{235} inventory, kg	163	227	196	163	227
Number of shipping casks	292	355	295	280	341
Final poison fraction	0.27	0.21	0.25	0.13	0.10
Final isotope concentration, g/liter					
U^{234}	1.22	1.36	1.28	0.74	0.90
U^{235}	12.2	16.0	13.2	5.52	7.60
U^{236}	13.9	13.1	14.0	12.2	11.5
U^{238}	223	311	223	217	306
Np^{239}	0.03	0.04	0.03	0.04	0.04
Pu^{239}	3.54	6.12	3.95	1.97	3.65
Pu^{240}	3.62	6.06	4.04	2.12	3.96
Pu^{241}	1.24	2.05	1.38	0.74	1.38
Estimated costs, mills/kwhr					
Uranium inventory	0.08	0.12	0.11	0.08	0.12
D_2O inventory and losses	0.19	0.19	0.19	0.19	0.19
Uranium feed	2.12	2.01	2.12	1.78	1.63
Chemical processing	0.18	0.25	0.18	0.16	0.23
Hydroclones	0.04	0.04	0.04	0.04	0.04
Shipping	0.04	0.04	0.04	0.04	0.04
Plutonium sale (credit)	0.07	0.12	0.08	0.04	0.08
Diffusion plant (credit)	0.12	0.15	0.12	0.01	0.01
Total (fuel cost)	2.42	2.34	2.44	2.24	2.16

*Same conditions as listed in Table 7.1.

gases and no letdown from the high-pressure system, there will be virtually complete retention of the fission fragments and the fission-product gases within the reactor system. Under such conditions, partial or total reactor shutdown would lead to an increase in Xe^{135} concentration, which might, in turn, lead to difficulties in maintaining criticality or reaching criticality upon subsequent full-power demand. Calculations were therefore performed,[2] to investigate the above effect, for a 4-ft-dia spherical reactor operating at 280°C, containing U^{235}, heavy water, I^{135}, and Xe^{135}, and operating at initial fluxes of 10^{13} to 10^{15} neutrons/cm²·sec. For these cases the reactor power was reduced either to zero or to one-tenth the initial value, and the fuel

concentration required for criticality was obtained for times following the power reduction. At the time that the xenon concentration reached a maximum value the power was returned to its original level, and at this point the maximum rate of reactivity addition associated with xenon burnout was obtained. The rate of change in fuel concentration required to maintain criticality at this point was also obtained. In addition, the time required for the xenon concentration to reach a minimum value following return to power was evaluated. The maximum change in xenon concentration was used to estimate the total reactivity addition associated with xenon buildup and was interpreted in terms of fluid temperature changes required to maintain criticality if the fuel concentration were maintained constant. Table 7.3 summarizes the results obtained and, for comparison purposes, also includes results for a reactor of infinite diameter.

---

[2]M. Tobias, *Effect of Xe^{135} Retention upon Homogeneous Reactor Behavior,* (CF memorandum to be issued).

TABLE 7.3. EFFECT OF Xe^{135} UPON REACTOR CONDITIONS FOLLOWING SHUTDOWN
AND RETURN TO POWER

Case	Reactor Diameter (ft)	$\phi_0^{(a)}$ (neutrons/cm²·sec)	$\dfrac{P^{(b)}}{P_0}$	$\dfrac{-1}{N(25)}\dfrac{dN(25)^{(c)}}{dt}$ (sec⁻¹)	$\dfrac{dk_e^{(d)}}{dt}$ (sec⁻¹)	$\Delta k_e^{(e)}$	$\Delta T^{(f)}$ (°C)	$t_{min}^{(g)}$ (hr)
1	4	10^{13}	0.1	2.7×10^{-6}	6.5×10^{-7}	0.0075	2	10
2	4	10^{13}	0	3.0×10^{-6}	7.4×10^{-7}	0.0086	2	10
3	4	10^{14}	0.1	6.8×10^{-5}	1.7×10^{-5}	0.090	20	5
4	4	10^{14}	0	8.5×10^{-5}	2.1×10^{-5}	0.13	30	5
5	4	10^{15}	0.1	6.9×10^{-4}	1.7×10^{-4}	0.17	60	1
6	4	10^{15}	0	3.5×10^{-4}	8.6×10^{-5}	0.33	(b)	3
7	∞	10^{15}	0	6.9×10^{-4}	3.6×10^{-4}	0.52	(b)	2

[a] Initial value of thermal flux before shutdown; averaged over high-pressure system.

[b] Power during shutdown relative to power before and after shutdown.

[c] Relative rate of change in fuel concentration required to maintain criticality at time of return to power (no change in fluid temperature).

[d] Rate of reactivity addition due to xenon burnout at time of return to power.

[e] Estimate of reactivity associated with removal of Xe^{135} at time of maximum xenon concentration.

[f] Estimate of fluid temperature decrease if reactivity addition associated with xenon buildup were compensated by fall in reactor temperature.

[g] Estimate of the time required for xenon concentration to reach a minimum value following return to power.

[h] Cannot maintain criticality by decrease in reactor temperature alone.

As given in Table 7.3, the rates of reactivity addition associated with xenon burnout are low, being less than 0.03% Δk_e/sec for an extreme case. Since permissible rates of reactivity addition are usually greater than 0.1% Δk_e/sec, no immediate reactor safety problem appears to be associated with xenon burnout. Of more concern would be the method of maintaining criticality during the period of xenon buildup. The methods considered here were concentration control and temperature control.

The primary disadvantage in concentration control alone appears to be the relatively high fuel concentrations required to maintain criticality during xenon transients. For example, if the flux were initially 10^{14}, maintenance of criticality following a 90% reduction in power would require a 35% increase in fuel concentration (for 10^{15} initial flux, the fuel concentration would have to be doubled). Also, although the rates of fuel concentration or dilution required for criticality may appear to be small, they are probably as large as might be reasonably attained in an actual reactor system.

An alternative to concentration control would be to allow the reactor temperature to drop during xenon buildup and to rise during a decrease in xenon concentration. On the basis of Table 7.3 results, this appears to be a reasonable method if the initial flux is no greater than about 10^{14} neutrons/cm^2·sec. However, the results were for a specific reactor (bare, 4-ft-dia sphere), and, while this method shows promise, its application to different reactors would require individual evaluation.

For initial fluxes of 10^{15} followed by power reductions of 90% or greater, the decrease in temperature required for criticality would be undesirably and perhaps impractically large; so removal of xenon by means other than burnout should be considered. Possible ways of accomplishing this include continuous letdown of fuel solution from the high-pressure system and gas sparging. While preliminary calculations indicate that the xenon can be removed safely at rates as high as ~3% per second, it is clear that a gas-sparging system must be designed with care so that the attainment of higher rates will be prevented.

7.3 MATH AND COMPUTATION

H. C. Claiborne   T. B. Fowler
C. W. Nestor, Jr.

Previous Oracle codes were changed to comply with recent changes in Oracle operation.

The Oracle code for calculating heat generation in materials due to gamma-ray absorption was used to calculate gamma-ray heating in lead, iron, and aluminum samples placed near the Bulk Shielding Reactor.[3] The calculation is based on six energy groups (average energies of 0.5, 1.5, 2.5, 4, 6, and 8 Mev), with a buildup factor and an attenuation coefficient for each group and region considered. A total of 1485 source regions was considered. The following assumptions were used in the calculations:

1. The partially attenuated beam of gammas leaving the core is adequately expressed in terms of an equivalent gamma current of source energy by means of a buildup factor.

2. The gamma current leaving the core is considered as the source term for the reflector.

3. The original direction is preserved in travel through the reflector.

4. The attenuation through the reflector is only a function of the reflector material and the original source energy.

The calculated results checked experimental measurements in the BSF to within ±23% for lead, iron, and aluminum samples placed from 0 to 6 in. from the reactor core face (the calculated values for lead were about 23% high, those for iron were 20% low, and those for aluminum varied from 4% low to 6% high).

---

[3]H. C. Claiborne and T. B. Fowler, *The Calculation of Gamma Heating in Reactors of Rectanguloid Geometry*, ORNL CF-56-7-97 (July 20, 1956).

Part III

ENGINEERING DEVELOPMENT

J. A. Lane

8. DEVELOPMENT OF FUEL-SYSTEM COMPONENTS

C. B. Graham

C. H. Gabbard
B. A. Hannaford
P. H. Harley
P. P. Holz

I. K. Namba
W. L. Ross
I. Spiewak
D. S. Toomb

H. D. Willis

8.1 RECOMBINER DEVELOPMENT

8.1.1 High-Pressure Recombiner Loop

The high-pressure recombiner loop was not operated during this quarter. Titanium and zirconium samples exposed during previous runs were examined;[1] these materials appear to be unsatisfactory for rebuilding the loop.

Two cracks that appeared in type 347 stainless steel during the last run[2] were examined metallographically. One of the cracks, in a weld, was apparently caused by stress-corrosion originating in the poorly penetrated root of the weld. The other was an intergranular crack in a pipe bend; its cause has not yet been determined.

It is planned to rebuild the loop with either type 309 stainless steel or Incoloy, depending on availability of materials. These materials should be superior to type 347 stainless steel in resistance to corrosion cracking.

8.1.2 Battelle and Syracuse Subcontracts

The Battelle investigation of explosive limits was completed, and their final report will be available shortly.

Syracuse University completed the phases of their work dealing with viscosity of steam-gas mixtures and the detonation of H_2-O_2-steam mixtures in a long 0.434-in.-ID tube. The final reports are in preparation.

The reaction limits of stoichiometric H_2-O_2 in steam in the 0.434-in.-ID tube, as determined by Syracuse, are shown below.

Type of Reaction	Mole % $2H_2$-O_2
Detonation	50 and up
Explosion	44–50
Partial reaction	22.4–44
No reaction	Below 22.4

8.2 SMALL REACTOR COMPONENTS

8.2.1 20-cfm Canned-Rotor Blower

The 20-cfm canned-rotor blower failed to achieve the specified head-flow characteristics during the initial performance test by Allis-Chalmers. A new main impeller is being fabricated, and Allis-Chalmers expects to retest the unit late in July. The blower must also undergo a hydrostatic test before it is accepted by ORNL.

Fabrication of the test-loop facilities at ORNL was completed as far as practicable prior to the actual receipt of the gas-circulating unit.

8.2.2 Small Circulating Pumps

Three 5-gpm ORNL pumps with series-connected stator windings are being operated with water. They continue to perform well, with the exception of one stator failure on a pump operating at 250°C and 1000 psi. The failure, after 2618 hr of stator operation, is attributed to excessive moisture on the stator windings as a result of condensation on the cooling-water coils and cooling-water leakage.

8.3 4000-gpm LOOP

A run of 481 hr was made[3] in order to determine the effect of low oxygen concentration on the corrosion of materials in UO_2SO_4 solution containing 10 g of uranium per liter. During the major part of the run, the oxygen concentration was below 20 ppm. A rapid rise in concentration of dissolved cobalt was noted, indicating probable wear of Stellite pump parts.

The accumulated loss of Stellite from the wearing surfaces of the Byron Jackson pump was about 410 g. Examination of the hot region of the pump

---

[1]See Sec. 14.1.4, "Recombiner-Loop Corrosion and Hydrogen Pickup by Zirconium and Titanium," this report.

[2]C. B. Graham et al., HRP Quar. Prog. Rep. April 30, 1956, ORNL-2096, p 65.

[3]J. C. Griess, R. S. Greeley, and S. R. Buxton, HRP Dynamic Corrosion Studies Summary of Run 4000–6; Corrosion in Dilute Uranyl Sulfate Solution with Very Low Oxygen Concentration, ORNL CF-56-6-12 (June 1, 1956).

showed localized attack that had completely penetrated the Stellite in some places.

The pump will be further disassembled to inspect the Stellite in the cooler region of the pump and to inspect the bearings.

8.4 TITANIUM-LINED EQUIPMENT

The construction of the titanium-lined pipe and the small heat exchangers by Crane Co. and The Pfaudler Co., respectively, has been delayed because of difficulties in procuring materials. The lined pipe is scheduled for completion in October; the delivery date for the heat exchanger is uncertain, since a supplier for the titanium tubing has not yet been found.

8.5 HIGH-PRESSURE FLANGE TEST

The 4-in. 1500- and 2500-lb ring-joint flanges with stainless steel rings were tightened to 32,000 psi bolt stress, after leakage developed in earlier thermal cycles.[4] Considerable leakage was still present when the joints were cycled between room temperature and 600°F. Increasing the stress to 40,000 psi did not improve the situation; leakage became greater with each succeeding thermal cycle. According to strain-gage readings, the bolts relaxed slightly after each cycle. This is

believed to have resulted from plastic deformation of the gaskets.

The flange grooves were remachined and new O-ring gaskets were placed in both the 1500- and 2500-lb flanges. A good fit on all gasket sealing surfaces was verified by the uniform transfer of wet dye from ring to groove. The flanges were made up with a bolt stress of approximately 25,000 psi, as determined by bolt elongation, and then thermal cycled. The leakage per pair of flanges to a vacuum leak detector now averages about 8×10^{-5} g of water per day cold at low pressure and 2×10^{-3} g of steam per day hot at 2000 psi.

8.6 THERMAL-CYCLE TEST FACILITY

The preliminary design of a thermal-cycle facility for testing various reactor components has been started. This system will be used to cycle the spare 5-Mw HRT steam generator according to HRP specification 1113. It is planned also to cycle titanium-lined pipe, the Pfaudler titanium heat exchanger, flanges, and other equipment. The standard thermal cycle will consist in heating from 380 to 580°F in 20 min, a 10-min hold period at 580°F, an 80-min cooling period back to 380°F, and a 10-min hold period at 380°F.

Specifications for a 2000-psi 5000-lb/hr-capacity steam boiler were released for bids. Specifications are being prepared for the other system components.

---

[4]C. B. Graham *et al.*, *HRP Quar. Prog. Rep. April 30, 1956*, ORNL-2096, p 66.

9. DEVELOPMENT OF BLANKET-SYSTEM COMPONENTS

R. B. Korsmeyer

D. G. Davis	C. G. Lawson	M. Richardson
H. N. Fairchild	L. E. McTaggart	A. N. Smith
R. B. Gallaher	I. M. Miller	D. G. Thomas
A. S. Kitzes	R. H. Nimmo	R. P. Wichner
	L. F. Parsly	

9.1 REVIEW OF THORIUM OXIDE CAKING EXPERIENCE

D. G. Thomas

Thorium oxide slurries have been circulated for about 25,000 hr in 100- and 200-gpm loops since October 1953. These tests were made at temperatures from 250 to 300°C and at concentrations from 200 to 1200 g of thorium per kilogram of H_2O, with very pure slurries and with slurries having additives or impurities of sulfate, phosphate, chromate, fluoride, oxygen, hydrogen, and carbon dioxide.

Under a variety of circumstances the slurry did not drain freely from the system at the end of the test. Five different types of accumulated solids have been observed:

1. highly flocculated slurry of low density, having a definite yield stress;
2. soft plug in pressurizer and bypass lines;
3. thin, hard film in regions of high velocity or high impact;
4. thick, hard deposit in interstices of the pump impeller;
5. thick, hard layer deposited uniformly throughout the system.

These types are listed in increasing order of seriousness in a reactor system. The first three would not particularly hinder the circulation of the slurry in the main stream, although the third type could cause a great deal of trouble if it should form in a heat exchanger. The fourth type might tend to unbalance the impeller as well as to impede flow. The fifth deposit would be the most serious one; it would have an adverse effect on heat transfer, be difficult to resuspend, could cause a flow stoppage and pump damage if pieces of cake spall off, and would decrease the concentration of the circulating streams as the deposit builds up.

A typical type 2 plug observed in the pressurizer of T-loop is shown in Fig. 9.1. Note that a small channel was kept open by the flow required to supply the condensate for injection into the rotor cavity of the pump, and as a result there was no interference with the operation of the pressurizer.

A typical type 4 deposit is shown in Fig. 9.2. Two of the five vanes contained the deposit; the remainder were clean.

Two types of deposit (types 2 and 3), that occurred during the same test[1] in CS-loop, in a pin holder in one of three parallel flow lines are shown in Fig. 9.3. The inner deposit was soft and cracked as it dried out, whereas the outer deposit was hard and brittle and did not crack.

A type 5 deposit from the 200A loop[2] is shown in Fig. 9.4. This deposit covered all surfaces in the circulating part of the loop, was from $\frac{1}{8}$ to

---

[1]E. L. Compere *et al.*, *HRP Quar. Prog. Rep. Jan. 31, 1956*, ORNL-2057, p 88.

[2]R. B. Korsmeyer *et al.*, *HRP Quar. Prog. Rep. April 30, 1956*, ORNL-2096, p 67.

Fig. 9.1. Type 2 Plug in Pressurizer.
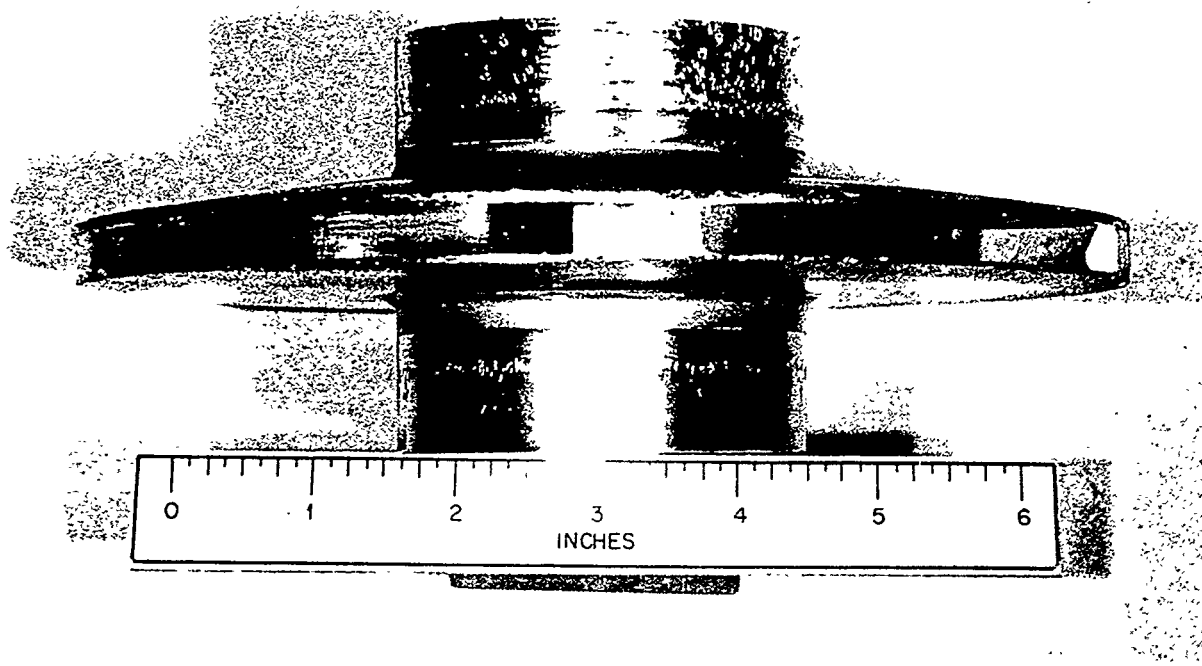
Fig. 9.2. Type 4 Deposit in Impeller.

$\frac{1}{4}$ in. thick, was quite hard and dense, and had a modulus of rupture of 368 psi. The machine tool marks were modeled by the oxide as it was deposited.

Table 9.1 summarizes the experience at ORNL in circulating ThO_2 slurries in the 100- and 200-gpm loops. As can be seen, there was no recognized difficulty in circulating slurry in about 75% of the tests, which accounted for almost 90% of the circulation time.

Since the single occurrence of the hard type-5 cake in October 1955, there have been 30 tests and over 5000 hr of operating experience with no repetitions of this occurrence. In one test in S-loop, boiling and cavitation took place, and a hard cake was observed in the eye of the impeller at the conclusion of the run when the pump was dismantled.

Factors contributing to, if not the sole cause of, cake formation in the cases of type 2, 3, and 4 cakes can be inferred from the conditions of the experiments, although the relationships have not been established. In the only case where a hard cake was deposited throughout a loop, the reason

for the deposition remains completely obscure; it does not appear to have been associated with either heated or cooled surfaces, nor does centrifugal action appear to have been present. The fact that it has not been possible to form such a cake again has made the study of caking problems particularly difficult.

9.2 RHEOLOGY OF THORIUM OXIDE SLURRIES

9.2.1 Laminar Flow

R. H. Nimmo

A survey[3] was made of data for the various ThO_2 slurries which have been tested in a capillary-tube viscometer.[4-6] Analysis of the collected data

---

[3]R. H. Nimmo and A. S. Kitzes, *Collected Data on the Rheologic Properties of ThO_2 Slurries* (to be published).

[4]R. N. Lyon *et al., HRP Quar. Prog. Rep. Jan. 31, 1955,* ORNL-1853, p 147–148; B. A. Kress and D. S. Toomb, *HRP Quar. Prog. Rep. April 30, 1955,* ORNL-1895, p 147–148.

[5]A. S. Kitzes and R. N. Lyon, *Aqueous Uranium and Thorium Slurries,* paper 811, Session 20B, International Conference on the Peaceful Uses of Atomic Energy, August 1955, Geneva.

[6]P. R. Crowley, unpublished material in data books.

Fig. 9.3. Types 2 and 3 Deposits in Pin Holder.

TABLE 9.1. THORIUM OXIDE CAKING EXPERIENCE IN 100- AND 200-gpm LOOPS

(October 1953 to July 1956)

	Number of Tests	Total Circulation Time (hr)
Hard cake deposited throughout system (type 5)	1	143
Thick, hard deposit in interstices of impeller (type 4)	(1)*	(95)*
Thin, hard film in regions of high velocities or high impact (type 3)	2	449
Soft plugs in pressurizers (type 2)	20	1,442
Bypass lines plugged (type 2)	12	996
No circulating difficulties	95	21,584
		24,614

*A type 2 deposit was also observed during this test; therefore the data are not used in calculating the totals.
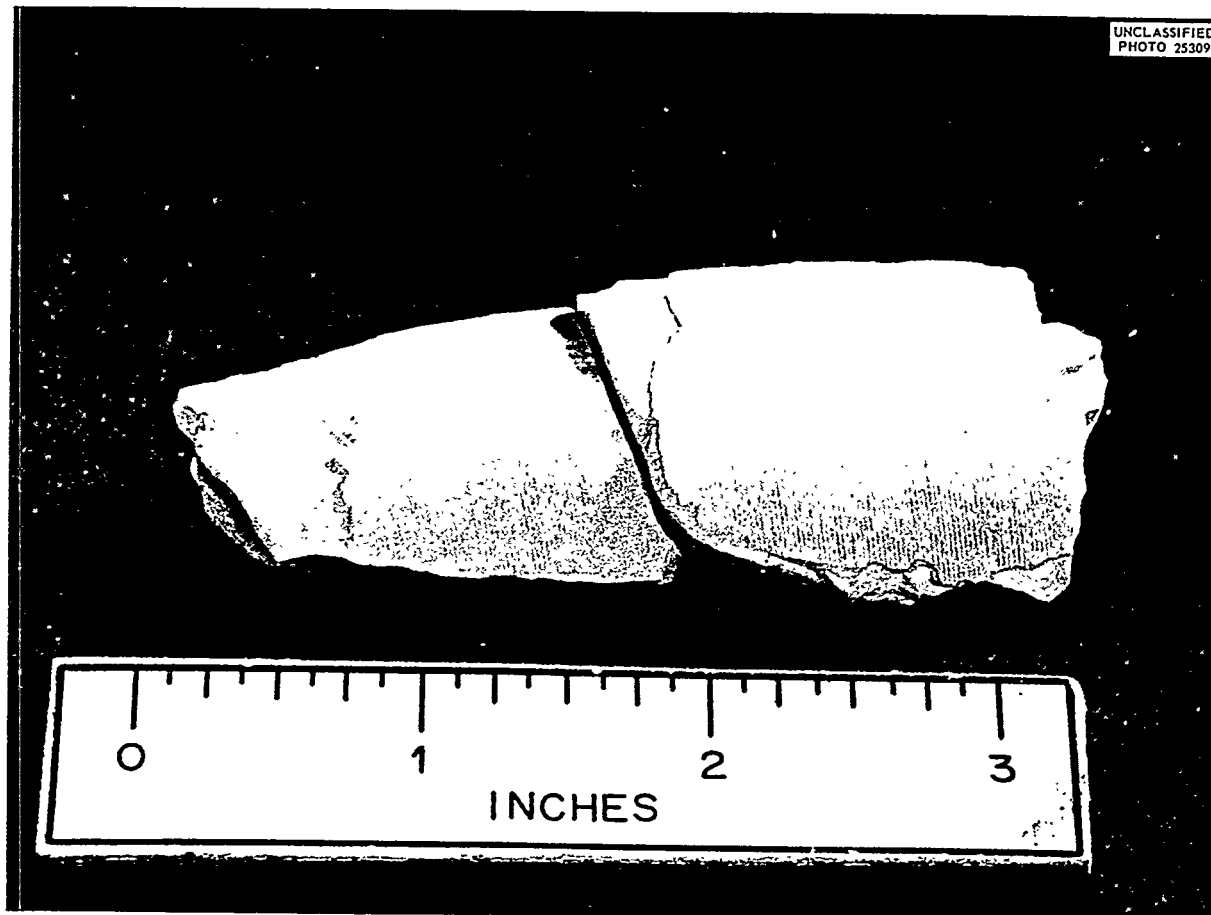
Fig. 9.4. Type 5 Deposit from 200A Loop.

reveals a simple relationship between the yield stress and concentration and that there is no evidence for thixotropy in thorium oxide slurries.

It has been reported[7] that, for a particular Bingham plastic–clay–water suspension, the effect of solids concentration upon the yield stress, τ_y, may be expressed by an equation of the form

(1) $$\tau_y = AC^n ,$$

where

τ_y = yield stress, force per unit area,

C = concentration, volume fraction of solids in relation to total volume,

n = constant = 3 for data of ref. 7,

A = a constant which is characteristic for each slurry.

The data for five different ThO_2 slurries, which were tested in three different viscometer tubes at room temperature over a range of concentrations from 300 to 1500 g of thorium per kilogram of water, are plotted in Fig. 9.5 as log τ_y vs log volume fraction of solids. (Yield-stress values were obtained from data uncorrected for end effect.) As can be seen, there is a linear relationship between these variables, and the average value of the exponent in Eq. 1 is 3.64 ± 0.44.

The presence of thixotropy may be detected from capillary-tube viscometer data by varying the length of the viscometer tubes, a decrease in the apparent viscosity with an increase in tube length being indicative of thixotropy.[8] The pseudo-shear diagrams for such sets of experiments made with

[7]F. H. Norton, A. L. Johnson, and W. G. Lawrence, *J. Am. Ceram. Soc.* **27**, 149–164 (1944).

[8]G. E. Alves, D. F. Boucher, and R. L. Pigford, *Chem. Eng. Prog.* **48**, 385 (1952).
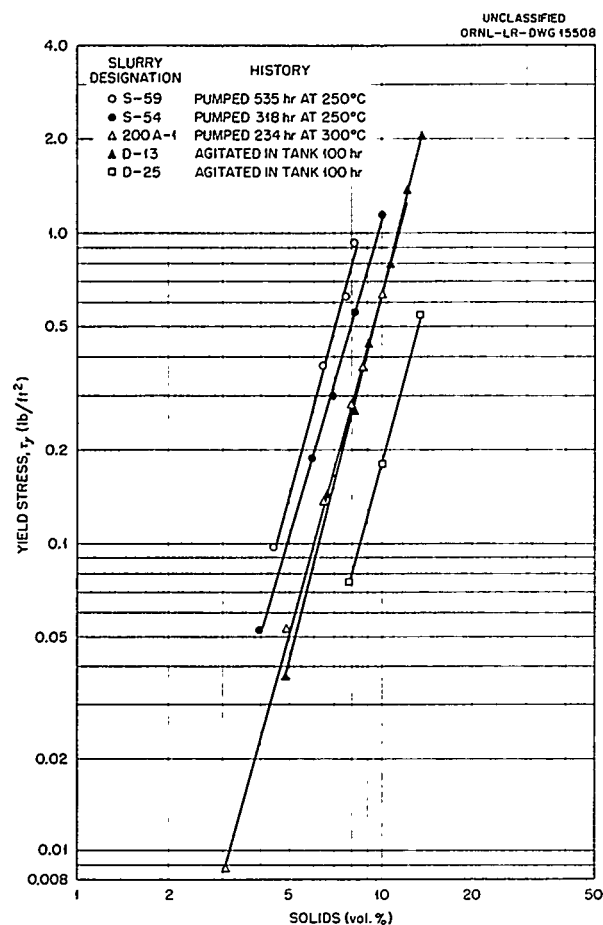
Fig. 9.5. Effect of Slurry Concentration on Yield Stress.

Fig. 9.6. Effect of Tube Length on Pseudo-Shear Diagrams.

different thorium oxide slurries and different-diameter tubes are shown in Fig. 9.6 after correction for end effects by calculating values of $(\Delta P_L - \Delta P_s)/(L_L - L_s)$ for the same slurry velocity through two tubes of different lengths.

Since there is a unique pseudo-shear diagram for each slurry (with no decrease in apparent viscosity with increase in tube length), there is no evidence that these ThO_2 slurries were thixotropic.[9]

9.2.2 Turbulent Flow

C. G. Lawson

It has been shown that the pressure drop for Newtonian and plastic aqueous slurries in turbulent flow can be calculated from the usual friction-factor–Reynolds-number plot, provided that the density is taken as that of the slurry and the viscosity as that of water.[10-17] This relationship has been tested for the data presented last quarter[18] in the form of a Hedstrom[19] plot. The data are plotted in Fig. 9.7 on a standard friction-factor

[9]R. N. Lyon *et al.*, *HRP Quar. Prog. Rep. Jan. 31, 1955*, ORNL-1853, p 147–148.

[10]D. H. Caldwell and H. E. Babbitt, *Trans. Am. Inst. Chem. Engrs.* **37**, 237 (1941).

[11]G. W. Howard, *Proc. Am. Soc. Civil Engrs.* **64**, 1377 (1938).

[12]A. P. Yufin, *Izvest. Akad. Nauk. S.S.S.R., Otdel. Tekh. Nauk.*, No. 8, 1146 (1949).

[13]M. P. O'Brien and R. G. Folsom, *Univ. Calif. Publ., Eng.*, **3**, No. 7, 343 (1937).

[14]A. Hazen and E. D. Hardy, *Trans. Am. Soc. Civil Engrs.* **57**, 307 (1906).

[15]N. S. Blatch, *Trans. Am. Soc. Civil Engrs.* **57**, 400 (1906).

[16]G. E. Alves, D. F. Boucher, and R. L. Pigford, *Chem. Eng. Prog.* **48**, 385–393 (1952).

[17]H. C. Ward and J. M. Dallavalle, *Chem. Eng. Progr., Symposium Ser. No. 10*, 50(1954), p 1.

[18]C. G. Lawson, *HRP Quar. Prog. Rep. April 30, 1956*, ORNL-2096, p 70–74.

[19]B. O. A. Hedström, *Ind. Eng. Chem.* **44**, 651–656 (1952).
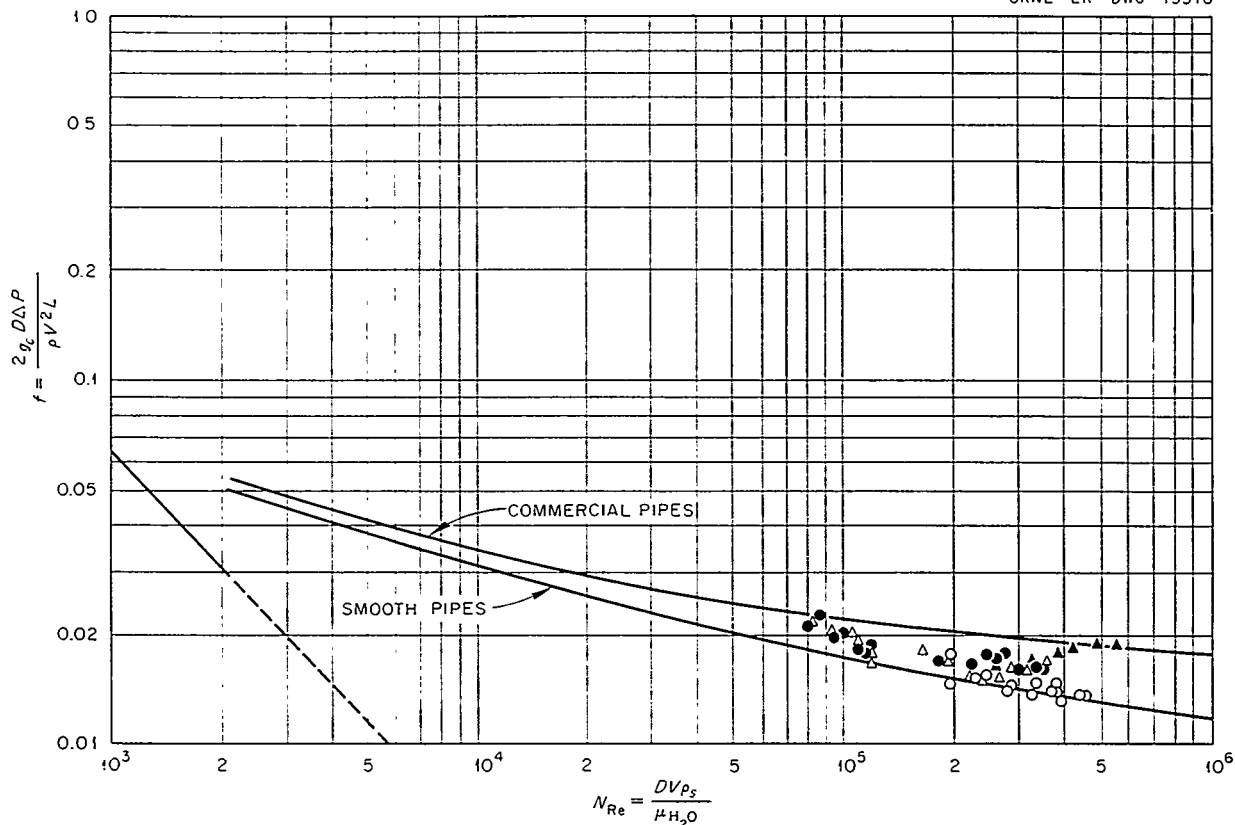
Fig. 9.7. Friction-Factor—Reynolds-Number Diagram for ThO_2 Slurries.

chart[20] containing the curves for commercial pipes and smooth pipes. Essentially all the data are between the two curves, indicating that for the particular ThO_2 slurry and the conditions of these measurements, the pressure drop was that predicted by the method given above.

This suggested the modification of the Hedstrom plot for plastic slurries, shown in Fig. 9.8. The Reynolds number is defined as $DV\rho_s/\eta$, where η is the coefficient of rigidity (instead of $DV\rho_s/\mu_{H_2O}$ used in Fig. 9.7, where μ is the viscosity of water), which translates the Newtonian turbulent-friction-factor curve by the ratio η/μ_{H_2O}. A family of turbulent-friction-factor curves is obtained for slurries with η/μ_{H_2O} as a parameter, thus providing a generalized method for calculating the pressure drop of Bingham-plastic material in turbulent flow as well as in laminar flow.

9.3 HEAT-TRANSFER PROPERTIES OF SLURRIES

C. G. Lawson

The following equation has been derived for forced-convection laminar heat transfer to Bingham plastics:[21]

$$\frac{hD}{k} = 1.615 \left(\frac{WC}{kL}\right)^{1/3} \left(\frac{1 + g_c \tau_y D}{24 \eta V}\right)^{1/3} .$$

Although the equation has not been checked experimentally, it should furnish reasonably accurate predictions of heat-transfer rates when the slurry particles remain homogeneously suspended.

[20] J. H. Perry (ed.), *Chemical Engineers Handbook*, 3d ed., p 382, 1950.

[21] R. V. Bailey, *Forced Convection Heat Transfer to Slurries in Tubes*, ORNL CF-52-11-189 (Nov. 24, 1952).
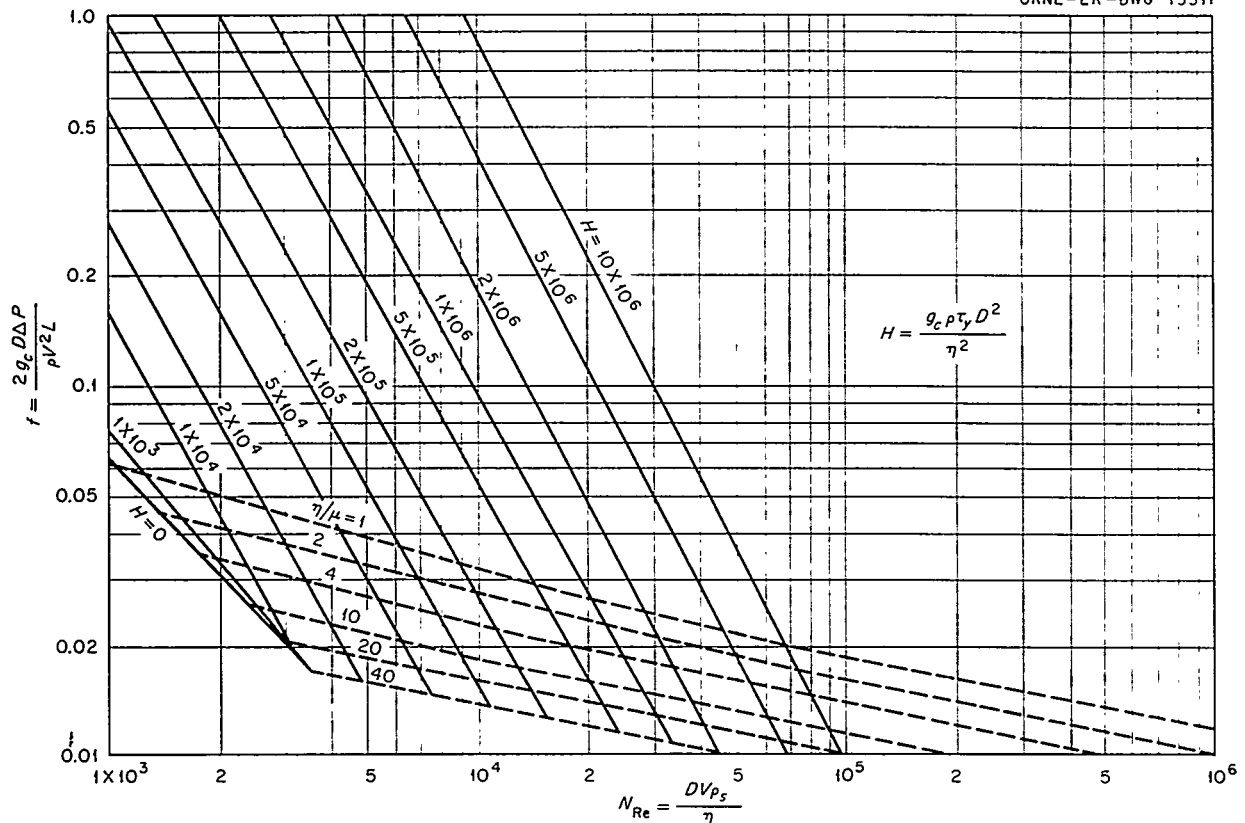
Fig. 9.8. Generalized Friction-Factor Plot for Bingham-Plastic Slurries Flowing in Smooth Pipes.

Forced-convection heat-transfer studies with slurries in turbulent flow have been conducted by several investigators.[22-26] Their results indicate that, for slurries having Newtonian flow characteristics, the heat-transfer coefficients can be calculated from the usual expressions by using the physical properties of the homogeneous slurry.[27]

Atmospheric-pressure heat-transfer data are being obtained for slurries having an appreciable yield stress, and the results are being compared with measurements on water in the same system. Typical data for such tests are shown in Fig. 9.9 in which the heat-transfer coefficient is plotted against the velocity for a slurry having a concentration of 900 g of thorium per kilogram of H_2O, a yield stress of 0.50 lb/sq ft, and a coefficient of rigidity of 0.0024 lb mass/ft-sec. The ratio τ_y/τ_w (where τ_y = yield stress of slurry and τ_w = shear stress at tube wall) was greater than 0.1 for all slurry data in Fig. 9.9, even though the velocities were as high as 24 fps. As can be seen, it is possible to obtain high heat-transfer coefficients for slurries having a definite yield stress, but only at velocities high enough to make τ_y/τ_w small.

[22]J. J. Salamone and M. Newman, *Ind. Eng. Chem.* **47**, 283–288 (1955).

[23]C. J. Bonilla *et al.*, *Am. Inst. Chem. Engrs., Heat Transfer Symposium*, December 1951, Atlantic City.

[24]C. Orr, Jr., Ph.D. Thesis: *The Transference of Heat Between a Pipe Wall and a Liquid-Solid Suspension Flowing Turbulently Inside the Pipe. The Thermal Conductivity and Viscosity of a Liquid-Solid Suspension*, Georgia Institute of Technology (1953).

[25]C. White, M.S. Thesis, Georgia Institute of Technology (1955).

[26]A. P. Miller, Ph.D. Thesis: *A Study of Heat Transfer to Liquid Solid Suspensions in Turbulent Flow in Pipes*, University of Washington (1954).

[27]C. G. Lawson, *A State-of-the-Art Survey on Engineering Calculations for Slurry Systems*, ORNL CF-55-9-165 (Sept. 22, 1955).

UNCLASSIFIED
ORNL-LR-DWG 15512
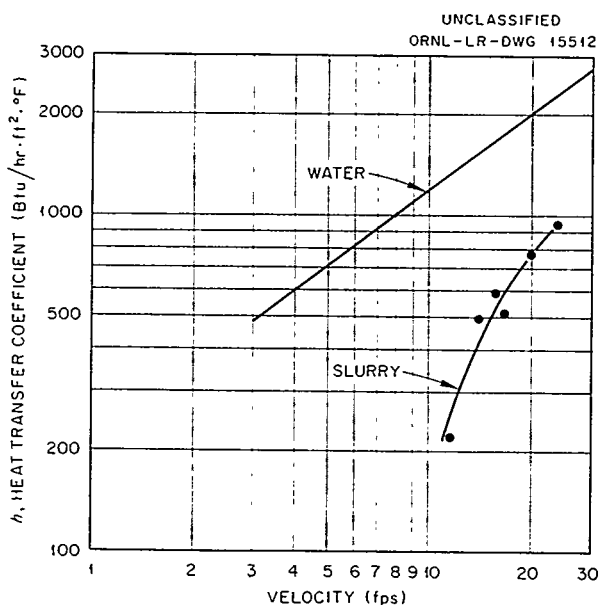
Fig. 9.9. Heat-Transfer Measurements on Thorium Oxide Slurries at Atmospheric Pressure.

9.4 SLURRY COMPONENT DEVELOPMENT AND LOOP OPERATION

9.4.1 200A Pump Loop

R. B. Gallaher

One run, 200A-5B, was completed in the 200A pump loop during the quarter to check the operation of the pump and to demonstrate the feasibility of circulating concentrated slurries at 300°C for extended periods of time. The run was terminated after a total of 1994 hr of operation.

The loop was loaded to give a thorium concentration of 1000 g of thorium per kilogram of H_2O, a sulfate concentration of 1500 ppm as thorium sulfate, and an O_2 partial pressure of 100 psi. During the initial startup,[28] the loop operated normally until the temperature was raised to above 175°C, at which point an erratic behavior of the pump power demand was noted. At the same time, a microphone attached to the stator casing picked up hissing and screeching sounds simultaneously with the larger power peaks. Successive additions of 1 N H_2SO_4 elevated the temperature of the apparent instability until the loop operated at 300°C with no further evidence of such instability.

_____
[28]R. B. Korsmeyer *et al.*, *HRP Quar. Prog. Rep. April 30, 1956,* ORNL-2096, p 67-70.

After the final acid addition the sulfate content of the slurry was 2808 ppm, and the loop was operated for 950 hr without any further changes, with an average slurry concentration of 1100 g of thorium per kilogram of H_2O; the pH of the slurry varied between 5 and 6 during this period.

After 1545 hr of circulation, the loop was cooled to room temperature and fresh oxide was added to increase the concentration to 1350 g of thorium per kilogram of H_2O. Subsequent sampling did not indicate the increase in thorium concentration. The thorium concentration varied between 1150 and 1280 g per kilogram of H_2O, before the addition was made, and between 1170 and 1250 g per kilogram after the addition of fresh slurry. The Fe/Th ratio, however, did decrease by 14.5% with the addition of fresh slurry, although a decrease of 25% in this ratio was expected. The pH of the slurry remained between 5 and 6. On draining the loop at the end of the run for a scheduled shutdown and inspection, substantially all the oxide charged was recovered. No caking or unusual accumulations of solids were found in the pressurizer or main circulating lines, and the solids were easily washed from the system. No satisfactory explanation has been found for the unexpectedly low concentration of oxide in the circulating slurry.

Some pump components suffered wear. The titanium seal rings were badly worn, and the stainless steel casing liner was attacked, as shown in Fig. 9.10. The titanium impeller (Figs. 9.11 and 9.12) was not pitted except on the surface where the accelerated fluid leaves the periphery, although it lost 14.5 g in weight. There was no damage to the Kingsbury thrust bearing or to the back radial bearing; however, the front radial bearing was severely worn, as shown in Fig. 9.13.

By visual inspection, the Graphitar appeared to be porous and powdery, indicating possible oxidation by the oxygenated purge water rather than abrasion by the slurry. This conclusion is supported by the fact that no Graphitar was found adhering to the rotor or stator can. Graphitar usually coated the motor end of the pump in past instances when the radial bearing was abraded by the slurry. The velocity of the slurry in the pipes was about 12 fps, and the generalized loop attack averaged less than 1 mpy, based on the iron contamination found in the slurry. However, the localized attack in areas of high velocity was much greater, as evidenced by the rates of attack listed in Table 9.2 for the stainless steel orifice

Fig. 9.10. 200A Pump Volute Showing Areas of Attack During Run 200A-5B.
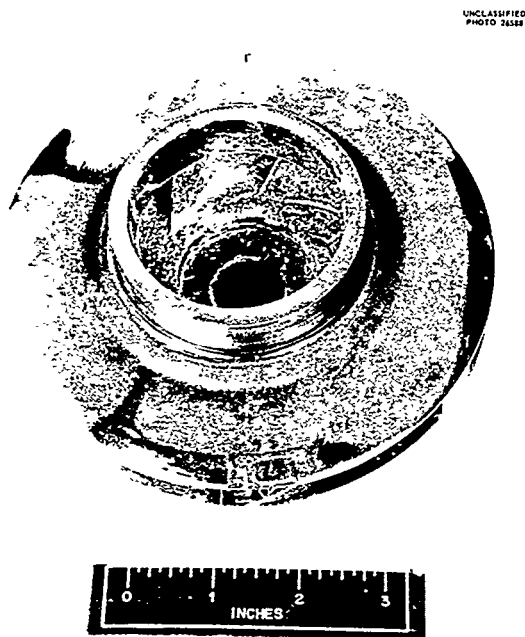
Fig. 9.11. Front Face of Titanium Impeller —
Run 200A-5B.

Fig. 9.12. Rear Face of Titanium Impeller —
Run 200A-5B.

plates (flow restrictors) shown in Fig. 9.14. The
attack rate on stainless steel appears to be pro-
portional to the square of the velocity.

(a) **Automatic Seal-Weld Cutter.** — In order to
eliminate leaks experienced in previous runs at

TABLE 9.2. ATTACK ON STAINLESS STEEL BY
OXYGENATED ThO_2 SLURRY

Orifice No.	Slurry Velocity (fps)	Attack Rate (mpy)
1	36	30
2	43	59
3	52	84
4	65	132

Fig. 9.13. Front Graphitar Radial Bearing —
Run 200A-5B.
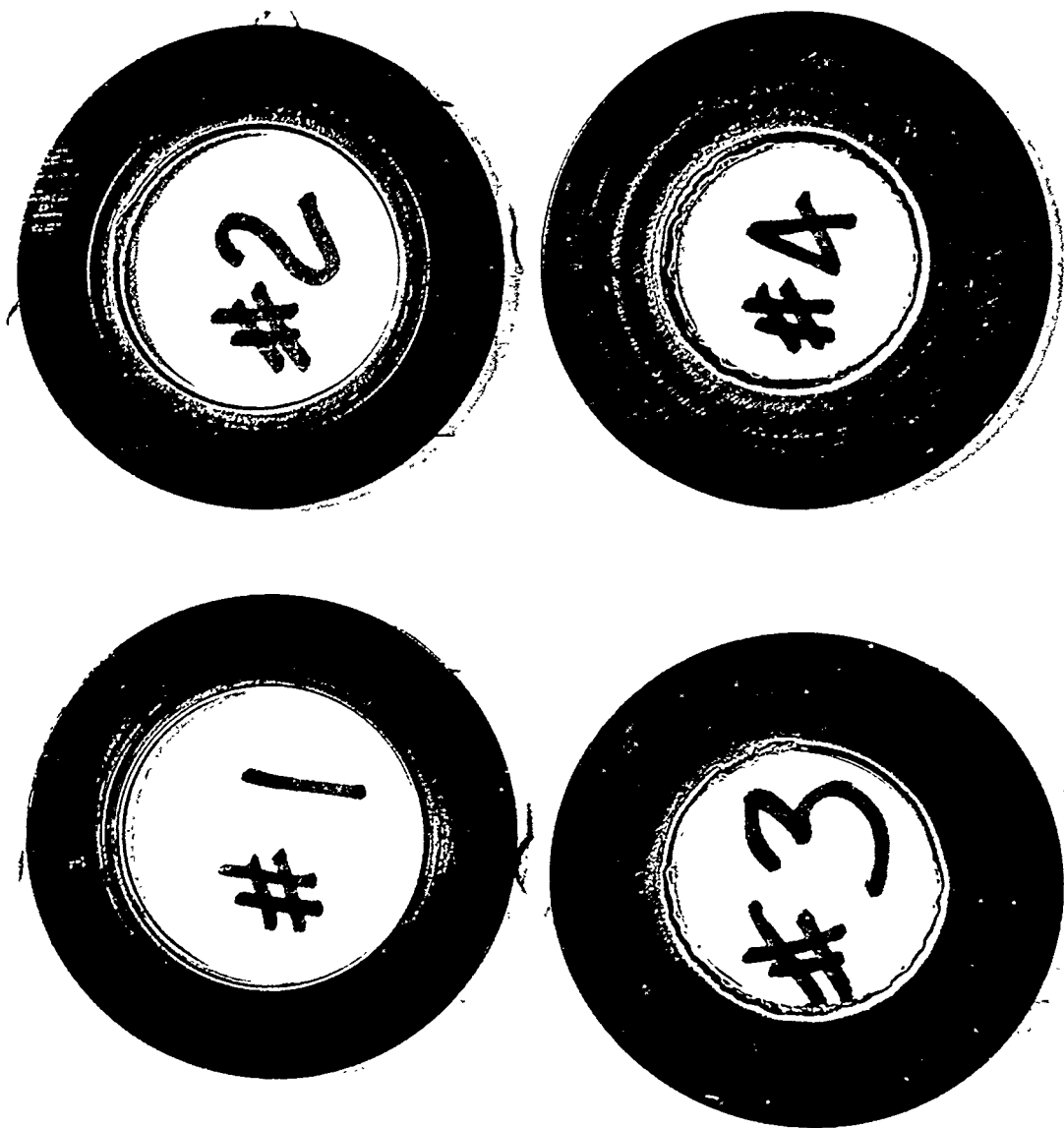
Fig. 9.14. Upstream Faces of Stainless Steel Orifices Showing Attack by Slurry. Run 200A-5B, 1994 hr at 300°C.

300°C and 2000 psi, the main pump flange and thermal barrier of the 200A pump were seal-welded prior to the startup of run 200A-5B. At the end of the run, these welds were removed successfully with the custom-built, manually operated, seal-weld cutter for Westinghouse 150C pumps. Based on this one experience, it is estimated that the pump can be removed from the loop, disassembled, and cleaned within 3 to 4 hr.

9.4.2 Dump Tanks

M. Richardson

The first stage of the project for the development of types of dump tanks feasible for use with slurries has been completed. Two types of dump tanks, one horizontal and the other vertical, have been demonstrated, in small-scale models, to be practical with some slurries.

(a) **Combination Race Track–Vertical Gas Lift.** — The system[28,29] was operated intermittently for several thousand hours with a slurry containing 900 to 925 g of thorium per kilogram of water and approximately 1000 ppm of sulfate as thorium sulfate. No difficulties were encountered in maintaining homogeneity or in resuspending the solids after shutdowns for varying lengths of time up to 30 days.

After the 30-day shutdown, with the bed in each riser leg approximately 18 in. deep, a steam pressure of 3 psig was required to set the bed in motion and keep the solids suspended in 100 liters of slurry.

(b) **Conical Dump Tank with Vertical Gas Lift.** — The vertical-cone dump tank[28,30] was operated successfully for 1400 hr with slurries containing 900 to 2300 g of thorium per kilogram of H_2O and 1000 to 4800 ppm sulfate. A steam pressure of 9 psig was required to move the settled bed; once in motion, only 3.5 psig steam was needed to maintain homogeneity to within ±50 g of thorium per kilogram of H_2O.

The system was operated continuously for 1000 of the 1400 hr of operation with an average slurry concentration of 1100 g of thorium per kilogram of H_2O and 1000 ppm of sulfate. During this phase of the studies, the thorium concentration was varied from 900 to 1500 g per kilogram of H_2O, and

[29]R. N. Lyon *et al.*, *HRP Quar. Prog. Rep. Oct. 31, 1955*, ORNL-2004, p 68–71.

[30]M. Richardson and A. N. Smith, *HRP Quar. Prog. Rep. Jan. 31, 1956*, ORNL-2057, p 80.

the slurry volume for part of the run was reduced from 65 liters, the normal operating volume, to 30 liters to simulate a withdrawal. During the withdrawal of slurry and during the operation with the reduced slurry volume, the thorium concentration remained at 1100 g per kilogram of H_2O, and the system was always under control when a slurry was either withdrawn or added.

To check the operation of the system with a slurry similar to the slurries being circulated in the high-temperature loops, the sulfate content was increased from 1000 to 3000 ppm by adding 1 N H_2SO_4 while maintaining the thorium concentration at 1100 g per kilogram of H_2O. The system operated normally for 365 hr with the sulfated slurry; no additional steam pressure was required either to move the settled bed after a week's shutdown or to maintain homogeneity.

To further demonstrate the operation of the system at reduced volumes with a sulfated concentrated slurry, the system was operated successfully with slurry containing 2300 g of thorium per kilogram of H_2O and 4800 ppm of sulfate; it was then opened for inspection without being refilled to its normal operating volume. Some deposit was found (Figs. 9.15 and 9.16) on all surfaces, particularly on the auxiliary heater and steam-injector tubes which extend through the vapor space. These accumulations did not appear to be detrimental to operation of the unit and were easily removed by flushing with water.

9.5 SLURRY BLANKET SYSTEM TEST

H. L. Falkenberry

| L. F. Parsly | I. M. Miller |

During the report period, the high-pressure system of the blanket test facility has had three shakedown runs on water, with one brief and one extended shutdown between runs. Major alterations to the system included installation of a high-pressure condenser and flow-control system to provide purge water for the slurry circulating pump, removal of the pulsafeeder and associated piping, installation of an "acid egg" type of high-pressure feed system, and replacement of the aluminum-foil insulation with conventional insulation. A number of minor changes were also made in an effort to provide a more easily operated and a safer system. Operation of the system on the latest shakedown run has been good, and the high-pressure system is ready to operate on slurry.

UNCLASSIFIED
PHOTO 26637
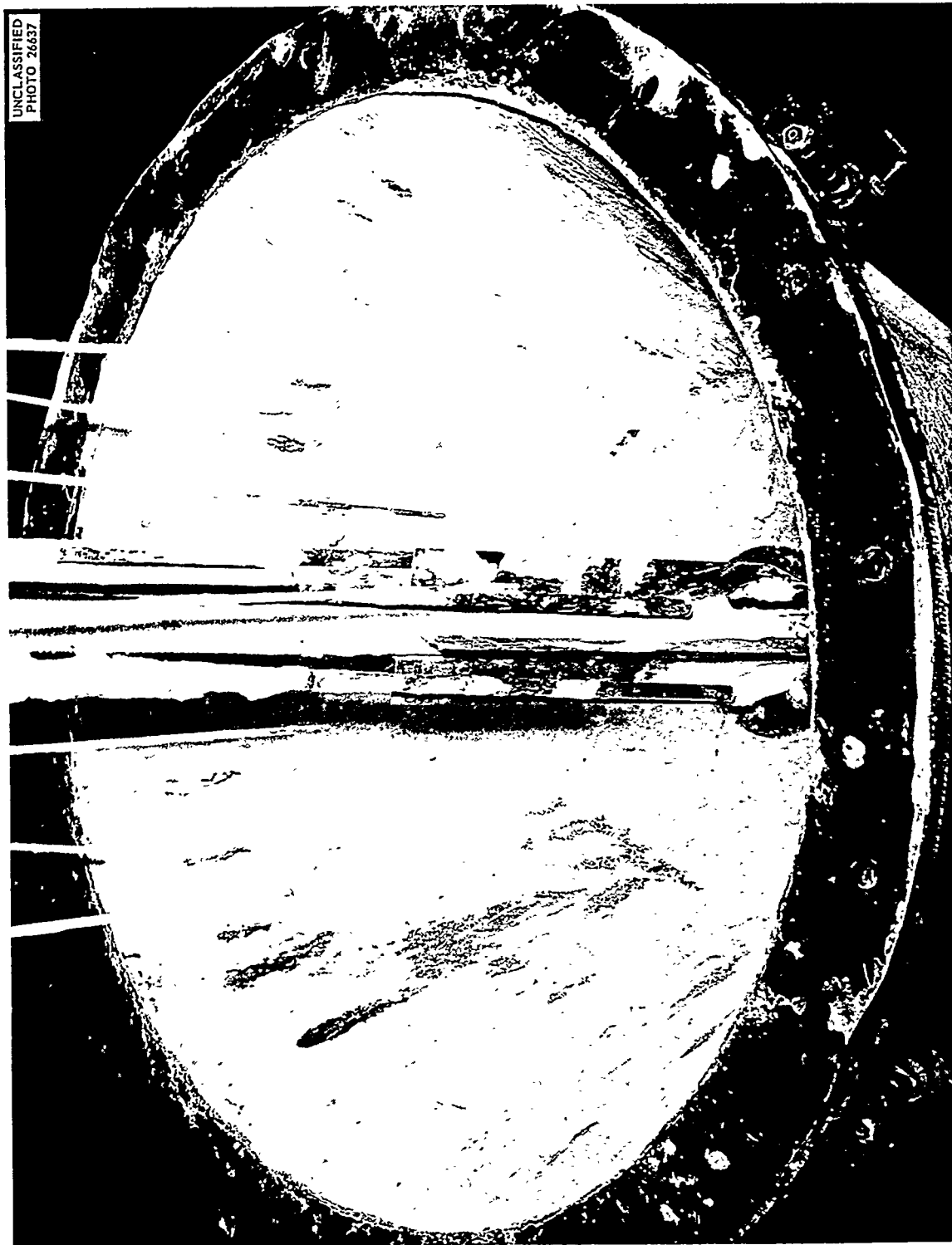
Fig. 9.15. Condition of Cone-Shaped Dump Tank After 1400 hr of Operation (Before Removing Slurry from Bottom of Tank).

UNCLASSIFIED
PHOTO 26636
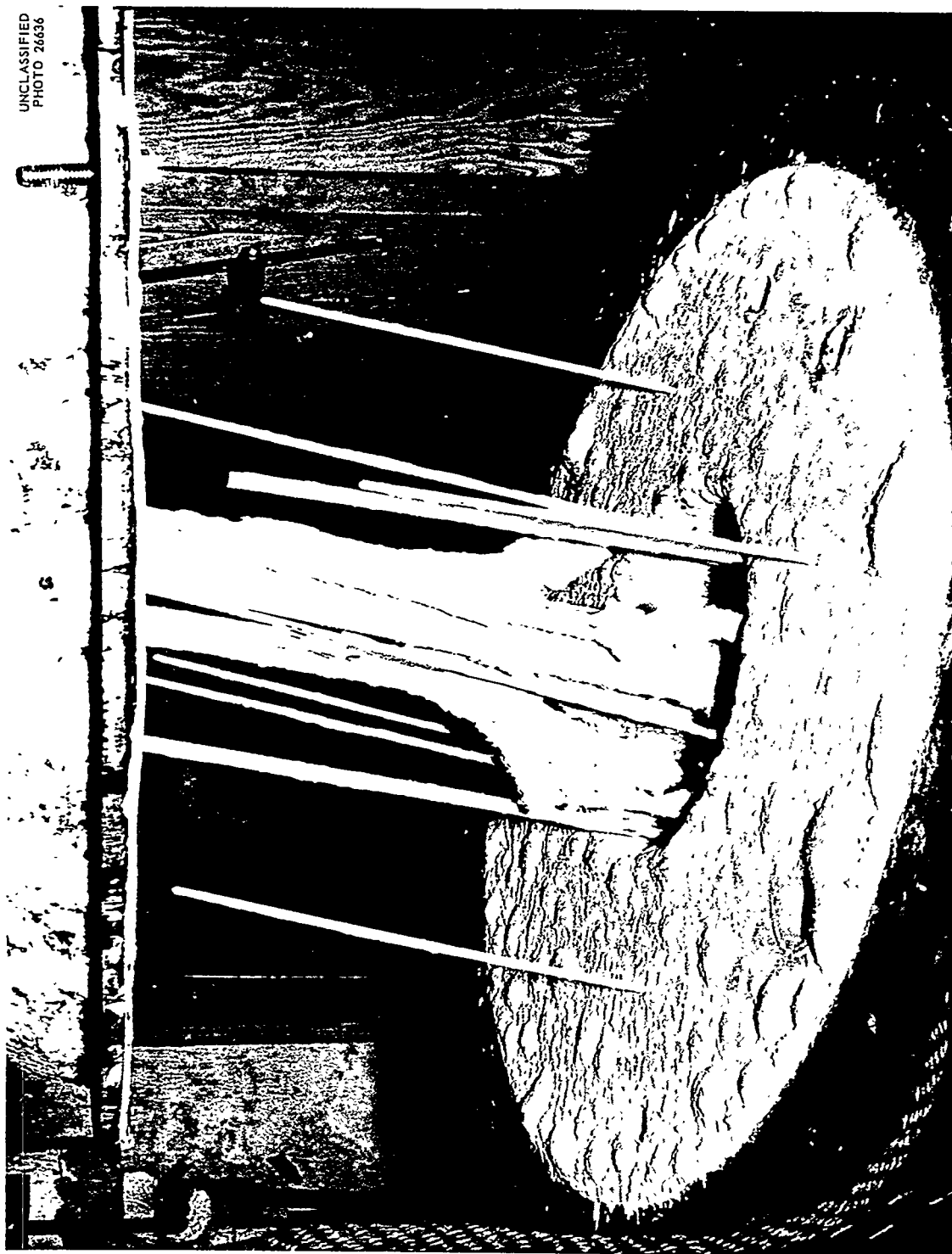
Fig. 9.16. Condition of Lift Tubes and Heaters After Operation at One-Third Normal Volume.

The high-pressure condensate and purge flow-control system was added because it had become evident that the original high-pressure feed system would have to be used to feed slurry whenever the loop cooled for any reason and thus could not be kept available for feeding purge water. At the same time, it was believed that the use of the pulsafeeder for feeding slurries would lead to excessive maintenance problems, and it was decided to withdraw it from the blanket test facility. As a replacement, an "acid egg" arrangement was devised (Fig. 9.17), which permits addition of slurry in batches of approximately 1 liter.

A review of heat balances computed during the first three runs on water indicated that heat losses

from the piping were excessive and that the losses became progressively greater on each run. This resulted from crushing of the aluminum foil originally installed as insulation. It was impossible to attain the design temperature of 300°C on the second or the third run, in spite of the addition of 8 kw to the loop heaters between the second and third runs. Therefore the aluminum foil was replaced with conventional insulation (both 85% magnesia and Hi-Temp); the system can now readily be heated to 300°C, and there is ample reserve for heat-transfer experiments.

During the shutdown following the third water run, the thermal barrier was seal-welded to the

UNCLASSIFIED
ORNL-LR-DWG 15513

2500 psi AIR

HIGH-LEVEL PROBE

SLURRY
FEED TANK

AIR
ACCUMULATOR

OPERATING SEQUENCE

1. FILL SLURRY TANK WITH SLURRY;
   FILL AIR ACCUMULATOR WITH AIR TO
   ~125 % OF OPERATING PRESSURE.

2. DISPLACE SLURRY INTO LOOP
   WITH AIR FROM ACCUMULATOR.

3. VENT SLURRY FEED TANK.

TO
SLURRY
TANKS

FROM
SLURRY
FEED PUMP

TO
LOOP
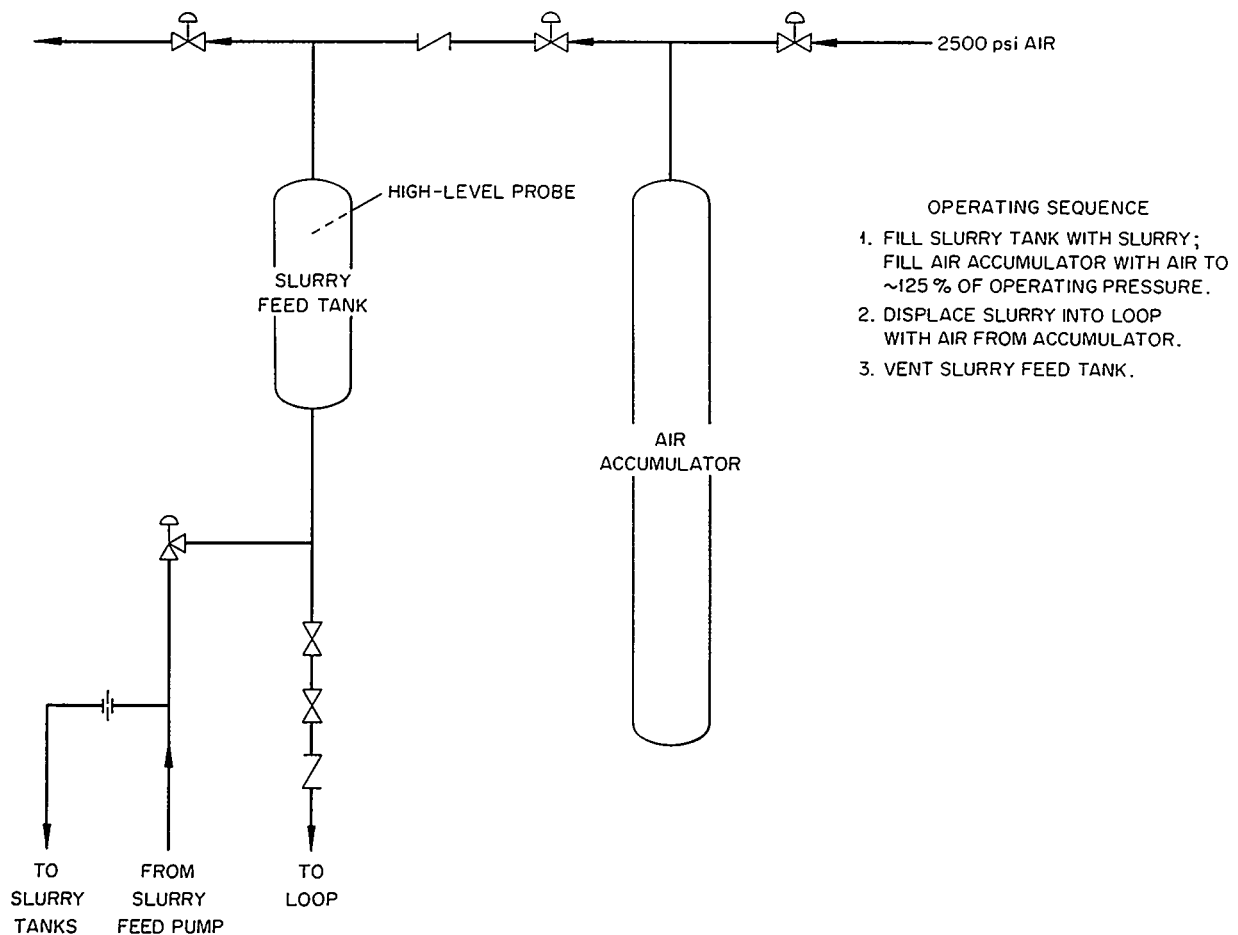
Fig. 9.17. Slurry Blanket Test — High-Pressure Feed System.

pump stator assembly, and the pump motor assembly was seal-welded to the casing.

Other than minor valve trouble, no operational difficulties were experienced in the water runs. A large number of bar-stock needle valves were utilized, and experience with these was generally unsatisfactory. Wherever such valves were required to hold pressure, it was necessary to install a more positive closure, such as a tube fitting and cap, downstream of the valve. Roughly half the valves of this type had to be repacked in less than 1000 hr of operation. Valves of other types are now being procured for evaluation.

10. INSTRUMENT AND VALVE DEVELOPMENT

D. S. Toomb

A. M. Billings   H. D. Wills

10.1 INSTRUMENT DEVELOPMENT

10.1.1 Heated-Thermocouple-Type Liquid-Level Indicator

An experimental liquid-level indicator suitable for use at 2000 psi and 335°C was fabricated. The indicator, shown in Fig. 10.1, consists of 12 thermocouple-heater assemblies (weld-sealed and stainless steel sheathed) extending through a 3-in. ring joint flange. Each 0.250-in.-OD sheath contains a Chromel-Alumel thermocouple and a pair of heater wires that extend to the sealed tip.

The wires are insulated with compressed magnesium oxide powder.

In operation, the heaters will be connected in series and supplied with a constant current; an equal amount of heat will be generated near the junction of each thermocouple and the temperature at each thermocouple will be dependent on the resistance to heat-transfer from the sheath to the process fluid. This resistance is less when the sheath is in the liquid phase than when in the vapor phase, and consequently an appropriate scan of the thermocouples will define the liquid-vapor
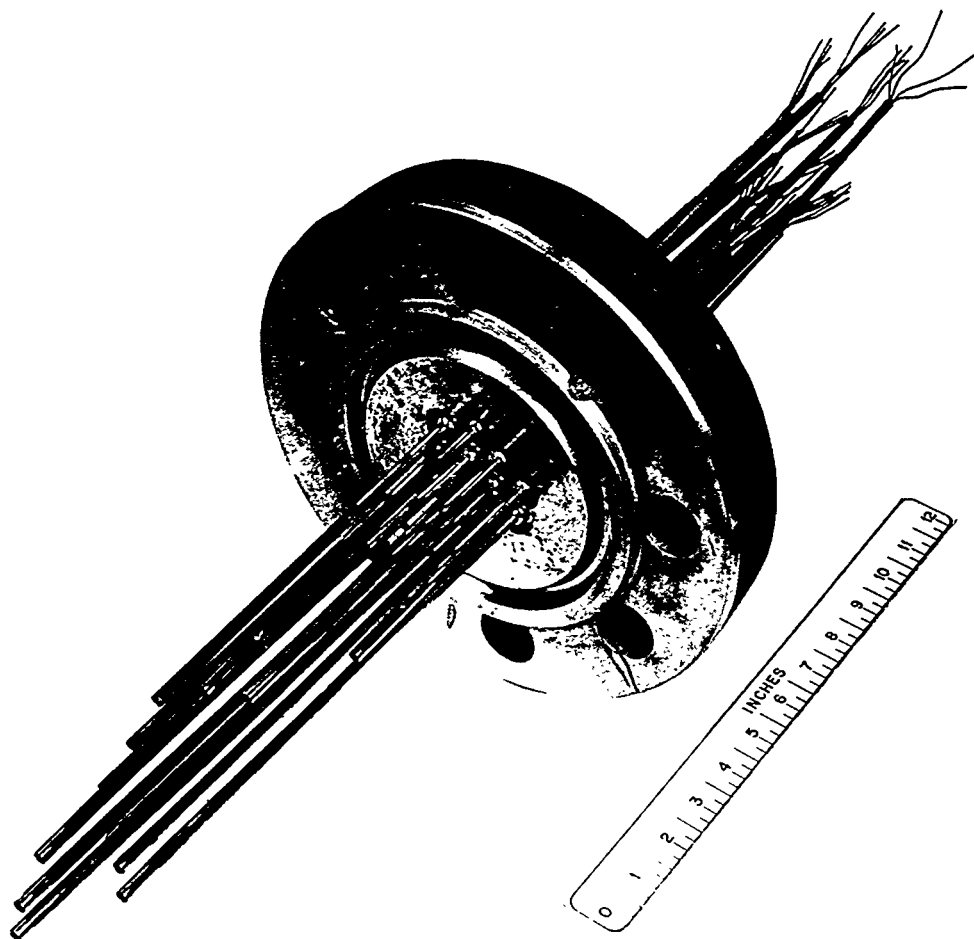
Fig. 10.1. Heated-Thermocouple-Type Liquid-Level Indicator.

interface. For satisfactory performance the sheaths must be heated to 10 to 20°C above system temperature.

Advantages of this type of level indicator are (1) the absence of moving parts and (2) no shift of zero point with changes in temperature and pressure.

10.2 VALVE DEVELOPMENT

10.2.1 Sealing Bellows

Six HRE-type bellows, manufactured by Fulton-Sylphon Division, suitable for sealing a $\frac{3}{4}$-in.-dia shaft, were tested in uranyl sulfate at 2000 psi and 300°C; they had an average life of 43,000 cycles for a stroke of $\frac{1}{8}$ in.

An additional series of six HRT-type low-pressure bellows, followed by a series of six HRT-type high-pressure bellows, all designed and fabricated by Fulton-Sylphon Division, will be tested under the same conditions.[1]

10.2.2 Valve Trim

In continuation of the investigation of materials for valve-trim use, five additional sets of trim were checked for performance in the valve test loop.[2]

Two sudden and unpredicted failures of titanium alloy valve trim occurred. The first was a Mallory-Sharon alloy MST 6AL-4V, which failed suddenly after 75 cycles in the test loop. At the time of the failure, the loop was "dumping" uranyl sulfate through the test valve from 1150 psi and 220°C to the receiver tank at atmospheric pressure. Figure 10.2 shows this trim before testing, and Fig. 10.3, after testing. The second failure, Rem-Cru titanium alloy Ti-130-AM, occurred with the loop dumping trisodium phosphate rinse solution at 1300 psi and 200°C through the test valve. This set of trim had been subjected to 112 cycles with uranyl sulfate followed by 292 dumps with the trisodium phosphate solution. As shown by

[1]D. S. Toomb *et al.*, *HRP Quar. Prog. Rep. April 30, 1956*, ORNL-2096, p 75.

[2]A. M. Billings, *HRP Experimental Valve Program*, ORNL CF-56-2-42 (Feb. 14, 1956).

Figs. 10.4 and 10.5, this failure was very similar to the first.

Two sets of trim, consisting of type 347 stainless steel seats and plugs hard-faced with Stellite 6, torch-applied by The Cleveland Hardfacing Company, were tested and gave performance inferior to that of plugs hard-faced with Stellite 6 at ORNL by the Heliarc technique.

UNCLASSIFIED
T 10567
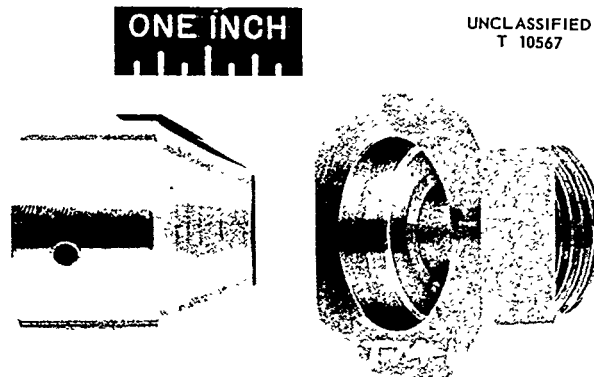
Fig. 10.2. MST 6AL-4V Titanium Valve Trim Before Test.

UNCLASSIFIED
T 10542
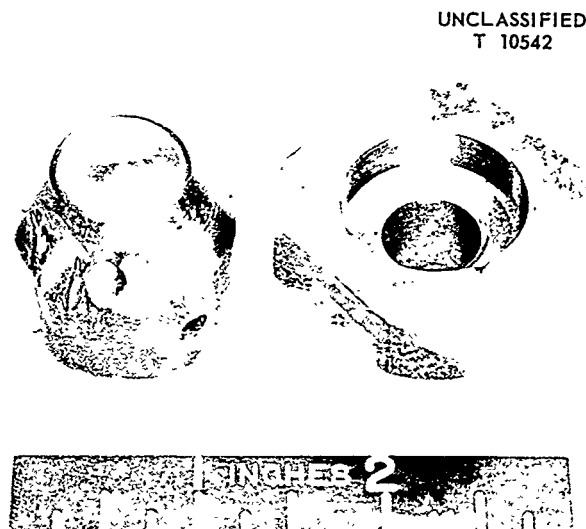
Fig. 10.3. MST 6AL-4V Titanium Valve Trim After Failure.

Fig. 10.4. Ti-130-AM Titanium Valve Plug After Failure.
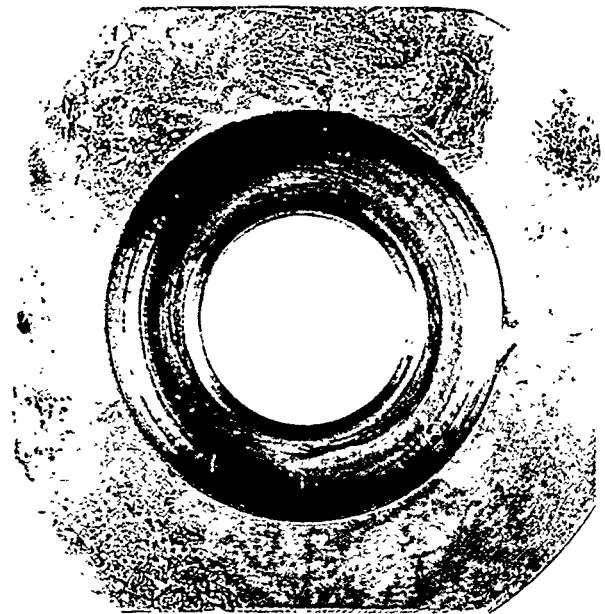
Fig. 10.5. Ti-130-AM Titanium Valve Seat After Failure.

Part IV

CORROSION AND MATERIALS

E. G. Bohlmann

11. SOLUTION CORROSION[1]

J. C. Griess   H. C. Savage

S. R. Buxton   T. H. Mauney
J. L. English   R. M. Pierce[2]
R. S. Greeley   J. A. Russell
E. F. House   R. M. Warner

11.1 PUMP LOOPS

J. C. Griess   H. C. Savage

S. R. Buxton   R. M. Pierce[2]
R. S. Greeley   J. A. Russell
T. H. Mauney   R. M. Warner

11.1.1 Loop Engineering

(a) **Loop F — Mockup of HRT Core-Vessel Expansion Joint and Zircaloy-Stainless Steel Gasket.** — A mockup of the expansion joint[3] and Zircaloy-to-stainless-steel transition joint[4] as used in the HRT reactor vessel was installed in 100A dynamic corrosion loop F. The mockup test assembly is shown in Fig. 11.1.

The purpose of the test is to determine corrosion of the component parts by uranyl sulfate solution, as well as the integrity of the bellows and Zircaloy–stainless steel joint, under reactor conditions of temperature and pressure. Reactor startup and shutdown will be simulated by thermally cycling the entire unit between 300 and 100°C and by mechanically deflecting the bellows to simulate the expansion and contraction expected under service conditions.

As presently installed in loop F, the inside of the bellows expansion joint is filled with distilled water and connected through a condenser into the vapor space of the loop pressurizer. A side stream of fuel from the main pump loop circulates through the test assembly on the outside of the bellows and joint. A pressure differential of approximately 50 psia is maintained across the joint and is recorded and interlocked with the system to prevent overpressure. A schematic diagram of the installation is shown in Fig. 11.2.

Periodic helium leak checks of the joint will be made. In addition, attempts will be made to detect and monitor leakage of fuel solution through the test unit by sampling the water inside the bellows. The fuel-solution side of the bellows is at a higher pressure than the water side.

Standard corrosion-specimen arrays are installed in the main loop circuit, and corrosion coupons and stressed specimens are installed in various locations in the bellows joint. These specimens (Zircaloy-2, titanium, and stainless steel) will be used as an aid in correlating the corrosion rates of the test components in localized fuel environments.

(b) **Loop O — Beryllium Solution Loop.** — A new loop, designed to handle solutions of uranyl sulfate containing beryllium as an additive, was completed. This loop is described in detail in another report.[5]

(c) **Aluminum Oxide Pump Bearings.** — Pure sintered aluminum oxide bearings and journals have given longer and more reliable service than other bearing and journal materials used in the 5-gpm pumps in in-pile loops.[6] Based on this experience, bearings and journals of pure sintered aluminum oxide were installed in a Westinghouse model 100A pump for use in the dynamic corrosion test loops. Figure 11.3 is a photograph of the aluminum oxide bearings and journals after approximately 1500 hr of operation — for 200 hr in water at 190°C and for 1300 hr at 300°C in 0.04 m uranyl sulfate solution containing 0.015 m sulfuric acid and 0.005 m copper sulfate. There was no visual or measurable wear. This pump has now been installed in slurry loop BS, where the use of aluminum oxide in pumps circulating thorium oxide slurries will be evaluated.

---

[1] Reported in greater detail in J. C. Griess *et al.*, *HRP Dynamic Solution Corrosion Studies, Quarter Ending July 31, 1956*, ORNL CF-56-7-52 (to be issued).

[2] On loan from TVA.

[3] R. B. Briggs *et al.*, *HRP Quar. Prog. Rep. Jan. 31, 1955*, ORNL-1853, p 8–9.

[4] W. R. Gall *et al.*, *HRP Quar. Prog. Rep. Jan. 31, 1956*, ORNL-2057, p 11 and Fig. 2.1.

[5] H. C. Savage and R. M. Pierce, *HRP Dynamic Corrosion Studies: 100A Loop O Design*, ORNL CF-56-7-42 (to be issued).

[6] G. H. Jenks *et al.*, *HRP Quar. Prog. Rep. Oct. 31, 1955*, ORNL-2004, p 121.
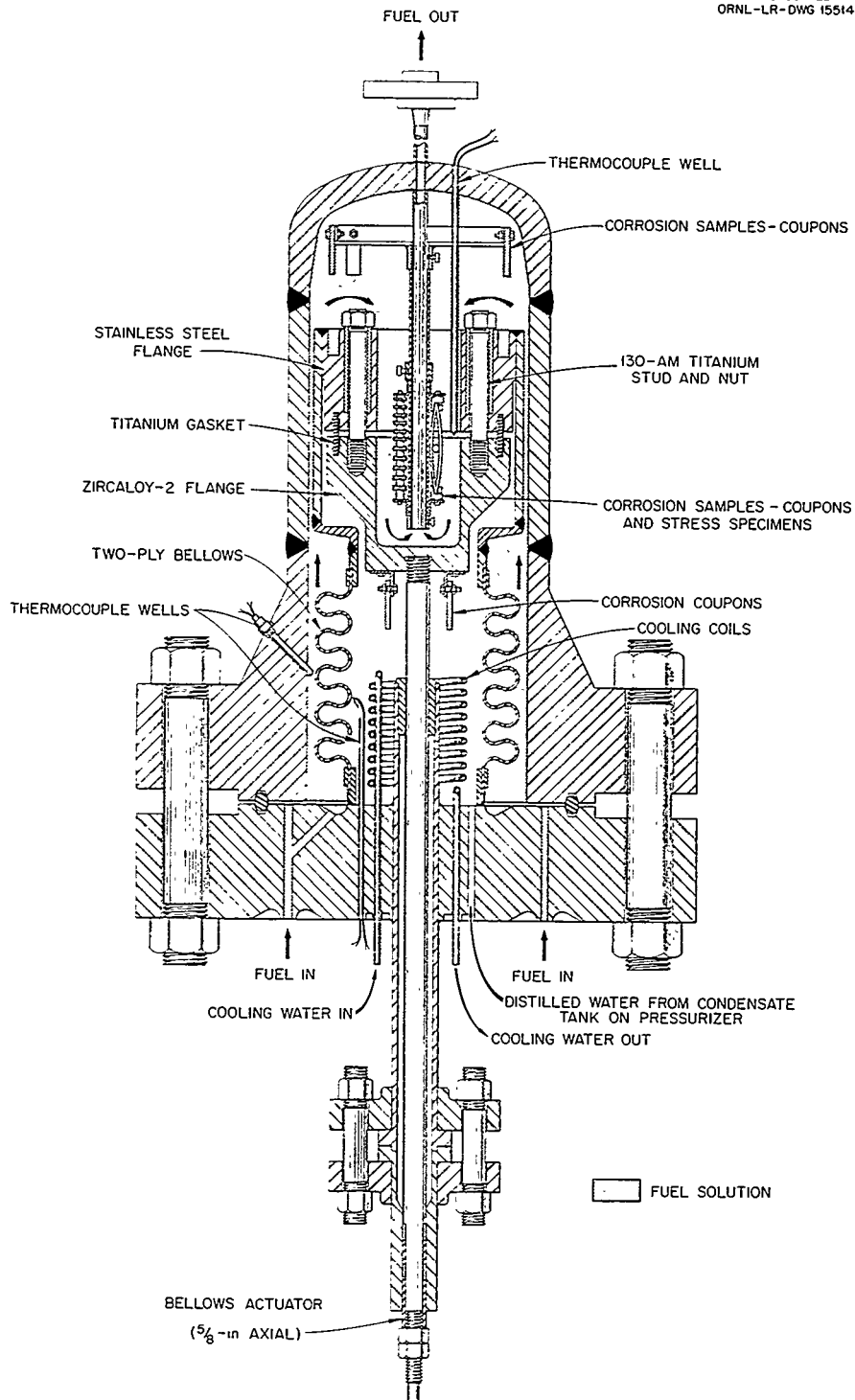
Fig. 11.1. Expansion Joint and Zircaloy–Stainless Steel Transition Joint.
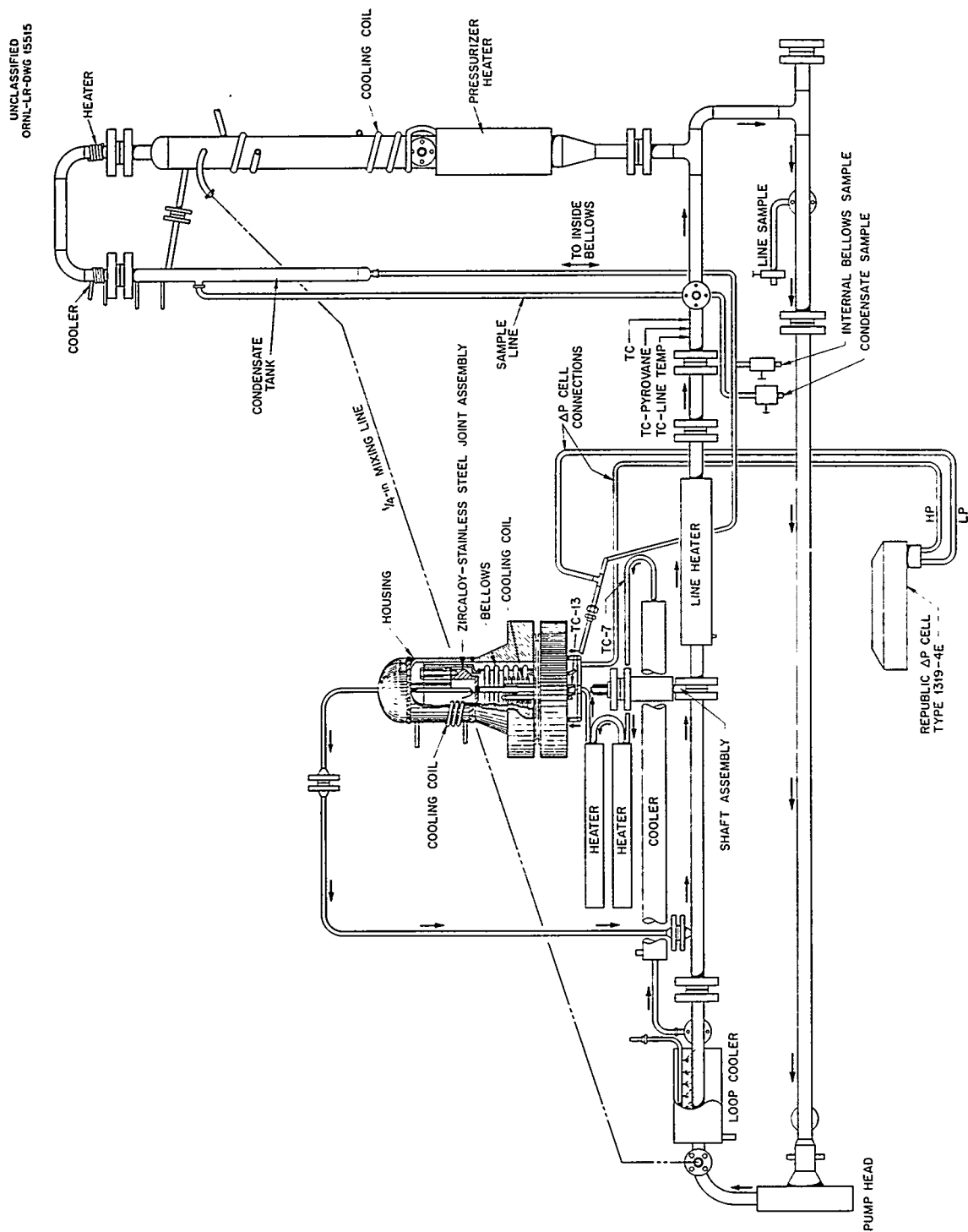
Fig. 11.2. Bellows Flange – Loop F Schematic.

ALUMINUM OXIDE BEARING INSERT

BEARING HOUSING

ROTOR

ALUMINUM OXIDE BUSHING

SHAFT

CLAMPING RINGS
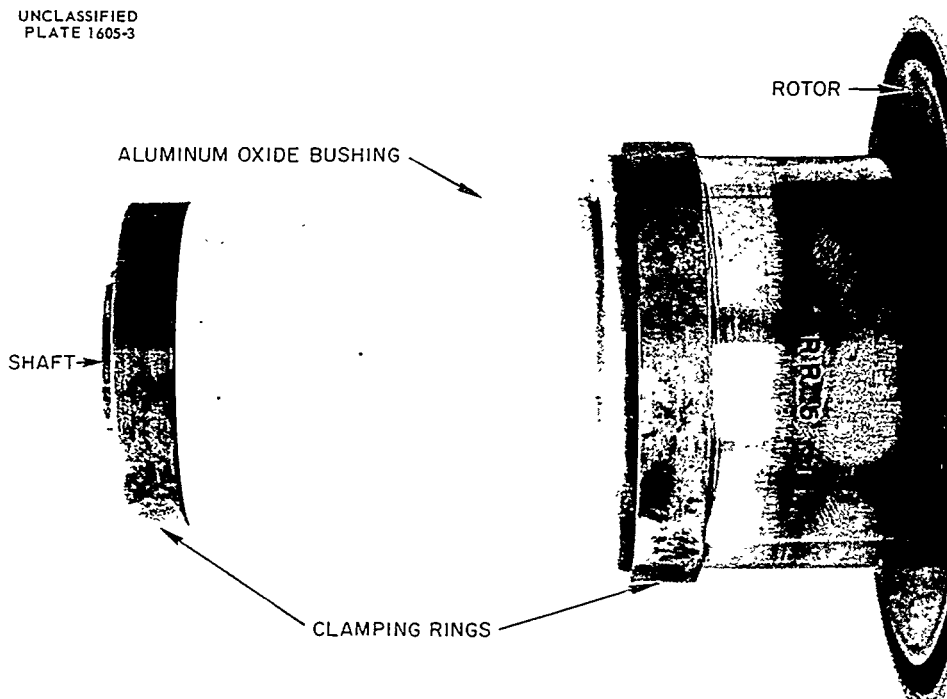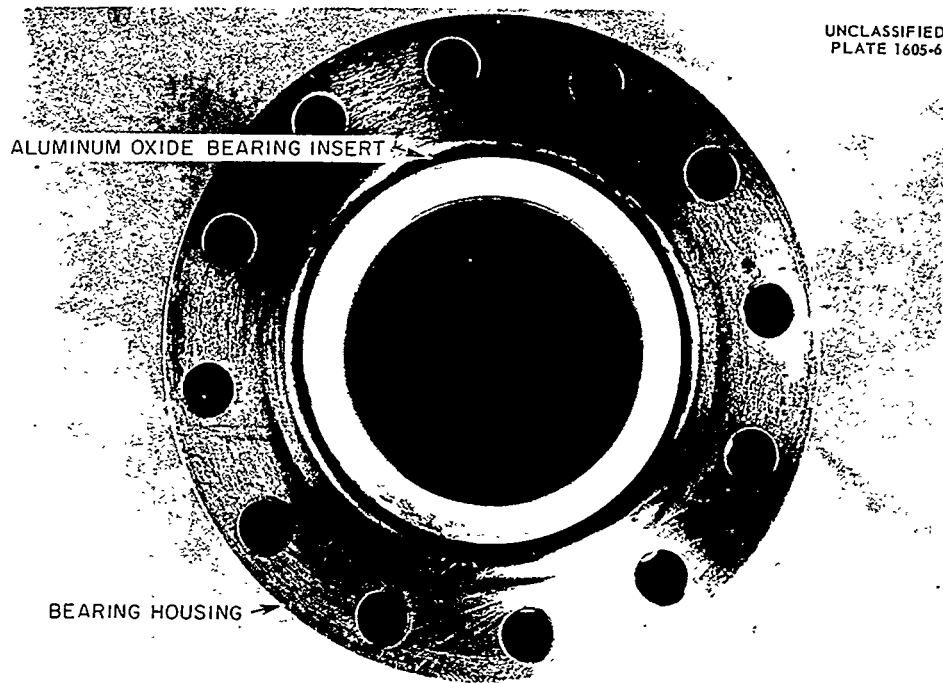
Fig. 11.3. Aluminum Oxide Bushing and Bearing — Westinghouse Model 100A Pump.

76

11.1.2 Loop Test Results

The out-of-pile corrosiveness and the stability of a solution proposed for use in the HRT (0.04 m UO_2SO_4, 0.005 m $CuSO_4$, and 0.015 m H_2SO_4) were determined at 200, 250, and 300°C. Previous runs[7] had been made under the same conditions, except with less acid, and had demonstrated low corrosion rates for stainless steel but had shown that the solution was not hydrolytically stable at 250 and 300°C during long periods of exposure.

Despite the increased acid concentration in these tests, 15 to 20% of the copper and 5 to 10% of the uranium precipitated from the solutions at 250 and 300°C after 4151 and 3231 hr of circulation, respectively; during the 4093-hr test at 200°C uranium and copper were lost from solution very slowly, probably as the result of slow hydrolysis.

The average corrosion rates of the pin-type specimens at different flow rates are shown in Table 11.1. These pins were newly machined before the tests. At the end of the runs all pins except those exposed at 34 and 42 fps at 200°C were completely covered with a protective film and were corroding at very low rates. Pins that had been tested previously and that were covered with oxide film before these tests began were not corroded during the tests; in fact, they all showed

slight weight gains. Even at 200°C at 34 to 42 fps, where new pins did not develop films, pins that had been previously exposed retained their films. This observation suggests that there may be some merit in a pretreatment, contrary to what has been observed previously.[8] The effect of pretreatment will be investigated further.

Type 347 stainless steel coupons were exposed in all runs and showed the following critical velocities: 25 to 35 fps at 200°C, 35 to 45 fps at 250°C, and greater than 45 fps at 300°C.

The results of the tests clearly showed that more than 0.015 m H_2SO_4 is necessary to stabilize 0.04 m UO_2SO_4 containing 0.005 m $CuSO_4$ at 250 and 300°C. Runs are now in progress with solutions containing the same copper and uranium concentrations but with 0.020 m H_2SO_4. On the basis of previous data, the corrosion of stainless steel is expected to be substantially worse at the higher acid concentration.

Results obtained during the operation of the 4000-gpm pump loop were given in the last quarterly report.[9] One additional run has been made. A solution containing 0.04 m UO_2SO_4, 0.02 m H_2SO_4, and 0.005 m $CuSO_4$ was circulated at 250°C for the purpose of determining the solution stability and the corrosion of stainless steel when the system contained low oxygen concentrations. The oxygen concentration was maintained at less than 25 ppm for 225 hr and at approximately 3 ppm for more than 100 hr. There was no evidence of solution instability, and the corrosion rate of stainless steel was about the same as that observed with a solution of the same composition but containing between 1000 and 2000 ppm oxygen.

A series of runs was made in which 0.17 and 1.3 m UO_2F_2 solutions were circulated at 250 and 300°C in 100A loops. A previous series of runs with uranyl fluoride has already been reported,[10] but the present runs were made to determine the effect of added lithium or sodium fluoride on corrosion and to evaluate the corrosion of titanium, zirconium, and stainless steel in the vapor above uranyl fluoride solutions.

---

[7] J. C. Griess et al., Quarterly Report of the Solution Corrosion Group, Jan. 31, 1956, ORNL CF-56-1-167, p 24.

TABLE 11.1. AVERAGE CORROSION RATES FOR PIN-TYPE STAINLESS STEEL SPECIMENS IN 0.04 m UO_2SO_4 CONTAINING 0.015 m H_2SO_4 AND 0.005 m $CuSO_4$

| Flow Rates (fps) | Average Corrosion Rates (mpy) | | |
	L-34, 200°C, 4093 hr	M-28, 250°C, 4151 hr	K-16, 300°C, 3231 hr
8	1.8		
13		0.36	0.24
20	3.3	0.66	0.20
26		0.50	0.27
34	13	0.68	0.37
42	17		

[8] J. C. Griess and R. E. Wacker, HRP Quar. Prog. Rep. April 30, 1954, ORNL-1753, p 76.

[9] J. C. Griess et al., HRP Quar. Prog. Rep. April 30, 1956, ORNL-2096, p 84.

[10] J. C. Griess and R. E. Wacker, HRP Quar. Prog. Rep. April 30, 1954, ORNL-1753, p 80.

The corrosion results with 1.3 m UO_2F_2 at 250°C, which were in good agreement with data obtained previously,[10] showed that stainless steel was attacked to a lesser extent than it is in uranyl sulfate solutions under the same test conditions. With 1.3 m UO_2F_2 the attack of stainless steel was less at 300°C than it was at 250°C; that is, the critical velocity was higher and, at flow rates less than the critical velocity, a smaller amount of metal dissolved during the period of film formation. In general, the temperature-corrosion relationship with uranyl fluoride solutions was the same as that observed with uranyl sulfate solutions.

The addition of 1.3 m NaF to 1.3 m UO_2F_2 at 250°C substantially reduced the corrosiveness of the solution to stainless steel, by a factor of about 30 at low velocity and a factor of 2 at high velocity, although it did not change the critical velocity. A similar effect was noted when 0.10 m LiF was added to 0.17 m UO_2F_2.

Titanium corroded at low, although measurable, rates in the uranyl fluoride solutions. The attack rate increased as the uranyl fluoride concentration increased, and the addition of either sodium or lithium fluoride increased the corrosion rate still further. Under all conditions, however, the corrosion of titanium and its alloys was located almost exclusively in the crevices where the pins were held in the holders.

In the gas phase, type 347 stainless steel was attacked at rates of 1 to 2 mpy and titanium at less than 1 mpy. Zirconium specimens, however, exposed with the titanium and stainless steel specimens, were completely destroyed in every case, presumably by hydrofluoric acid in the steam.

The studies with uranyl fluoride solutions have been concluded, at least for the time being. While stainless steel is more resistant to corrosion in uranyl fluoride solutions than it is in uranyl sulfate solutions, the difference is not sufficiently great to warrant further consideration. The rate at which titanium corrodes is greater in uranyl fluoride than it is in uranyl sulfate, and in crevices or in solutions with very low oxygen concentrations, titanium corrodes at excessively high rates. Furthermore, zirconium is completely incompatible with uranyl fluoride solutions.

Previous studies[11] have shown that Cr(VI) ions in uranyl sulfate solutions markedly affect the corrosion rate of stainless steel. Those studies were carried out in stainless steel loops, and since the uranyl sulfate solutions are capable of oxidizing chromium from the metal or from the oxide film to the hexavalent state, it was not possible to maintain a given Cr(VI) concentration; hence, only qualitative results were obtained. The results indicated clearly, however, that the presence of Cr(VI) ions increased the critical velocity, increased the film-free corrosion rate of the stainless steel, and decreased the amount of metal that dissolved during the period of film formation at low flow rates. Chromium(VI) does not appear to be stable in-pile. It is necessary to know its effect on the corrosion of stainless steel so that the out-of-pile studies in stainless steel systems can be correlated with in-pile studies.

The all-titanium loop was used to determine, in a more controlled manner, the effect of additions of potassium dichromate to 0.17 m UO_2SO_4 at 250°C. Since it was desirable to keep the exposed surface area of stainless steel as small as practical to minimize the accumulation of Cr(VI) in the solution, only two flow rates (10 to 12 fps and 68 to 70 fps) were used and only two type 347 stainless steel pins were exposed at each flow rate. No data concerning critical velocity were obtained. The results of this study are shown in Fig. 11.4. It should be noted that at the high flow rate small amounts of Cr(VI) (10 to 50 ppm) increased the corrosion rate substantially. At low flow rates the corrosion rate decreased, during the period of film formation, as the concentration of Cr(VI) increased. Further studies are planned in which the effects of Cr(VI) additions on the critical velocity of stainless steel will be investigated.

Previous tests[12] have shown that the addition of equimolar concentrations of lithium sulfate to 0.4 to 4 m UO_2SO_4 not only decreases the corrosiveness of such solutions but also increases the temperature at which a second liquid phase appears by as much as 50 to 100°C. (See Fig. 11.5, which shows the temperature at which a second liquid phase forms in a number of different solutions.) However, the addition of lithium

[11] J. C. Griess and R. S. Greeley, *HRP Quar. Prog. Rep. July 31, 1955*, ORNL-1943, p 89.

[12] *Ibid.*, p 70.
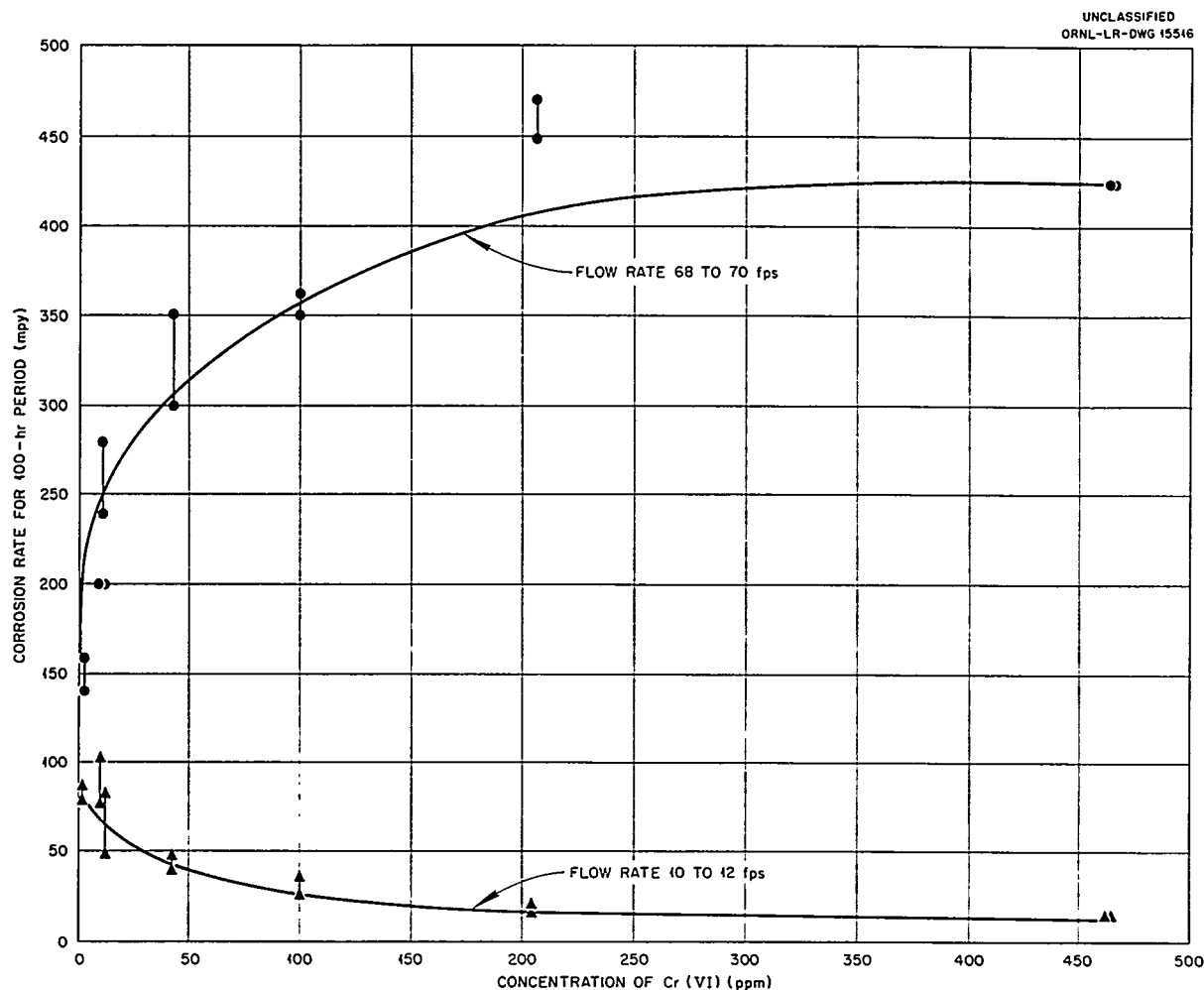
Fig. 11.4. Corrosion Rates of Type 347 Stainless Steel as a Function of Cr(VI) Concentration in 0.17 m UO$_2$SO$_4$ at 250°C.

sulfate to dilute uranyl sulfate solutions (<0.2 m) in amounts that increase appreciably the temperature of appearance of a second liquid phase causes a slow precipitation of uranium, lithium, and sulfate at temperatures below 300°C. Beryllium sulfate, on the other hand, had not been investigated, and the possibility existed that it might remain soluble in dilute uranyl sulfate solutions and give some corrosion inhibition. Also, beryllium sulfate solutions are known to dissolve appreciable quantities of beryllium oxide, and thus it was of interest to investigate the solubility of uranium trioxide in beryllium sulfate solutions.

A quartz-tube technique was used for all the tests to be described in this section.

Beryllium sulfate solutions form two liquid phases at high temperatures as do uranyl sulfate and uranyl fluoride solutions. Figure 11.6 shows the temperature at which the second liquid phase forms as a function of beryllium sulfate concentration. On the same graph are shown the temperatures at which two liquid phases form in solutions of uranyl sulfate containing equimolal concentrations of beryllium sulfate. In 0.04 m UO$_2$SO$_4$-BeSO$_4$ solution, crystals were observed to form near 300°C. In one test, not shown on the graph,
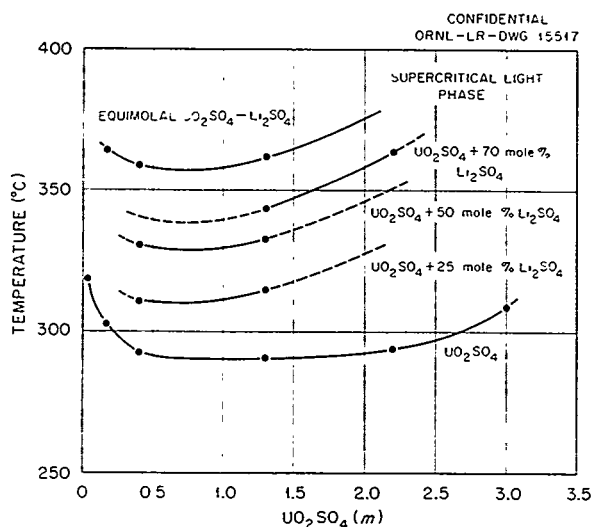
Fig. 11.5. The Temperature at which a Second Liquid Phase Appears in Uranyl Sulfate Solutions Containing Lithium Sulfate. The temperatures indicated for UO_2SO_4 are slightly lower than those given by C. H. Secoy, *J. Am. Chem. Soc.* **72,** 3343–5 (1950), and slightly higher than those given by E. V. Jones, *HRP Quar. Prog. Rep. March 15, 1952,* ORNL-1280, p 181.
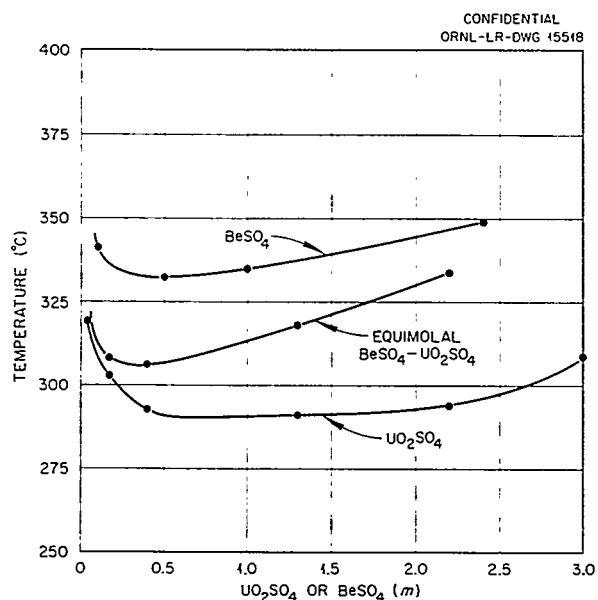
Fig. 11.6. The Temperature at which a Second Liquid Phase Appears in Uranyl Sulfate and Beryllium Sulfate Solutions.

a solution containing 0.04 m $BeSO_4$, 0.04 m UO_2SO_4, 0.005 m $CuSO_4$, and 0.02 m H_2SO_4 was heated to 320°C, and no crystals were observed.

Other quartz-tube studies have shown that beryllium sulfate solutions are capable of dissolving appreciable quantities of uranium trioxide and remaining phase-stable. Figure 11.7 represents the results to date. These solutions have relatively high pH values; for example, the solution of 1.0 m $BeSO_4$ containing 40 g of uranium per liter added as uranium trioxide has a pH of 2.8; a uranyl sulfate solution containing 40 g of uranium per liter has a pH of 2.4.

Since it has already been shown that the hydrolysis of some solutions is a very slow process, prolonged runs at high temperatures are necessary to verify the phase stability of the solutions.
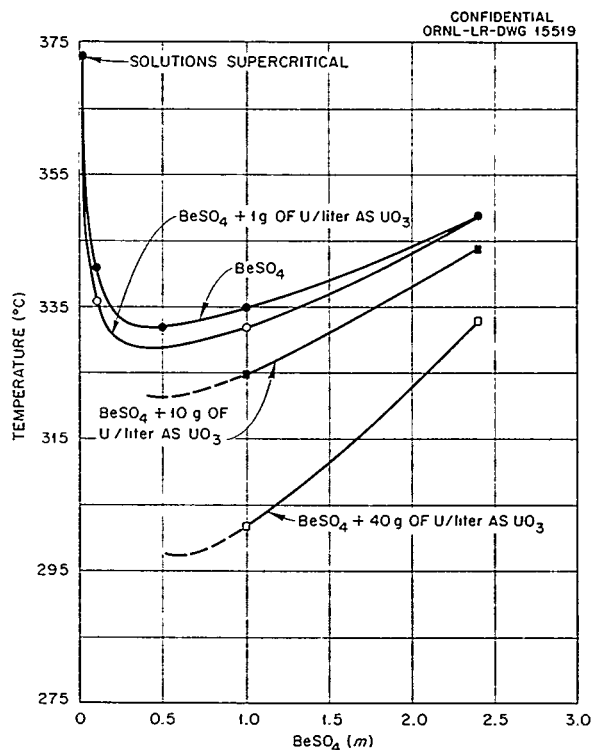
Fig. 11.7. The Temperature at which a Second Liquid Phase Appears in $BeSO_4$-UO_3 Solutions.

11.2 LABORATORY TESTS

J. L. English
E. F. House   J. C. Griess

A laboratory-scale corrosion study was initiated to examine the susceptibility of type 347 stainless steel to stress-corrosion cracking in boiling 0.04 m UO_2SO_4 containing 0.02 m H_2SO_4, 0.005 m $CuSO_4$ and halide ions. To determine the effect of chloride ions, specimens of stainless steel were exposed in solution to which had been added, 0, 5, 10, 25, 50, and 100 ppm chloride as potassium chloride. In each test one specimen was stressed to 15,000 psi and one to 30,000 psi; duplicate unstressed specimens were included in each test for control purposes.

All specimens were removed from the test solutions for examination after total elapsed times of 50, 100, 200, and 500 hr. With a single exception, cracking occurred on all stressed specimens exposed in solutions containing 25 and 50 ppm chloride ions. In all cases the cracks appeared in the region of maximum applied stress and were first observed between 100 and 200 hr inspections. Only the specimen stressed at 15,000 psi and exposed in the solution containing 25 ppm showed no cracking after 500 hr. No cracking occurred on the stress specimens exposed in the solutions containing 0, 5, 10, and 100 ppm chloride. Only one of the unstressed specimens showed signs of cracking. Several cracks, possibly attributable to stresses produced by polishing prior to use, were noted on the unstressed sample in the solution containing 25 ppm chloride.

The generalized corrosion rates were the same for all specimens exposed in the boiling solutions containing 5 and 10 ppm chloride and in the additive-free solution; no pitting was observed. The generalized attack on the specimens exposed in solutions containing 25, 50, and 100 ppm chloride was accelerated appreciably as a result of the additions. The most severe generalized corrosion was observed in the solution containing 100 ppm chloride. The most severe pitting occurred on the specimens exposed in solutions containing 25 and 50 ppm chloride; the incidence and severity of pitting attack were considerably less on the specimens exposed in the 100 ppm chloride solution. Figure 11.8 shows a plot of weight loss and corrosion rate during the 500-hr test as a function of chloride-ion concentration.
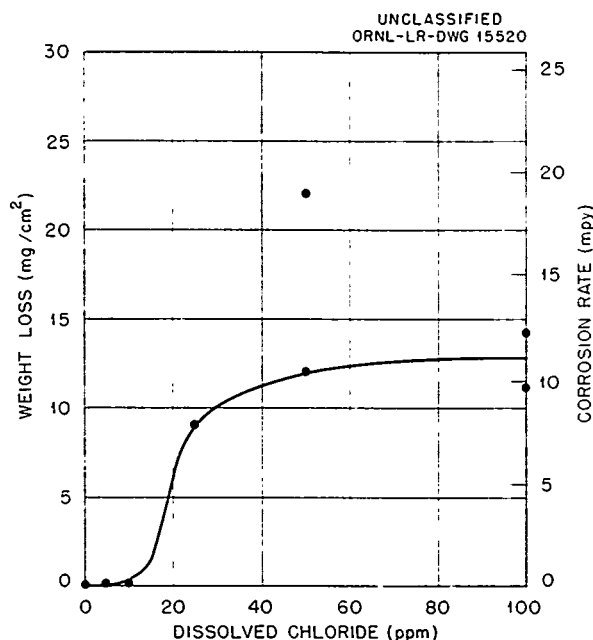
Fig. 11.8. The Effect of Chloride-Ion Concentration on the Corrosion of Unstressed Type 347 Stainless Steel After 500 hr in Boiling and Aerated 0.04 m UO_2SO_4 + 0.02 m H_2SO_4 + 0.005 m $CuSO_4$ Solution.

Preliminary tests with solutions containing 100 ppm iodide or 100 ppm bromide have failed to show any evidence of cracking. Further testing with bromide and iodide additions, as well as with chloride ions, is in progress.

One phase of a test program to examine the corrosion-fatigue behavior of type 347 stainless steel bellows in uranyl sulfate solution at elevated temperature was completed. Five HRE-type low-pressure bellows fabricated by the Fulton Sylphon Division (Fulton Sylphon drawing No. SS 94639-28-2R) were tested to failure. The bellows were of three-ply construction with a 0.0085-in. wall thickness for each ply; the outer diameter was $1\frac{1}{8}$ in. The rating of the bellows (number of cycles to failure) was 70,000 cycles at room temperature with a pressure differential of 1090 psi or 70,000 cycles at 538°C with a pressure differential of 500 psi.

The corrosion-fatigue test apparatus consisted of an electrically heated stainless steel autoclave. The total vertical movement effected by a Foxboro pneumatic operator was $\frac{1}{8}$ in. per cycle ($\frac{1}{16}$ in. in compression and $\frac{1}{16}$ in. in expansion). The

bellows were operated at 10 cpm until rupture occurred.

The environment on the outside of the bellows in four of the tests was 0.04 m UO_2SO_4 containing 0.02 m H_2SO_4 and 0.005 m $CuSO_4$; in the other test distilled water was the corrodent. A volume of 600 ml of solution pressurized with about 1200 psi oxygen at 285°C was used, so that the pressure differential across the bellows was 2100 to 2300 psi.

Results of the tests are presented in Table 11.2. In the one test with distilled water nearly 53,000 cycles were completed before failure. In three of the four tests with the uranyl sulfate solutions 41,000 to 46,000 cycles were logged before rupture; in the other test approximately half as many cycles produced failure. Figure 11.9 shows an enlarged cross-sectional view of the bellows which ruptured after 43,680 cycles (test J42-2). Figure 11.10 shows corrosion-fatigue cracks on the middle ply of the same bellows.

While not enough tests were run to draw any firm conclusions, it appears that the bellows have an adequate life in solutions proposed for use in the HRT. The use of uranyl sulfate solution in place of distilled water possibly decreased the time to rupture, but the effect was not a large

one. Further corrosion-fatigue tests with different bellows are planned.
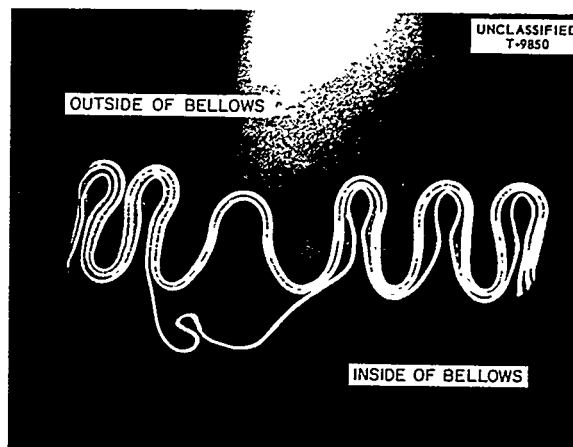
Fig. 11.9. Enlarged Cross-Sectional View of Type 347 Stainless Steel Bellows Showing Area of Rupture After 43,680 Cycles in 0.04 m UO_2SO_4 + 0.02 m H_2SO_4 + 0.005 m $CuSO_4$ Solution at 285°C and 2200 psi Total Pressure. 5X. Reduced 32.5%.
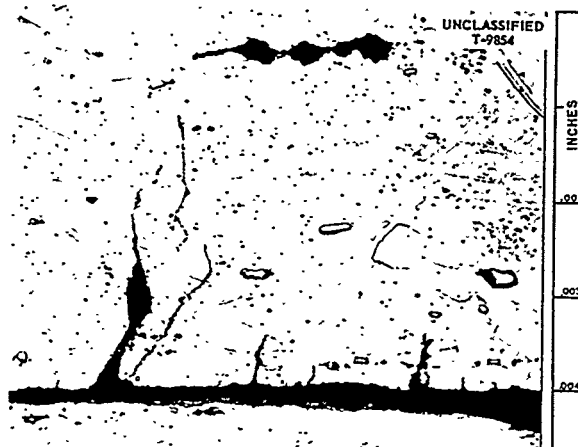
Fig. 11.10. Corrosion-Fatigue Cracks on Middle Ply in Ruptured Area of Three-Ply Type 347 Stainless Steel Bellows After 43,680 Cycles in 0.04 m UO_2SO_4 + 0.02 m H_2SO_4 + 0.005 m $CuSO_4$ Solution at 285°C and 2200 psi Total Pressure. Etchant: aqua regia. 750X. Reduced 32%.

TABLE 11.2. CORROSION-FATIGUE TESTS WITH TYPE 347 STAINLESS STEEL HRE-TYPE LOW-PRESSURE BELLOWS AT 285°C AND 2200 psi IN 0.04 m UO_2SO_4 WITH 0.02 m H_2SO_4 AND 0.005 m $CuSO_4$

Test No.	Operating Time (hr)	Number of Cycles to Failure
J42-1*	88.0	52,800
J42-2	72.8	43,680
J42-3	69.1	41,460
J42-4	41.0	24,600
J42-5	76.6	45,960

*Control test operated with distilled water at 285°C and 2200 psi.

12. SLURRY CORROSION

E. L. Compere   H. C. Savage

S. R. Buxton   S. A. Reed
G. E. Moore   J. A. Russell, Jr.
R. M. Pierce[1]   R. M. Warner

D. B. Weaver[1]

12.1 PUMP LOOPS

12.1.1 100A Loops

Two slurry tests,[2] runs CS-25 and CS-27, were made in the 100A pump loop CS during the quarter. Each test was preceded by an operational performance test with oxygenated water at 300°C. The performance tests were designated CS-24W and CS-26W, respectively.

In the last report[3] a description was given of the operational instabilities and pump cavitation which occurred in run CS-23, a 312-hr corrosion test at 300°C with a circulating concentration of 1000 g of thorium per kilogram of water. The difficulties were attributed to excessive flow of slurry (via the mixing line) to the pressurizer, where slugs of gas were entrained in the slurry and carried to the pump. This occurred when a 1-in. mixing line was being used with a flow of 31 gpm based on water flow measured at room temperature. Prior to run CS-25, the 1-in. mixing line was replaced by a $\frac{1}{2}$-in. sched-80 pipe, and flow was reduced by appropriate restrictors to 9 gpm.

A second modification to the system consisted in changing the bearings in the 100A centrifugal pump. Formerly the pump was equipped with Graphitar No. 14 bearings in combination with 98M2 Stellite journals. The front Graphitar bearings wore severely in nearly every run, even though the cavity of the pump was purged continuously with condensate at the rate of 5 to 6 liters/hr. Front-bearing wear ranged from 0.0050 in. to 0.0200 in. in run periods of 30 to 350 hr and necessitated terminating the runs before scheduled shutdown. The front Graphitar bearing was therefore replaced by a bearing of 98M2 Stellite in combination with a 98M2 Stellite journal.

Run CS-24W, a 49-hr performance test, was made with oxygenated water at 300°C to determine the operational characteristics of the modified system. In general, system operation was very steady. Pump performance, which was followed by means of an oscilloscope and a microphone affixed to the pump housing, was quite satisfactory. There was no measurable bearing wear when the pump was disassembled after the test.

In run CS-25 the three sample barrels loaded with pin-type corrosion specimens contained flow restrictors to give velocities of 11, 21, and 41 fps across the specimens with a total flow of 43 gpm, based on water flow measured at room temperature. Slurry flow through the mixing line at room temperature was approximately 8 gpm.

The system, after the usual evacuation, was charged to a concentration of 958 g of thorium per kilogram of water; 17.3 liters of slurry prepared from batch LO-2A thorium oxide was used. The thorium oxide had been made at ORNL from especially pure thorium nitrate by oxalic acid precipitation and calcination at 800°C. Before being used to charge the loop, the slurry was passed while wet through a 200-mesh screen.

The initial slurry sample was withdrawn from the system after 3 hr of operation. By chemical analysis, it contained 572 g of thorium per kilogram of water. A second sample taken 20 hr later contained 496 g of thorium per kilogram of water. During the period between run-hours 26 and 29.4, additional slurry was charged to the system by means of the slurry-addition device[4] in order to increase the circulating concentration to 1000 g of thorium per kilogram of water. The addition was made in two increments: the first charge contained 2785 g of thorium, and the second contained 872 g of thorium.

A characteristic rise in pump power occurred during the first addition; however, during the second addition the pump power decreased steadily. A sample taken after this addition contained only 580 g of thorium per kilogram of water. A period of

---

[1]On loan from TVA.

[2]E. L. Compere *et al.*, *HRP Dynamic Slurry Corrosion Studies, Quarter Ending July 31, 1956*, ORNL CF-56-7-51 (to be issued).

[3]E. L. Compere *et al.*, *HRP Quar. Prog. Rep. April 30, 1956*, ORNL-2096, p 87.

[4]*Ibid.*

erratic operation followed, and a noise developed in the pump. After 42.7 hr the automatic control on the lower pressurizer heater shut the system down because of overheating. After circulation was resumed, the pressurizer was surveyed with a scintillometer. Scintillometer readings indicated that a heavy accumulation of thoria extended from the lower pressurizer section, which contained the straightening vanes, up to the bypass-line inlet. The system was sampled and temporarily shut down after 46 hr of operation.

After the loop had cooled to 190°C, the run was continued. An additional 2.75 liters of water and 650 ml of 0.9 N H_2SO_4 were charged to the system with a Pulsafeeder after circulation began. It was calculated that, with these additions, the expanded volume at 300°C operating temperature would be sufficient to fill the pressurizer with liquid to a point above the level of solids indicated by scintillometer readings. The acid was added to aid in resuspending the solids which adhered to the pressurizer walls. Scintillometer values remained unchanged after the addition of acid. Subsequently, 60 psi of oxygen was charged rapidly to the system to provide a sparging action.

Scintillometer readings after sparging indicated that the thoria had been dislodged from the upper section of the pressurizer, but readings remained high adjacent to the heaters and around the vanes, indicating that heavy accumulations remained on the walls there. Overheating of the lower pressurizer heater continued, and general operation of the system was very erratic.

An additional 350 psi of oxygen was charged to the system when the loop temperature reached 285°C, but no improvement in operation resulted. Therefore the run was terminated after 49 hr total circulation time.

The loop was cooled to room temperature and disassembled without draining or flushing. The upper section of the pressurizer was found to be free of solids; however, a heavy plug of thoria (av density, 3.0), which extended from just above the top pressurizer heater to the bottom of the vanes, had accumulated in the lower section of the 4-in. pipe. With the exception of a small hole, approximately 1 to 1.5 in. in diameter through the center of the plug, the pipe was filled. No other obstructions were found in the system.

Comparative chemical analytical data and particle-size analyses of samples withdrawn from the system during circulation and samples of the plug are shown in Table 12.1.

Pump components were worn considerably during the 49-hr test. The pump impeller lost 8.5 g. No localized attack was apparent, although both front and rear surfaces of the impeller were highly polished. The front bearing and journal of 98M2 Stellite wore, respectively, 0.0026 in. and 0.0195 in.; the back Stellite journal, 0.0005 in.; and the back Graphitar bearing, 0.0002 in.

No modifications in loop geometry were made before run CS-27; however, the pump was refitted with No. 14 Graphitar bearings, and a new rotor, fabricated with a solid shaft having 98M2 Stellite journals, was used. Before run CS-27 a 30-hr performance test, run CS-26W, was made at 300°C with oxygenated water; no measurable wear of any of the pump parts was detected after the test.

For run CS-27, a new method of charging slurry to the system was used. Initially the loop was charged with 17.3 liters of water and 120 psi of oxygen at room temperature. After water was circulated in the system at 300°C for a period of 66 hr, sufficient slurry was added to the system, while the loop was operating at 300°C and 1500 psi pressure, to provide a circulating concentration of 500 g of thorium per kilogram of water. Five batch additions of a slurry prepared from lot LO-2 thoria were required to obtain the desired concentration. After each addition, the loop was sampled to determine what percentage of the added thoria was being circulated. Concentration changes were followed by withdrawing samples into special sample vials, weighing, precisely measuring the volume of the sample with a cathetometer, and calculating the sample density.

After each of the first four additions the circulating concentration reached the calculated concentration level within 30 min after the charge was added. The fifth charge of 1965 g of thorium oxide was injected into the loop at run-hour 78 to provide a final calculated circulating concentration of 500 g of thorium per kilogram of water. A sampled concentration of 490 g of thorium per kilogram of water was obtained 1 hr after the addition was made. Concentration changes were then followed by sampling at 48-hr intervals for the duration of the test. A gradual downward trend to 410 g of thorium per kilogram of water occurred over the following 222-hr period to run-hour 300.

TABLE 12.1. SUMMARY OF SAMPLE DATA – RUN CS-25

	Slurry Samples Taken After the Following Pumping Times						Solids Removed from Pressurizer After Shutdown	
	0 hr	3.0 hr	23.2 hr	29.4 hr[a]	46.0 hr[b]	49.0 hr	Center of Plug	Adjacent to Wall
Slurry concentration								
g of Th per kg of H_2O	958	572	496	580	506	562	2700 (density 3.12)	2340 (density 2.85)
mg of Th per g of slurry	458	345–347	317–319	348–350	321–322	339–343	660–665	638–640
H_2O, mg per g of slurry							229	252
Solid phase, mg per g of slurry								
Fe	0.016	0.037	0.142	0.133	0.172	0.235	0.480	0.470
Cr	0.003	0.036	0.054	0.119	0.116	0.102	0.199	0.185
Ni	0.006	0.017	0.024	0.037	0.095	0.030	0.062	0.074
Ti	0.002	0.027	0.071	0.059	0.099	0.078	0.146	0.132
Co	0.005	0.005	0.005	0.16	0.21	0.05	0.005	0.005
Cl	0.015	0.015	0.01	0.01	0.01	0.01	0.01	0.01
Si	0.01	0.01	0.01	0.01	0.01	0.03	0.07	0.07
SO_4^{--}	0.01	0.01	0.01	0.01	0.01	2.49	4.90	3.93
Mg	0.010	0.020	0.011	0.020	0.013	0.016	0.020	0.023
Al	0.010	0.015						
Average sedimentation particle size,[c] wt %								
Over 10 μ	28	0	1	2	0	0	1	0
3–10 μ	20	8	7	3	3	2	16	3
1–3 μ	27	25	19	21	23	30	20	20
<1 μ	25	67	73	74	73	68	63	77
X-ray crystallite size, Å	240	245	240	245	255	245		
Surface area N_2, m^2/g	16.5			21.1		21.5		

[a]Slurry addition made between run-hours 26 and 29.4.

[b]650 ml of 0.9 N H_2SO_4 added after 46 hr.

[c]Determined by neutron activation analysis using 0.001 M $Na_4P_2O_7$.

The scheduled 300-hr test was terminated without incident. With the exception of a moderate deposit of slurry in the annulus between the specimen holder and one sample barrel, in which the flow of slurry was approximately 6 gpm, no accumulations of thoria were found in the system. The pump impeller lost a total of 11.5 g, as a result, principally, of localized erosive attack of the front hub and impeller vanes. No measurable wear of other pump parts occurred.

Corrosion rates calculated from weight losses of defilmed pin specimens exposed for 49 hr at an average concentration of 534 g of thorium per kilogram of water in run CS-25 at 11, 21, and 41 fps, respectively, included (in mpy): gold, 0.4, 0.4, and 4; austenitic stainless steels, 2 to 4, 5 to 9, and 18 to 23; titanium and alloys, <0.1 to 1, 3 to 5, and 7 to 11; Zircaloy-2, 0.1, 1, and 6; and mild steel, 140 to 160, 120 to 210, and 190 to 220. The high rate on mild steel could be due to the sulfuric acid addition during the last few hours of the run. Generalized system corrosion averaged 4 mpy, based on stainless steel corrosion products found in the slurry.

Corrosion rates observed on pin specimens exposed for 300 hr at an average concentration of 426 g of thorium per kilogram of water in run CS-27 at 10, 22, and 41 fps, respectively, were (in mpy): gold, 0.1, 0.1, and 0.6; austenitic stainless steels, 0.7 to 1, 2 to 4, and 6 to 9; titanium and alloys, 0.2, 2, and 6; Zircaloy-2, 0.1, 0.1, and 2; mild steel, 11, 13, and 20 to 28. Incoloy corroded at rates of 1 and 8 mpy at 11 and 21 fps, respectively; nickel corroded at a rate of 6 mpy at 40 fps. Generalized system corrosion averaged 2 mpy.

For run CS-25 the velocity was 9.5 fps in the main loop, 13 fps in the bypass mixing line, and 0.26 fps in the pressurizer. In run CS-27 the velocity was 9.6 fps in the main line, 14 fps in the mixing line, and 0.26 fps in the pressurizer. These values were obtained by metering the flow of water in the loop at room temperature.

12.1.2 In-Pile Slurry Loop Development

Some short-term water runs were made in the experimental in-pile slurry loop, and one run was made in an attempt to add thorium oxide to the loop. During the runs with water the various flow rates in the loop and pressurizer were measured, calibrated, and adjusted. One run with water at 250°C was made for approximately 80 hr to further

evaluate the operational stability of the system and the reliability of the condensate system used to provide purge water feed to the pump rotor cavity. A steady condensate production rate of approximately 1.9 liters/hr was obtained. Although this rate is sufficient for purge water feed to the pump rotor cavity, more condensate is needed to operate the slurry addition device.[4]

It was decided that for slurry run HT-17 the loop would be started up with water, and thorium oxide would be added by means of the 325-ml addition tank after operating temperature and pressure were reached. This decision was made because it had not been possible to produce sufficient condensate at temperatures below about 200°C to purge the pump bearings properly.

The loop was charged with distilled water, and 60 psi of oxygen was added at room temperature. The loop was then operated at 250°C in the line and at 257°C and about 600 psia in the pressurizer for 26 hr to demonstrate stable operation. During this period the condensate production rate was approximately 3.4 liters/hr. The slurry addition tank was charged with 350 g of thorium oxide from batch LO-2 and 290 g of water so that a slurry concentration of 310 g of thorium per kilogram of water would be obtained when the slurry was charged to the loop and replaced with an equal volume of condensate. The tank was then opened to the loop and flushed through with condensate at a rate of approximately 0.5 liters/hr. After 24 hr of operation under these conditions, a sample from the circulating loop contained less than 1 g of thorium per kilogram of water.

An examination of the contents of the slurry addition tank revealed that most of the thorium oxide had remained in the tank. The solids had settled on the wall of the tapered reducer at the bottom of the tank, and the purge-water feed had channeled through. This reducer was changed to one with a more gradual taper in an attempt to eliminate the channeling in future tests.

12.2 TOROIDS

It has been postulated[5] that the behavior of thorium oxide slurries is critically dependent on the calcination temperature of the oxide and on its particle size, as well as on the solution in which

---

[5]V. D. Allred *et al., HRP Quar. Prog. Rep. Jan. 31, 1955,* ORNL-1853, p 178; G. E. Moore and E. L. Compere, *HRP Quar. Prog. Rep. July 31, 1955,* ORNL-1943, p 140.

the oxide particle is immersed. Studies of the attack rate of thorium oxide slurries, circulated in toroids, as a function of the calcination temperature of the oxide have been completed and reported.[6] Some information is now available on the effect of the particle size of the oxide, and on the effect of the addition of phosphate ions to the aqueous slurry system.

12.2.1 Effect of Thorium Oxide Particle Size

It has been difficult to evaluate the effect of particle size of the thorium oxide upon the attack of materials by circulating aqueous thorium oxide slurries. The particles studied so far (oxalate precipitated, multistage calcined to the oxide) often become degraded upon circulation[7] so that, at least during the early stages of circulation, the average particle size is decreasing. Ultimately, a steady state or equilibrium is reached, and the length of time required to reach equilibrium probably affects the degree of attack. Evaluation of the effect of particle size is also complicated by the usual errors inherent in small samples of large quantities, the limited range of sizes of thorium oxide particles so far available for study, and, when the attack is severe, the contamination of the thorium oxide by corrosion products. The contamination may produce errors in the methods used for particle-size determination.[8]

A correlation between attack rate of type 347 stainless steel and ultimate (degraded) thorium oxide particle size was attempted, based on the assumption that the time required to degrade the particles and the amount of metal corroded in the process are small as compared with the time and corrosion for the entire run. Examined were data for 109 type 347 stainless steel pins that had been exposed at 250°C, 26 fps, and under oxygen pressure to slurry containing 1000 g of thorium per kilogram of water. Thorium oxide used in the tests consisted chiefly of unsized D17 material (ORNL Chemical Technology Division production)

recalcined at temperatures up to 1600°C, although other oxides produced at ORNL and some sized D17 oxide were used also. Some of the slurries had been circulated in 100A loop CS prior to use in the toroids.

There was no clear relationship between corrosion rate and ultimate particle size. In tests with 79% of the pins the final average particle size was less than 1.4 μ and on the average it was 0.7 μ. The maximum corrosion rate was 14 mpy but the average for the pins was 3 to 4 mpy. In tests with the remaining 21% of the pins the ultimate average particle size was from 2.1 to 4.5 μ. For two-thirds of those pins the corrosion rates were less than 13 mpy but the average was greater than 6 mpy. The remaining pins were attacked at rates from 24 to 40 mpy; the thorium oxide contained relatively large amounts of corrosion products and there was evidence of oxygen depletion due to the severe attack. The effect of these factors on the correlation has not yet been determined.

As an alternate approach to the problem, thorium oxide produced by the ORNL Chemical Technology Division was separated by repeated gravitational sedimentation into several fractions, each composed of a definite range of sizes of thorium oxide particles. The procedure for accomplishing this fractionation involved the production of a relatively stable suspension of thorium oxide containing from 100 to 300 g of thorium per kilogram of water by the addition of a suitable concentration of oxalic acid. This suspension was then permitted to settle for calculated periods of time, and Stokes' law was assumed to be valid even for the extreme conditions of this particular system. The respective fractions were again allowed to sediment, according to the operational scheme given by Fischer.[9] Fractions were accumulated which corresponded to diameters larger than 3 μ, between 1 and 3 μ, and less than 1 μ. The thorium oxide was dried, and the oxalic acid was removed by thermally decomposing it at a temperature of 550°C, which was less than the maximum calcination temperature of any of the oxides. Each fraction averaged at least 70% purity, as illustrated in the typical fractionation shown in Table 12.2. Over-all recoveries of 83 to 99% were obtained.

The sized thorium oxide at a concentration of 1000 g of thorium per kilogram of water was then

---

[6]G. E. Moore and E. L. Compere, *Dynamic Slurry Corrosion Studies, Quarter Ending Jan. 31, 1956,* ORNL CF-56-1-168 (March 27, 1956), p 33.

[7]E. L. Compere *et al., HRP Dynamic Slurry Corrosion Tests: Quarter Ending April 30, 1956,* ORNL CF-56-4-139, p 16; C. E. Schilling, *HRP Quar. Prog. Rep. Oct. 31, 1955,* ORNL-2004, p 179.

[8]G. W. Leddicotte and H. H. Miller, *Anal. Chem. Semiann. Prog. Rep. Oct. 20, 1954,* ORNL-1788, p 21.

[9]E. K. Fischer, *Colloidal Dispersions,* p 37, Wiley, New York, 1950.

circulated in toroids at 26 fps relative velocity, at 250°C, and under an oxygen atmosphere. The results of these runs on the attack of type 347 stainless steel are summarized in Table 12.3. Although the results are not perfectly definitive, qualitative microscopic examination of the pins confirms for all the runs the trend shown by the 1200, 1400 (96 hr), and 1600°C oxide experiments; that is, slurries of the smaller sized thorium oxide caused less attack than slurries prepared from larger sized thorium oxide. Attack by slurries of larger sized particles was usually characterized by definite metal loss, apparently through excessive polishing action, and usually localized attack at the root of the pin. This was probably due either to the centrifuging action of the motion imparted to the toroid or to the turbulence of flow in that vicinity. The slurries of particles less than 1 μ in diameter (fraction C) did not produce any effect on the pins.

TABLE 12.2. FRACTIONATION BY GRAVITATIONAL SEDIMENTATION IN OXALIC ACID OF
D-17 THORIUM OXIDE RECALCINED AT 1600°C

Particle Size*	Weight Per Cent Found			
	As Calcined	Fraction A (>3 μ)	Fraction B (1 to 3 μ)	Fraction C (<1 μ)
>3 μ	40	70	7	5
1 to 3 μ	44	26	70	9
<1 μ	16	4	23	86
$\overline{d\mu}$	2.4	4.9	1.4	0.7

*Particle size distribution determined by gravitational sedimentation in 0.001 M Na$_4$P$_2$O$_7$ (ref. 8).

TABLE 12.3. ATTACK ON TYPE 347 STAINLESS STEEL BY CIRCULATING THORIUM OXIDE
SLURRIES OF VARYING THORIUM OXIDE PARTICLE SIZE

Sized D-17 thorium oxide
1000 g of thorium per kilogram of water
250°C
26 fps
100 psi oxygen

Calcination		Duration of Run (hr)	Average[a] Attack Rate on Type 347 Stainless Steel (mpy)			
°C	Hours		Fraction A (>3 μ)	As Calcined (85% >1 μ)	Fraction B (1 to 3 μ)	Fraction C (<1 μ)
650	b	316	2	4[c]	7	3
1200	7	232	12	3	4	1
1400	2	261	5	4	2	4
1400	96	214	6	7	9	1
1600	4	260	7	4	1	1

[a]Average of two pins for each oxide; deviation not more than ±1 mpy.

[b]Original batch D-17 thorium oxide, ORNL Chemical Technology Division product.

[c]From average of many runs.

The attack on titanium showed a similar trend with original particle size, while Zircaloy-2 generally showed little attack under any of these conditions (generally less than 4 mpy, with an average of 2 mpy).

Interesting qualitative observations were made on the slurries themselves after these runs. For the oxides recalcined at 1200, 1400, or 1600°C, the slurry prepared from the smallest sized fraction (fraction C) invariably produced the thickest slurry of all the fractions after circulation, was also the whitest, settled the slowest (although apparently flocculated), and adhered most strongly to glass. On the other hand, the slurry prepared from fraction A particles yielded the thinnest slurry of all fractions after circulation, was the darkest (brown or black, indicating relatively large amounts of corrosion products), generally settled rapidly, and adhered to glass only slightly. All the settled solids were readily redispersed. The properties and behavior of the slurries of the as-calcined thorium oxide and fraction B were between the two extremes described.

12.2.2 Effect of Calcination Time

As a corollary to the study of the effect of thorium oxide calcination temperature, a study was made of the effect on the attack rates of calcination time at a given temperature. Portions of D-17 thorium oxide were recalcined in platinum dishes for periods of 2, 4, 24, or 96 hr at 1400°C. Marked changes in the crystallite size and in the specific surface area were observed[10] (see Table 12.4); however, there was no detectable change in the particle-size distribution.

Table 12.4 also presents the rates of attack of stainless steel, titanium, and Zircaloy-2 exposed to circulating slurries of these oxides. The slurries had a concentration of 1000 g of thorium per kilogram of water and were circulated for 263 hr at 26 fps relative velocity, at 250°C, and under an oxygen atmosphere. The attack rates, determined from weight-loss data of the corrosion pin specimens, appear to be independent of the length of time of calcination up to 96 hr. However, microscopic examination of the type 347 stainless steel corrosion pin specimens showed a localized attack near the root of some of the pins; the 96-hr oxide showed the greatest localized attack, while the oxides calcined for shorter times did not produce

---

[10]V. D. Allred and J. P. McBride, *HRP Quar. Prog. Rep. July 31, 1955*, ORNL-1943, p 181.

TABLE 12.4. EFFECT OF LENGTH OF CALCINATION TIME AT 1400°C ON THORIUM OXIDE PROPERTIES

D-17 thorium oxide
1000 g of thorium per kilogram of water
250°C — 263 hr circulation
26 fps
100 psi oxygen

	Hours of Recalcination at 1400°C				
	0	2	4	24	96
Crystallite size, Å	107	2500	3700	4600	>5000
Specific surface area, m²/g	30.3	1.40	1.31	1.16	0.89
Average particle diameter, as calcined	2.2	2.7	2.2	2.8	2.6
Average particle diameter, after circulation	0.7*	1.2	2.1	2.5	2.4
Attack rate, mpy					
Type 347 SS	4*	4, 4	4, 4	4, 5	6, 6
Titanium 75A	4*	3	2	2	7
Zircaloy-2	1*	3		2	2
Type 347 SS toroid	1*	2	3	2	3

*Previous data.

this attack (except for one of two pins exposed to the 4-hr calcined thorium oxide). The 4- and 96-hr oxides produced thin slurries after circulation, the 24-hr slurry was somewhat less fluid, and the 2-hr slurry was moderately thick.

It thus appears that, at least under the conditions of this test, 2-hr calcination was sufficient to produce marked changes in the physical properties of the thorium oxide, while 4-hr and longer calcinations produced only relatively minor further changes. However, upon circulation the 2-hr-calcined thorium oxide degraded to a greater extent than oxides calcined for longer periods of time. There again seemed to be a correlation in the degree of degradation and the production of a thick slurry. The 96-hr calcination produced an oxide whose aqueous slurry appeared to yield relatively high attack rates, especially of a localized nature.

12.2.3 Effect of Phosphate Additions

The behavior and properties of aqueous thorium oxide slurries are dependent upon the electrolytic character of the medium in which the thorium oxide is suspended. Some properties of thorium oxide in a number of such electrolytes have been studied.[11] One of the aqueous media in which thorium oxide can be readily dispersed and which yields fairly concentrated suspensions of thorium oxide is a solution of tetrasodium pyrophosphate, $Na_4P_2O_7$. Such solutions are used in the gravitational sedimentation of thorium oxide for particle-size distribution determinations[8] and have often been mentioned in regard to engineering studies to provide aqueous dispersions of thorium oxide. The effect of additions of aqueous tetrasodium pyrophosphate solutions and other phosphate buffer solutions to thorium oxide slurries on the attack rates of materials of interest was determined in some preliminary tests. The effect of phosphoric acid additions has been reported previously.[12]

Various concentrations of tetrasodium pyrophosphate solutions with and without thorium oxide present were circulated in toroids at 250°C, at 26 fps relative velocity, and with either oxygen or hydrogen atmospheres. In fewer experiments the phosphate buffer system of disodium hydrogen phosphate–sodium dihydrogen phosphate was cir-

culated. These tests are summarized in Table 12.5. Some static autoclave experiments (not included in the table) are also under way. Where several runs under identical conditions except for the length of the run have been completed, the average attack rate is reported, although the data for titanium have so far shown a relatively large dispersion.

Although the data are preliminary and the rates may be altered somewhat by further experimentation, there is no doubt that titanium can be severely attacked in both neutral (NaH_2PO_4-Ha_2HPO_4, pH ~ 7) and alkaline ($Na_4P_2O_7$, pH ~ 11) circulating slurries under both oxygen and hydrogen atmospheres at 250°C. Further investigations into the use of hydrogen-gas atmospheres are planned, and a few more experiments involving the phosphate system are indicated.

Figure 12.1 illustrates the severity of the attack
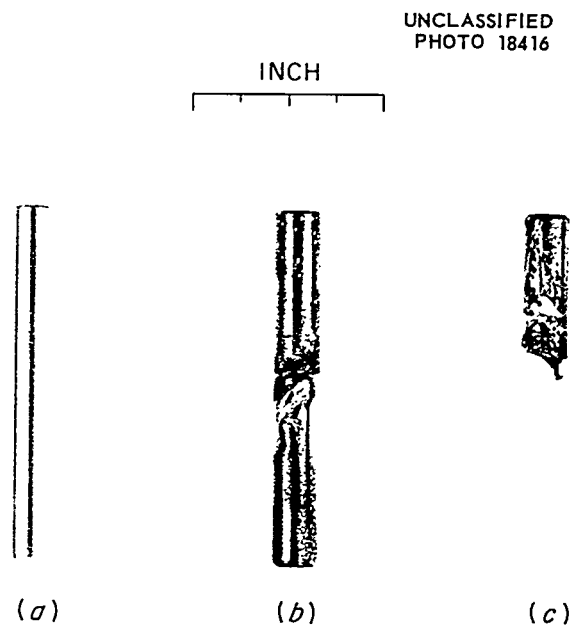
Fig. 12.1. Titanium 75A Corrosion Pin Specimens. (a) Unexposed control specimen. (b),(c) Pins after exposure in atmospheres of (b) approximately 100 psi oxygen at 250°C and (c) 1 atm of hydrogen at room temperature. Exposures were made for 294 hr in toroids at 26 fps relative velocity and 250°C to 0.1 M $Na_4P_2O_7$ slurries of 1000 g of thorium per kilogram of water (D-17-800-8 thorium oxide) at pH 10.9. The approximate attack rates were (b) 90 mpy and (c) greater than 1900 mpy. Only the lower approximate half of the pins were exposed to the circulating fluid.

[11] D. G. Thomas, J. D. Perret, and R. Buxton, *HRP Quar. Prog. Rep. Oct. 31, 1954,* ORNL-1813, p 125; D. E. Ferguson *et al., ibid.,* p 145; V. D. Allred and J. P. McBride, *HRP Quar. Prog. Rep. Oct. 31, 1955,* ORNL-2004, p 172.

[12] R. N. Lyon *et al., HRP Quar. Prog. Rep. July 31, 1954,* ORNL-1772, p 118.

on titanium 75A exposed to circulating thorium oxide slurries (1000 g of thorium per kilogram of water) containing 0.1 M $Na_4P_2O_7$ at 250°C and 26 fps relative velocity for 294 hr. Under the oxygen atmosphere an attack rate of 90 mpy was calculated from weight-loss data; with hydrogen a rate in excess of 1900 mpy was obtained.

TABLE 12.5. EFFECT OF PHOSPHATE ADDITIONS TO THORIUM OXIDE SLURRIES CIRCULATED IN TOROIDS AT 250°C AND 26 fps RELATIVE VELOCITY

Concentration (g of Th per kg of H_2O)	PO_4 (M)	Additive	Initial pH	Atmosphere	Average Attack Rate (mpy)		
					Type 347 SS	Titanium	Zircaloy-2
0	0.02	$Na_4P_2O_7$	10	O_2	1	+	+
0	0.2	$Na_4P_2O_7$	10	O_2	4	17	1
1000	0.00	NaOH	11	O_2	3	3	1
1000	0.01	$Na_4P_2O_7$		O_2	7	4	0
1000	0.02	$Na_4P_2O_7$	10	O_2	10	8	2
1000	0.2	$Na_4P_2O_7$	11	O_2	14	60	+
1000	0.00	NaOH	11	H_2	35	8	2
1000	0.2	$Na_4P_2O_7$	11	H_2	5	>1900	0
1000	0.00	None	7	O_2	2	4	1
1000	0.2	NaH_2PO_4-Na_2HPO_4	7	O_2	15	>300	1
1000	0.00	None	7	H_2	6	1	0
1000	0.2	NaH_2PO_4-Na_2HPO_4	7	H_2	6	>1400	1

13. RADIATION CORROSION

G. H. Jenks   H. C. Savage

A. L. Bacarella	B. O. Heston	F. J. Walter
J. E. Baker	D. T. Jones	R. M. Warner
S. E. Bolt	R. A. Lorenz	K. S. Warren
R. J. Davis	T. H. Mauney	D. B. Weaver[1]
H. O. Day	J. R. McWherter	S. H. Wheeler
V. A. DeCarlo	A. R. Olsen	L. F. Woo
H. A. Fisch	J. A. Russell	W. C. Yee
	M. D. Silverman	

13.1 IN-PILE LOOPS

J. R. McWherter   H. C. Savage

J. E. Baker	A. R. Olsen
S. E. Bolt	J. A. Russell
D. T. Jones	F. J. Walter
R. A. Lorenz	R. M. Warner
T. H. Mauney	D. B. Weaver

S. H. Wheeler

13.1.1 Development and Construction

(a) **General.** — Construction of in-pile loop assemblies for operation in beam holes HB-2 and HB-4 at the LITR is continuing. Modifications to the loop design are continually being made and incorporated in loops to improve operation and/or meet the varying operational demands. These modifications include an increase in loop cooling capacity to allow operation with greater fission power in the core and a redesign of the loop layout to make use of the Byron Jackson 5-gpm circulating pump instead of the ORNL 5-gpm pump.

(b) **HB-4 Loop Package.** — Loop L-4-13[2] is still awaiting installation in beam hole HB-4. Revisions to the equipment and instrument panel at the LITR to permit operation at temperatures and pressures to 300°C and 2000 psia have not been completed.

(c) **HB-2 Loop Package.** — The all-titanium in-pile loop, L-2-14, was completed and tested. This loop is ready for installation in beam hole HB-2 of the LITR. The corrosion specimen holders (type 75A titanium, tapered-channel) in the core and line positions of loop L-2-14 contain corrosion coupons of types 347 and 309 SCb stainless steel, titanium type 55AX, titanium alloy containing 6% Al and 4% V, crystal-bar zirconium, Zircaloy-2, and a zirconium alloy, containing 15% Nb, in two crystal-structure forms: monoclinic and cubic. Impact specimens of titanium type RC-A40 are included in the core and line positions, as well as tensile test specimens of titanium type RC-A40 and C-130-AM. Installation of the loop in beam hole HB-2 of the LITR may be delayed until loop L-2-15 has been operated, in order to allow time for further laboratory exploration of the operating conditions which have been proposed.

Construction of in-pile loop L-2-15 (a type 347 stainless steel loop) is essentially complete. Additional cooling capacity is being incorporated in this loop to allow operation at higher fission power in beam hole HB-2. The loop cooler of L-2-15 is designed to provide 4 to 5 kw of cooling capacity, as compared with the 2 to 3 kw in previous in-pile loops.

(d) **Byron Jackson Pumps.** — Ten Byron Jackson canned-rotor pumps have been ordered for use in in-pile loops. These pumps are of a two-stage centrifugal type, designed to circulate solution at 300°C and 2000 psia at a rate of 5 gpm against 40 ft of head. They are of stainless steel, all-welded construction and have aluminum oxide bearings and journal bushings. The over-all pump dimensions are $3\frac{1}{2}$-in. OD × $20\frac{1}{2}$-in. length, as compared with the $6\frac{1}{16}$-in. OD × 12-in. length for the ORNL in-pile pump presently in use. Redesign of the present loop layout was required to accommodate the increased pump length. The pump motor operates on 145-v, a-c, 60-cycle three-phase power supply. Two of the ten pumps have been received and are currently under test.

(e) **ORR Loop.** — Design layout of the in-pile corrosion loop facility for the ORR has begun. The design power density for the core has been increased from the 33 w/ml reported previously[3]

---

[1]On loan from TVA.

[2]G. H. Jenks *et al., HRP Quar. Prog. Rep. April 30, 1956,* ORNL-2096, p 90.

[3]*Ibid.,* p 90–92.

to 66 w/ml (average); a density of 100 w/ml will be obtained on the leading specimen.

13.1.2 Metallographic Examination of In-Pile Loop EE

The metallographic examination of components and specimens from in-pile loop EE was completed, and results were reported[4] during the quarter. A description of the operation and the results of an examination of this loop were included in a previous quarterly progress report.[5] The following summary of the metallographic findings completes the report on the postirradiation examination of the loop.

Metallographic examination of the type 347 stainless steel components indicates qualitatively that there was some attack of the loop pressurizer above the liquid level and of the core cap. The remaining sections below the solution level in the pressurizer, the pressurizer heater, and the pump outlet line showed no indication of corrosive attack after film formation. As with previous metallographic examinations, uniform generalized attack of the components cannot be determined because of the fabrication tolerances on the original stock.

Various coupons from the loop, together with all the stress specimens, were also examined. The results of these examinations are summarized in Table 13.1. The metallographic findings closely parallel the weight-loss determinations. The originally sand-blasted surfaces of the Zircaloy-2 stress specimens made essentially impossible a postirradiation evaluation of corrosive attack based on surface appearance.

13.1.3 General Description of In-Pile Loop Experiment L-4-11

Except for metallographic examination, the sixth in-pile loop experiment, L-4-11, was completed. Details of this experiment and the results will be reported.[6] A summary is presented below.

The purpose of this experiment was to compare a large number of samples of various materials under irradiation conditions similar to those in

previous loops.[4,7,8] For the first time, straight-channel coupon holders were used in the core and in-line positions to maintain a uniform velocity over the materials in the holders.

Identical sets of corrosion coupons (24 each) in Zircaloy-2 coupon holders were installed in the core and in-line positions. Eight rod assemblies containing uncoupled coupons were mounted around the core coupon holder, and four were mounted around the in-line coupon holder. Type 347 stainless steel rods and spacers were used in these assemblies. Four slender, pin-type, Zircaloy-3 specimens were also mounted around the coupon holders in both positions. A type 347 stainless steel bracket containing two sapphire specimens was mounted on the forward end of the core coupon holder.

Many different zirconium alloys were tested. Their code numbers and compositions are given in Table 13.2. In addition to the zirconium alloys, stainless steel, titanium alloys, platinum, Incoloy, and sintered alumina specimens were exposed in the loop. The stainless steel specimens included types 347, 350A, 443, and 446. The titanium specimens included types Ti-75A, Ti-110AT, and Ti-130AM.

The initial operating conditions employed in this experiment were similar to those reported for previous loop experiments (0.17 m UO_2SO_4, 0.031 m $CuSO_4$, 0.04 m H_2SO_4, loop at 250°C, pressurizer at 280°C); however, as a result of decreasing pressurizer flow rate, the pump speed was increased about 40% after 100 hr of circulation time. Later an attempt was made to loosen any plug in the pressurizer by changing the pressurizer temperature. The temperature of the pressurizer, initially 280°C, was decreased to 260°C for a short time and then raised to 270°C, where it was maintained for the remainder of the experiment. This appeared to have little effect on the pressurizer flow rate, and after 344 hr of circulation time the loop was drained, given a standard pretreatment,[7] and charged with fresh solution. Operation was continued for an additional 786 hr of circulation time. The pressurizer flow rate during the latter part of the run was only 12% of the initial rate. The main-stream temperature was maintained at 250°C

[4]A. E. Richt, *Metallographic Examination of HRP In-Pile Loop "EE" Components and Coupons,* ORNL CF-56-7-17 (July 6, 1956).

[5]H. C. Savage et al., *HRP Quar. Prog. Rep. Oct. 31, 1955,* ORNL-2004, p 123—150.

[6]E. G. Bohlmann et al., *HRP Radiation Corrosion Studies (In-Pile Loop L-4-11),* ORNL-2152 (in press).

[7]G. H. Jenks et al., *HRP Quar. Prog. Rep. July 31, 1955,* ORNL-1943, p 109.

[8]G. H. Jenks et al., *HRP Quar. Prog. Rep. Jan. 31, 1956,* ORNL-2057, p 92—95.

TABLE 13.1. SUMMARY OF METALLOGRAPHIC EXAMINATION RESULTS FOR HRP IN-PILE LOOP EE

Identification	Alloy	Specimen No.	Specimen Weight Change (mg)	Metallographic Results
Coupon	Type 347 stainless steel	787A	−0.1	No evidence of corrosive attack
		740A		A few pits, approximately $\frac{1}{2}$ mil deep
		747A	2.5	Numerous pits, approximately 1 mil deep
		743A	−105.5	Severely attacked; over 4 mils of surface removal
	Zircaloy-2	Z-12		No evidence of corrosive attack
		Z-37	−1.6	Slight surface roughening
		Z-24	−2.9	Slight surface roughening
		Z-19	−5.1	Numerous pits, approximately $\frac{1}{2}$ mil deep
	Ti-55AX	T-3		No evidence of corrosive attack
		T-16	−0.4	No evidence of corrosive attack
		T-8	−0.5	No evidence of corrosive attack
		T-12	−1.4	No evidence of corrosive attack
Stress specimen	Type 347 stainless steel	SS-11	−33.7	Slight pitting attack, less than 1 mil deep
		SS-12	−35.5	Slight pitting attack, less than 1 mil deep
		SS-13	−26.1	Slight pitting attack, less than 1 mil deep
		SS-14	−30.6	Slight pitting attack, less than 1 mil deep
	Zircaloy-2	Zr-2	−93.1	Very rough, uneven surface
		Zr-3	−94.0	Very rough, uneven surface
		Zr-4	−76.4	Very rough, uneven surface
		Zr-5	−72.4	Very rough, uneven surface
	Ti-55AX	Ti-1	−3.2	No evidence of corrosive attack
		Ti-2	−3.1	No evidence of corrosive attack
		Ti-11	−4.5	No evidence of corrosive attack
		Ti-12	−3.8	No evidence of corrosive attack

throughout the experiment. The total circulation time was 1130 hr, of which 1109 hr was in the reactor. The energy output of the LITR during this time was 2175 Mwhr, and essentially all of this power was liberated at the 3-Mw level. The initial solution and the solution used when the loop was recharged were of approximately the same composition:

UO_2SO_4	0.17 *m* (U^{235}/total U = 0.927)
$CuSO_4$	0.031 *m*
H_2SO_4	0.04 *m*

The first solution also contained 504 ppm of nickel, which was added as $NiSO_4$.

During the normal shutdown operation, the drain line on the loop plugged during the third rinse, and the loop had to be drained through the pump drain line. Since the loop cannot be completely drained through this line, a portion of the rinse water was still in the loop when it was removed from the reactor.

The average fission power during operation, as determined from cesium analyses, was 709 w when the LITR was at 3 Mw. The power density at a given location was determined from measurements of the induced activities of the zirconium-alloy specimens. The power densities thus determined ranged from about 7.2 w/ml at the forward end of the coupon holder to 1.3 w/ml at the rear. Although the power density at the forward end is higher, the

average power density is about the same as that reported for loop GG.[7]

The average corrosion rate as calculated from the oxygen data, which was in agreement with the rate based on nickel data, was 2.8 mpy for the first 344 hr of exposure, at which time the initial solution was drained. The rate for the next 300 hr, with the second solution, was about 4.1 mpy, and for the remainder of the run was about 2.0 mpy. This compares with 4.0 mpy during the first 300 hr and 0.7 mpy during the remainder of the run for experiment L-4-8.[8]

TABLE 13.2. ZIRCONIUM ALLOYS IN EXPERIMENT L-4-11

Code Letters	Alloy	Alloy No.	Composition or Description					
			Sn(%)	Fe(%)	Cr(%)	Nb(%)	Other (%)	N_2 (ppm)
ZA	Zr-1							
ZB	Zr-2							
ZC	Zr-3						3 (Ag)	
ZD	Zr-3	6	0.26	0.19				40
ZE	Zr-3	12A	0.50	0.44				
ZF	Zr-3	13A	0.50	0.24			0.25 (Ni)	
ZG	Zr-3	19	1.46	0.25			0.21 (Mo)	50
ZH	Zr-2						Various H_2 additions	
ZI	Zr-3	32B	0.47	0.85			0.78 (Ni)	50
ZJ	Zr-3	38	0.56				0.71 (W) 60 ppm H_2	
ZK	Zr-3	44	0.52				5.71 (Ti)	40
ZL	Zr-3	51	0.52	0.28			5.66 (Ti)	60
ZM	Zr-3	57		0.24		0.32		70
ZN	Zr-3	61	1.54	0.26		0.83		80
ZO	Zr-3	73					3.84 (Al), 2.5 (Mn)	
ZP	Zr-3	70	0.69				0.69 (Cu)	40
ZQ	Zr-3			0.81	0.77			
ZR	Zr-3		0.45	0.72	0.73			
ZS	Zr-3		0.50		1.5			
ZT	Zr-3					15		
ZU	Zr-3					2		
ZZ	Zr-3[a]							
WA	Zr-2[b]							
WB	Zr-2[c]							
WC	Zr-2[d]							
Rod I	Zr-3			0.7				
Rod II	Zr-3			1.4				
Rod III	Zr-3			3.5				
Rod IV	Zr-4			0.7	2.8			

[a]Crystal bar.

[b]Cut from Newport News top weld.

[c]Cut from Newport News bottom weld

[d]Cut from Newport News weld.

13.1.4 Qualitative Results of Inspection and Evaluation of Loop L-4-11

As with previous loop experiments, all stainless steel surfaces outside the core were covered with a heavy rustlike scale. The deposit of scale in the pressurizer was heavier in the liquid-phase region than in the vapor-phase region. There was no apparent localized attack on any of the components inspected.

Both in-line sample arrays were covered with a bulky rustlike scale. The sintered alumina coupon in the in-line holder disintegrated. There was a white oxide film under a bulky gray-white deposit which completely covered the zirconium alloy containing aluminum and manganese. Otherwise, all in-line holder coupons had the same general appearance. As with all previous loops, cathodic defilming of the in-line coupons was only partially effective; some film was retained by the coupons. In fact, all but two of the zirconium-alloy coupons showed weight gains following the final defilming. Some peculiarities in attack were observed on the defilmed Zircaloy-2 in-line coupon holder. The middle portions of both halves on both inside and outside surfaces were heavily etched, while the ends of the holder retained their smooth machined surfaces.

On dismantling, the core was found to be full of solution, probably rinse water which could not be completely drained from the system upon completion of the experiment. All surfaces in the core were found to be coated with a dark, loosely adherent deposit, possibly a result of having remained in contact with the solution for several weeks between termination of the experiment and dismantling of the loop. This is the first loop in which any scale was retained on coupons in the Zircaloy-2 core coupon holder.

The single sintered-alumina coupon in the core holder disintegrated. A small piece of the single core rod-coupon was found to be intact, but it fell apart upon handling. Two core rod-coupon assemblies, A and H, were very difficult to disassemble. The coupons could not be completely removed from the rods until the rod assemblies had been cathodically defilmed.

An examination of the pump showed no measurable wear of the sintered-alumina bearings.[9]

13.1.5 Quantitative Results of Inspection and Evaluation of Loop L-4-11

Corrosion-rate values reported below were calculated from weight-loss data, with the exposed specimen areas and total radiation time (equivalent to 725 hr of LITR operation at 3 Mw) used as a basis for the calculations. This is the first loop in which straight-channel coupon holders were used; hence no effect of velocity gradient on core and in-line coupons could be observed. Solution velocity through the holders was about 13.3 fps.

(a) **Zirconium and Zirconium Alloys.** – The corrosion results obtained on Zircaloy-2 specimens were in good agreement with those obtained for Zircaloy-2 specimens in previous loops.[10] Rates observed varied from 2 mpy at 2 w/ml power density to 4 mpy at 6 w/ml power density. One of the striking results is that most of the other zirconium alloys tested corroded at about the same rate as Zircaloy-2 did in the core region, with the same general power-density dependency. The ZC, ZK, and ZL specimens corroded at two to three times the Zircaloy-2 rates under similar conditions. The ZO coupons, zirconium with aluminum and manganese, corroded at rates of 59 to 121 mpy in the core region. The zirconium-alloy pin-type specimens, rods I and III, corroded at about 5 mpy, while rods II and IV corroded at 12 mpy. These pin specimens were at an average power density of 3.8 w/ml.

The ZT specimens, zirconium with 15% niobium, exhibited a negligible corrosion rate at 1.9 w/ml and a low rate of 1.2 mpy at 5.6 w/ml. The latter is less than one-third the rate observed for Zircaloy-2 at the same power density.

Most of the zirconium alloys in the in-line positions could not be defilmed completely, and weight gains were observed after the final defilming. Some of the exceptions were the ZO, ZC, and ZU specimens. In-line corrosion rates for the ZO specimens ranged from 59 to 82 mpy. Rates for the ZC coupons ranged from 3 to 5 mpy. The single ZU coupon corroded at 17 mpy. The in-line ZT specimen showed a weight gain of two to three times that of the Zircaloy-2 in-line specimens.

The Zircaloy-2 weld specimens and the Zircaloy-2 specimens with added H_2 did not appear to corrode at rates higher than those observed for Zircaloy-2.

[9]A. R. Olsen, *Examination of In-Pile Loop Pump from Loops EE and L-4-11,* ORNL CF-56-6-135 (June 18, 1956).

[10]J. E. Baker *et al., HRP Radiation Corrosion Studies — In-Pile Loop L-4-8,* ORNL-2042 (Aug. 8, 1956).

(b) Titanium Alloys. — The average corrosion rates of titanium coupons in the core and in-line positions were 0.6 and 0.7 mpy, respectively. No significant difference was noted between the various alloys tested. The corrosion rate of the holder coupons at 13.3 fps velocity was about 1 mpy, as compared with an average of 0.4 mpy exhibited by the core rod coupons at low velocity. Very little effect of power density was noted. Two of six Ti-75A in-line rod-coupon specimens exhibited rates of over 1 mpy, as compared with a maximum rate of 0.43 mpy for a core rod coupon of this material.

(c) Stainless Steel. — Two stainless steel specimens were located in the core holder — one of type 347, the other of type 443. Both specimens were exposed at a power density of about 1.3 w/ml and to a solution velocity of 13 fps. The corrosion rate determined for each specimen was 2.2 mpy. This rate is approximately 1.3 times the rate observed for type 347 stainless steel under similar conditions in experiment L-4-8.[10]

Core rod coupons of types 347, 350A, 443, and 446 stainless steel were exposed at power densities below 4 w/ml. The observed corrosion rate in each case was less than 1 mpy. One specimen of type 350A and one of type 446 were exposed at higher power densities, about 5.5 w/ml. The observed rate for the type 350A was 2.2 mpy. That for the type 446 was 15.8 mpy.

The corrosion rate of the type 443 stainless steel coupon located in the in-line holder was about the same as that for the coupon in the core holder. However, the type 347 stainless steel coupon in the in-line holder had a corrosion rate of only 0.2 mpy. The corrosion rates of the in-line rod coupons were not appreciable.

(d) Incoloy. — The core coupon array contained one Incoloy specimen in the low-flux region of the holder. The core rod-coupon assembly contained three Incoloy specimens. With the exception of the core rod specimen of Incoloy in the high-flux region (4.2 w/ml), which had a high corrosion rate of 5.4 mpy, the corrosion rates were about the same as those for the stainless steel core rod specimens at the same power densities. The in-line Incoloy specimens showed lower corrosion rates than the core specimens. Single specimens in the in-line holder and in-line rod arrays gave rates of 0.1 mpy each.

(e) Platinum. — Platinum corroded very slightly. Core coupons and core rod coupons gave corrosion rates of from 0.03 to 0.3 mpy. One coupon exhibited a rate of 1.6 mpy; however, this may have occurred as a result of damage to the specimen during removal from the loop. The in-line specimens showed either no weight change or a weight increase after the final defilming.

(f) Sintered Alumina. — Two alumina specimens located in the core region and one in an in-line position disintegrated. A very small portion of the core rod coupon was in place after disassembly.

(g) Synthetic Sapphire. — Two synthetic sapphires, which were held in a special bracket in front of the regular core-specimen assemblies, acquired a loose flaky deposit of transported iron oxides and lost much of their transparency. The power density in the sapphire location was about 8 w/ml, and the corrosion rate of the specimens was about 12 mpy.

13.1.6 In-Pile Loop L-4-12

Exposure of in-pile loop experiment L-4-12 in the LITR was completed. Disassembly and examination of the loop and loop specimens are in progress.

Unlike the previous experiments, this one contained a titanium core, coupled to the stainless steel loop with titanium-to-type-347-stainless-steel unions, and tapered titanium coupon holders in both the core and in-line positions.

Over-all stainless steel corrosion rates obtained from nickel and oxygen data are in good agreement. There was no initial period of high corrosion rate as observed in previous experiments.[10] As calculated from oxygen data, the corrosion rate during the first 300 hr was 1.4 mpy. During the final 1720 hr the average rate was 1.1 mpy.

13.1.7 In-Pile Loop L-2-10

Stainless steel loop L-2-10 is now being exposed in the new loop facility in beam hole HB-2 at the LITR. The available thermal-neutron flux in this facility is over twice the flux in the HB-4 facility, where all previous loop experiments were conducted. The L-2-10 core contains specimens of stainless steel, zirconium alloy, and titanium alloy. The core and in-line sample coupon holders are tapered-channel holders fabricated from type 347 stainless steel. The solution charged to the

loop for in-pile operation was of the following composition:

UO_2SO_4	0.04 m (U^{235}/total U = 0.927)
$CuSO_4$	0.0075 m
H_2SO_4	0.02 m

The operating temperature and pressure for this loop have been increased over those for previous loops and are as follows:

Main-stream temperature	280°C
Pressurizer temperature	305°C
O_2 pressure	200 psi
Total pressure	1546 psia

13.2 IN-PILE AUTOCLAVE TESTS

R. J. Davis

H. O. Day	A. R. Olsen
V. A. DeCarlo	R. M. Pierce
H. A. Fisch	J. A. Russell
D. T. Jones	F. J. Walter
R. A. Lorenz	K. S. Warren

L. F. Woo

13.2.1 LITR Tests

(a) **Correlation of Zircaloy-2 Corrosion Data from LITR.** — Inspection of the data obtained in the various Zircaloy-2 corrosion experiments in the LITR has provided evidence that the rate of radiation-induced corrosion of Zircaloy-2 by uranyl sulfate solutions is not directly proportional to the intensity of reactor radiations prevailing in the experiment. Instead, the data indicate that the rate is proportional to a fractional power of the radiation intensity. This nonlinear relationship between corrosion rate and fission power density was observed first with the data obtained in loop experiments and has been mentioned in previous reports.[10,11] Data presently available from both loop and rocking-autoclave experiments can be expressed by equations of the form:

$$CR = K(PD)^{2/3} ,$$

where CR is the corrosion rate (mpy) based on radiation time, PD is the fission power density (w/ml) which prevailed in solution during exposure, and K is a constant, the value of which depends

upon exposure temperature and solution composition. In Fig. 13.1, data from the various rocking-autoclave experiments are plotted in accordance with the above equation. The approximate experimental conditions for the different sets of data are listed in the legend. More detail may be found by reference to Table 13.3 and to previous quarterly reports.[12-14] The corrosion-rate values plotted in Fig. 13.1 are those obtained from oxygen measurements, except the value for experiment Z-3, for which oxygen data are known to be in error. For each experiment exposed in HB-5 of the LITR a value of 0.3 w/ml, the estimated value of the power generated from absorption of fast-neutron energy, has been added to the value for the fission power density in the experiments. The justification of this addition is as follows: Experiments with depleted-uranium solutions in the MTR and LITR have demonstrated that reactor radiation alone accelerates the corrosion of Zircaloy-2. The rate determined in the MTR experiment is about the same as that anticipated, if the power density estimated as being due to absorption of fast-neutron energy was, instead, due to absorption of fission energy.[15] This addition of 0.3 w/ml, for the majority of the experiments, does not alter the power-density values appreciably. However, it is important in the case of Z-17, which was at a low fission power density. The fast flux in HB-6 is assumed to be negligible because there is a beryllium moderator between the fuel and the beam hole.

As can be seen in Fig. 13.1, the majority of the rocking-autoclave experiments were with solutions which were 0.17 m in UO_2SO_4 and which were either without added acid or with 0.04 m excess H_2SO_4. The temperature of the experiment was either 250 or 280°C. In general, a straight line which passes through the origin can be drawn through the points for those experiments which were at 280°C and were without added acid. Another line can be drawn through the points for experiments which were at 280°C and were with 0.04 m excess H_2SO_4. Other lines can be drawn

[11]G. H. Jenks *et al.*, *HRP Quar. Prog. Rep. July 31, 1955*, ORNL-1943, p 121–124.

[12]G. H. Jenks *et al.*, *HRP Quar. Prog. Rep. April 30, 1956*, ORNL-2096, p 93.

[13]G. H. Jenks *et al.*, *HRP Quar. Prog. Rep. Jan. 31, 1956*, ORNL-2057, p 97.

[14]G. H. Jenks *et al.*, *HRP Quar. Prog. Rep. Oct. 31, 1955*, ORNL-2004, p 154.

[15]G. H. Jenks *et al.*, *HRP Quar. Prog. Rep. Jan. 31, 1956*, ORNL-2057, p 98.

Bomb No.	LITR Beam Hole	Bomb Material	Solution Composition			
			UO_2SO_4 (m)	$CuSO_4$ (m)	H_2SO_4 (m)	Other
Z-18	HB-5	Zircaloy-2	0.042	0.056	0.040	557 ppm Cr as CrO_3
Z-19	HB-5	Zircaloy-2	0.160	0.010	0	546 ppm Mo as H_2MoO_4
Z-20[d]	HB-5	Zircaloy-2	0.168[e]	0.040[e]	0.040[e]	
H-78	HB-6	Titanium-75A	0.168	0.040	0.040	
H-59	HB-6	Zircaloy-2	0.31	0.036		
H-60	HB-6	Zircaloy-2	0.158	0.019	0.040	
Z-2	HB-6	Zircaloy-2	0.165	0.011	0.040	
Z-9	HB-6	Zircaloy-2	0.172	0.007	0	
Z-8	HB-6	Zircaloy-2	0.178	0.021	0.046	0.004 m Cr
Z-14	HB-5	Zircaloy-2	1.363	0.043	0.043	
Z-16	HB-5	Zircaloy-2	1.355	0.043	0.043	
Z-17	HB-5	Zircaloy-2	0.169	0	0.040	
H-95	HB-6	Type 347 stainless steel	0.042	0.049	0.039	
H-96	HB-6	Type 347 stainless steel	0.172	0.010	0	0.0011 m $KTcO_4$
Z-11	HB-6	Zircaloy-2	0.172	0.010	0	0.0054 m $KTcO_4$

[a]Zircaloy-2 pins.
[b]85% Zr, 15% Nb pins.
[c]83.5% Zr, 15% Nb, 1.5% Sn pins.
[d]Deuterium replaced 96.9% of the light hydrogen in the solution.
[e]Concentrations calculated as moles solute per 1107-g solvent D_2O.
[f]LITR operated at 1.5 Mw power level.
[g]Rates based on 1.5-Mwhr radiation time scale. Reactor operated at 1.5 Mw.
[h]Rate based on 2.5-Mwhr radiation time scale. Reactor operated at 2.5 Mw.

3. LITR IN-PILE BOMB DATA

Enrichment (% U^{235})	Exposure Temperature (°C)	Fission Power Density (w/ml)	Irradiation Time (hr) (1 hr = 3 Mwhr)	Total Penetration		Corrosion Rate O_2 Data (mpy)
				O_2 Data (mils)	Pin Weight Data (mils)	
93.2	280	~4	158.9	0.18	0.16	9.9
93.2	280	~17	53.5	0.22	0.22^a	23.8
	300	~16	18.1		0.12^b	32.9
					0.12^c	
93.2	250	$\sim 8.5^f$	64.0	0.17		7.2^g
		~17	124.8			9.7
93.2	280	~10	107.8	0.05	0.05	2.7
	250	~10.5	280.6			0.3
	280	$\sim 5^f$	64.0			0.1^g
	225	~11	124.8			0.0
93.2	250	11.9 ± 0.2^b	120.0	0.198	$0.0188^i \pm 0.004$	6.11 ± 0.08
		7.1 ± 0.1^g	69.8		0.234 ± 0.011^j	4.89 ± 0.06
93.2	250	8.6 ± 0.3^k	250.6	0.261	0.237 ± 0.004^i	5.29 ± 0.08
	275	8.2 ± 0.3^l	77.3		0.253 ± 0.005^j	10.7 ± 0.3
93.2	280	10.8 ± 0.6	109.2	0.178	0.153 ± 0.002	13.1 ± 0.5
93.2	250	7.94 ± 0.04	101.3	0.213	0.204	8.3 ± 0.3
	280	7.49 ± 0.04	58.9		0.202^m	15.9 ± 0.3
93.2	250	11.4 ± 0.2	368.2	0.246	0.270 ± 0.005	5.4 ± 0.45
14.01	250	26.3 ± 1.4	1.8	n	0.11	n
	280	24.8 ± 1.3	104.2			
14.01	250	24.6 ± 1.3	125.5	0.123	0.120 ± 0.003	6.1 ± 0.1
	280	23.6 ± 1.2	40.4			7.5 ± 0.2
6.01	250	1.51 ± 0.03	533.5	0.17	0.150 ± 0.003	1.5
	280	1.43 ± 0.02	165.8			3.4
93.2	250	2.38 ± 0.04	580.2	0.056	0.085 ± 0.003	3.0 → 0.2
	280	2.42 ± 0.04	481.9			~0.3
93.2	250	15.3 ± 0.3	604.3	0.148	0.194 ± 0.012	Variable^o
93.2	250	8.6 ± 0.2	125.1	0.275	0.288 ± 0.004	7.64 ± 0.08
	280	8.1 ± 0.2	51.1			16.1 ± 0.12
	232	8.9 ± 0.2	116.0			5.6 ± 0.34

[i]Annealed pins.

[j]Unannealed pins.

[k]Probably high, due to fuel element change in middle of run.

[l]Probably low, due to fuel element change in middle of run.

[m]Alloy pins 50% Sn, 1.50% Cr, bal, Zr.

[n]Not available.

[o]Previously described by G. H. Jenks *et al.*, *HRP Quar. Prog. Rep. April 30, 1956*, ORNL-2096.
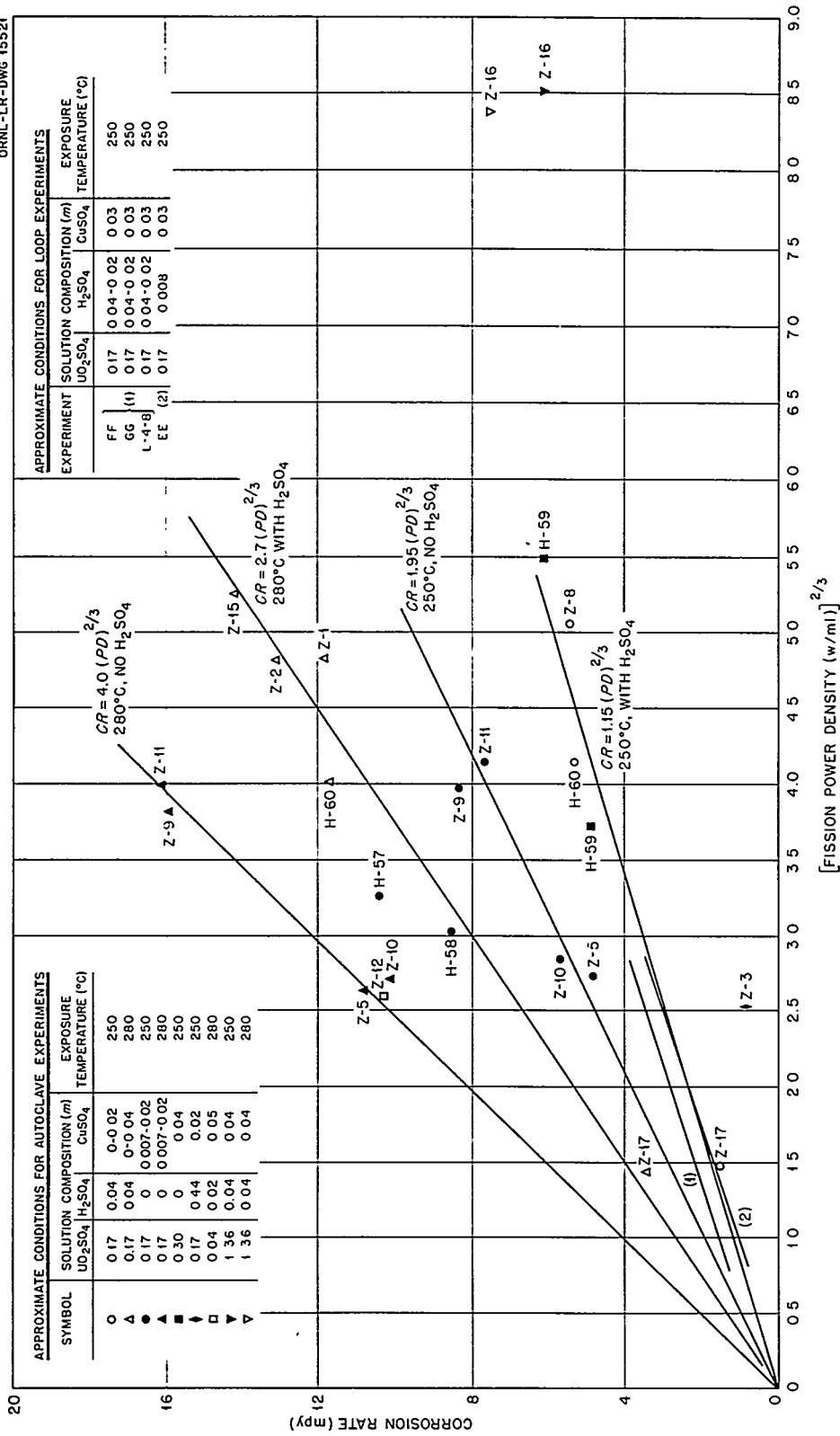
Fig. 13.1. Radiation-Corrosion Data for Zircaloy-2.

through the points for experiments which were at 250°C. The results of experiments H-57 and H-58 are definitely out of line with other results under comparable conditions, and have been ignored in drawing the line. Those two experiments were the first of the series of Zircaloy-2 experiments, and the H series of experiments were with a metal stock which differed from that of the later Z series.

Loop results are included in Fig. 13.1 for comparison with the autoclave data. Line 1 is the least-squares straight line determined for the data from loops FF, GG, and L-4-8. Line 2 is the similarly determined line for the data from loop EE. Reasonable agreement between the loop data and autoclave data is apparent.

In another report[16] it was shown that preliminary results for some of the autoclave experiments shown in Fig. 13.1 indicated that the corrosion rate under irradiation is proportional to the square root of the fission power density. Experimental values for the thermal-neutron flux which prevailed in each experiment are now available, and for these data a better fit is obtained with the $\frac{2}{3}$ power dependence than with the 0.5 or 0.6 power if it is assumed that the straight lines must pass through the origin. It should be emphasized that this value for the power dependence is not final. Future revisions of the present data may indicate a somewhat different value. Experimental points which will be obtained at higher power densities will aid in establishing a more precise value.

It is important to note that the present data indicate that the rate for experiment Z-12, for which the solution was 0.04 m UO_2SO_4, 0.02 m H_2SO_4, and 0.05 m $CuSO_4$, is appreciably higher than for those experiments for which the solution was 0.17 m UO_2SO_4, 0.04 m H_2SO_4, and 0 to 0.04 m $CuSO_4$. It is possible that this difference in rates is due to the lower excess H_2SO_4 concentration in the 10-g/liter experiment. However, it is also possible that the difference in rates is, in part, due to the lower UO_2SO_4 concentration in Z-12. The results of several experiments have demonstrated that for UO_2SO_4 concentrations greater than 0.17 m the radiation-induced corrosion is less than that obtained with 0.17 m solutions under conditions which are otherwise

similar. The results of experiment H-59, solution 0.30 m in UO_2SO_4, are examples of this effect. Another example shown in Fig. 13.1 is experiment Z-16, which was with a solution 1.3 m in UO_2SO_4. The results may possibly be related to the acid supplied by hydrolysis of the UO_2SO_4 in the more concentrated solutions.

The beneficial effect of acid exhibited in Fig. 13.1 has been discussed previously.[17]

(b) General. — One titanium experiment (H-78) was run in beam hole HB-6, and three Zircaloy-2 experiments (Z-18, Z-19, and Z-20) were operated in HB-5. The data available are presented in Table 13.3. Data from earlier experiments have become available since the last report, and are included in Table 13.3.

Approximate values of fission power density for the four recent experiments were obtained by using an estimated slow neutron flux of 1.2×10^{13} neutrons/cm^2·sec for HB-5 and 7.5×10^{12} for HB-6. Where the values of fission power density are not indicated as approximate, the number was obtained from slow neutron flux values as indicated by analyses of Zr^{95}-Nb^{95} activation in the pins.

As usual, the values listed for radiation time are those obtained by setting 3 Mwhr of LITR energy output equivalent to 1 hr. Corrosion rates are based on this radiation time (3 Mwhr) scale except when the LITR was operating at one-half full power. The corrosion rates observed during the half-power operation of the LITR were based on a 1.5-Mwhr radiation time scale. The plus-or-minus values are standard probable errors computed from the spread of the data.

The Ti-75A experiment, H-78, was conducted in an attempt to evaluate the effect of power density and temperature on the corrosion under irradiation. Operation was first at 280°C with the LITR at full power, next at 250°C at full power, next at 280°C with the reactor at half power (1.5 Mw), and, finally, at 225°C with the LITR at full power. Termination of the experiment was caused by a plugged capillary.

Corrosion, as indicated by oxygen consumption, was negligible after the initial exposure at 280°C. The rate during this initial period, however, remained constant at 2.7 mpy. The corrosion

---

[16]H. F. McDuffie, *Minutes of HRP Monthly Information Meeting, March 15, 1956,* ORNL CF-56-4-45, p 7 (April 4, 1956).

[17]G. H. Jenks *et al., HRP Quar. Prog. Rep. April 30, 1956,* ORNL-2096, p 92—94.

penetration as determined by weight gain of the pin specimens is in near agreement with that determined by oxygen consumption. The interpretation of these results is not clear. No tendency has been observed in previous experiments for the radiation-induced attack to level off with time.[18-21] The effect of power density and temperature on titanium corrosion remains obscure.

A Zircaloy-2 experiment, Z-18, with chromate added, was conducted. The results of solution analyses of a previously reported steel experiment, H-95, showed an appreciable amount of chromium in the solution after exposure. One interpretation of this result is that Cr(VI) was stable under the conditions of the experiment, probably due to a combination of a low pressure of radiolytic gas and a high temperature in the experiment. The solution for the Zircaloy-2 experiment, Z-18, was the same as that employed in H-95 (0.04 m UO_2SO_4, 0.056 m $CuSO_4$, 0.040 m H_2SO_4) except that approximately 500 ppm of Cr(VI) was added to the charge for the autoclave. The exposure temperature, 280°C, was the same as that employed in the final portion of the exposure of the previous experiment. No large difference in rate was observed between this experiment and a similar one,[22] Z-12 (10.3 mpy), without chromate added. It should be noted, however, that the power density in Z-18 is not yet known accurately. Chromium was lost from solution during exposure. The final solution was reported to contain 60 ppm, whereas, as noted above, the initial solution contained 500 ppm. This loss may have been due to reduction to insoluble Cr(III). However, it may also have been due to adsorption of Cr(VI) on ZrO_2. There is no method of establishing whether Cr(VI) was stable during exposure.

A second Zircaloy-2 experiment, Z-19, was run in HB-5 with a small amount of H_2MoO_4 added to test the possible effect of this additive on corrosion. The solution as added to the bomb was not clear at room temperature but did clarify on heating. Essentially no molybdenum was found in the final solution. Molybdenum was found in the oxide scale from the Zircaloy-2 surfaces. It appears likely that all the added molybdenum was absorbed on the oxide.

Comparison of the corrosion rate with an extrapolated estimate from Fig. 13.1 indicates that H_2MoO_4 did not have much effect on the corrosion rate. A more exact comparison can be made when the power density is more accurately known.

This bomb contained two pin specimens of each of three zirconium alloys. One alloy was 85% Zr, 15% Nb; another was 83.5% Zr, 15% Nb, and 1.5% Sn; and a third was Zircaloy-2. The corrosion penetration in each of the Nb alloys, as indicated by defilmed weight losses of the specimens, was about half that in the two Zircaloy-2 pins (see Table 13.3).

A Zircaloy-2 experiment, Z-20, was operated in HB-5 to ascertain the effect on corrosion of substituting D_2O for H_2O. The UO_2SO_4 solution was deuterated by taking the salt to dryness several times and taking it up in 99.8% D_2O. The $CuSO_4$ used was recrystallized as the pentadeuterate several times from 99.8% D_2O; D_2SO_4 was made by adding SO_3 to 99.8% D_2O. The Baldwin strain gage and capillary were filled with D_2O. Oxygen was added to the bomb, however, by means of 85.4% H_2O_2. The light water in the solution amounted to 3.1% of the total solution. It appears from Fig. 13.1 that the corrosion rate is somewhat higher than that observed with light-water solutions. A more accurate comparison will be meaningful only when the power density measurements by activation analysis are available.

13.2.2 MTR Tests – ORNL-15-6

An all-stainless-steel system was operated in HB-3 of the MTR for 26 hr in the retracted position and for 14 hr in the inserted (high flux) position. The corrosion rates and other data are given in Table 13.4. This experiment was rocked continuously at 36 rpm, twice the rate of previous experiments, to ensure wetting of all surfaces. In view of the relatively high density of steel and the correspondingly high heat flux in the gamma field, the rapid rocking was considered desirable.

The stainless steel bomb differed from previous MTR bombs in that the outside diameter of the bomb was reduced to 0.640 in., the inside diameter

[18]G. H. Jenks *et al.*, *HRP Quar. Prog. Rep. Jan. 31, 1955*, ORNL-1853, p 112.

[19]G. H. Jenks *et al.*, *HRP Quar. Prog. Rep. April 30, 1955*, ORNL-1895, p 121.

[20]G. H. Jenks *et al.*, *HRP Quar. Prog. Rep. Oct. 31, 1955*, ORNL-2004, p 154.

[21]G. H. Jenks *et al.*, *HRP Quar. Prog. Rep. Jan. 31, 1956*, ORNL-2057, p 97.

[22]G. H. Jenks *et al.*, *HRP Quar. Prog. Rep. July 31, 1955*, ORNL-1943, p 127.

TABLE 13.4. MTR BOMB DATA FOR EXPERIMENT
ORNL-15-6

Bomb Material: Type 347 stainless steel
Solution: $0.038\ m\ UO_2SO_4$, $0.044\ m\ CuSO_4$,
$0.036\ m\ H_2SO_4$

	Position	
	Inserted	Retracted
Fission power density, w/ml	~31	~1
Fast-neutron power density, w/ml	~4	~0.8
Gamma power density, w/ml	~4	~1
Temperature, °C	280	280
Corrosion rate (O_2 consumption), mpy	12	4
Operating time, hr	14.0	26.0

remaining the same (0.406 in.). There was an enlarged section, 0.750 in.-OD, about 1 in. long in the open end of the bomb to accept the pin rack.

A rather large temperature difference between the ends of the bomb occurred in this experiment, amounting to 45°C when the reactor was down, 65°C when retracted, and 90°C while inserted. In each case the higher temperature was at the end of the bomb nearest to the reactor lattice.

At the end of the 40 hr of operation some difficulty was experienced with the equipment which necessitated temporary removal of the experiment. The total penetration which had been observed for the system at this time was ~0.04 mil. The calculated concentration of nickel in the bomb solution which corresponds to this penetration is 0.016 m. The calculated excess H_2SO_4 concentration at this time was 0.019 m, that is, one-half the initial concentration. Solution stability data, which became available after this experiment was under way, indicate that the solution in the bomb would have become unstable at the exposure temperature of 280°C after a small additional amount of corrosion had taken place.[23] Because the solution was approaching the conditions of instability and because of the large temperature gradients along the length of the bomb during exposure, it appeared likely that further exposure would not yield significant results. Hence, the bomb was not reinserted.

The initial rate of 12 mpy under irradiation does not necessarily indicate an increase in corrosion rate over that observed at lower power densities in the LITR. An LITR experiment,[12] H-95, which employed the same initial solution as this MTR experiment but which was exposed initially at 250°C, exhibited a rate of about 3 mpy until the corrosion penetration reached about 0.03 mil. After this initial period, the observed rate was about 0.3 mpy. It is possible that ORNL-15-6 would have exhibited similar corrosion behavior if it could have been exposed longer.

[23]F. E. Clark *et al.*, *HRP Quar. Prog. Rep. April 30, 1956*, ORNL-2096, p 130–135.

14. METALLURGY

G. M. Adamson

R. G. Berggren   J. K. White
W. J. Fretague   J. C. Wilson
W. J. Leonard   C. H. Wodtke
M. L. Picklesimer   O. Zmeskal

14.1 PHYSICAL METALLURGY

M. L. Picklesimer

14.1.1 Zirconium-Hydrogen Alloys

Crystal-bar zirconium specimens were hydrided to nominal contents of 10, 25, 50, 100, 250, 500, and 1000 ppm H_2 and quenched from 800, 850, and 900°C in mercury in the hydrogenation equipment.[1] Zircaloy-2 specimens were hydrided to nominal contents of 100 and 500 ppm H_2 and mercury-quenched from 600 and 800°C or step-cooled 100°C every 30 min from 600, 900, and 1000°C. The examination of the specimens is still under way. Difficulties with metallographic techniques have prevented the examination of a sufficient number to permit any major conclusions to be drawn. The specimens examined so far indicate that at least 130 ppm H_2 can be dissolved in the alpha phase of crystal-bar zirconium at 600°C and returned to room temperature by quenching in mercury. X-ray diffraction analysis of several of the crystal-bar zirconium specimens which contained visible hydrides after quenching revealed no hydride other than the normal cubic $ZrH_{1.75}$, the hydride structure in equilibrium with alpha zirconium. Transition hydrides with other crystal structures have been reported in the literature, but none have been found in this examination so far. It is possible that the diffraction-analysis techniques used have not been sufficiently refined.

14.1.2 Morphology of Zircaloy-2

Specimens of Zircaloy-2 plate used in fabricating the HRT core tank were held at 840, 860, and 880°C for seven days and water-quenched. The specimens show the same amount and the same distribution of beta phase as reported previously for specimens that had been heated for 30 min to 2 hr. Thus the phase-boundary temperature,

810°C for the alpha/alpha-plus-beta temperature, is valid for the equilibrium boundary.[2]

Results of x-ray diffraction analysis of the Zircaloy-2 specimens which received the randomization treatments (1000°C for 30 min, air-cooled or water-quenched, cold-rolled 20%, and annealed at 800°C for 30 min) discussed in the last report[3] were received from C. J. McHargue, ORNL Metallurgy Division. The intensity of the orientation peaks of an inverse pole figure indicated that some preferred orientation was still present; however, it had been reduced by about half and had undergone a small shift in position. Less preferred orientation was found in the quenched than in the air-cooled specimens.

A Zircaloy-2 weldment (not in core-tank material) was examined metallographically. The microstructures are presented in Figs. 14.1 through 14.4. The base material was partially recrystallized and contained numerous long thin stringers that could not be resolved clearly at magnifications less than 500X. Figures 14.1 and 14.2 show the bright-field and polarized-light photomicrographs of the same area at the root of the weld with both weld metal and base metal in the field of the photomicrograph. The stringers present in the base material opened into voids, probably because of the very fast heating and the high local stresses present during welding. No clearly defined fusion line is present, and the beta grains present in the base material during welding clearly grew into the deposited weld metal without change in grain size or orientation, or in any way delineating the fusion line. Figure 14.3 is a photomicrograph of the heat-affected zone in the parent metal. It shows the structures from the unaffected base metal (in the lower left corner), through an alpha recrystallization texture, into a zone of alpha plus beta, into the all-beta

---

[1]W. O. Harms *et al.*, *HRP Quar. Prog. Rep. Jan. 31, 1955*, ORNL-1853, p 158.

[2]M. L. Picklesimer and G. B. Wadsworth, *HRP Quar. Prog. Rep. Jan. 31, 1956*, ORNL-2057, p 101–104.

[3]M. L. Picklesimer and G. B. Wadsworth, *HRP Quar. Prog. Rep. April 30, 1956*, ORNL-2096, p 96–99.

Fig. 14.1. Zircaloy-2 Weld Fusion Zone Showing Absence of Transition Region and Enlarging of Stringers. Bright field, 50X. Reduced 31%.

Fig. 14.3. Weld Heat-Affected Zone Showing Rapid Change in Structure of Parent Metal. Polarized light, 100X. Reduced 31%.

Fig. 14.2. Weld Fusion Zone Under Polarized Light Showing Similarity of Structure. Polarized light, 50X. Reduced 31%.
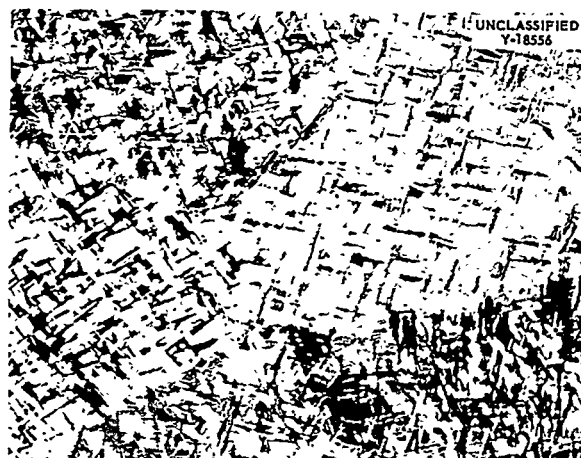
Fig. 14.4. Deposited Weld Metal Showing Coarse Transformed Beta Grains. Polarized light, 100X. Reduced 31%.

structure, and into the start of the coarse-grained beta structure. The distance from one corner of the photomicrograph along the diagonal to the other corner is approximately 0.050 in. on the specimen. The photomicrograph of the deposited weld metal, Fig. 14.4, shows the "basket weave" texture typical of coarse-grained beta phase that has been transformed to alpha at a cooling rate slightly greater than a "still air" cooling rate. A macrograph of the weld is shown in Fig. 14.5, and the hardness traverse and DPH values are shown in

Fig. 14.6. Both the hardness traverse and the microscopic examination indicate very rapid changes in structure and properties. Difficulties are often experienced with welds in which rapid changes in structure and properties occur.

14.1.3 Zirconium-Alloy Development

Specimens of all the zirconium alloys so far prepared[3] containing Nb, Mo, Ta, and Fe were held for 2 hr at 600, 700, 800, 900, 1000, and 1100°C; 48 hr at 400, 500, and 600°C; and two
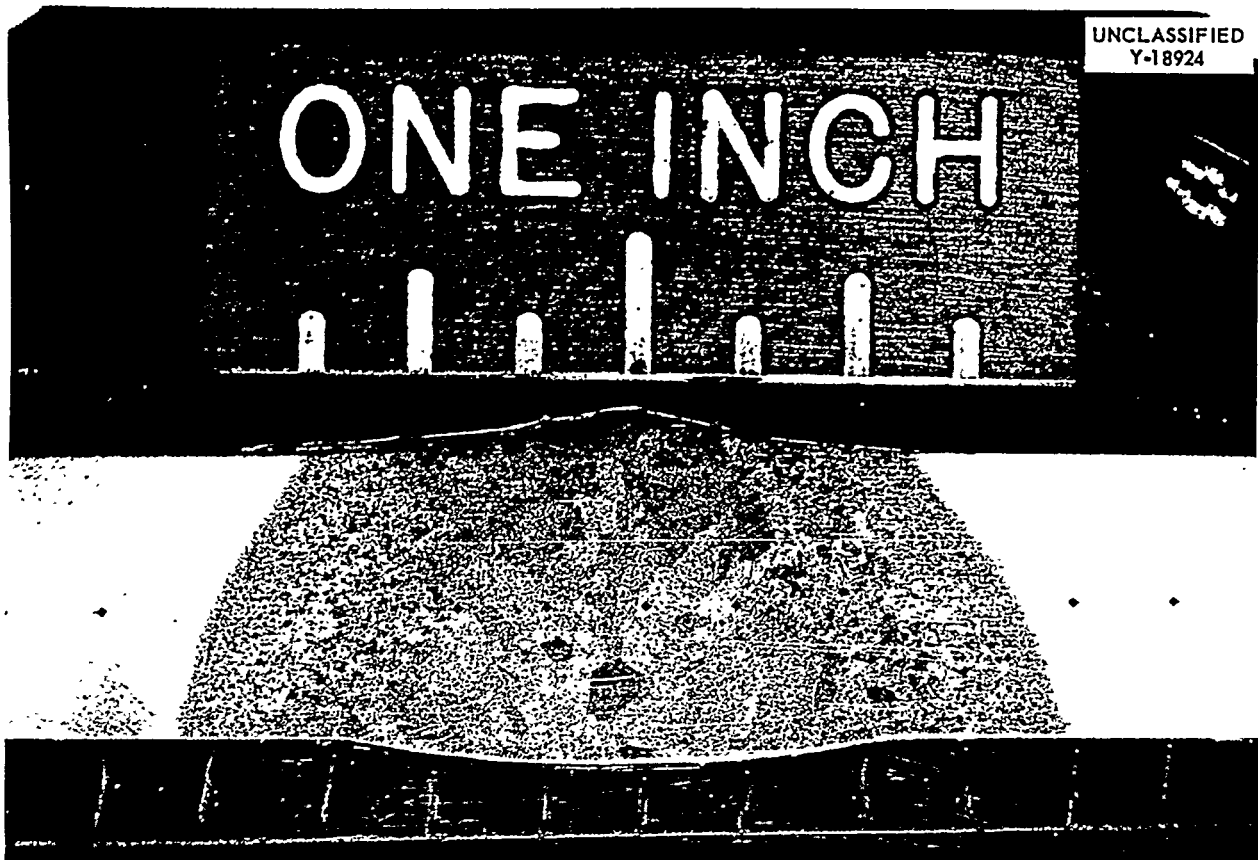
Fig. 14.5. Macrograph of Zircaloy-2 Weld Showing Rapid Change in Structure. Oblique Lighting.

weeks at 300, 400, 500, and 600°C and were then water-quenched. Alloy specimens containing (in wt %) 5 and 10 Pd, 10 Nb + 1 Pd, 10 Nb + 2 Pd, 15 Nb + 1 Pd, and 15 Nb + 2 Pd were also held at each of the times and temperatures listed above, except that none were held at 1000 or 1100°C. Most of the specimens have been mounted. Polishing and etching difficulties have prevented the examination of all the specimens held at 600°C and below, except for the 5 and 10% Pd alloys. Examination of the specimens held at 700°C and above permits the following conclusions to be drawn: (1) fully retained beta phase can be obtained by quenching in only the 5% Pd alloy; (2) quenching the 10% Pd alloy from 800 or 900°C results in retained beta plus a second phase which is not alpha zirconium; (3) the addition of 2% Pd to the alloys containing niobium results in a decrease in the amount of alpha zirconium formed on quenching but does not eliminate it; (4) the 10% Mo alloy quenched from 800°C and above

shows a second phase, which has not been identified, as a dot precipitate throughout the grains. Examination of some of the 5 and 10% Pd alloy specimens heat-treated at 700°C and below indicates that the eutectoid of the Zr-Pd alloy system occurs near 5% Pd and between 700 and 800°C and that the complete transformation of the retained beta occurs in less than 1 hr at 600 and 700°C.

14.1.4 Recombiner-Loop Corrosion and Hydrogen Pickup by Zirconium and Titanium

Specimens of A-55 titanium, Ti–6% Al–4% V alloy, crystal-bar titanium, crystal-bar zirconium, and Zircaloy-2 were prepared and submitted for corrosion testing and hydrogen contamination in a recombiner loop operated by the Engineering Development Section of REED. The specimens labeled RL were held in a vapor flow of 0.5 to 0.6 cfm at 500 psi and 350 to 425°C in the recombiner section of the loop. A variation was
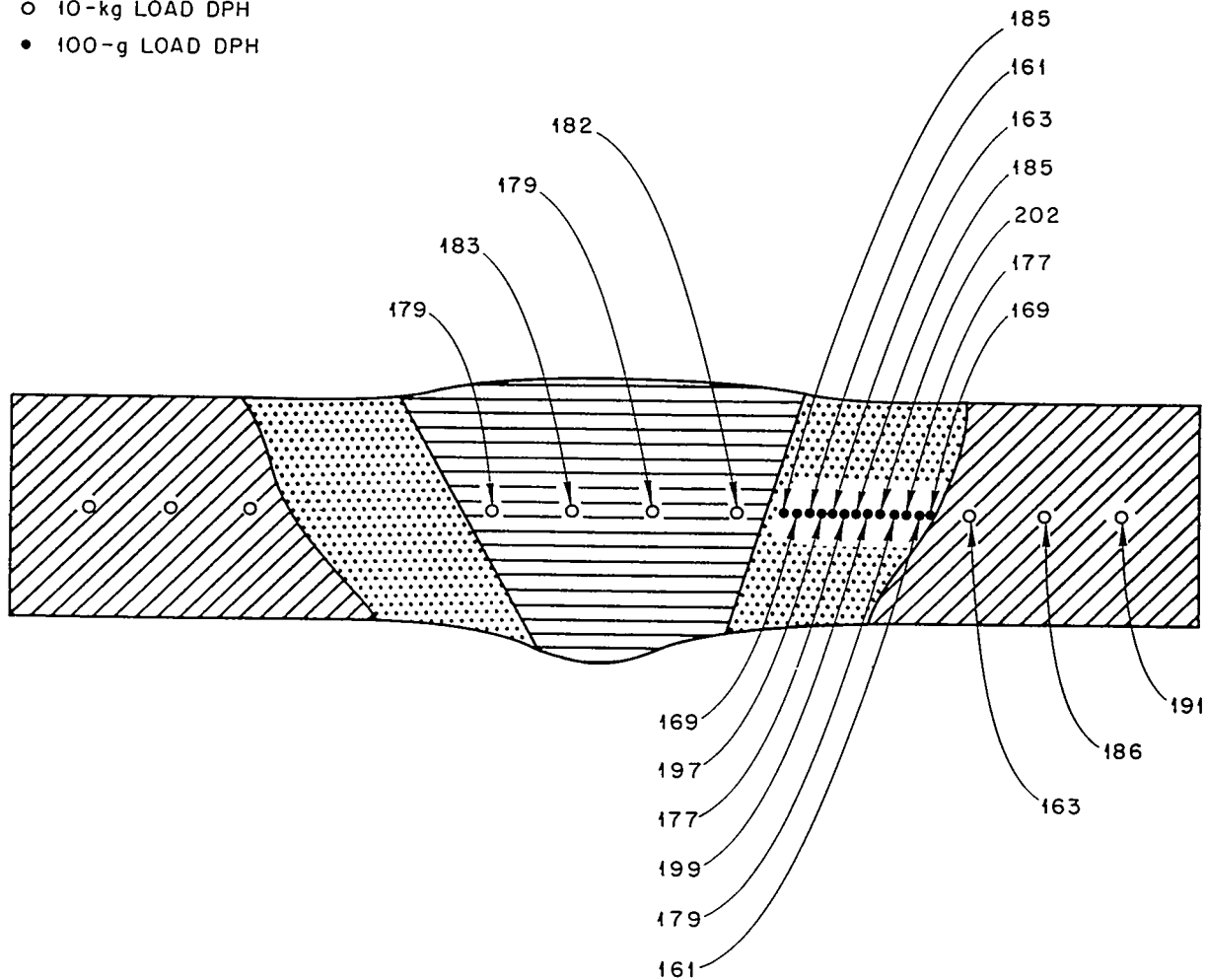
Fig. 14.6. Hardness Traverse of Weld Shown in Fig. 14.5.

reported in the vapor composition in this section, but ranges and averages, in mole %, were: steam, 79.6 to 83% (av 82.15%); argon, 16.8 to 17.2% (av 17.0%); H_2, 0 to 3.0% (av 0.55%); O_2, 0 to 1.5% (av 0.28%). The specimens labeled CL were held in the vapor over the electrolytic cell at a temperature of 230 to 240°C. The vapor composition was: steam, 78.6%; argon, 16.8%; H_2, 3.0%; and O_2, 1.5%. The loop was operated for a total of

188 hr, and there were several shutdowns during that period. Half of each specimen was submitted for hydrogen analysis, and the other half was mounted for metallographic examination. The hydrogen analyses are given in Table 14.1.

Metallographic examination of the mounted specimens confirmed approximately the hydrogen contents given in Table 14.1; photomicrographs are shown in Figs. 14.7 through 14.11.

TABLE 14.1. HYDROGEN CONTENTS OF RECOMBINER-LOOP CORROSION SPECIMENS

	Ti–6% Al–4% V		A-55 Titanium		Crystal-Bar Titanium		Crystal-Bar Zirconium		Zircaloy-2	
	Specimen No.	H$_2$ (ppm)	Specimen No.	H$_2$ (ppm)	Specimen No.	H$_2$ (ppm)	Specimen No.	H$_2$ (ppm)	Specimen No.	H$_2$ (ppm)
Recombiner	RL-1	73	RL-5	33	RL-2	120	RL-3	1600	RL-4	23
Cell	CL-3	230	CL-5	290	CL-4	1200	CL-1	37	CL-2	71
Control	RL-1C	140	RL-5C	25	RL-2C	120	RL-3C	18	RL-4C	13

The structures of the Ti–6% Al–4% V specimens (Fig. 14.7) are not appreciably different. The apparent second phase present in CL-3 is thought to be due to pitting and staining, although it was reproducible through several repreparations of the specimen. The difference in hydrogen content between the recombiner specimen, RL-1, and the control specimen, RL-1C, probably resulted from a hydrogen concentration gradient in the alloy bolt from which the specimens were cut.

The structure of the A-55 titanium control specimen, RL-5C, shows evidence of considerable cold work, with no visible hydrides; the recombiner specimen, RL-5, shows evidence of the beginning of recrystallization of the cold-worked structure; and the cell specimen, CL-5, shows complete recrystallization, with numerous hydride platelets (needles as viewed in the polished surface) in the grain boundaries (see Fig. 14.8). The reasons for this recrystallization of CL-5, taking place as it did at a reported lower temperature than that for RL-5, are not known unless the process of dissolving the hydrogen in some way aided and increased the rate of recrystallization considerably. A re-examination of the specimens eliminated the possibility of a mixup in specimens or photomicrographs or that specimen CL-5 did not come from the same A-55 titanium plate as RL-5 and RL-5C. An experiment in the hydrogenation equipment used for the preparation of hydrided specimens will be scheduled to see if this "anomaly" can be duplicated in a different type of test.

The crystal-bar titanium specimens (Fig. 14.9) show the same type of recrystallization – that is, RL-2C, the control specimen, shows a considerable amount of cold working; RL-2, with the same hydrogen content, shows complete recrystallization and redistribution of the hydrides; and the cell specimen, CL-4, shows tremendous grain growth and very large hydride particles. The effects appear to be real but cannot be explained at the present time.

The crystal-bar zirconium specimens (Fig. 14.10) do not show the same change in structure as the A-55 and crystal-bar titanium specimens, presumably because the zirconium was not cold-worked. The control specimen shows no hydrides present; the cell specimen, CL-1, shows a few hydride needles in the grain boundaries; and the recombiner specimen, RL-3, shows many massive hydride needles, consistent with the very large amount of hydrogen absorbed.

The Zircaloy-2 specimens (Fig. 14.11) show a cold-worked structure with no identifiable hydrides in the control specimen, RL-4C, complete recrystallization into very fine grains in the recombiner specimen, RL-4, and complete recrystallization with considerable grain growth (in comparison with RL-4) with hydride needles in the grain boundaries in the cell specimen, CL-2. The stringer phase observed in the direction of rolling in RL-4 is not entirely hydride but contains the iron, nickel, and chromium intermetallics. All the specimens have been examined in polarized light to confirm the conclusions stated.

Fig. 14.7. Ti–6% Al–4% V Specimens Exposed in Recombiner Loop. (*a*) Recombiner specimen RL-1. (*b*) Cell specimen CL-3. (*c*) Control specimen RL-1C. 500X. Reduced 32%.

Fig. 14.8. A-55 Titanium Specimens Exposed in Recombiner Loop. (*a*) Recombiner specimen RL-5. (*b*) Cell specimen CL-5. (*c*) Control specimen RL-5C. 500X. Reduced 32%.

Fig. 14.9. Crystal-Bar Titanium Specimens Exposed in Recombiner Loop. (*a*) Recombiner specimen RL-2. (*b*) Cell specimen CL-4. (*c*) Control specimen RL-2C. 500X. Reduced 32%.

Fig. 14.10. Crystal-Bar Zirconium Specimens Exposed in Recombiner Loop. (*a*) Recombiner specimen RL-3. (*b*) Cell specimen CL-1. (*c*) Control specimen RL-3C. 500X. Reduced 32%.
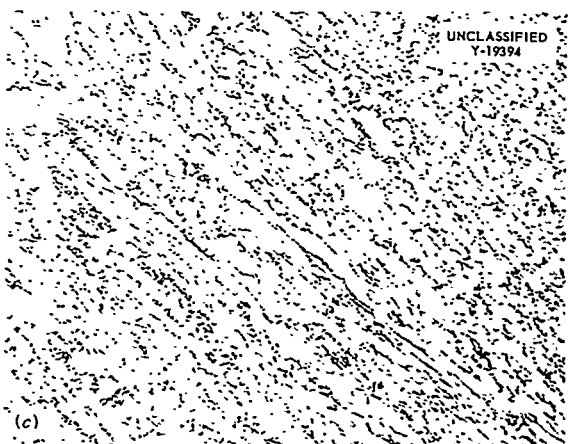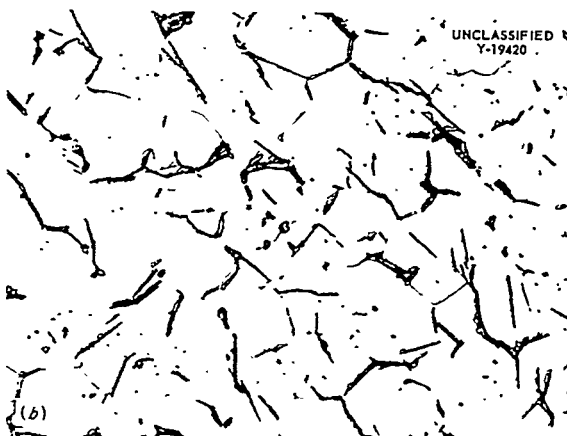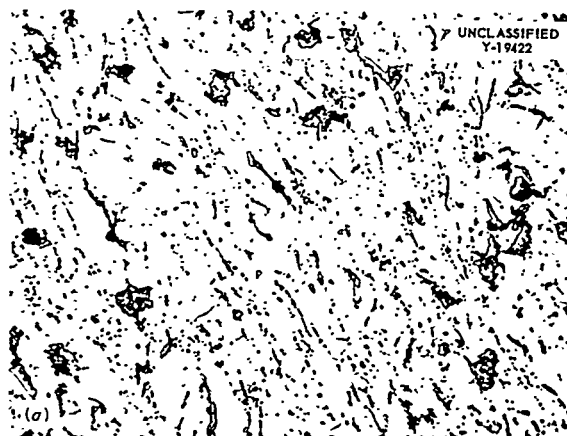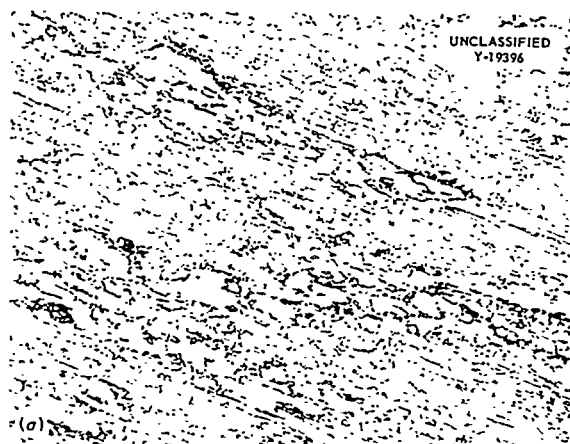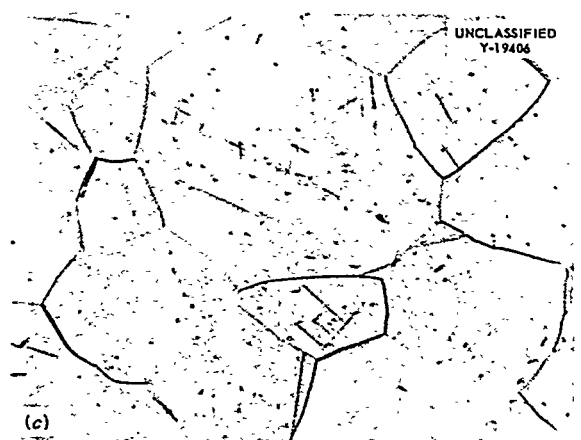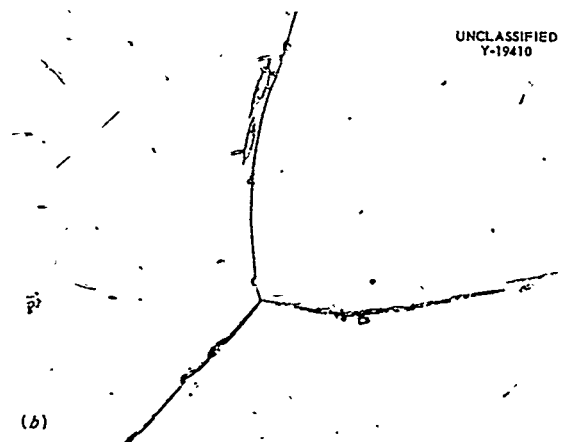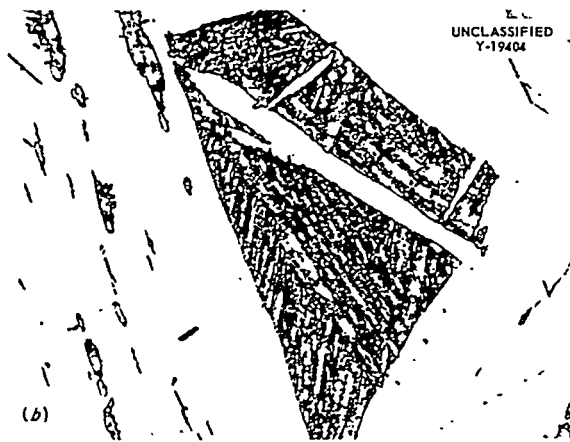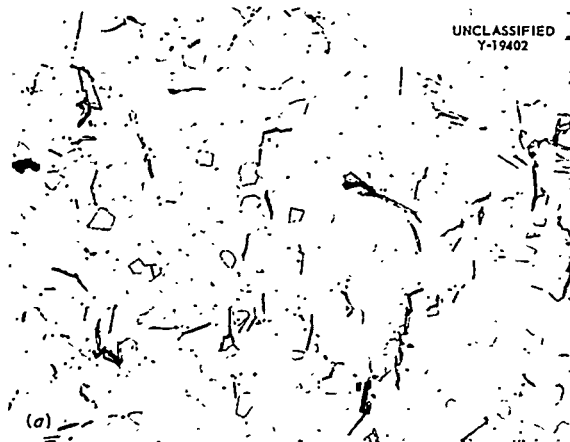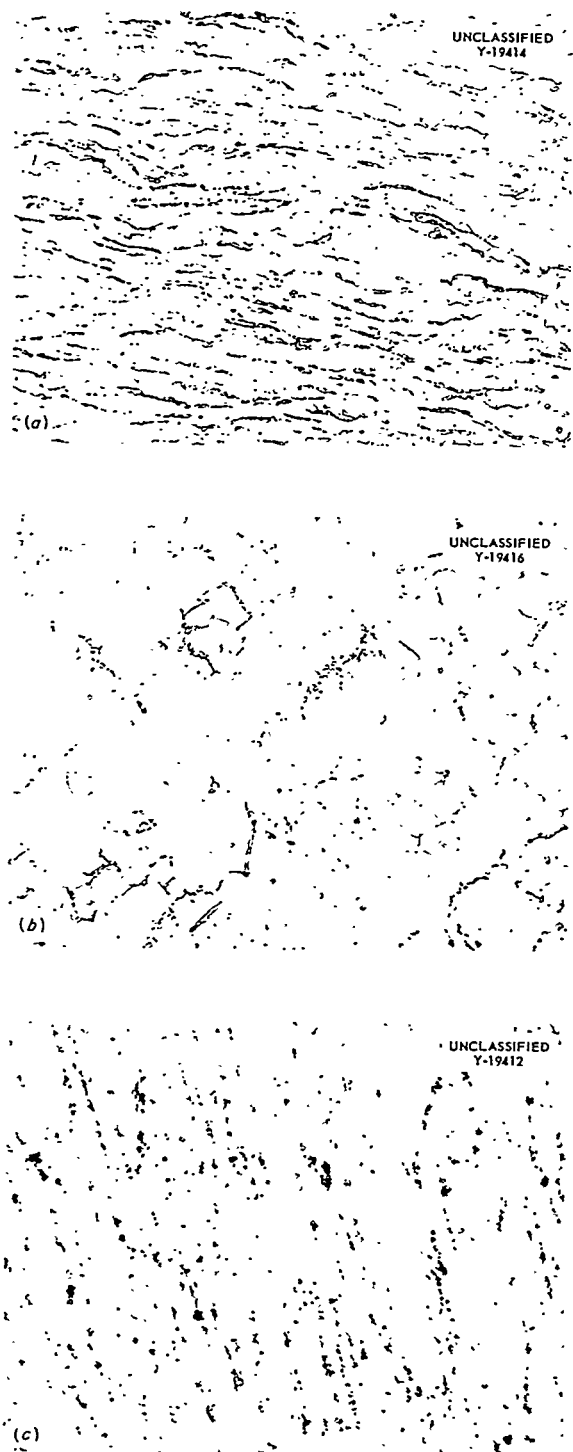
Fig. 14.11. Zircaloy-2 Specimens Exposed in Recombiner Loop. (*a*) Recombiner specimen RL-4. (*b*) Cell specimen CL-2. (*c*) Control specimen RL-4C. 500X. Reduced 32%.

14.2 MECHANICAL METALLURGY

W. J. Fretague   M. L. Picklesimer

Zircaloy-2 specimens of the multibreak, impact, subsize type were aged for 1008 hr at 300, 350, 400, and 450°C. The specimens were encapsulated in evacuated Vycor tubing, held at temperature for the desired time, and air-cooled in the capsule. Then they were broken at temperatures from −100 to 250°C in an Izod-type impact tester. The data are presented in Fig. 14.12, with similar data for the specimens aged at 250°C and 1085 hr and for the control specimens of the prior series (250°C for 500, 1000, and 1500 hr).[4] The curve was drawn to be a "best fit" for the control specimens. All the data points for the temperature series lie above the control-specimen curve, except for the specimens that were broken at 250°C. The 250°C break points are not representative of the true impact strength at 250°C, since none fractured completely on the first strike; most of them broke on the rebound swing of the impact head. Although the strengths for the aged specimens lie consistently above the control curve, the difference is not believed to be of major significance. Thus aging times up to 1500 hr and at temperatures up to 450°C do not appear to have an appreciable effect on the impact strength of Zircaloy-2.

14.3 OXIDATION STUDIES ON ZIRCONIUM ALLOYS

O. Zmeskal

The study of the oxidation of zirconium alloys has as its objective the development of an alloy with superior resistance to corrosion by uranyl sulfate solutions under irradiation conditions. The direction of the study is based on the premise that the monoclinic oxide film found on zirconium and on Zircaloy-2 is not sufficiently protective under irradiation because it tends to transform more or less abruptly to a more densely packed oxide phase, producing cracks in the film, and, hence, entries for the corrodent. The immediate goal is to develop a zirconium alloy on which the oxide film will be almost completely free of the monoclinic phase and hence may be expected to be stable under irradiation and thus be fully protective.

[4]W. J. Fretague, *HRP Quar. Prog. Rep. April 30, 1956*, ORNL-2096, p 99.
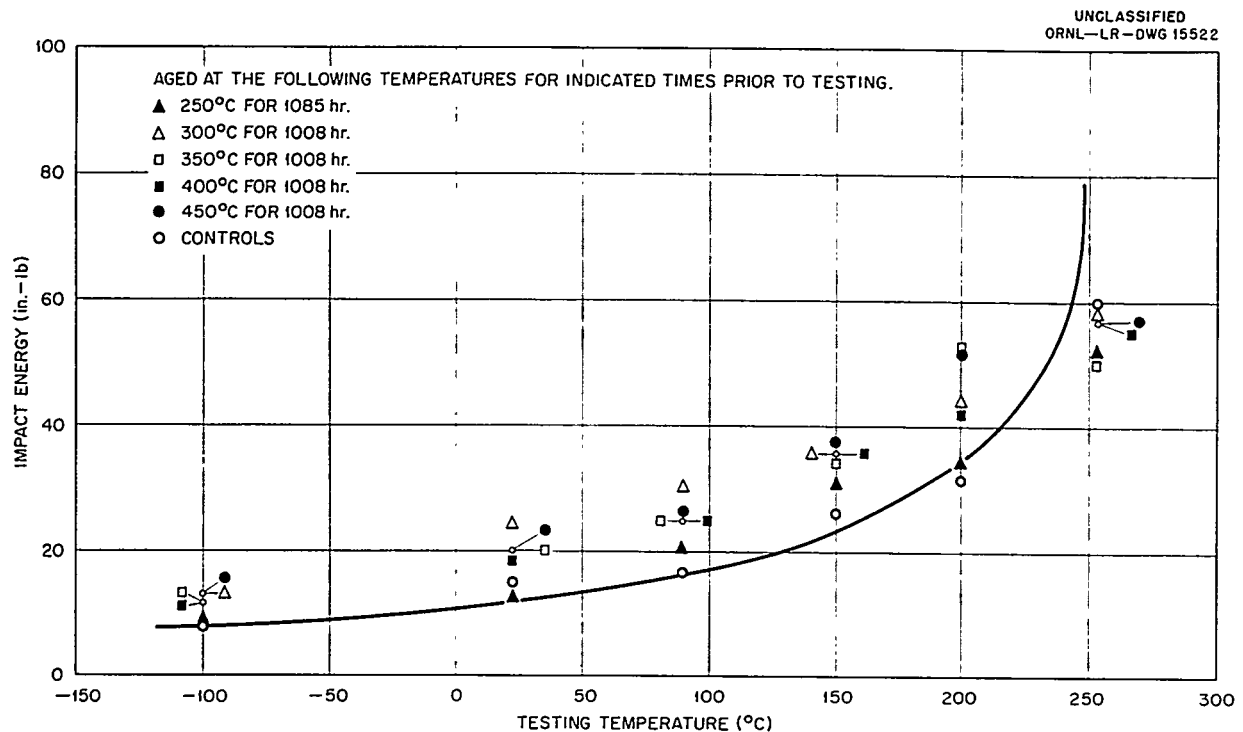
Fig. 14.12. Impact Strengths of Subsize Zircaloy-2 Specimens. ($\frac{3}{8}$-in. rod swaged to 0.217-in.-dia rod, sand blasted, pickled, vacuum annealed at 750°C for 2 hr, and furnace cooled)

The program began under the leadership of J. R. Johnson and was restricted to finding those oxide systems that contained the cubic or tetragonal zirconia-rich solid solutions.[5] The promising systems were then to be reproduced as alloys, and it was expected that the alloys would oxidize to form the cubic or tetragonal phases of zirconia solid solutions. The most promising elements from the oxide studies could not be made to alloy with zirconium, but the study did serve to point the way to the study of zirconium-niobium alloys.

The zirconium-niobium alloys have proved to be superior to Zircaloy-2 in corrosion resistance under irradiation conditions in both bomb and loop tests. The films which form on these alloys are mixtures of monoclinic zirconia and the compound $6ZrO_2 \cdot Nb_2O_5$, which has an orthorhombic structure.

Since the present stage of the study is a preliminary examination to permit the selection of the most promising alloys for more extensive studies, oxidation procedures were selected which

would yield oxides that could be most readily analyzed by x-ray diffraction. Low-temperature oxidation of massive specimens is not a satisfactory procedure, as the films are highly stressed and have a marked preferred orientation. The method chosen is that of oxidizing the powdered alloys, separating the oxide from the metal by crushing, and using the fine dust in the x-ray diffractometer. Oxidation temperatures of 600, 800, and 1100°C were selected for this preliminary study.

A large number of alloys of zirconium with niobium and molybdenum and zirconium-niobium with various amounts and combinations of tantalum, iron, palladium, tin, vanadium, yttrium, manganese, and indium are being used.

Except for the 5 and 10% molybdenum alloys, which probably lost molybdenum during the oxidation, all the alloys oxidized to produce the orthorhombic oxide in amounts that increased as the temperature increased. The 5 and 10% molybdenum alloys were the only ones that did not contain niobium.

[5]J. I. Federer *et al.*, *HRP Quar. Prog. Rep. Oct. 31, 1955*, ORNL-2004, p 159.

Zirconium with molybdenum alone does not produce a cubic or a related, densely packed oxide phase. Molybdenum increases the amount of orthorhombic $6ZrO_2 \cdot Nb_2O_5$ formed on the zirconium-niobium alloys, however, as does tantalum. Iron is of no value in this respect.

The alloys made from sponge zirconium produce significantly more orthorhombic oxide than do alloys made from iodide zirconium. A clue as to the nature of the impurity that causes this effect may be obtained from Wittels' analyses[6] of natural zirconia, which transforms from monoclinic to cubic structure on irradiation whereas high-purity ZrO_2 does not.[6]

It has been shown that many alloying elements that stabilize the body-centered cubic phase in zirconium tend to stabilize the more densely packed phase of zirconia. It has not yet been determined whether oxidation of a beta-stabilized alloy produces more of the densely packed zirconia than is obtained by oxidation of the equilibrium alpha-plus-beta structure.

14.4 WELDING DEVELOPMENT

W. J. Leonard

14.4.1 Titanium Welding

Previous attempts to weld $2\frac{1}{2}$-in. sched-40 RC-55A titanium pipe by using preplaced consumable inserts have resulted in welds having hardnesses of 40 to 60 VPN higher than those of welds obtained when filler wire was used for the root pass. The higher hardnesses are thought to be due to the higher heat input necessary to obtain a crack- and porosity-free weld when the insert is used.

By changing the included angle and the position of the insert, a weld design was obtained in which the same heat input was possible for an insert-type weld as for a filler-wire weld. An insert was made by flattening a ring of $\frac{3}{32}$-in.-dia RC-40A wire to an approximate rectangular cross section

---

[6]Unpublished paper by M. C. Wittels, Solid State Division, *Neutron Irradiation Induced Phase Transformations in ZrO_2*, dated June 22, 1956.

$\frac{1}{8}$ in. wide and $\frac{1}{16}$ in. thick. A weld made with this insert was similar in quality and hardness to the filler-type welds. Additional work is required to confirm that welds of constantly high quality can be obtained by using the modified weld design and the inexpensive flat insert.

Manufacturers' data list the 6% Al–4% V titanium alloy as being weldable; however, some bend test data cast doubt on this claim. A single-pass inert-gas-shielded arc weld was made in a $\frac{1}{16}$-in. sheet of this material by using a $\frac{3}{32}$-in. filler wire. The weld appeared to be clean and sound to visual and x-ray examinations and to a micro-examination. The microhardnesses of the weld metal averaged 338 VPN, those of the heat-affected zone of the base metal, 363 VPN, and the unaffected base metal, 355 VPN. With a guided root and face bend of a 4T radius, all specimens broke in the heat-affected zone of the base metal after bending through an angle of 10 to 40 deg. A similar weld in pure titanium will bend 180 deg without failure. This indicates that if the 6% Al–4% V titanium alloy is used in critical structures, the welds must be heat-treated.

14.5 EFFECTS OF RADIATION ON STRUCTURAL METALS AND ALLOYS

R. G. Berggren   J. C. Wilson

14.5.1 Equipment and Facilities

A beam-hole irradiation of impact and tensile specimens was completed in the HB-3 facility of the MTR. The apparatus has been disassembled, and testing of the impact specimens has commenced. Parts for the elevated-temperature apparatus for use in the MTR are machined, and assembly will start soon. The mockup of apparatus for irradiation of titanium- and zirconium-alloy specimens at 575°F in the MTR is being operated to check design calculations. Assembly of the experiment for irradiation in a lattice piece of the MTR is continuing.

An impact testing machine designed by Bell Laboratories has been received and is being modified for remote operation and temperature control.

Part V

CHEMICAL ENGINEERING DEVELOPMENT

F. R. Bruce

15. FUEL PROCESSING

D. E. Ferguson   E. O. Nurmi   W. D. Burch

S. D. Clinton   R. W. Horton
J. R. Engel   R. A. McNees
P. A. Haas   S. Peterson

15.1 REACTOR SOLIDS DISSOLUTION

R. A. McNees

Further studies on the dissolution of solids expected from the operation of the HRT Chemical Plant have shown that the dissolution of 1 g of simulated reactor solids requires only 3 to 5 ml of 10.8 M H_2SO_4. When solids were refluxed with acid in that proportion, the oxides were converted to sulfate salts which, although insoluble in 10.8 M H_2SO_4, dissolved easily when the acid was diluted to 1 to 2 M with water. During the conversion of oxide to sulfate, agitation of the solids was necessary in order to prevent formation of a mass containing unreacted solids. Beneficial results were also obtained by adding to the reaction mass an amount of concentrated (18 M) H_2SO_4 equivalent to the oxides being dissolved. The addition was made in five equal portions at 15-min intervals after a temperature of 165 to 170°C had been reached.

Uranium could not be satisfactorily leached from simulated reactor solids by mixtures of hydrochloric and nitric acids, whether concentrated or dilute. No uranium was leached by such mixtures from solids containing more than traces of zirconium; from a solid containing only traces of zirconium, however, 69% of the original uranium content was extracted, while only 30% of the total solids was dissolved.

15.2 IODINE CHEMISTRY

R. A. McNees   S. Peterson

15.2.1 Effect of Radiation on Iodine Chemistry

The effect of gamma radiation on the valence distribution of iodine in 0.02 m UO_2SO_4–0.005 m H_2SO_4 at 250°C is opposite to that at 100°C. It was previously reported[1] that at 250°C the F/C ratio (ratio of free to combined iodine), in the absence of radiation, was approximately 7/1. In the presence of a gamma field of 8.1×10^{17} ev per gram of H_2O per minute (15,000-r/min source), the F/C ratio increased sharply to approximately 20/1. Repeated experiments in the presence of this gamma field showed F/C ratios varying from 18.5/1 to 27/1. Tests with the same equipment before and after radiation experiments gave maximum ratios of 7.7/1.

At 100°C with an O_2 pressure of 200 psi, the F/C ratio was repeatedly measured as 0.5/1 to 1.2/1. When exposed to the same gamma source mentioned above, the ratio dropped to the range 0.02/1 to 0.03/1. In three other experiments the gamma source was brought into position after a few samples had been taken at 100°C. The F/C ratio, which was in the range 0.52/1 to 0.55/1 without the source, dropped to 0.032/1, 0.023/1, and 0.020/1, respectively, after the gamma source was introduced. Gross effects due to varying the oxygen pressure from 200 to 20 psi at 100°C were not observable in the absence of radiation, but apparently 8 to 12 hr is needed for equilibrium to be reached at this temperature.

15.2.2 Volatility of Iodine Under Reactor Conditions[2]

Modifications of the ejector test loop were made which increased the gas/liquid mole ratio from 0.005/1 to 0.01/1 at 250 to 270°C. A single test of iodine stripping with the loop was made. In this test traced iodine as potassium iodide was injected into the circulating uranyl sulfate stream while the circulating gas stream was scrubbed with a dilute silver sulfate solution. The rate of removal of iodine from the fuel stream was faster than could be accounted for by using known data. Precipitation of iodine by silver carried over into the fuel stream was probably the cause. Use of a solid silver absorber in the scrubber section will be tried. The vapor/liquid mole ratio of free iodine in 0.02 m UO_2SO_4–0.005 m H_2SO_4–0.005 m $CuSO_4$ at 100°C was 0.37/1, as compared with a value of 7/1 at 250°C. In the fuel stream at 100°C in the

---

[1]D. E. Ferguson *et al.*, HRP Quar. Prog. Rep. April 30, 1956, ORNL-2096, p 118.

[2]Work done at Vitro Laboratory; KLX-10034 (to be issued).

absence of oxygen the F/C iodine ratio was 25/1 when no simulated fission products were present. In the presence of simulated mixed fission and corrosion products, including ruthenium, the vapor/liquid equilibrium distribution ratio was 2.4/1, while the F/C iodine ratio in the liquid phase was 1/1.

In water solutions, pH 4.4 to 4.8, at 100°C the vapor-liquid distribution coefficient for elemental iodine was 0.013 at iodine concentrations of 1 mg per kilogram of H_2O. The F/C iodine ratio was 10/1 in the liquid phase. Variation of the distribution coefficient with pH was from 0.03 at pH 1.9 to 0.008 at pH 8.0.

In other experiments iodine vapor at low partial pressures in oxygen and water vapor was effectively retained by platinized Alundum at 350 to 400°C. This indicates that fission-product iodine may build up in a recombiner catalyst bed.

15.3 BEHAVIOR OF SOLIDS IN HRT MOCKUP

R. A. McNees   W. D. Burch
J. R. Engel

The behavior of simulated fission and corrosion products in the HRT mockup at Y-12 has been studied by injecting into that system fuel containing iron, zirconium, and rare-earth sulfates. Radiation detectors were placed in various positions about the loop circuit in order to follow the buildup of tracer activity introduced along with the metal salt solution. A hydroclone with its accessory equipment was also installed on the loop.

Two separate experiments were performed: in the first, La^{140} tracer was used for studying the behavior of rare-earth sulfates, and in the second, Zr^{95} tracer was used for observing the behavior of corrosion products. The results of these runs may be summarized as follows: The lanthanum concentration in the underflow pot was four times greater than in the loop; the total rare-earth concentration in the underflow pot was six times greater than in the loop. Only a small fraction of the solids that formed in the loop remained suspended in the circulating stream. Only 3% of the solids that formed in the loop were isolated in the hydroclone underflow pot, the remainder being dispersed throughout the system, with notable concentrations in the gas separator and heat exchanger.

In each experiment salt solution was pumped into the system to produce 60 g of solids per day for the first six days of the run; no salt was added in the final three days of the run. In order to simulate the proposed intermittent operation of the HRT Chemical Plant, the hydroclone was operated only during the first and last three days of each run.

During the run in which La^{140} tracer was used, a gradual increase in activity in the system was noted. Samples taken from the high- and low-pressure portions of the system showed no significant difference. After the $La_2(SO_4)_3$ content of the system reached 12 mg per kilogram of H_2O, there was no further increase of activity in the solution samples and this soluble activity remained essentially constant for the duration of the run. Radiation surveys showed about the same level of activity in the high- and low-pressure portions of the system. Activity accumulated in the heat exchanger and hydroclone underflow pot. The hydroclone underflow pot was dumped twice. In the first discharge a small amount of liquid flowed through the system while the hydroclone assembly was cooling. Under these conditions no concentration of rare earths above that present in the loop was found. In the second discharge there was no flow through the hydroclone system during cooling, and the total rare-earth concentration was six times greater than in the loop. Lanthanum-140 activity measurements indicated a fourfold concentration in the underflow pot. After the loop system had been cooled and dumped, the only measurable activity remaining in the system was in the heat exchanger.

In the Zr^{95}-traced run, an equilibrium activity was reached almost immediately; the first sample showed essentially the same Zr^{95} activity shown for all subsequent samples. In these samples approximately 10 mg of zirconium per kilogram of H_2O was in solution. No activity buildup in the low-pressure system could be observed, but the gas separator soon became the most radioactive part of the entire system. A smaller accumulation of activity in the heat exchanger and hydroclone underflow pot was noted. In the underflow-pot samples, 2% of the activity found was in solution; 98% was in the solid phase. However, in this and the preceding experiment only 8 to 10 g of solids was recovered out of 360 g added, and only in the hydroclone-pot dump samples. This, coupled with the fact that samples taken during the course of both experiments showed either no solids or only a trace, indicates that some portions of the loop system, especially the gas separator, provided

excellent sites for solids accumulation. Further additions of solids are planned to determine whether such sites have a finite capacity for solids or whether the sites will continue to accumulate them indefinitely.

15.4 LOOP STUDIES

S. D. Clinton   R. W. Horton

Tests run in loop A indicated that mounting the hydroclone upstream from the preheater had little effect on the removal of soluble rare-earth fission-product precipitates. The results from two tests,[3,4] LR-45 and LR-48, are compared in Table 15.1 with results from a run[5] (LR-38) in which the hydroclone was downstream from the heater.

Zirconium oxide precipitated in the loop by hydrolysis from zirconium sulfate exhibited a tendency to plate out on all surfaces in the loop regardless of temperature or stream velocity. In a series of five tests 32.5 g of zirconium was added to loop B-2; 17.5 g was recovered. Examination of the loop and pump showed a uniform scale film on all surfaces, including the pump impeller.[4]

---

[3]W. K. Eister, *Chemical Technology Division Unit Operations Section Monthly Progress Report for April 1956*, ORNL CF-56-4-210.

[4]W. K. Eister et al., *Chemical Technology Division Unit Operations Section Monthly Progress Report for May 1956*, ORNL CF-56-5-197.

[5]W. K. Eister, *Chemical Technology Division Unit Operations Section Monthly Progress Report for November 1955*, ORNL CF-55-11-176.

15.5 HYDROCLONE DEVELOPMENT STUDIES

P. A. Haas

Examination of a 0.25-in.-dia, 1.50-in.-long titanium-lined hydroclone showed no significant corrosion after 3975 hr at 300°C on REED loop K. The titanium walls of the cross-sectioned unit (Fig. 15.1) were covered with a uniform golden film; the only visible attack was a slight enlargement of the sharp-edged underflow port. The loop circulated a solution of 0.04 M UO_2SO_4, 0.005 m $CuSO_4$, and 0.010 to 0.015 m H_2SO_4. The hydroclone was operated at 37 psi pressure drop for a throughput of 0.23 ppm. The hydroclone test was incidental to the operation of the loop for corrosion studies.[6] A 0.40-in.-dia, 3.14-in.-long hydroclone, cross-sectioned (see Fig. 15.2) after a total of 1366 hr on corrosion loops circulating UO_2SO_4 solutions at concentrations from 10 to 300 g of uranium per kilogram of H_2O at 250 to 300°C, demonstrated the durability of titanium units for use with more concentrated UO_2SO_4 solutions.

Literature correlations reported for hydroclones of 3-in.-dia and larger were tested and revised to cover the Unit Operations data for 0.16- to 0.50-in.-dia units. This information is now available in a form that permits selection of hydroclone units to give desired capacities or efficiencies.[4]

---

[6]J. C. Griess et al., *HRP Quar. Prog. Rep. Jan. 31, 1956*, ORNL-2057, p 85.

TABLE 15.1. COMPARISON OF HYDROCLONE PERFORMANCE WITH HYDROCLONE UPSTREAM AND DOWNSTREAM FROM THE HEATER

	Hydroclone Downstream from Heater	Hydroclone Upstream from Heater	
	Run 38	Run 45	Run 48
Milligrams of $Nd_2(SO_4)_3$ recovered from underflow pot	17	20	31
Grams of $Nd_2(SO_4)_3$ precipitated per square foot of loop	0.004	0.184	0.093
Grams of $Nd_2(SO_4)_3$ precipitated per square foot of preheater	6.76	5.28	*

*Loop was cooled before draining; preheater precipitate was redissolved.

DIAMETER: 0.25 in
LENGTH: 1.50 in.
MATERIAL: TITANIUM 55A
CONDITIONS: 10 g of U/kg of H_2O, 300°C

TEST PERIOD: 3975 hr
TEST LOOP: REED LOOP K
FEED FLOW: 0.23 gpm
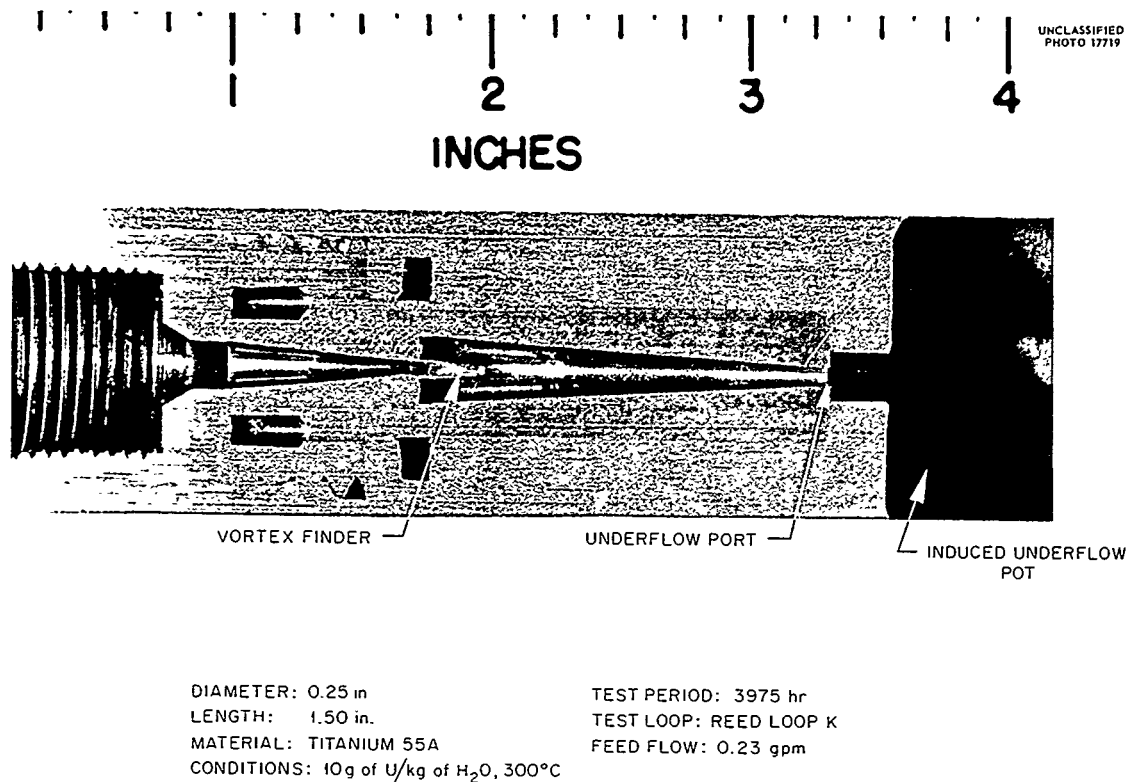
Fig. 15.1. Corrosion of a 0.25-in.-dia Titanium-Lined Hydroclone.

DIAMETER: 0.40 in.
LENGTH: 3.14 in.
MATERIAL: TITANIUM 55A
CONDITIONS:
        10 - 300 g of U/kg of H_2O
        250 - 300°C

TEST PERIOD: 1366 hr
TEST LOOP: REED LOOPS
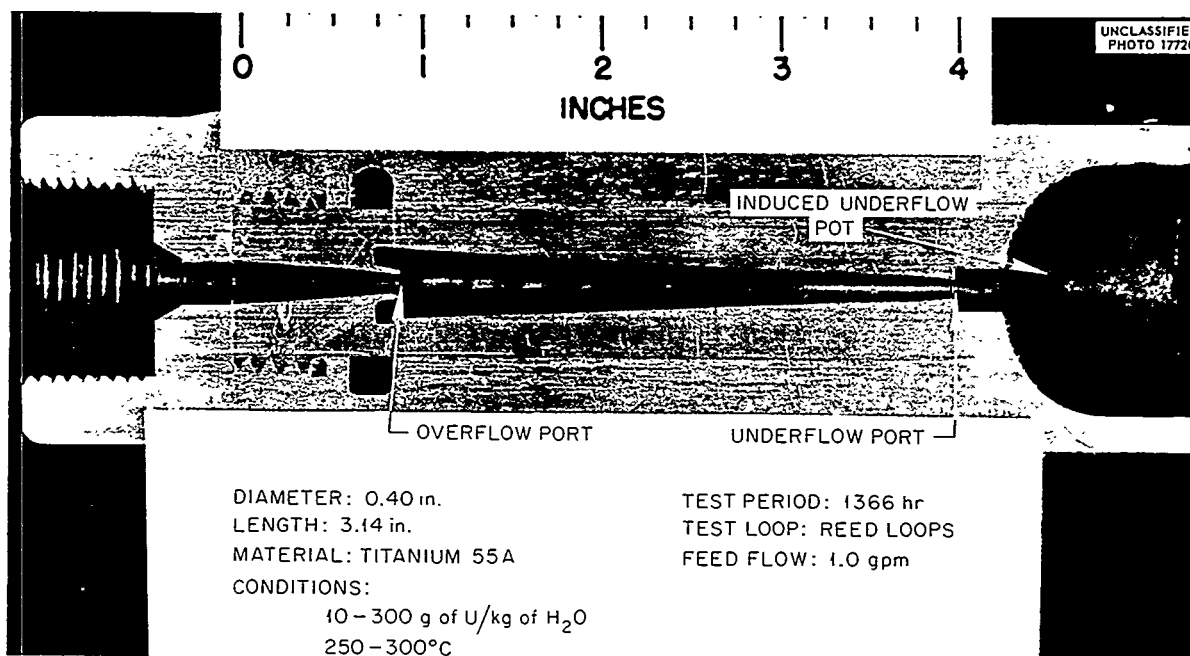FEED FLOW: 1.0 gpm

Fig. 15.2. Corrosion of a 0.40-in.-dia Titanium-Lined Hydroclone.

16. PLUTONIUM-PRODUCER BLANKET PROCESSING

D. E. Ferguson

R. E. Leuze   R. D. Baybarz   J. M. Chilton

The study of plutonium-producer blanket chemistry included investigation of the adsorption of plutonium on metals, plutonium behavior in uranyl sulfate solution at 250°C, and dissolution of corrosion product oxides.

16.1 ADSORPTION OF PLUTONIUM ON METALS

J. M. Chilton

The experimental determination of plutonium adsorption on titanium and Zircaloy-2 at 250°C from 1.4 m UO_2SO_4 containing 0.5 to 10 mg of plutonium per kilogram of H_2O and under 90 psi O_2 and 180 psi H_2 pressure was continued. The equations presented earlier[1] indicated that, when no precipitation occurred, the amount of plutonium adsorbed was proportional to the square root of the exposure time. Although the data scatter considerably, it now appears that, for conditions where PuO_2 does not precipitate, the plutonium adsorbed on titanium and Zircaloy-2 reaches a maximum, or equilibrium, amount which is different for each metal. For example, at 250°C in contact with 1.4 m UO_2SO_4 containing 4 mg of plutonium per kilogram of H_2O, approximate maximum adsorption values were 0.3 $\mu g/cm^2$ on titanium and 3.5 $\mu g/cm^2$ on Zircaloy-2. This amount of plutonium adsorption is insignificant compared with the amount of PuO_2 expected to adhere to the walls in an actual reactor system. In previous studies,[2] when PuO_2 precipitated, larger amounts deposited on the metal walls without reaching a saturation value.

The rate of plutonium adsorption in the absence of PuO_2 precipitation seems to depend on the surface condition of the metal. In the case of polished titanium, equilibrium was reached in about 100 hr. Titanium with a heavy oxide film required less time to reach equilibrium. About 400 hr was required for maximum plutonium adsorption on polished Zircaloy-2.

Plutonium adsorbed on metal surfaces under these conditions (i.e., no PuO_2 precipitation) was

not completely removed by exposure at 250°C to uranyl sulfate containing no plutonium. An average of 68% of the plutonium was removed from titanium-metal samples during a 15-hr exposure to 1.4 m UO_2SO_4 at 250°C. No additional plutonium was removed during the next 30 hr. Zircaloy-2 metal exposed to 1.4 m UO_2SO_4 at 250°C lost 54% of the adsorbed plutonium in 15 hr and 66% of the plutonium in 45 hr.

In order to estimate the rate of plutonium buildup on reactor walls, experimental methods must be used in which the rates of plutonium production, hydrolysis, and precipitation are approximated. This can probably be accomplished best in circulating loops to which plutonium solution is added continuously.

16.2 PLUTONIUM BEHAVIOR IN UO_2SO_4 SOLUTION AT 250°C

J. M. Chilton

It has been established[3] that dissolved plutonium in 1.4 m UO_2SO_4 at 250°C under a stoichiometric mixture of hydrogen and oxygen will rapidly change to Pu(IV), hydrolyze, and precipitate as PuO_2. Under these conditions the plutonium remaining in solution is about 3 mg per kilogram of H_2O and is essentially all Pu(IV). Since solubilities greater than this were obtained in in-pile experiments and during plutonium adsorption studies, additional investigations were made to determine the reason for this behavior. When 1.4 m UO_2SO_4 containing less than 25 mg of plutonium per kilogram of H_2O was heated at 250°C in pyrex under 200 psi H_2 and 100 psi O_2, PuO_2 was not always precipitated; in many cases precipitation occurred, but considerably more than 3 mg of plutonium per kilogram of H_2O remained in solution and in some cases precipitation was complete, leaving in solution 0.5 to 3 mg per kilogram of H_2O. For initial plutonium concentrations of 30 to 50 mg per kilogram of H_2O, some PuO_2 always formed, but often more than 3 mg of plutonium per kilogram of H_2O remained in

[1]D. E. Ferguson *et al.*, *HRP Quar. Prog. Rep. April 30, 1956*, ORNL-2096, p 120.

[2]D. E. Ferguson, R. E. Leuze, and R. H. Rainey, *HRP Quar. Prog. Rep. Oct. 31, 1955*, ORNL-2004, p 189.

[3]D. E. Ferguson *et al.*, *HRP Quar. Prog. Rep. Jan. 31, 1955*, ORNL-1853, p 192–194.

solution. For initial plutonium concentrations of 100 mg per kilogram of H_2O or greater, precipitation was essentially complete, leaving in solution about 3 mg per kilogram of H_2O. The solubility measurements previously reported were made with initial plutonium concentrations equal to or greater than 100 mg per kilogram of H_2O. When these solutions contained 100 mg of iron per kilogram of H_2O, added as ferrous sulfate, the iron hydrolyzed and precipitated, leaving in solution about 20 mg per kilogram of H_2O; however, this had no significant effect on the plutonium behavior.

Valence determinations during these experiments indicate that some of the high plutonium solubilities were partly due to the presence of Pu(VI). However, this is not the sole reason, since Pu(IV) concentrations after heating were as much as 18 mg per kilogram of H_2O. When uranyl sulfate preconditioned by heating under oxygen at 250°C was used to prepare the feed for these tests, there was a greater tendency for oxidation of plutonium to Pu(VI), and hence no precipitation or only partial precipitation occurred more often than when the uranyl sulfate was untreated or was preconditioned under stoichiometric hydrogen and oxygen. This oxidizing material has not been identified, and attempts to remove it by boiling or by sparging with hydrogen at room temperature were not successful. It is important to note that, with initial plutonium concentrations greater than 100 mg per kilogram of H_2O (even when uranyl sulfate preconditioned under oxygen was used), precipitation was essentially complete at 250°C, leaving in solution about 3 mg of plutonium, essentially all as Pu(IV).

16.3 BLANKET SOLIDS DISSOLUTION

R. D. Baybarz

In order to obtain a representative sample of the material expected to be removed by the hydroclone during operation of an HRT blanket processing plant, it is necessary to completely dissolve all the solids. It is expected that solids collected from the HRT blanket will contain about 70% Fe_2O_3, 18% Cr_2O_3, 9.8% NiO, 1.2% ZrO_2, and 1.0% UO_3. Simulated solids with this composition, prepared by hydrolysis at 250°C, were completely dissolved in anhydrous H_3PO_3 or H_3PO_4 at 230°C and were partially dissolved in 0.4 M $CrSO_4$–1.0 M H_2SO_4 at 80°C.

When simulated reactor solids were added to either H_3PO_3 or H_3PO_4 at 230°C, they were immediately dissolved, giving a clear solution. When the H_3PO_3 solution was diluted, dissolved zirconium tended to hydrolyze and precipitate; however, this tendency was not noted in the case of H_3PO_4 solutions. It was also noted that H_3PO_4 is stable at 270°C but that H_3PO_3 showed some decomposition at temperatures above 200°C.

The chromous sulfate–sulfuric acid solution at 80°C did not completely dissolve the solids. A small amount of a light-gray precipitate, which was primarily ZrO_2, did not dissolve.

Since the solids from a plutonium-producer blanket will also contain PuO_2, the effect of these dissolution reagents on solids containing PuO_2 will be investigated.

17. THORIUM OXIDE SLURRY DEVELOPMENT

D. E. Ferguson   J. P. McBride

V. D. Allred   N. A. Krohn
A. R. Jones   L. E. Morse
E. V. Jones   C. E. Schilling

W. M. Woods

17.1 SLURRY IRRADIATION STUDIES

N. A. Krohn   J. P. McBride
W. M. Woods

17.1.1 Slurry Irradiations in the LITR

The primary objective of the thorium oxide slurry irradiation studies has been to demonstrate as quickly and as definitively as possible that under irradiation conditions approximating those of a TBR blanket there is no gross deterioration of slurry properties. In the slurry irradiations carried out during this period, there was no gross radiation-damage effect on slurries; concentrated thorium oxide slurries were repeatedly and successfully stirred in the LITR at 300°C for as long as 200 hr, at power densities approximately equal to the average power density of a TBR blanket, with no apparent deterioration in slurry properties (Table 17.1).

Five irradiations were carried out in the LITR on slurries of thorium-uranium mixed oxides which contained 750 g of thorium and 3.75 g of 93% enriched uranium per kilogram of H_2O. The irradiations were carried out at 300°C in the stainless steel dash-pot-stirred irradiation bomb.[1]

---

[1]A. R. Jones *et al., HRP Quar. Prog. Rep. Jan. 31, 1956,* ORNL-2057, p 111.

TABLE 17.1. IN-PILE BEHAVIOR OF THORIUM-URANIUM OXIDE SLURRIES

Temperature: 300°C

Flux: 3×10^{13} neutrons/cm^2·sec

	Concentration (g of Th per kg of H_2O)	Approximate Power Density (w per g of ThO_2)	Irradiation Time (hr)	Time of Stirring In-pile (hr)	Viscosity[a] (centistokes) Before Irradiation	During Irradiation
D-16 ThO_2 — 0.5 mole % natural UO_3, wet-autoclaved at 300°C, calcined at 900°C	1000[b]	0.06	151	77[c]	7	
	1000[b]	0.06	68	72[c]	7	
	1000[b]	0.06	172	264	7	
	1000[b]	0.06	200	171[d]	7	
900°C calcined coprecipitated thorium-uranous oxalates, 93.14% enriched uranium	500[e]	5	85	111	4	4
	750[f]	7	168	211	7	5
	750[g]	7	92	121	5	5
	750[g]	7	192	219	4	4.5

[a]*HRP Quar. Prog. Rep. April 30, 1956,* ORNL-2096, p 109.

[b]*HRP Quar. Prog. Rep. Jan. 31, 1956,* ORNL-2057, p 109.

[c]Stirring terminated as a result of instrument failure.

[d]Slurry ceased stirring in middle of run for unknown reason but continued stirring to end of run after stirring was restarted.

[e]*HRP Quar. Prog. Rep. April 30, 1956,* ORNL-2096, p 107.

[f]Contained 1000 ppm of PdO.

[g]Contained 20,000 ppm of MoO_3 (0.15 *m*).

In two of the experiments the mixed oxide was prepared by wet-autoclaving at 300°C a mixture of 650°C calcined D-16 ThO_2 and the UO_3 and recalcining the recovered solids at 900°C. One thousand ppm of PdO was mixed with the dry solid before it was dispersed in water for irradiation. In both experiments the bombs were removed from the reactor after less than one day of irradiation — in the first because of a short circuit in the stirrer drive coils and in the second because of difficulties in stirring. Similar stirring difficulties were encountered in the out-of-pile control experiment.

The other three experiments were successfully carried out with a thorium-uranium oxide prepared by calcining at 900°C the coprecipitated thorium-uranous oxalates. In these experiments the slurries were stirred in-pile for 211, 121, and 219 hr, with 168, 92, and 192 hr, respectively, of irradiation at full reactor power (Table 17.1). In the first experiment 1000 ppm of PdO was mixed with the dry solid before it was dispersed for irradiation, and in the last two experiments 20,000 ppm of MoO_3 (0.15 m) was used to recombine the radiolytic hydrogen and oxygen. Less than 100 psi gas pressure in excess of steam was noted in all experiments, indicating excellent radiolytic-gas recombination. Radiolytic-gas production in the irradiated slurry should have been approximately 1 cc/min.

17.1.2 Development of Equipment and Irradiation Facilities

The common cause of stirring failure in-pile has been the development of a short circuit in the stirrer drive coils. The drive coils are wound with double-glass-insulated aluminum wire. The insulation frays easily, giving rise to short circuits. Impregnating the insulation with Sauereisen thinner No. 1 and cementing the coils in place with Sauereisen cement have greatly improved the durability of the insulation.

Modification of cell 7 in the High-Radiation-Level Analytical Facility for use in opening and sampling slurry irradiation bombs is essentially complete.

A small-scale slurry circulating system for use in-pile, which incorporates a dash-pot type of slurry pump and a slurry-viscosity measuring device that uses the falling-ball technique, was designed and is under construction.

17.2 GAS-RECOMBINATION STUDIES

L. E. Morse   J. P. McBride

Out-of-pile reaction-rate studies of stoichiometric mixtures of hydrogen and oxygen in thorium oxide–uranium oxide slurries as a function of molybdenum oxide catalyst concentration (0.025 to 0.2 m) were continued. In a slurry of thorium-uranium mixed oxides containing 0.025 m MoO_3, the combination rate was more than sufficient to maintain a slurry blanket at less than 2000 psi total pressure under TBR conditions. The slurry contained 1000 g of thorium and 3.75 g of uranium per kilogram of H_2O and was activated by heating at 200°C with a hydrogen overpressure of 1000 psi at room temperature. Maximum catalytic activity was obtained with 0.05 m MoO_3 both in the slurry as prepared and after treatment with hydrogen (see Table 17.2).

The slurries used in the combination experiments were prepared from 900°C-recalcined D-16 ThO_2. The uranium, as $UO_3 \cdot H_2O$, and the MoO_3 were added to the dry oxide, tumbled for 1 hr, and then dispersed in water. Before being used in the combination experiments, the slurries were heated for 3 hr at 200°C with an oxygen overpressure (300 psi at room temperature). The MoO_3 was prepared by heating ammonium paramolybdate at 480°C for 16 hr in a covered dish.

The slurries as prepared showed low combination activity, with a maximum combination rate (3 moles of H_2 per hour per liter of slurry at 500 psi H_2 partial pressure) at 0.05 m MoO_3 concentration. Heating the slurries at 280°C for 1.5 hr with a hydrogen overpressure (1000 psi at room temperature) greatly increased the catalytic activity of MoO_3 at concentrations less than 0.1 m but had only a slight effect on the slurries containing 0.15 and 0.20 m MoO_3 (Table 17.2). Subsequent treatment of the reduced slurries with O_2 (at 280°C for 2 to 3 hr) did not affect their combination activity.

Experimental details and methods of analysis have been described previously.[2,3] The specific reaction-rate constant, k_T, and the rates of hydrogen consumption were obtained from the rate of pressure decrease, assuming a first-order dependence on the hydrogen partial pressure and the applicability of the perfect gas law. Linear dependence of the reaction rate on total pressure (steam, H_2, O_2) has already been demonstrated.[2]

[2]D. E. Ferguson *et al.*, *HRP Quar. Prog. Rep. Oct. 31, 1954*, ORNL-1813, p 143–144.

[3]H. F. McDuffie *et al.*, *Reactor Sci. Technol.* 4(2), 23 (1954) (TID-2013).

TABLE 17.2. HYDROGEN-OXYGEN COMBINATION RATES IN THORIUM-URANIUM OXIDE SLURRIES CONTAINING MOLYBDENUM OXIDE CATALYSTS

Slurry: thorium, 1000 g per kg of H_2O, ThO_2 calcined at 900°C; uranium, 5 g per kg of H_2O added as $UO_3 \cdot H_2O$; MoO_3

MoO_3 Concentration (m)	Slurry as Prepared, Temperature 280°C		Reduced Slurry,[a] Temperature 150°C	
	k_π (hr^{-1})	H_2 Combination Rate P_{H_2} = 500 psi (moles/hr/liter)	k_π (hr^{-1})	H_2 Combination Rate P_{H_2} = 500 psi (moles/hr/liter)
0.025	0.4	0.1	28	19
0.05	7.8[b]	3[b]	44[c]	29[c]
0.075	1.7	0.5	40	27
0.10	2.8	0.8	34	21
0.15	20	5	7.7	5
0.20	31	9	15	10

[a]Heated with hydrogen overpressure for 1.5 hr at 280°C; 1000 psi H_2 added at room temperature.
[b]Extrapolated from rate data obtained at 250°C and below.
[c]Extrapolated from rate data obtained at 102°C and below.

It is of interest to note that the thorium-uranium slurries containing 0.15 m MoO_3 which were irradiated in the LITR (Table 17.1) were not activated by heating under hydrogen before being irradiated. Yet less than 100 psi of gas pressure in excess of steam pressure was observed under irradiation, indicating excellent gas recombination. The radiation power densities in these experiments were approximately equal to the expected average power density in a TBR blanket, and hence the radiolytic-gas production was also comparable to the average expected in the reactor blanket system.

17.3 SLURRY CHARACTERIZATION AND PREPARATION STUDIES

V. D. Allred   E. V. Jones
J. P. McBride

17.3.1 Surface-Area–Crystallite-Size Relations

Previous reports[4,5] indicated a close correlation between the specific surface area as determined by low-temperature nitrogen adsorption and the average crystallite size obtained from x-ray-diffraction line

[4]V. D. Allred and S. R. Buxton, *HRP Quar. Prog. Rep. July 31, 1955,* ORNL-1943, p 182–188.

[5]V. D. Allred, *HRP Quar. Prog. Rep. Oct. 31, 1955,* ORNL-2004, p 172.

broadening. By considering the measured surface area to represent the available surface for gas adsorption and equating this with the theoretically available surface — that is, calculated from the crystallite size — a relation was developed which has been useful in correlating the data on oxide prepared by various methods and is indicative of the nature of the crystallite packing in the thoria particles.

Thorium oxide has a cubic crystal structure; hence the total surface area θ of a gram of thorium oxide composed of discrete crystallites of cube edge D should be calculated by

$$(1) \qquad \theta = \frac{6}{\rho D} ,$$

where ρ is the x-ray or theoretical density of thoria and for which it is assumed that no correction is required for roughness or loss of surface in packing. The relative crystallite surface area available for gas adsorption in a gram of thorium oxide may then be defined as

$$(2) \qquad \frac{S}{\theta} = \frac{\rho D S}{6} ,$$

where S is the nitrogen-adsorption surface area.

With D in angstrom units, S in square meters per gram, and ρ equal to 10.02, the relation becomes

$$(3) \qquad \frac{S}{\theta} = 1.67 \times 10^{-4} DS \; .$$

The relative surface areas available for gas adsorption were calculated for a large number of oxide preparations by Eq. 3; they are plotted in Fig. 17.1 as a function of the oxide firing temperature.

For pure oxides prepared by hydrothermal methods the relative surface available for gas adsorption is approximately 1:1 over a wide calcination temperature range, indicating that the crystallites are discrete particles. This is consistent with the observation that there is little or no crystallite growth with increasing firing temperature until temperatures in excess of 900°C are reached.[5]

The observation that S/θ for oxide from thermally decomposed thorium oxalate has an average value of about 0.6 over a considerable calcination temperature range leads to the equation[4]

$$SD = 3.6 \times 10^3 \; ,$$

which is useful in estimating nitrogen-adsorption surface area from crystallite data. However, as seen from Fig. 17.1, caution must be used in applying this relation in other than the 500 to 900°C range and it must be applied only for pure oxide prepared by thermal decomposition of the oxalate.

17.3.2 Crystallite Growth Studies

No crystallite growth was observed in a typical thorium oxide which was heated as an aqueous slurry in a rocking autoclave (500 g of thorium per kilogram of H_2O) at 300°C for 1766 hr. The oxide had been prepared by thermal decomposition of
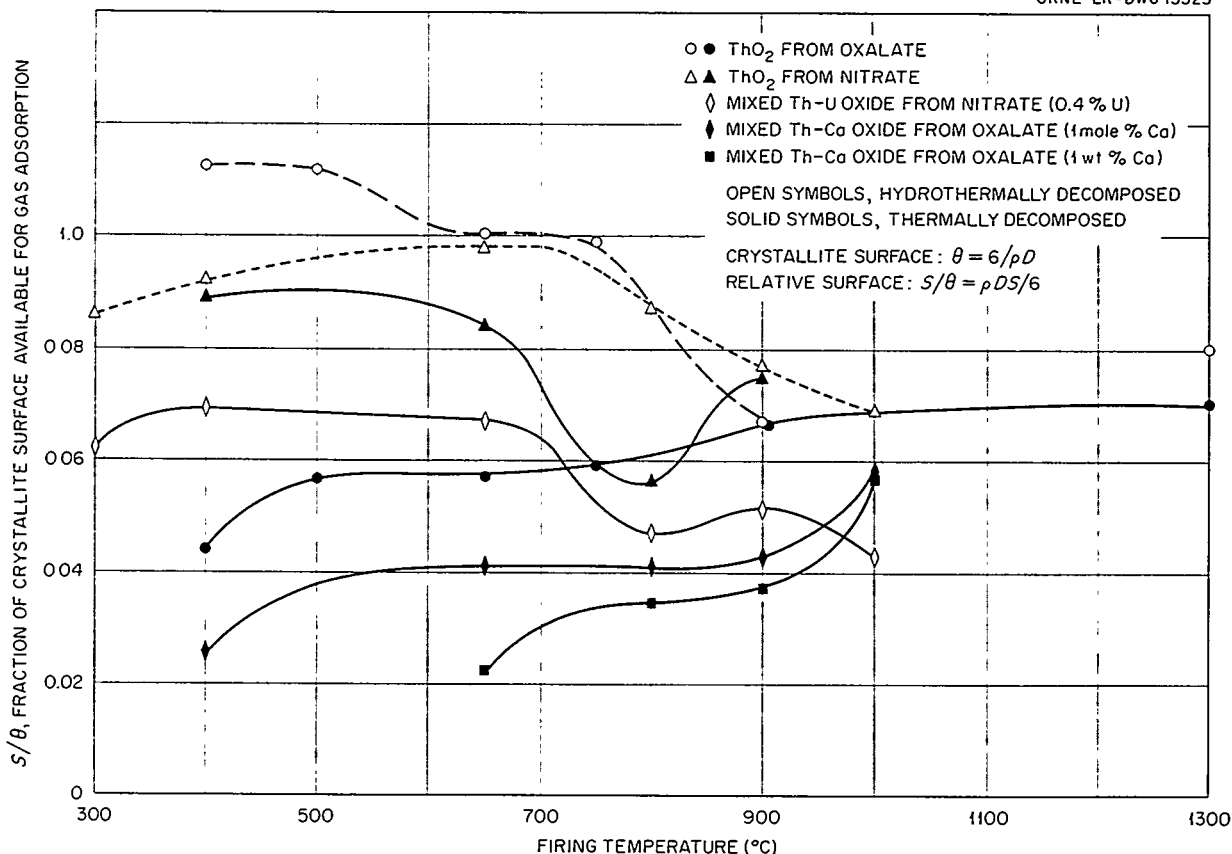
Fig. 17.1. Effect of Method of Preparation on Available Crystallite Surface.

10°C-precipitated oxalate and had been fired at 900°C for 2.5 hr. Samples removed from the autoclave at various time intervals failed to show any significant change in average crystallite size (Table 17.3). Lack of crystallite growth probably indicates an extremely low solubility of thorium oxide in water at 300°C.

TABLE 17.3. EFFECT OF TIME OF HEATING ON THE AVERAGE CRYSTALLITE SIZE OF AN AQUEOUS THORIUM OXIDE SLURRY AT 300°C

Time (hr)	Average Crystallite Size (Å)	Remarks
0	385	
140	373	Supernatant foamy
279	360	
443	368	
706	357	Slurry agglomerated into soft lumps
1236	345	Slurry flocculated; no lumps
1766	338	Slurry very flocculated

17.3.3 Oxide Preparation

Thorium oxide and mixed thorium-uranium oxide (0.4 mole % uranium) suitable for use in the preparation of aqueous suspensions was prepared by the hydrothermal decomposition at 300°C of the nitrate solutions. The oxides are characterized by their small crystallite size (100 to 150 Å), which does not change significantly when the oxide is fired at temperatures up to 900°C. This and other properties are similar to those of oxide produced by the hydrothermal decomposition of the oxalate.[5]

The formation of oxide by the hydrothermal method is postulated to proceed by a hydrolysis of the nitrate salt, liberating nitric acid:
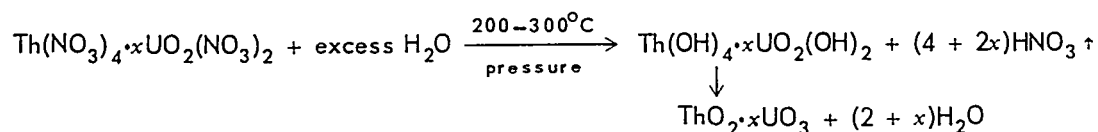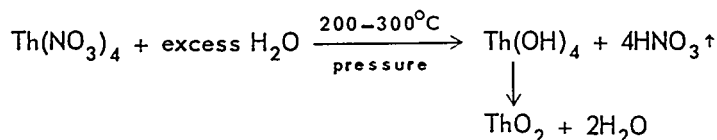
The reactions were carried out in a gold-lined autoclave with nitrate solutions about 1 M in thorium. Slow bleeding of the water and oxides was required to force the reaction to proceed in the direction of oxide formation. The characteristic properties of the oxides are summarized in Table 17.4. Data for the oxide prepared by the thermal decomposition of thorium nitrate are included for comparison.

Figure 17.2 shows the normality of the acid distillate as a function of the total volume of distillate. Good nitric acid recovery is indicated, the first 85% being recovered as a 2 N solution and the remainder as a 13 N solution.

It appears that a process could be devised in which a slurry of oxide could be produced from nitrate solution by separating the acid by steam distillation in a pressurized vessel. Concentrated acid could be recovered by an ordinary distillation step. The acid could be recycled to the chemical processing plant and the oxide sent to a continuous drier and kiln to remove the last traces of nitrate before reslurrying for use in the reactor blanket.

17.3.4 High-Temperature Settling Characteristics of Pumped Oxides

Slurry-settling studies with the use of the high-temperature x-ray absorption sedimentation apparatus[6] showed the settling rates and settled concentrations of pumped oxides to be markedly changed by the presence of sulfate. Typical settling data obtained as a function of temperature are shown in Fig. 17.3. The settling-rate–temperature-dependence curves for the slurries containing sulfate show marked deviations from predicted behavior and from the settling-rate–temperature-

---

[6]V. D. Allred, E. V. Jones, and J. P. McBride, *HRP Quar. Prog. Rep. April 30, 1956*, ORNL-2096, p 112–114.

$$Th(NO_3)_4 + \text{excess } H_2O \xrightarrow[\text{pressure}]{200-300°C} Th(OH)_4 + 4HNO_3\uparrow$$
$$\downarrow$$
$$ThO_2 + 2H_2O$$

$$Th(NO_3)_4 \cdot xUO_2(NO_3)_2 + \text{excess } H_2O \xrightarrow[\text{pressure}]{200-300°C} Th(OH)_4 \cdot xUO_2(OH)_2 + (4 + 2x)HNO_3\uparrow$$
$$\downarrow$$
$$ThO_2 \cdot xUO_3 + (2 + x)H_2O$$

dependence curves obtained for the pure oxides that had been pumped (X-29, U-8, U-37).[7]

A thorium oxide slurry in which no change in flocculation characteristics occurred with increasing slurry temperature would be expected to show a gradually increasing settling rate with

increasing slurry temperature, the settling-rate–temperature-dependence curve having a slope similar to the curve for the change in water fluidity (reciprocal viscosity) with increasing temperature.[6] This behavior was exhibited by the pure oxide slurries that had been pumped, and it may be assumed that little or no change in flocculation characteristics occurred in these materials

[7]V. D. Allred, E. V. Jones, and J. P. McBride, *HRP Quar. Prog. Rep. Jan. 31, 1956*, ORNL-2057, p 115–117.

TABLE 17.4. EFFECT OF FIRING TEMPERATURE ON CHARACTERISTIC PROPERTIES OF THORIUM AND THORIUM-URANIUM OXIDES PRODUCED BY DIRECT DECOMPOSITION OF NITRATE SALTS

Firing Conditions[a]		Nitrate Content	Average Crystallite Size ($\overset{\circ}{A}$)	Specific Surface Area, S (m^2/g)	S/θ[b]
Temperature (°C)	Time (hr)				
Thermal Decomposition of Thorium Nitrate[c]					
400	1		50	106	0.89
650	1		80	63	0.84
800	1		134	25	0.56
900	1		250	18	0.75
1000	1		475	1.2 (?)	0.10 (?)
900	24		565	0.7 (?)	0.07 (?)
Hydrothermal Decomposition of Thorium Nitrate[d]					
e		3.45%	95	54	0.86
400	1	1.69%	96	57	0.92
650	1	16 ppm	94	62	0.98
800	1	<5 ppm	101	51	0.87
900	1	<5 ppm	111	42	0.77
1000	1	<5 ppm	134	31	0.68
650	24		100	56	0.94
900	24		136	27	0.60
Hydrothermal Decomposition of Thorium-Uranium Nitrate[f]					
e		1.02%	142	26	0.62
400	1	0.70%	144	29	0.69
650	1	49 ppm	133	30	0.66
800	1	20 ppm	136	21	0.47
900	1	20 ppm	149	21	0.51
1000	1	20 ppm	158	16	0.43
650	24	65 ppm	145	28	0.67
900	24	10 ppm	174	16	0.46

[a]After initial decomposition.

[b]See Sec. 17.3.1.

[c]Prepared by heating at 200 to 400°C.

[d]Prepared by autoclaving 1 M thorium nitrate solution at 300°C.

[e]As received from the autoclave.

[f]Prepared by autoclaving 1 M thorium—0.4 M uranium nitrate solution at 300°C.
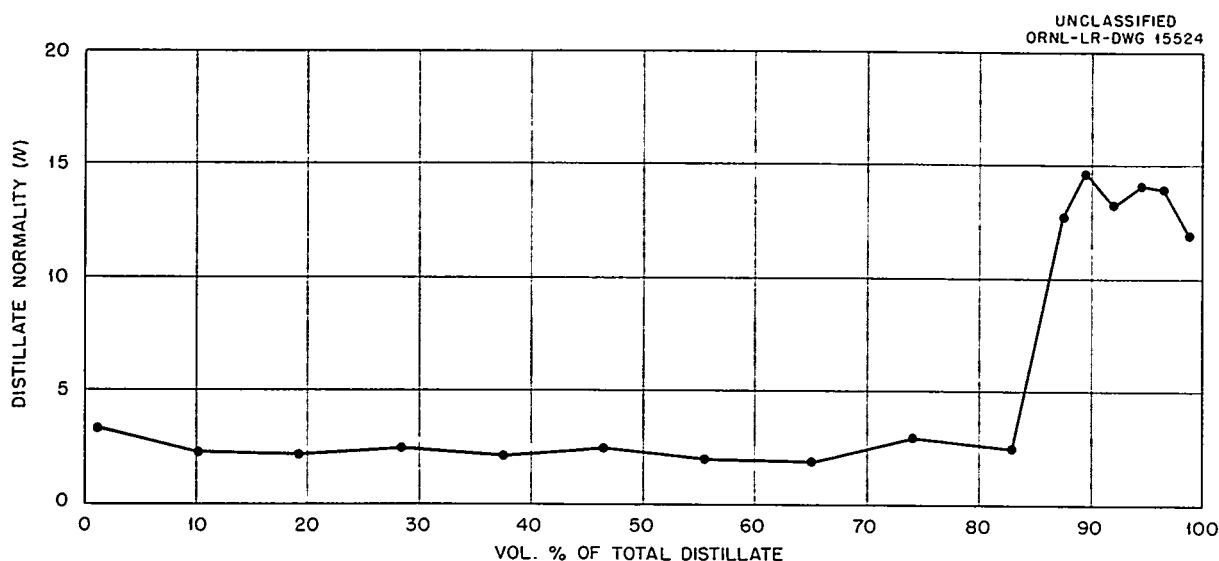
Fig. 17.2. Acid Recovery from Hydrothermal Decomposition of Thorium Nitrate at 300°C.
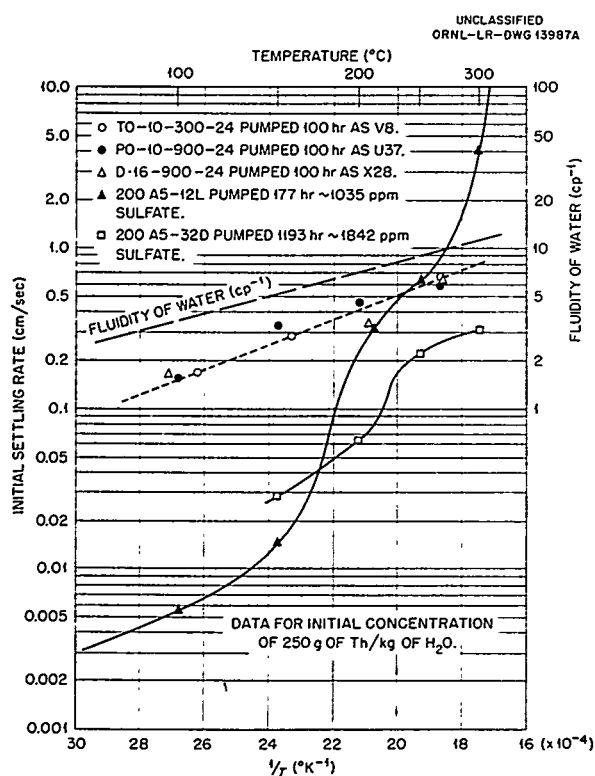

Fig. 17.3. Effect of Temperature on the Sedimentation Rates of Pumped Thorium Oxide Slurries.

with increasing slurry temperature. However, results obtained with the sulfate-containing material indicate that marked changes in the flocculation characteristics took place with increasing temperature.

A preliminary investigation of the effect of sulfate concentration and temperature on the settling characteristics of a thorium oxide slurry was carried out with an 800°C-calcined thorium oxide which had been pumped in run CS-23.[8] Thorium sulfate was added at various concentrations to a suspension of the pumped material, 250 g of thorium per kilogram of H_2O, and the suspension was heated for 3 to 4 hr at 300°C before the settling experiments were carried out. A marked increase in the settled density of this material occurred at all temperatures (100 to 300°C) upon the addition of 500 to 1000 ppm of sulfate (0.7 to 1.4×10^{-3} meq/m^2 of surface) and at 5000 ppm of sulfate (6.8×10^{-3} meq/m^2 of surface). The relative effect was less at the higher temperature (Fig. 17.4). These data indicate a marked change in the flocculation characteristic at these sulfate concentrations.

[8]E. L. Compere *et al.*, *HRP Quar. Prog. Rep. April 30, 1956,* ORNL-2096, p 87–89.
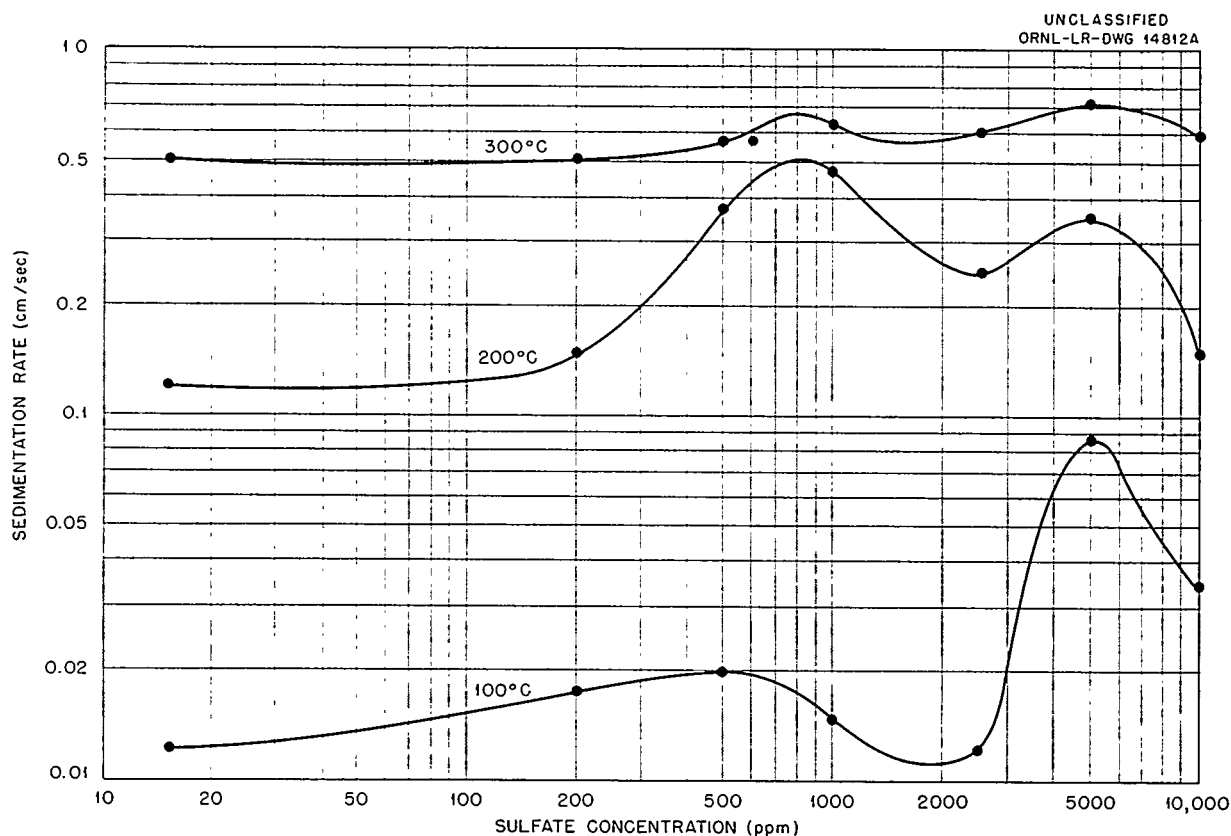
Fig. 17.4. Effect of Sulfate on the Sedimentation Rate of a Thorium Oxide Slurry (i.e., CS-23, 800°C Oxide Containing 250 g of Thorium per kilogram of H_2O).

Figure 17.5 shows the relation between the settling rate, the settled concentration, and the critical concentration (concentration at which the slurry enters the compaction zone of settling).[9] The fact that the settled concentration and critical concentration increase in the same manner as the settling rate indicates that the flocs found in the regions where sulfate produces a marked change in the flocculation characteristics are dense and tightly bound.

17.4 THE PREPARATION OF THORIA SOLS[10]

The preparation of thoria sols by an improved dialysis process was continued. In the improved process the sols are concentrated to a glass and redispersed in water, repeatedly, at intermediate stages of the dialysis. This results in a con-

densation of the thoria micels and a release of nitrate ion, which is then readily removed from the system. Nineteen sol samples containing nine different inorganic stabilizers — NO_3, Cr_2O_3, CrO_3, Fe_2O_3, MoO_3, La_2O_3, Bi_2O_3, PdO, and Y_2O_3 — were prepared and tested for stability at high temperatures. All the sols were stable for long periods at 100°C; all decomposed to slurry in 16 hr or less at 300°C in unstirred bombs, as shown by examination at temperature by x-radiography. The presence of nitrate ion in all the sols may have masked the effect of the additives.

Electrophoresis experiments showed that a thoria sol, containing less than 4% nitrate on the thoria basis, consists of positively charged micels. X-ray-diffraction crystallite size measurements indicated that crystallite growth is proportional to the nitrate/thoria ratio in sol-slurry systems.

Thorium phosphate gel beads were made with an average diameter of about 2 mm. A study of the

---

[9]E. V. Jones, *HRP Quar. Prog. Rep. Oct. 31, 1955*, ORNL-2004, p 172—175.

[10]Work done by Houdry Process Corp.

hydrothermal stability and physical properties of these beads is in progress.

Electrophoresis apparatus for studying the electrical properties of micels and particles at elevated temperatures is being designed. Arrangements were made with Sperry Products, Inc., for laboratory tests of ultrasonic apparatus for measuring slurry settling rates.
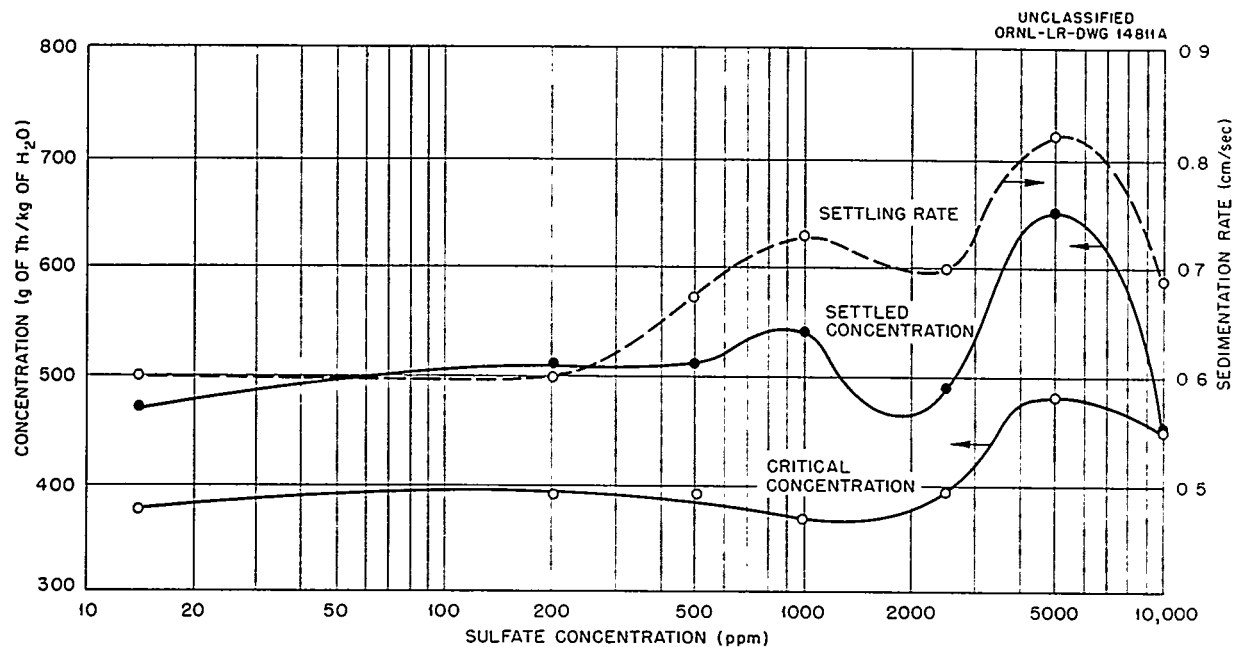

Fig. 17.5. Effect of Sulfate on the Settling Characteristics at 300°C of a Thorium Oxide Slurry (i.e., CS-23, 800°C Oxide Containing 250 g of Thorium per kilogram of H_2O).

18. EQUIPMENT DECONTAMINATION

D. E. Ferguson

R. E. Leuze   R. D. Baybarz

A treatment with chromous sulfate in dilute sulfuric acid, followed by alkaline-tartrate-peroxide, and phosphorous acid–hypophosphite solutions removed corrosion oxides and fission products deposited on type 347 stainless steel in an in-pile loop used for circulating uranyl sulfate solutions at 250°C. A treatment with chromous sulfate solution followed by alkaline-tartrate-peroxide removed thorium daughters deposited on type 347 stainless steel by ThO_2 slurries at 250°C.

18.1 EQUIPMENT USED TO CONTAIN URANYL SULFATE SOLUTION

R. D. Baybarz

Additional studies confirmed the effectiveness of chromous sulfate in dilute sulfuric acid for dissolving corrosion oxides and fission-product contamination from type 347 stainless steel that had been in contact with uranyl sulfate solutions at 250°C. The activity of short lengths of type 347 stainless steel pipe from in-pile loop L-4-11 was reduced from 30 r/hr to 200 mr/hr by placing the pipe samples in 0.4 M $CrSO_4$–0.5 M H_2SO_4 at 85°C for 2 hr. The activity remaining on the metal was 99% ruthenium, which had apparently replated from the chromous sulfate solution. Contacting the metal with 10% NaOH–2.5% sodium tartrate–2.5% H_2O_2 solution for 4 hr at room temperature further reduced the activity to about 6 mr/hr. This gave an over-all decontamination factor of 5 × 10^3. Since this pipe was taken from a portion of the loop that had not been in the neutron flux, there was essentially no induced activity. About 80% of the original gamma activity was zirconium-niobium, and 15% was ruthenium.

In 3 hr, molten phosphorus at 110°C removed the oxide film deposited on type 347 stainless steel by uranyl sulfate at 250°C, but unfortunately the base metal was heavily corroded. Solutions containing less than 25% H_3PO_3 were ineffective for oxide removal, even at 250°C for 48 hr. However, solutions containing only 2% H_3PO_3 and 2% NaH_2PO_2 at 150 to 180°C removed the oxide film in 20 to 30 hr, with only moderate corrosion to the base metal, that is, 50 to 100 mpy in static

corrosion tests. Attempts to dissolve ZrO_2 and PuO_2 in this solution were unsuccessful.

Decontamination of in-pile loop specimens by the phosphorous acid–hypophosphite solution was somewhat erratic. Short lengths of type 347 stainless steel pipe from in-pile loop L-4-11 were completely descaled by contact with 2% H_3PO_3–2% NaH_2PO_2 at 150 to 180°C for 20 to 30 hr. However, the fission-product activity apparently replated on the metal. Pipe samples whose original activity was 8 r/hr had activities of 0.3 to 5 r/hr after being descaled. This activity was zirconium-niobium and ruthenium; it was readily removed by 10% NaOH–2.5% sodium tartrate–2.5% H_2O_2. Although the phosphorous acid–hypophosphite solution is easier to prepare, chromous sulfate in dilute sulfuric acid is a more satisfactory decontaminant, since it dissolves PuO_2 and since it contains no materials that would interfere with reactor operation if not completely removed from the system.

18.2 EQUIPMENT USED TO CONTAIN THORIUM OXIDE SLURRIES

R. D. Baybarz

Surface contamination of thorium daughters deposited on type 347 stainless steel from ThO_2 slurries at 250 to 300°C was reduced from about 10^6 to 50 alpha counts/min/in.^{2} by 0.4 M $CrSO_4$–0.5 M H_2SO_4 solution at 80°C followed by 10% NaOH–2.5% sodium tartrate–2.5% H_2O_2 at 23°C.

A type 347 stainless steel loop used for circulating ThO_2 slurries at elevated temperature was thoroughly washed to remove all loose oxide. The surface contamination due to thorium daughters was estimated to be 10^6 alpha counts/min/in.^{2} The loop was charged with 1600 ml of 0.4 M $CrSO_4$–0.5 M H_2SO_4 solution, which was circulated at 80°C for 2 hr. After this solution was discharged, the loop was washed with water and disassembled for inspection. All surfaces were bright and were free of ThO_2 and iron oxide corrosion film. The alpha activity on the pump impeller was 5 × 10^3 counts/min/in.^{2} The loop was reassembled, and 10% NaOH–2.5% sodium tartrate–

2.5% H_2O_2 was circulated at room temperature for 4 hr. After this treatment, the alpha activity on the pump impeller was about 50 counts/min/in.[2], giving an over-all decontamination factor of greater than 10^4.

Average corrosion of the loop by the chromous sulfate treatment was 0.11 mil, or about 500 mpy (based on dissolved iron and exposed surface area). Although the loop had been thoroughly washed before the chromous sulfate treatment, a considerable amount of ThO_2 was removed in the decontaminating solutions. However, these solutions contained essentially no dissolved thorium.

Part VI

SUPPORTING CHEMICAL RESEARCH

E. H. Taylor

19. AQUEOUS SYSTEMS AT ELEVATED TEMPERATURES

C. H. Secoy

H. H. Stone   F. H. Sweeton

19.1 STABILIZATION OF ThO$_2$ SOLS

The previously reported study of sol E,[1] a ThO$_2$ sol stabilized by Th(NO$_3$)$_4$, was extended. Its refractive index was found to be 1.3895 at 24.6°C. The specific conductivity of the sol was found to be 0.0125 mho at 25°C. This conductivity was about one-fifth that of a Th(NO$_3$)$_4$ solution having essentially the same nitrate concentration; thus it appears that there was considerable interaction in the sol between the ThO$_2$ and the Th(NO$_3$)$_4$.

A program was started to find the effect of peptization conditions on particle size, since particle size theoretically has a pronounced effect on sol stability. A supply of hydrous ThO$_2$ suitable for peptizing was prepared by fast mixing of flowing streams of Th(NO$_3$)$_4$ and NH$_4$OH. The resulting precipitate was washed by successive decantations until all soluble impurities should have been removed. However, analysis showed that about 13% of the original nitrate remained, evidently adsorbed on the ThO$_2$ in some manner. It was found that a little of this ThO$_2$ could be slowly peptized in solutions of Th(NO$_3$)$_4$ at room temperature but that, as more of the oxide was added, the rate became too low to be useful. At 50°C, however, the rate was faster, and higher concentration of sols could be achieved in reasonable times. At 80°C the rate was even faster.

However, x-ray analysis[2] of these sol preparations showed no appreciable differences in average crystallite size. All samples fell in the apparent range of 30 to 50 Å. A later analysis of the washed ThO$_2$ used in making these sols showed a crystallite size in the same range. There is evidence that these crystallites grew after preparation of the washed ThO$_2$ sample. According to the assumption that large crystallites can be produced by digesting very fine crystallites in the presence of a few of somewhat larger size, it appears desirable to repeat this work, taking particular pains to have a ThO$_2$ material made up of extremely fine crystallites.

During the course of the above studies an attempt was made to estimate particle size of the sol preparations by use of a spectrophotometer to measure their light transmission. The transmission is, of course, decreased both by the light scattering that indicates average particle size and by normal absorption. Unfortunately, for the nitrate-peptized sols, Th(NO$_3$)$_4$ has absorption peaks in the ultraviolet region, which is the most sensitive region for studying light scattering. The results of these measurements indicated that the particles may have been several times as large in diameter on the average as the reported average crystallite diameter. This method appeared to be worth further study, as it was fast and easy to carry out. Its sensitivity and accuracy should improve as sol concentrations are increased, as particle size is increased, and as shifts to peptizing agents that are more transparent in the ultraviolet region are made.

19.2 EFFECT OF AN ADDED SOLUBLE SALT ON SETTLING RATE OF A THORIUM OXIDE SLURRY

In an earlier report[3] it was suggested that the use of high-concentration salt solution as a suspension medium for thorium oxide might provide a more attractive slurry system than the use of pure water or water containing very small amounts of ionic material. More specifically, it was suggested that the settling rates might be affected to an extent beyond the effect due to physical properties such as viscosity and density.

Recently an investigation to determine the gross effects was instituted. The apparatus consisted of a 100-ml graduate suspended in a water bath. The only two temperatures that were investigated are 26 and 90°C, one being the thermostatted room temperature and the other the temperature as recorded in boiling water. In each case the system was given time to come into equilibrium at the desired temperature; then an electric stirrer was used to stir the slurry for 2 or 3 min. The settled volumes, in milliliters, were recorded against time,

[1] F. H. Sweeton, HRP Quar. Prog. Rep. Jan. 31, 1956, ORNL-2057, p 133.

[2] These analyses were made by R. D. Ellison of the Chemistry Division and R. L. Sherman of the Analytical Chemistry Division.

[3] F. J. Loprest, W. L. Marshall, and C. H. Secoy, HRP Quar. Prog. Rep. April 30, 1956, ORNL-2096, p 129.

in seconds. All studies to date have employed D-16 ThO_2 suspended in a 53.5% $Ca(NO_3)_2$ solution. Calcium nitrate was chosen for no special reason other than having been the subject of previous vapor-pressure studies.

Figures 19.1 and 19.2 show the results obtained with slurries containing, respectively, 444 and 1150 g of ThO_2 per liter. A logarithmic scale was used for the time variable in order to show, on the same graph, times varying over several orders of magnitude. The dissolved salt obviously has a considerable effect, especially during the early unhindered part of the settling process.

So far, only the variables of temperature and ThO_2 concentration have been investigated, and these only in a very limited manner. It should be of interest to investigate higher temperatures and other ThO_2 concentrations, as well as other salt concentrations and salts other than calcium nitrate. The effect of time factors such as repeated settling and mixing cycles on the same suspension is also of interest. In spite of the increased neutron loss and other possible objections to such systems, the delayed settling and lowered vapor pressure may be advantageous in reactor applications.
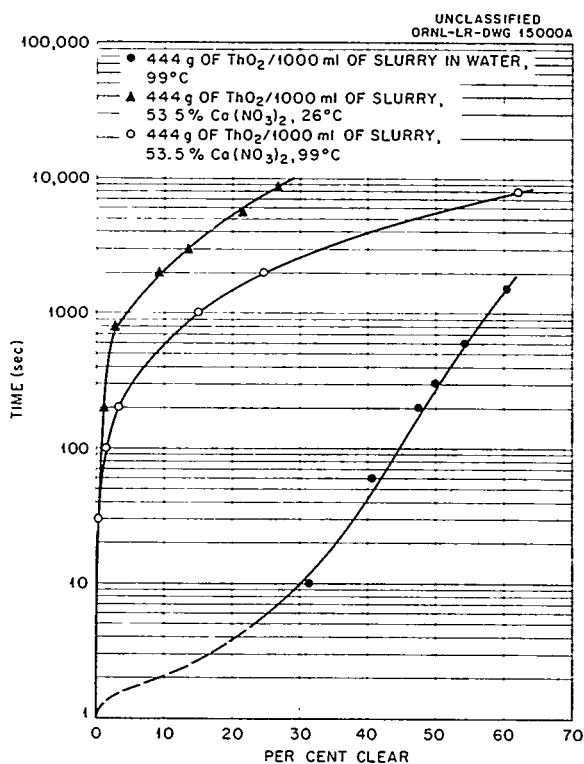

Fig. 19.1. Settling Rates of ThO_2 (444 g/liter) Suspended in H_2O and in $Ca(NO_3)_2$ Solutions.
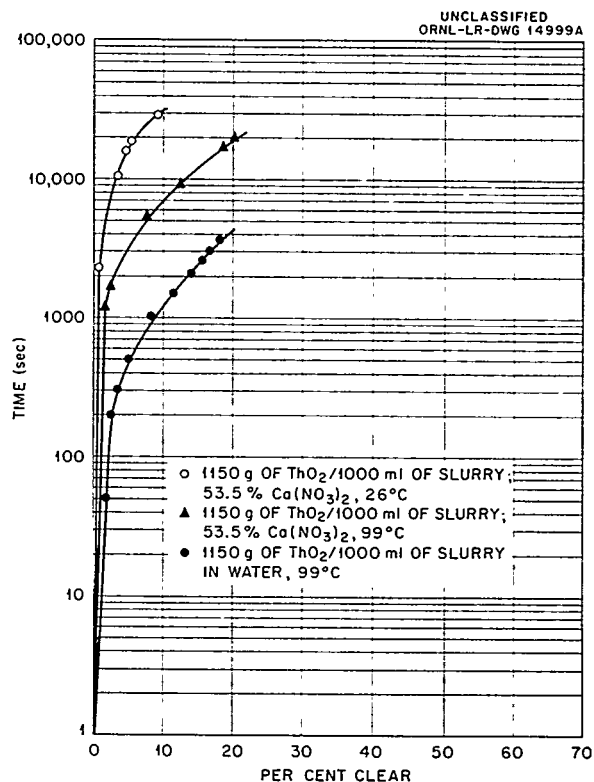
Fig. 19.2. Settling Rates of ThO_2 (1150 g/liter) Suspended in H_2O and in $Ca(NO_3)_2$ Solutions.

20. RADIATION STUDIES OF THORIUM NITRATE SOLUTIONS

J. W. Boyle   H. A. Mahlman

A platinum-lined stainless steel autoclave suitable for in-pile studies at temperatures up to 300°C was prepared,[1] and the irradiation of thorium nitrate solutions was extended to this temperature. The solution,[2] irradiated at a thermal-neutron flux of 3.7×10^{11} neutrons/cm²·sec, was 7 m $Th(NO_3)_4 \cdot Be(NO_3)_2$ and 0.05 m highly enriched $UO_2(NO_3)_2$. Ninety-five per cent of the total absorbed energy was from fissioning taking place in the solution. The conclusions from the experi-

ment were that the rate of formation of N_2 is independent of temperature and that any radiation-induced or thermal back reaction of the N_2 is negligible up to 300°C.

The nitrogen yield for the 49.3 wt % nitrate solution was found to be 0.16 ± 0.016 molecule of N_2 per 100 ev. This agrees with the value obtained from the extrapolation of less concentrated solutions.[3] The gas analyzed 98.8% oxygen and nitrogen with an O_2/N_2 ratio of 2.44. The theoretically expected ratio is 2.50 if N_2 and O_2 are the only nitrate decomposition products.

[1]H. H. Stone and J. W. Boyle, "Description of an All Platinum System for High Temperature, High Pressure Studies," *Chem. Semiann. Prog. Rep. June 20, 1956,* ORNL-2159 (to be issued).

[2]J. W. Boyle and H. A. Mahlman, "Radiation Studies on Nitrate Solutions," *Chem. Semiann. Prog. Rep. June 20, 1956,* ORNL-2159 (to be issued).

[3]J. W. Boyle and H. A. Mahlman, *HRP Quar. Prog. Rep. Jan. 31, 1955,* ORNL-1853, p 201.

21. HRP ANALYTICAL CHEMISTRY

M. T. Kelley   C. D. Susano

R. G. Ball	G. Goldstein	F. J. Miller
R. E. Biggers	T. H. Handley	T. C. Rains
C. M. Boyd	H. P. House	S. A. Reynolds
J. Y. Ellenburg	D. L. Manning	I. B. Rubin
C. Feldman	O. Menis	P. F. Thomason

21.1 ANALYSIS OF SOLUTIONS OF URANYL SULFATE

Studies were made which resulted in (1) the improvement of the cell that is used for the removal of copper by internal electrolysis; (2) the evaluation of interference with, and the precision of, an amperometric method for mercury; and (3) the development of a method for the differential titration of acid in solutions of uranyl sulfate.

In order to determine the copper content and to prevent its interference with other determinations, a method of internal electrolysis has been applied to the removal of copper from solutions of uranyl sulfate which contain corrosion products. Copper is deposited at the cathode of the cell

$$Cd \,|\, CdSO_4(H_2SO_4) \,||\, KCl \,||\, CuSO_4(UO_2SO_4) \,|\, Pt$$

A cell has been designed whereby 30 to 40 mg of copper can be deposited in 30 min. Satisfactory results have been obtained by the use of this method with simple equipment which requires a minimum of analyst skill and time.

An evaluation was made of interferences and of the precision of an amperometric method which had been developed previously[1] for the determination of microgram quantities of mercury in solutions of uranyl sulfate. The method is based on the titration of mercury in a dilute solution of nitric acid with standard tetraphenylarsonium chloride at −0.5 v vs the SCE. It was established that, in this titration, the reactants combine in the molar ratio 1:1. Concentrations of 10 mg of UO_2^{++}, 0.5 mg of Sn^{++}, and 0.5 mg of Cd^{++} per milliliter do not interfere, while nitric acid in concentrations greater than 5 M does interfere. Mercury in amounts as low as 25 μg in a volume of 15 ml can be titrated with a coefficient of variation of 4%, while for amounts up to 2 mg the coefficient of variation is 2%.

---

[1] O. Menis *et al.*, *HRP Quar. Prog. Rep. Oct. 31, 1955,* ORNL-2004, p 213.

A method was developed for the titration of acid in solutions of uranyl sulfate by means of the Sargent-Malmstadt automatic differential titrator. In the titration of a solution of uranyl sulfate with standard base, two inflection points occur: the first point, at a pH value of 3.5, corresponds to the neutralization of free acid; the other, at a pH value of about 9, indicates the completion of hydrolysis of the uranium salt. In order to produce a rate of change in potential large enough to terminate the titration at the desired end point, sodium fluoride was added to a solution of uranyl sulfate to complex the uranium and thus to reduce the buffering action of the salt. With this modification, 0.1 to 1.0 meq of acid can be titrated in the presence of as much as 500 mg of uranium, with a coefficient of variation of about 2%.

21.2 ANALYSIS OF THORIUM OXIDE

Studies, completed or in progress, include the following: conversion of pyrophosphate to orthophosphate in slurries of thorium oxide; modification of the Warren Spectracord for use in the spectrophotometric titration of fluoride; methods for the determination of aluminum in thorium oxide which contains a variety of interfering components; the determination of chlorine, bromine, and iodine by flame photometry; methods for the determination of the particle-size distribution of ThO_2; effect of graphite in slurries of thorium oxide on the determination of sulfate.

Thorium oxide in aqueous slurries was found to catalyze the conversion of sodium pyrophosphate to the orthophosphate. For slurries which contained 40 g of the oxide per liter of 0.05 M $Na_4P_2O_7$, the half-life periods for the conversion reaction at 25, 50, and 100°C, respectively, were 60, 7, and 0.1 hr. The reaction rate, which appears to be a nonlinear function of the weight ratio of ThO_2 to $Na_4P_2O_7$, does not conform to any single reaction order throughout the conversion.

The Warren Spectracord was modified to render it applicable to the automatic spectrophotometric titration of fluoride with thorium nitrate, with alizarin red S being used as the indicator. The modification was accomplished by attaching a time-drive accessory and a feed assembly for the titrant to the instrument. The feed assembly consists of a 10-ml Micro-Metric syringe-type buret driven by a 1-rpm synchronous motor. This apparatus was used to titrate 5 to 75 μg of fluoride in thorium oxide, after separation of the fluoride by a distillation procedure. The coefficient of variation is approximately 3%.

Methods are being studied for the determination of aluminum in thorium oxide which contains small amounts of one or more corrosion products, principally Fe, Ti, Ni, Cr, and Zr in various combinations and proportions. The 8-quinolinol spectrophotometric method was modified to render it applicable to the determination of aluminum in the presence of titanium, nickel, and iron in moderate amounts. Work is continuing on the improvement of this method, particularly with regard to the elimination of interferences due to other combinations of impurities.

An indirect flame-photometric method for the determination of chloride, based on the reduction in emissivity of a solution of silver nitrate as a consequence of the addition of chloride,[1] was extended to the determination of bromide and iodide. Equimolar quantities of the three halides produce equal reduction of emissivity. By the adjustment of the acidity and the use of ammonium ions at controlled concentrations as a masking agent, chloride, bromide, or iodide can be determined in mixtures of the halides.

Studies were made of sedimentation methods for the determination of the particle-size distribution of thorium oxide in aqueous and xylene media. Variables given consideration included dispersing agents and the time and method of dispersion. As a consequence of this study, the Andreasen pipet method was selected for the actual determination of particle-size distribution of samples now being submitted to the laboratory. In this method, sedimentation is carried out in a xylene medium containing 0.06% oleic acid, following dispersion, by agitation for 3 min in a Waring Blendor. Comparative results obtained by the Wagner turbidimetric and the Andreasen pipet method are, in general, in reasonable agreement for particle sizes

with diameters in the range from 1.5 to 8 μ. For larger particles, a modified gravity-sedimentation method is being tested. Work is also in progress on a centrifugal-sedimentation technique for establishing the distribution of particles less than 2 μ in diameter.

A study was made in order to determine the cause of low and apparently erratic results in the volumetric determination of sulfate in slurries of thorium oxide which contained finely divided graphite. The sulfate was titrated with $BaCl_2$, with tetrahydroxyquinone (THQ) being used as the indicator. These tests revealed that graphite does not absorb and withhold any significant amount of sulfate, but that losses were due primarily to the difficulties which have been encountered in washing the sulfate completely from the filter paper which is used to remove the graphite, prior to the removal of thorium by ion-exchange resins. Satisfactory results were obtained by eliminating the filtration step, since tests indicated that solutions which contained suspended graphite could be added directly to the resin column without impairment of precision or accuracy.

21.3 ANALYTICAL CHEMISTRY FOR THE HRT AND THE HRT CHEMICAL PROCESSING PLANT

21.3.1 Radiochemical Analysis for the HRT

With respect to radioanalytical requirements for the HRT, a memorandum was prepared,[2] which summarizes the current status of the various analytical methods and lists estimates of the concentration of fission-product, heavy-element, and induced activities. Satisfactory radiochemical procedures for Cs, Cu, Nb, P, and S were developed and are described in detail in the memorandum. The future program — primarily development of instrumental methods and calibration of equipment — is described.

21.3.2 Ionic Analysis of HRT Samples

(a) Determination of Tellurium in Uranyl Sulfate Solutions. — In order to meet the requirements for the HRT chemical plant,[3] a study is being made

---

[2]T. H. Handley and S. A. Reynolds, *Development of Radioanalytical Methods for HRT*, ORNL CF-56-7-118 (July 23, 1956).

[3]W. L. Carter, *HRP-CP: Analytical Requirements for the HRT Chemical Processing Plant*, ORNL CF-56-4-101 (April 9, 1956).

of methods for the separation and determination of fission-product tellurium. The polarographic method of estimation seems to be the most suitable. A linear plot of diffusion current vs concentration over the range of 1 to 50 μg/ml has been obtained in an NH_4OH-NH_4Cl buffer solution of pH 8.4. An investigation is being made of the separation of tellurium from interfering cations by means of ion-exchange resin columns, using Dowex-50 resin. The use of anion-exchange resin columns for the same purpose will also be studied.

(b) New Spectrophotometric Reagents for the Determination of Uranium. — Two heterocyclic chelating agents, 2-benzoselenazole carboxaldehyde-*o*-hydroxy anil (I) and 2-benzoselenazole carboxaldehyde-*o*-hydroxy-*p*-sulfonic acid anil (II) were synthesized, and are being evaluated as possible selective colorimetric reagents for uranium in both the IV and VI valence states.

Under proper conditions, the UO_2^{++} chelate with compound I is apparently stable and has molar absorbency indexes from 4,076 to 14,600.

In the visible region, the UO_2^{++} chelate with compound II has molar absorbency indexes considerably less than those of the chelate with compound I, but in the ultraviolet region an index of 66,535 was observed. The effect of several parameters on the complex formation of both reagents is being studied.

The preparation of the sulfur analogues of these compounds is also contemplated.

21.3.3 Spectrochemical Analysis for the HRT

(a) Spectrographic Equipment in the High-Radiation-Level Analytical Facility. — An Ebert grating spectrograph and supporting devices were installed at cell 6 in the High-Radiation-Level Analytical Facility. The sample is placed in an excitation stand located inside the cell. The light emitted by the sample is conducted through a hole in the side wall of the cell by relay lenses and reflected into the spectrograph, which stands outside the cell near the operator. All chemical, sample-transfer, and excitation operations can be performed or controlled from outside the cell.

The spectrograph has a 15,000-line/in. grating used for conventional operation and a 7,500-line/in. grating used in higher orders for high-resolution work, for example, analyzing uranium or thorium preparations for impurities without preliminary chemical separation.

(b) Separation of Microgram Quantities of Rare Earths from Thorium. — The sample is converted to $Th(NO_3)_4 \cdot 12 H_2O$ and dissolved in ether (ethyl or, preferably, di-*n*-propyl) containing 5 to 15 vol % concentration of H_2O. This is then treated with dehydrated filter-paper pulp, which adsorbs the rare earths. The thorium solution is drained off. The pulp is washed, and the rare earths are stripped with aqueous HNO_3 at pH 2. The rare earths are separated from residual impurities by extraction with TTA.

(c) Separation of Microgram Quantities of Rare Earths from HRT Fuel Solution. — Uranium plus rare earths can be precipitated with NH_4OH, converted to the nitrate, and the above-described cellulose procedure applied. With very minor modifications, it works equally well for uranyl nitrate.

If the HRT fuel solution is made 2 N in HNO_3, uranium can be extracted by organic solvents from this solution, and the rare earths will remain in the aqueous phase. The rare earths can then be isolated with TTA.

Rare earths (even in microgram quantities) can be precipitated quantitatively from HRT fuel solution by the addition of Na_2CO_3, followed by Na_3PO_4. The carbonate forms a soluble complex with uranium, and partially precipitates iron and rare earths, as well as other elements. Addition of the phosphate is necessary, especially when only microgram quantities of rare earths are present, to ensure their complete coprecipitation on the iron. If no iron is present in the HRT fuel solution, it should be added.

(d) Separating Zirconium from HRT Fuel Solution. — In quantities of 250 μg or more, zirconium can be precipitated quantitatively from 2 N HCl solution with *p*-dimethylaminoazophenylarsonic acid.

If the aqueous phase is made 10^{-7} M in versene and 2 N in HNO_3, the uranium can be extracted with TBP, and the zirconium will remain in the aqueous phase.

(e) Separation of Niobium from HRT Fuel Solution. — If the fuel solution is made 10 N in HCl, niobium can be extracted from it with di-isopropyl ketone. The niobium can be stripped with 6 N HCl.

The versene-TBP procedure described for zirconium above works equally well for niobium.

(f) Quantitative Analysis of Mixtures of Microgram and Submicrogram Quantities of Rare Earths. — With the apparatus at hand, the most sensitive method of detection for rare earths is that of sparking a solution residue on the end face of a $\frac{1}{8}$-in. graphite rod in an argon-oxygen mixture. (It is assumed that only rare earths are present.) Ordinarily, the working curve of a given rare earth is displaced and/or rotated by a change in the proportions of the other rare earths in the mixture. This has been overcome by the addition of 30 μg of zinc to the electrodes. Standard deviations of 2 to 3% have been attained. Sensitivities range from hundredths to tenths of a microgram for various rare earths.

(g) Improvement of Precision of Air-Interrupted Spark Sources. — The day-to-day repeatability of results obtained with air-interrupted sources depends, among other things, on charging the condensers to a reproducible potential. This potential is conventionally set by adjusting the separation of the auxiliary spark gap. It was found, however, that if this gap was widened and then reset, the original breakdown potential was not always reproduced with sufficient accuracy. This was due to two factors: inability to reset the gap separation with sufficient accuracy, and possible interim changes in the atmosphere and/or surface condition (i.e., work function) of the electrodes. The difficulty was eliminated by using a different procedure for adjusting the auxiliary gap. The gap is first opened wide enough to prevent breakdown. The primary voltage is then carefully adjusted to a predetermined value, by use of an accurate a-c voltmeter. The auxiliary gap in the secondary is then narrowed until breakdown just barely occurs. This ensures that the breakdown potential will be equal to the secondary voltage corresponding to the preset primary voltage. This has a unique value, which does not have to be known accurately. There is thus no need to reproduce accurately the auxiliary gap separation or the condition of the atmosphere or electrode surfaces.

22. ISOLATION OF PROTACTINIUM-231

L. V. Jones

M. K. Barnett	R. E. Phillips
A. Elmlinger	M. L. Salutsky
H. W. Kirby	K. J. Shaver

During the past two years, personnel at Mound Laboratory have concentrated approximately 1 g of Pa^{231}, an amount sufficient to permit a study of its chemical and physical properties. The material concentrated is now being assayed to determine the exact amount available.

22.1 SOURCE OF PROTACTINIUM

The principal source of Pa^{231}, which occurs in the same decay chain as U^{235}, was the residue that appeared in the aqueous raffinate from the diethyl ether extraction step of the uranium processing scheme used at the uranium refinery plant operated by the Mallinckrodt Chemical Works. This residue contained between 0.1 and 0.2 ppm protactinium. Approximately 18 tons (80 drums) of this raffinate residue was separated from the raffinate streams by the Mallinckrodt Chemical Works and shipped to Mound Laboratory.

22.2 PROCESSING OF MALLINCKRODT RAFFINATE RESIDUE

22.2.1 Precipitation of the Protactinium on the Carrier

The raffinate residue was processed on a batch basis; a batch consisted of one drum; about 450 lb of wet solids. The contents of a drum were reacted with 2 N HCl (10 meq of HCl per gram of wet filter cake), and the resulting liquor was treated by boiling with NaCl (1.88 g of salt per gram of original filter cake). The precipitate yielded by this treatment carried the greater portion of the protactinium. The "carrier" was separated by decantation, washed with 0.5 N HCl, digested with 12% NaOH at 95°C, and finally washed twice with hot water. A total of 43 drums (2150 gal) containing 19,360 lb of raffinate residue was processed in this manner to yield 130 gal of carrier.

Because of the inhomogeneity of the raffinate residue, it was necessary that simulated process runs on samples from each of the 80 drums be made in order to determine the amount of protactinium (1) which would be recoverable by the adopted process, (2) which would dissolve in 2 N HCl but would not precipitate when the solution was heated with NaCl, and (3) which would not dissolve but would remain in the residue. The sum of these values indicated the total protactinium content of the residue.

Analysis indicated that in approximately half the drums, half or more of the protactinium would not dissolve in 2 N HCl; 37 drums have not been processed because of the indicated low yield. In about half the remaining drums, the protactinium that was dissolved by the 2 N HCl was not precipitated efficiently when the solution was treated with sodium chloride. To recover the protactinium in these cases, 0.4 mg of titanium, as titanium trichloride solution, per gram of raffinate residue was added during the initial solution step. When the liquor was heated with the sodium chloride, the titanium precipitated to act as a carrier to effect recovery of approximately 90% of the protactinium in solution.

22.2.2 Solvent Extraction

The protactinium in the carrier precipitate was concentrated by four solvent-extraction cycles; a summary of the concentration effected by each step is given in Table 22.1, and a summary of losses is presented in Table 22.2. In the first solvent-extraction cycle the carrier precipitate was reacted with concentrated HCl (1 vol of

TABLE 22.1. SUMMARY OF CONCENTRATION

	Volume (liters)
Raffinate residue, 19,360 lb	8170
Carrier precipitation	495
First solvent-extraction cycle	99
Second solvent-extraction cycle	16
Third solvent-extraction cycle	1.6
Fourth solvent-extraction cycle	0.16

TABLE 22.2. SUMMARY OF PROTACTINIUM LOSSES

	Recoverable Pa^{231} (g)	Losses (g)
Raffinate residue (total Pa^{231}, 1.63 g)	1.23*	0.25
Carrier	0.98	0.20**
Solvent-extraction cycles	0.78	0.15
Final product	0.63	

*Approximately 0.40 g of protactinium remained in the residue from the solution of the raffinate residue; it is believed that this is partially recoverable by the process contemplated for the remaining drums.

**This is the amount contained in the residue from the reaction of the HCl with the carrier; it is recoverable.

precipitate to 3 vol HCl) and contacted with a volume of di-isobutyl carbinol—Amsco mixture equal to the volume of the carrier precipitate. Protactinium was stripped from the organic phase with two concurrent strips into water. A 50-gal residue from the first solvent-extraction cycle contains about 200 mg of protactinium; a procedure has been developed which, according to estimates, will recover 90% of the protactinium from this residue.

Aqueous strip solutions from the first solvent-extraction step were acidified with HCl and extracted with isopropyl ether to remove gross amounts of iron. Then the aqueous solution of protactinium was acidified with 4/5 volume of concentrated H$_2$SO$_4$ and 2 volumes of concentrated HCl and extracted with isobutyl carbinol in Amsco. Protactinium was stripped from the organic phase by 3% H$_2$O$_2$ solution.

Strip solution from the second extraction was acidified by addition to 1/2 volume of concentrated H$_2$SO$_4$ and that solution was mixed with 4/3 volumes of concentrated HCl. Protactinium was extracted from the acid solution by isobutyl carbinol diluted with benzene and stripped into 10% H$_2$O$_2$ solution. Concentration of the material was completed in a fourth extraction cycle, which was similar to the third.

The protactinium from the fourth solvent-extraction cycle was stored in 500 ml of a solution of approximately 2.5 M H$_2$SO$_4$ and 7 M HCl. It is estimated that the 500 ml contains about 700 mg of protactinium; a quantitative analysis and assay are currently in process. The alpha spectrum indicates the material to be free of radioactive contaminants. A preliminary analysis indicated iron, titanium, aluminum, and niobium as principal impurities. Since the solution from the final solvent-extraction cycle contains a relatively low concentration of impurities, it is believed that final purification of the protactinium can be effected by ion-exchange techniques.

22.3 PROCESSING OF REMAINING RAFFINATE RESIDUE

As stated previously, approximately half the raffinate residue received from Mallinckrodt Chemical Works could not be satisfactorily processed to recover the protactinium by the adopted process. A method has been developed for processing the remaining drums of raw material, and laboratory investigations have shown that this method gives higher yields of protactinium, as well as reduced process losses.